

**A COMPREHENSIVE
VIBRATION ASSESSMENT PROGRAM
FOR
THE PROTOTYPE SYSTEM 80
REACTOR INTERNALS
PALO VERDE
NUCLEAR GENERATING STATION
UNIT 1**

B207080383 B20702
PDR ADOCK 05000470
E PDR

LEGAL NOTICE

THIS REPORT WAS PREPARED AS AN ACCOUNT OF WORK SPONSORED BY COMBUSTION ENGINEERING, INC. NEITHER COMBUSTION ENGINEERING NOR ANY PERSON ACTING ON ITS BEHALF:

A. MAKES ANY WARRANTY OR REPRESENTATION, EXPRESS OR IMPLIED INCLUDING THE WARRANTIES OF FITNESS FOR A PARTICULAR PURPOSE OR MERCHANTABILITY, WITH RESPECT TO THE ACCURACY, COMPLETENESS, OR USEFULNESS OF THE INFORMATION CONTAINED IN THIS REPORT, OR THAT THE USE OF ANY INFORMATION, APPARATUS, METHOD, OR PROCESS DISCLOSED IN THIS REPORT MAY NOT INFRINGE PRIVATELY OWNED RIGHTS; OR

B. ASSUMES ANY LIABILITIES WITH RESPECT TO THE USE OF, OR FOR DAMAGES RESULTING FROM THE USE OF, ANY INFORMATION, APPARATUS, METHOD OR PROCESS DISCLOSED IN THIS REPORT.

A COMPREHENSIVE VIBRATION ASSESSMENT
PROGRAM FOR THE PROTOTYPE SYSTEM 80
REACTOR INTERNALS

(PALO VERDE NUCLEAR GENERATING
STATION UNIT 1)

TABLE OF CONTENTS

i

SUMMARY

xv

1.0	<u>SYSTEM 80 PROTOTYPE COMPREHENSIVE VIBRATION ASSESSMENT PROGRAM.</u>	1-1
1.1	<u>Introduction</u>	1-1
1.2	<u>CVAP Program</u>	1-4
1.3	<u>Test Conditions.</u>	1-7
1.4	<u>Pre-Core and Post-Core Testing.</u>	1-7
1.4.1	Core Support Barrel	1-9
1.4.1.1	Hydraulic Loads	1-9
1.4.1.2	Natural Frequency	1-10
1.4.2	Lower Support Structure	1-10
1.4.2.1	Hydraulic Loads	1-10
1.4.2.2	Natural Frequency	1-11
1.4.3	Upper Guide Structure	1-12
1.4.3.1	Hydraulic Loads	1-12
1.4.3.2	Natural Frequency	1-13
1.4.4	Summary	1-13
1.5	<u>Stress Margin</u>	1-19
1.5.1	Design Conditions	1-20
1.5.2	CVAP Test Conditions.	1-21
1.6	<u>Test Duration</u>	1-29
2.0	<u>DESCRIPTION OF THE STRUCTURAL ASSEMBLIES.</u>	2-1
2.1	<u>Core Support Barrel Assembly.</u>	2-1
2.1.1	Core Support Barrel	2-1
2.1.2	Lower Support Structure	2-3
2.2.	<u>Upper Guide Structure Assembly.</u>	2-4

TABLE OF CONTENTS

(Continued)

3.0	<u>STRUCTURAL RESPONSE OF THE CORE SUPPORT ASSEMBLIES TO DETERMINISTIC AND RANDOM HYDRAULIC LOADS.</u>	3-1
3.1	<u>General Methodology</u>	3-1
3.1.1	Methods for Calculating Hydraulic Loads	3-3
3.1.2	Structural Analysis Methods	3-4
3.1.3	Methods for Calculating Structural Response	3-5
3.2.	<u>Summary</u>	3-6
4.0	<u>CALCULATION OF THE FORCING FUNCTIONS.</u>	4-1
4.1	<u>General Methodology</u>	4-1
4.1.1	Transient Conditions.	4-1
4.2	<u>Core Support Barrel Assembly.</u>	4-3
4.2.1	Core Support Barrel	4-3
4.2.1.1	Deterministic Forcing Function.	4-3
4.2.1.2	Random Forcing Function	4-4
4.2.2	Lower Support Structure	4-4
4.2.2.1	Deterministic Forcing Function.	4-4
4.2.2.2	Random Forcing Function	4-5
4.3	<u>Upper Guide Structure</u>	4-5
4.3.1	Deterministic Forcing Function.	4-6
4.3.2	Random Forcing Function	4-6
5.0	<u>CALCULATION OF THE STRUCTURAL RESPONSE.</u>	5-1
5.1	<u>General Methodology</u>	5-1
5.1.1	Transient Conditions.	5-1
5.2	<u>Core Support Barrel Assembly.</u>	5-2

TABLE OF CONTENTS

(Continued)

5.2.1	Core Support Barrel-Analysis.	5-2
5.2.1.1	Natural Frequencies and Mode Shapes	5-2
5.2.1.2	Forced Response to Deterministic Loading.	5-3
5.2.1.3	Response to Random Loading.	5-3
5.2.1.4	Core Support Barrel-Results of the Analysis	5-4
5.2.1.4.1	Natural Frequencies and Mode Shapes	5-4
5.2.1.4.2	Response to Deterministic Loading	5-5
5.2.1.4.3	Response to Random Excitation	5-5
5.2.2	Lower Support Structure-Analysis.	5-20
5.2.2.1	Natural Frequencies and Mode Shapes	5-21
5.2.2.2	Response to Deterministic Loading	5-21
5.2.2.3	Response to Random Excitation	5-21
5.2.2.4	Lower Support Structure-Results of the Analysis	5-21
5.2.2.4.1	Response to Periodic Loading.	5-21
5.2.2.4.2	Response to Random Excitation	5-22
5.3	<u>Upper Guide Structure Assembly-Analysis</u>	5-33
5.3.1	Natural Frequencies and Mode Shapes	5-33
5.3.2	Response to Periodic Loading.	5-34
5.3.3	Response to Random Excitation	5-34
5.3.4	Upper Guide Structure-Results of the Analysis	5-35
5.3.4.1	Natural Frequencies and Mode Shapes	5-35
5.3.4.2	Response to Periodic Loading.	5-36
5.3.4.3	Response to Random Excitation	5-36
5.4	<u>Maximum Values of Stress and Values of Stress Margins</u>	5-51
5.4.1	Primary Stress.	5-51
5.4.2	Fatigue	5-51
6.0	<u>MEASUREMENT OF HYDRAULIC FORCING FUNCTIONS AND STRUCTURAL RESPONSE.</u>	6-1
6.1	<u>Requirements.</u>	6-2
6.2	<u>Instrument Locations.</u>	6-2
6.2.1	Core Support Barrel Assembly.	6-2
6.2.1.1	Core Support Barrel	6-2

TABLE OF CONTENTS

(Continued)

6.2.1.1.1	Hydraulic Input Function Measurement.	6-2
6.2.1.1.2	System Response Measurements.	6-3
6.2.1.2	Lower Support Structure	6-4
6.2.1.2.1	Hydraulic Input Function Measurement.	6-4
6.2.1.2.2	Structural Response Measurements.	6-4
6.2.2	Upper Guide Structure Assembly.	6-5
6.2.2.1	Hydraulic Input Function Measurement.	6-5
6.2.2.2	Structural Response Measurements.	6-5
6.2.3	Summary of Instrumentation.	6-6
6.3	<u>Specification for Instrumentation Systems</u>	6-21
6.3.1	Pressure Transducer System Requirements	6-21
6.3.2	Strain Gage System Requirements	6-22
6.3.3	Accelerometer System Requirements	6-23
6.3.4	Displacement Transducer System Requirements	6-25
6.4	<u>Preparation and Installation of Instrumentation Systems</u>	6-27
6.5	<u>Data Acquisition.</u>	6-27
6.5.1	Recording Equipment	6-27
6.5.1.1	Equipment Description	6-27
6.5.2	Data Acquisition Methods.	6-28
6.5.2.1	Documentation	6-29
6.5.2.2	Calibration	6-29
6.5.2.3	Data Monitoring	6-29
6.6	<u>Data Reduction Methods.</u>	6-31
6.6.1	Reduction During Tests.	6-31
6.6.2	Post Test Reduction	6-31
7.0	<u>ACCEPTANCE CRITERIA FOR TEST DATA</u>	7-1
7.1	<u>Basis for Acceptance Criteria</u>	7-2
7.1.2	Uncertainties	7-3
7.2	<u>Acceptance Criterion.</u>	7-4
7.2.1	Acceptance Values for Response Instrumentation.	7-8

TABLE OF CONTENTS

(Continued)

8.0	<u>INSPECTION PROGRAM</u>	8-1
8.1	<u>Phases of Inspection Program</u>	8-2
8.2	<u>Inspection Procedure</u>	8-2
8.2.1	<u>Procedure - Baseline</u>	8-2
8.2.1.1	Reactor Vessel	8-2
8.2.1.2	Core Barrel Exterior	8-5
8.2.1.3	Under Core Support Barrel	8-5
8.2.1.4	Core Barrel Interior	8-6
8.2.1.5	Under Upper Guide Structure	8-7
8.2.1.6	Outer Surface of the Upper Guide Structure	8-7
8.2.1.7	Hold Down Ring	8-7
8.2.1.8	Reactor Vessel Closure Head	8-7
8.2.1.9	CVAP Instrumentation	8-8
8.2.2	<u>Procedure - Post Hot Functional</u>	8-10
8.2.2.1	Reactor Vessel	8-10
8.2.2.2	Core Barrel Exterior	8-10
8.2.2.3	Under Core Support Barrel	8-10
8.2.2.4	Core Barrel Interior	8-12
8.2.2.5	Under Upper Guide Structure	8-12
8.2.2.6	Outer Surface of the Upper Guide Structure	8-12
8.2.2.7	Holddown Ring	8-13
8.2.2.8	Reactor Vessel Closure Head	8-13
8.2.2.9	CVAP Instrumentation	8-13
8.3	<u>Inspection Report</u>	8-15

REFERENCES

R-1

TABLE OF CONTENTS(Continued)APPENDICES

A.	<u>HYDRAULIC LOADS</u>	A-1
A.1	<u>Hydraulic Forcing Function for CSB Assembly</u>	A-1
A.1.1	Core Support Barrel	A-1
A.1.1.1	Deterministic Forcing Function.	A-1
A.1.1.2	Random Forcing Function	A-9
A.1.2	Lower Support Structure	A-9
A.1.2.1	Deterministic Forcing Function.	A-9
A.1.2.2	Random Forcing Function	A-22
A.2	<u>Hydraulic Forcing Function for UGS Assembly</u>	A-29
A.2.1	Periodic Forcing Function	A-29
A.2.2	Random Forcing Function	A-31
B.	<u>DESCRIPTION OF COMPUTER CODES UTILIZED IN CVAP ANALYSIS</u>	B-1
B.1	ASHSD	B-1
B.2	MRI/Stardyne.	B-3
B.3	ICES/STRU DL-II.	B-6
B.4	HYDRO	B-8
B.5	DPVIB	B-9
B.6	STEADY STATE.	B-10
C.	<u>Development of Relationships for Acceptance Criteria.</u>	C-1
C.1	Ratio of Measured to Predicted Stress	C-1
C.2	Acceptance Criterion based on RMS Value of Measured Response.	C-4

TABLE OF CONTENTS
(Continued)
LIST OF TABLES

<u>Table</u>	<u>Title</u>	
I	SUMMARY OF PREDICTED STRESSES	xviii
II	SUMMARY OF SYSTEM 80 CVAP INSTRUMENTATION	xvix
1.3-1	SUMMARY OF TEST CONDITIONS.	1-8
1.4-1	IN WATER FREQUENCIES (564°F) OF CSB WITH AND WITHOUT CORE . . .	1-15
1.4-2	PRE- AND POST-CORE FLOW PARAMETERS RELATED TO CSB RESPONSE. . .	1-16
1.4-3	PRE- AND POST-CORE FLOW PARAMETERS RELATED TO ICI RESPONSE. . .	1-17
1.4-4	PRE- AND POST-CORE FLOW PARAMETERS RELATED TO CEA TUBE RESPONSE.	1-18
1.5-1	DESIGN STRESSES-CSB ASSEMBLY.	1-23
1.5-2	DESIGN STRESSES-UGS ASSEMBLY.	1-24
1.5-3	FATIGUE MARGIN, DESIGN CONDITIONS	1-25
3.2-1	SUMMARY OF HYDRAULIC LOADS, STRUCTURAL ANALYSIS AND STRUCTURAL. RESPONSE ANALYSES	3-7
5.2-1	CSB FREQUENCIES IN AIR AND WATER, PRE-CORE, 564°F	5-7
5.2-2	LIQUID NATURAL FREQUENCIES IN CSB ANNULUS - 564°F	5-8
5.3-1	SUMMARY OF UGS NATURAL FREQUENCIES.	5-37
5.4-1	SUMMARY OF MAXIMUM STRESSES AND MARGINS	5-53
5.4-2	SUMMARY OF PEAK STRESSES AND FATIGUE MARGINS.	5-54
6.2-1	CSB FORCING FUNCTION INSTRUMENTATION.	6-7
6.2-2	CSB RESPONSE INSTRUMENTATION.	6-8
6.2-3	LSS FORCING FUNCTION INSTRUMENTATION.	6-9
6.2-4	LSS RESPONSE INSTRUMENTATION.	6-10
6.2-5	UGS FORCING FUNCTION INSTRUMENTATION.	6-11

TABLE OF CONTENTS(Continued)LIST OF TABLES

6.2-6	UGS RESPONSE INSTRUMENTATION.	6-12
6.2-7	CVAP INSTRUMENTATION.	6-13
6.6-1	SPECTRAL DENSITY DATA REDUCTION	6-33
7.1-1	DESIGN, CVAP AND MAXIMUM ACCEPTABLE VALUES OF MEASURED STRESS .	7-5
7.1-2	RANGE FOR MEASURED STRESS AND VALUE FOR ACCEPTANCE CRITERION. .	7-6
7.2-1	RESPONSE INSTRUMENTATION DATA ACCEPTANCE CRITERIA	7-9
A.1-1	PUMP INDUCED PERIODIC PRESSURE AT INLET NOZZLE STATION.	A-12
A.1-2	MAXIMUM PUMP INDUCED PERIODIC PRESSURE ON CORE BARREL	A-13
A.1-3	RANDOM FLUCTUATING PRESSURE ON CORE SUPPORT BARREL.	A-14
A.1-4	PUMP PULSATION LOADS IN THE LOWER SUPPORT STRUCTURE REGION. . .	A-25
A.1-5	PERIODIC LIFT/DRAG FORCE ON ICI TUBE 58 DUE TO VORTEX SHEDDING. .	A-26
A.1-6	RANDOM FLUCTUATING PRESSURE ON ICI TUBE 58.	A-27
A.2-1	PUMP PULSATION LOADS ON THE CEA TUBES AND FUEL ALIGNMENT PLATE. .	A-32
A.2-2	PUMP PULSATION LOADS ON UPPER GUIDE STRUCTURE COMPONENTS. . . .	A-33

TABLE OF CONTENTS(Continued)LIST OF FIGURESFigure

A.	REACTOR VERTICAL ARRANGEMENT SHOWING COMPONENTS REFERRED TO IN THE TEXT	xiv
I.	SYSTEM 80 VERTICAL ARRANGEMENT: ASSEMBLIES INSTRUMENTED FOR CVAP. . .	xx
II.	CORE SUPPORT BARREL - TYPICAL CVAP INSTRUMENTATION	xxi
III.	UPPER GUIDE STRUCTURE - TYPICAL CVAP INSTRUMENTATION	xxii
IV.	LOWER SUPPORT STRUCTURE - TYPICAL CVAP INSTRUMENTATION	xxiii
V.	COMPREHENSIVE VIBRATION ASSESSMENT PROGRAM	xxiv
1.1-1	REACTOR VESSEL ARRANGEMENT	1-3
1.2-1	INTERNAL ASSEMBLIES WITH CVAP INSTRUMENTATION	1-6
1.5-1	MATERIAL PROPERTIES.	1-26
1.5-2	MAXIMUM STRESS REGIONS-CSB ASSEMBLY.	1-27
1.5-3	MAXIMUM STRESS REGIONS-UGS ASSEMBLY.	1-28
2.0-1	REACTOR INTERNALS ASSEMBLY	2-2
3.1-1	SUMMARY OF ANALYTICAL METHODOLOGY.	3-2
5.2-1	CALCULATION OF CSB DYNAMIC RESPONSE TO PERIODIC PRESSURE FORCES. . . .	5-9
5.2-2	CSB: FINITE ELEMENT MODEL	5-10
5.2-3	CSB: BEAM MODE SHAPES	5-11
5.2-4	CSB: SHELL MODE SHAPES.	5-11
5.2-5	CSB: FORCING, LIQUID AND STRUCTURAL FREQUENCIES	5-12
5.2-6	CSB: MAXIMUM STRESS - UPPER FLANGE, LONGITUDINAL; INSTRUMENTS S1, S3	5-13
5.2-7	CSB: MAXIMUM CIRCUMFERENTIAL STRESS - UPPER FLANGE; INSTRUMENTS S2, S4	5-14

TABLE OF CONTENTS

(Continued)

LIST OF FIGURES

5.2-8	CSB: MAXIMUM LONGITUDINAL STRESS - MID PLANE; INSTRUMENTS S5, S7.	5-15
5.2-9	CSB: MAXIMUM CIRCUMFERENTIAL STRESS - MID PLANE; INSTRUMENTS S6, S8.	5-16
5.2-10	CSB: MAXIMUM STRAIN - UPPER FLANGE.	5-17
5.2-11	CSB: MAXIMUM STRAIN - MID PLANE	5-18
5.2-12	CSB: MAXIMUM DISPLACEMENT AT BOTTOM OF BARREL: INSTRUMENTS A1-A4	5-19
5.2-13	LOWER SUPPORT STRUCTURE INSTRUMENT NOZZLE; FINITE ELEMENT MODEL	5-23
5.2-14	ICI SUPPORT TUBE: OUTER POSITION FINITE ELEMENT MODEL	5-24
5.2-15	ICI NOZZLE MODE SHAPES AND FREQUENCIES.	5-25
5.2-16	INSTRUMENT NOZZLE ASSEMBLY - MODE SHAPES AND FREQUENCIES.	5-26
5.2-17	LSS; FORCING AND STRUCTURAL FREQUENCIES	5-27
5.2-18	ICI NOZZLE; STRAIN; INSTRUMENTS S13	5-28
5.2-19	ICI NOZZLE; STRAIN; INSTRUMENTS S14	5-29
5.2-20	ICI NOZZLE; STRESS; INSTRUMENTS S13	5-30
5.2-21	ICI NOZZLE; STRESS; INSTRUMENTS S14	5-31
5.2-22	ICI SUPPORT PLATE; DISPLACEMENT; INSTRUMENT A11	5-32
5.3-1	CONTROL ELEMENT SHROUD TUBE; FINITE ELEMENT MODEL	5-38
5.3-2	DYNAMIC RESPONSE MODEL OF UGS ASSEMBLY.	5-39
5.3-3	CEA SHROUD TUBE NATURAL FREQUENCIES AND MODE SHAPES	5-40
5.3-4	UGS SHROUD TUBE ASSEMBLY; NATURAL FREQUENCIES AND MODE SHAPES.	5-41
5.3-5	UGS BARREL ASSEMBLY; MODE SHAPES AND FREQUENCIES.	5-42
5.3-6	UGS ASSEMBLY; MODE SHAPES AND FREQUENCIES	5-43
5.3-7	UGS; FORCING AND STRUCTURAL FREQUENCIES	5-44
5.3-8	CEA GUIDE TUBES; STRAIN, INSTRUMENTS S9, S11.	5-45
5.3-9	CEA GUIDE TUBES; STRAIN, INSTRUMENTS S10, S12	5-46
5.3-10	CEA GUIDE TUBES; STRESS, INSTRUMENTS S9, S11.	5-47

TABLE OF CONTENTS(Continued)LIST OF FIGURES

5.3-11	CEA GUIDE TUBES; STRESS, INSTRUMENTS S10, S12	5-48
5.3-12	CEA GUIDE TUBES; DISPLACEMENT, INSTRUMENTS A5 to A9	5-49
5.3-13	FUEL ALIGNMENT PLATE DISPLACEMENT, INSTRUMENTS A10.	5-50
6.2-1	TRANSDUCER AXIAL LOCATIONS.	6-14
6.2-2	CIRCUMFERENTIAL LOCATIONS OF INLET AND OUTLET NOZZLES	6-15
6.2-3	CSB; INPUT FUNCTION MEASUREMENT TRANSDUCERS	6-16
6.2-4	CSB; RESPONSE MEASUREMENT TRANSDUCERS	6-17
6.2-5	LSS; INSTRUMENTATION.	6-17
6.2-6	UGS; INSTRUMENTATION FOR ONE QUADRANT	6-18
6.2-7	UGS; AXIAL LOCATIONS FOR INSTRUMENTATION.	6-19
6.2-8	CEA SHROUD TUBE TYPICAL INSTRUMENTATION MOUNTING.	6-20
7.1-1	BASIS FOR ACCEPTANCE CRITERIA	7-7
7.2-1	ACCEPTANCE CRITERION COMPARED TO MAXIMUM MEASURED STRESS INTENSITIES FOR ASSEMBLIES.	7-10
8.1-2	REACTOR VESSEL CVAP INSPECTION.	8-3
8.1-2	REACTOR INTERNALS ASSEMBLY CVAP INSPECTION.	8-4

TABLE OF CONTENTS(Continued)LIST OF FIGURES

A.1-1	DETERMINISTIC HYDRAULIC MODEL	A-15
A.1-2	CIRCUMFERENTIAL VARIATION IN PRESSURE	A-16
A.1-3	AXIAL VARIATION IN PRESSURE	A-17
A.1-4	MAXIMUM VALUES OF PRESSURE PULSATIIONS ON CSB.	A-18
A.1-5	LOCATION OF ICI TUBE 58	A-28
A.2-1	LOCATION OF CEA TUBE 6.	A-34
A.2-2	LOCATION OF PRESSURE TRANSDUCER FOR FLOW INDUCED VIBRATION TEST.	A-35
A.2-3	PRESSURE PSD AT CVAP CONDITIONS	A-36
C.1-1	DESIGN AND CVAP STRESS INTENSITIES.	C-3
C.2-1	IDEALIZED RESPONSE PSDs FOR DEVELOPMENT OF ACCEPTANCE CRITERIA.	C-6

NOMENCLATURE

Figure A shows the reactor assemblies and components referred to in the test.

Mathematical symbols are defined at appropriate places in the text.

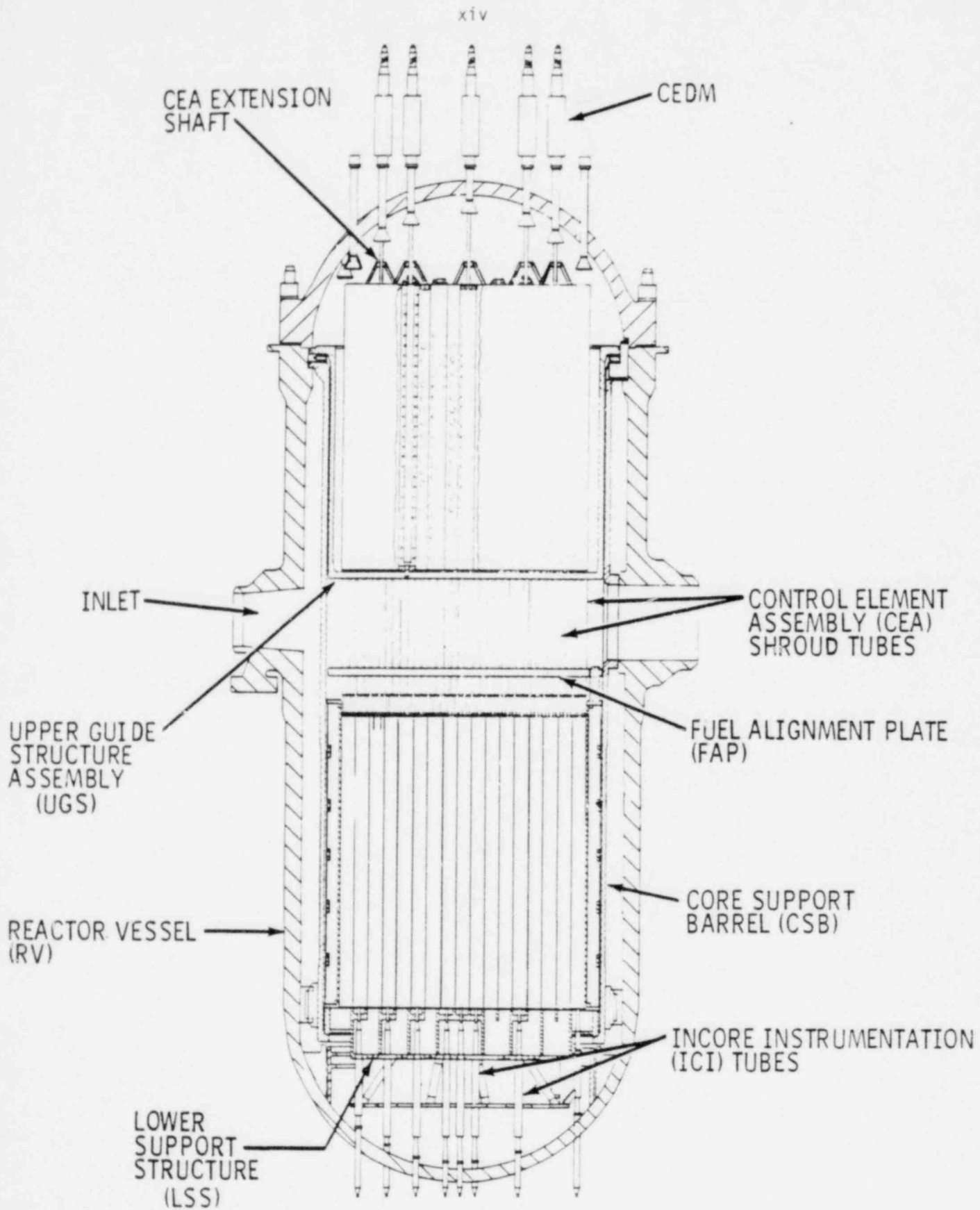


FIGURE A
 REACTOR VERTICAL ARRANGEMENT SHOWING COMPONENTS
 REFERRED TO IN THE TEXT

SUMMARY

In accordance with the United States Nuclear Regulatory Commission Regulatory Guide 1.20 (Rev. 2) a Comprehensive Vibration Assessment Program (CVAP) has been developed for Palo Verde Nuclear Generating Station Unit 1. This plant is prototypical of Combustion Engineering's 3800 Mwt System 80 pressurizer water reactor (Figure I).

The purpose of the CVAP is to verify the structural integrity of the reactor internals to flow induced loads prior to commercial operation. The dynamic flow related loads considered are associated with normal steady state operation and anticipated operating transients.

This comprehensive program, for a reactor prototype, consists of four individual Analysis, Measurement, Inspection, and Evaluation programs. The Analysis program provides theoretical evidence of the structural integrity of the internals and serves as a basis for both the Measurement and Inspection programs. Results of these programs form a basis for assessing, in the Evaluation program, the margin of safety for the reactor internals.

This report contains a summary of the Analysis program and descriptions of the Measurement and Inspection programs.

Analyses have been completed for the flow induced loading dynamic response of the two safety related assemblies; the core barrel support assembly (core support barrel and lower support structure) and upper guide structure assembly (Figure I). These analyses consider both random (e.g. turbulence) and deterministic (e.g. periodic pump induced pressure pulsations and vortex shedding related to cross flow velocity) flow related loads. The magnitude and frequency of the flow induced loads are a function of the thermal and hydraulic operating conditions. In addition, structural frequencies vary with temperature due to variations in hydrodynamic mass. An evaluation of both the loading and the response showed pre-core flow conditions to be conservative. Therefore dynamic response was calculated at pre-core conditions corresponding to normal operation with four pumps at the hot stand-by temperature of 564°F.

Response predictions were also done at combinations of flow (pump number) and temperature, occurring during pre-operational testing, that are not considered conditions of normal operation.

Standard modal analysis techniques were used to determine the forced response of the assemblies and their components. The appropriate set of equations describing the free vibration motion of the structure were solved to obtain its normal modes and frequencies. Hydrodynamic effects were included, for the core support barrel, by solving the coupled fluid-structure problem, and for the upper guide structure and lower support assemblies, by incorporating a hydrodynamic mass. Dynamic forces on the assemblies consisted of flow induced excitation due to both random and periodic variations in pressure. These forces were then used to obtain the forced vibration response to both random and deterministic flow induced excitation.

Maximum predicted stresses, summarized in Table I, are the alternating stress intensities due to flow induced dynamic loads predicted for CVAP test conditions corresponding to normal operation. Stresses were based on expected, or best estimate, values of flow. A margin for fatigue was defined as the ratio of the endurance limit stress to predicted stress. A margin of safety greater than one indicates that the internals are adequately designed to avoid fatigue damage due to flow induced loads. For flow induced loads at test conditions of normal operation, the margins of safety are summarized in Table I.

A measurement program was developed based on results of these analyses. The purpose of this program is to obtain data on both random and deterministic excitation (pressure) and structural response (displacement, strain acceleration). Instrumentation, consisting of pressure transducers, strain gages, accelerometers, and displacement transducers have been specified for each of the assemblies. A summary of the instrumentation is given in Table II. Instrumentation locations are shown schematically in Figures II, III, and IV.

Testing will be done at all steady state and transient (pump startup and shutdown) conditions corresponding to normal and part loop operation.

Additional tests will be done to verify the hydraulic forcing functions used in the analysis. Transducer signals will be conditioned and recorded on magnetic tape for post test reduction and analysis. Response during testing will be monitored by online evaluation of the spectral content of these signals. Root mean square values of all the signals related to structural response will be computed following each test and compared to an acceptance criterion based on the endurance stress from the ASME Code.

A pre-core inspection of the internals will be done before initiation and after completion of all pre-core flow tests. In both cases the internals will be positioned to permit visual inspection of the specified locations. Major load bearing surfaces, contact surfaces, welds, maximum stress locations identified in the analysis program and the CVAP instrumentation, mountings, and conduits will be examined. A photographic record will be made of all observations. A minimum of [] hours of pre-core flow testing will be completed to insure that the components are subject to a minimum of 10^6 cycles of vibration before inspection.

The Evaluation program will include analysis and critical review of the data required in both the Measurement and Inspection programs and comparison of these data with predictions of the Analysis program. This evaluation will include an assessment of the methods used to predict the response of the internals to dynamic forces and the resulting margins of safety. Preliminary and final reports of this evaluation will be submitted to the Nuclear Regulatory Commission, within the time limits specified in Regulatory Guide 1.20, after completion of all precritical testing.

An overview of the Comprehensive Vibration Assessment Program, showing the inter-relationship between the four individual programs, is presented schematically in Figure V.

TABLE I
SUMMARY OF PREDICTED STRESSES

Component	Predicted Stress (psi)	Fatigue Margin
Core Support Barrel	[]	[]
Upper Guide Structure	[]	[]
Lower Support Structure	[]	[]

Predicted Stress = Peak alternating stress at CVAP test conditions of 4 pump operation, 564°F.

Fatigue Margin = Endurance Limit/Predicted stress

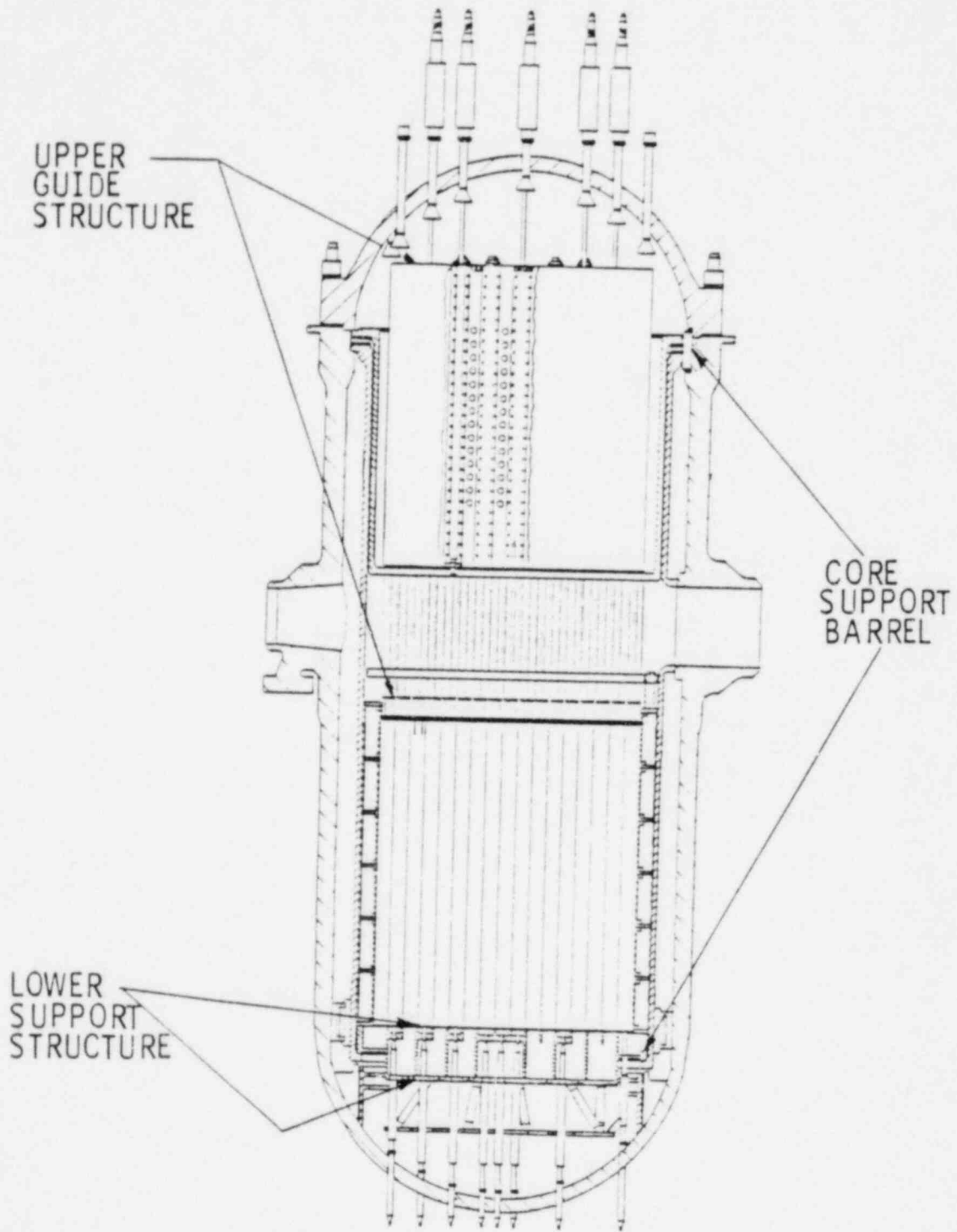
Endurance Limit = Stress limit for fatigue at 10^6 cycles (26,000 psi)

TABLE II
SUMMARY OF SYSTEM 80 CVAP INSTRUMENTATION

MAJOR COMPONENTS	INPUT FUNCTIONS			RESPONSE		
	TRANSDUCER	PRIMARY FUNCTION	QTY.	TRANSDUCER	PRIMARY FUNCTION	QTY.
Core Support Barrel	P. T.	Axial Dist.	2	S. G.	Shell Mode Response	4
		Circumferential Dist.	3	2-D Accl.	5-300 Hz Response (Beam & Shell Modes)	1
				E. D. D.	0.1-10 Hz Response (Beam Mode)	3
		Transient	1	S. G.	CSB Stress State Below Upper Flange	4
		Inlet Pressure	1			
Upper Guide Structure	P. T.	CEA Shroud Tube Loading (Max. Crossflow Velocity Location)	2	2-D Accl.	CEA Shroud Tube Response	5
				S. G.	CEA Shroud Tube Stress State	4
		UGS Support Plate Loading	1	3-D Accl.	Fuel Alignment Plate Vertical and Radial Response	1
Lower Support Structure	P. T.	ICI Tube-58 (Max. Turbulent Load)	1	S. G.	Axial Stress and Response of ICI Tube 58	2
				2-D Accl.	Lateral response of LSS	1
Summary	Pressure Transducers					
	13			2-D Accelerometers		7
				3-D Accelerometers		1
				Eddy Type Disp. Device		3
				Strain Gages		14
Total(Input)			13	Total(Response)	25	

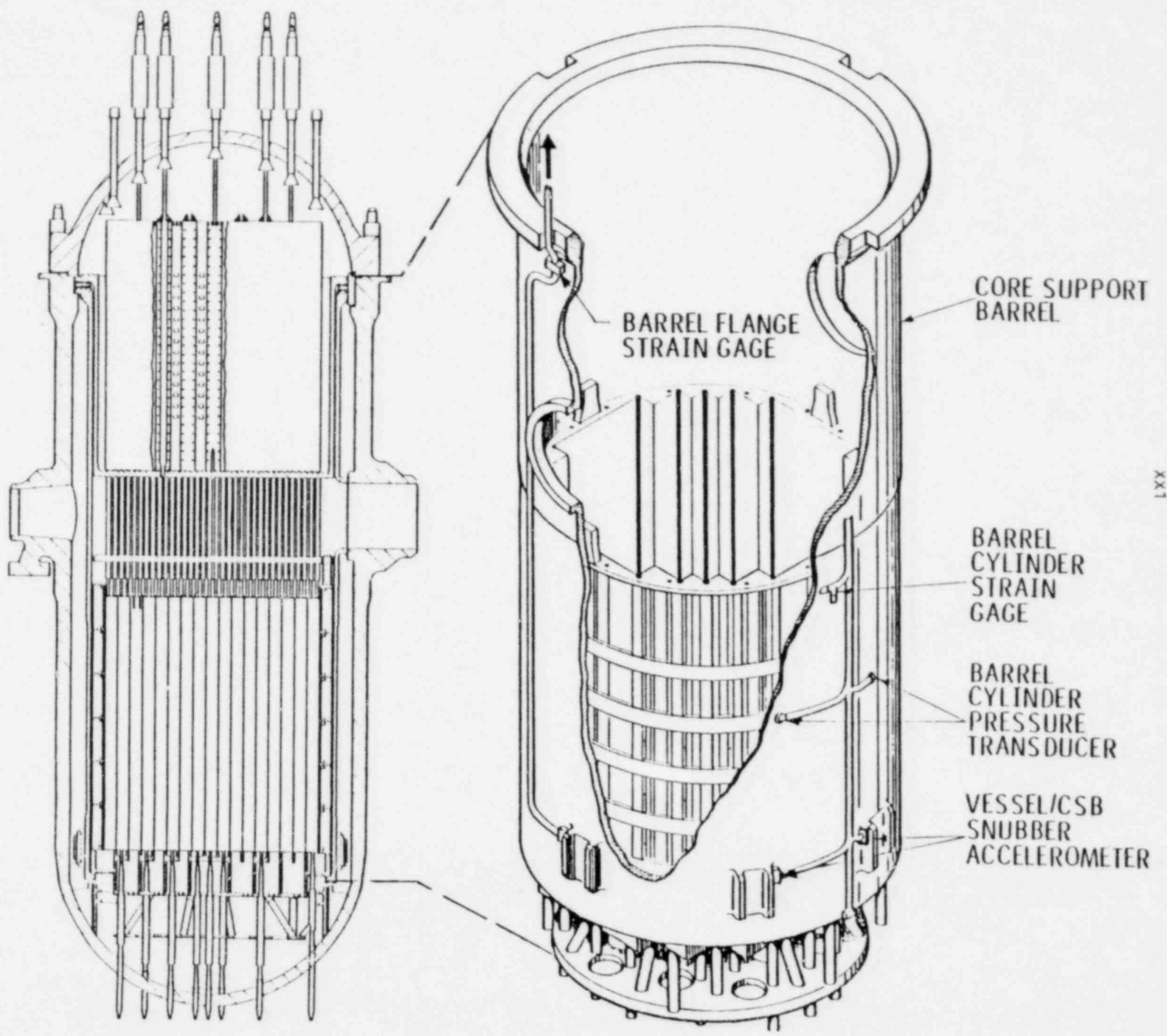
Total Instruments 38

P.T. Pressure Transducer
 S.G. Strain Gage
 E.D.D. Eddy Type Displacement Device
 Accl. Accelerometer (2-D, Two Directions, 3-D, Three Directions)

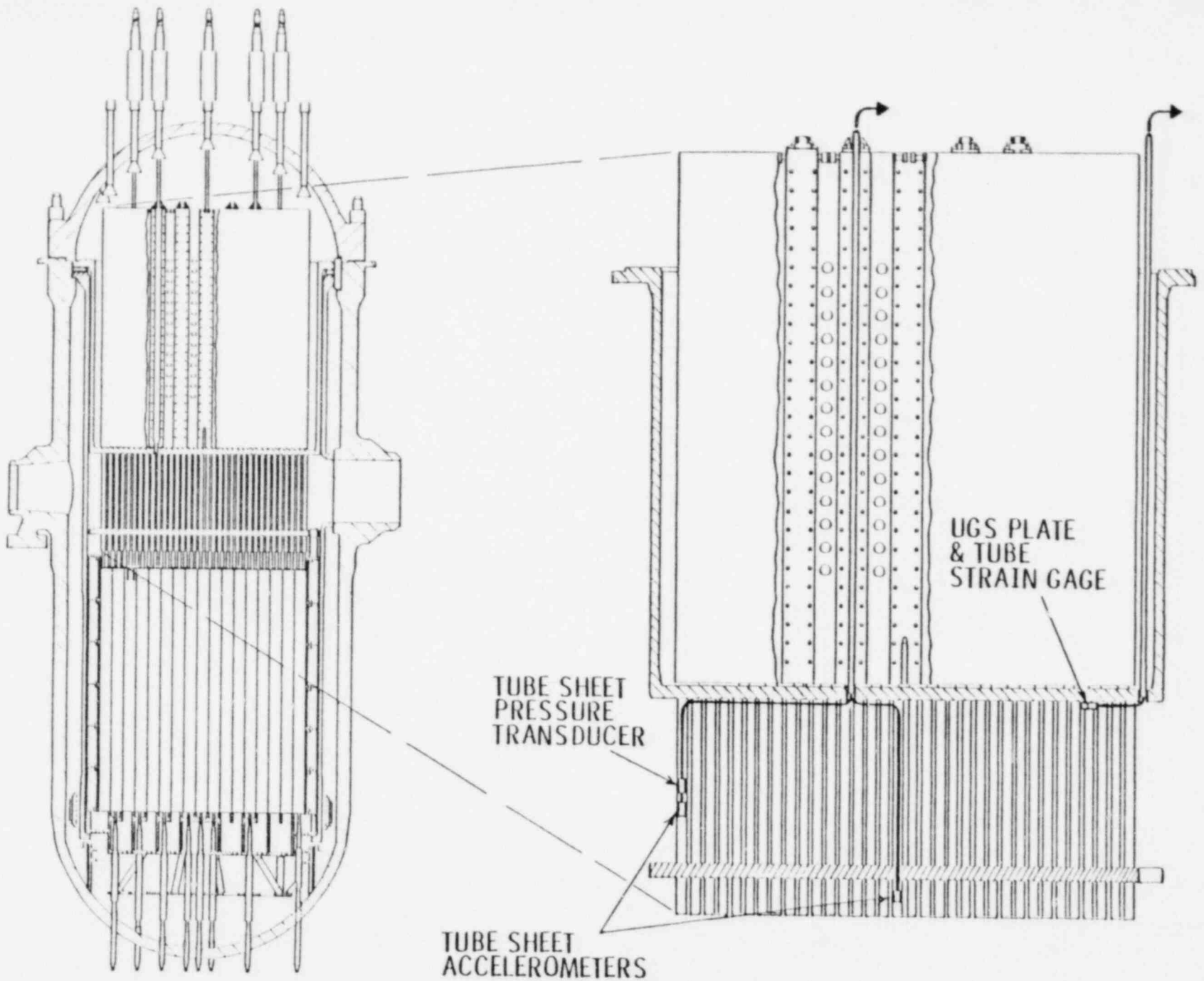


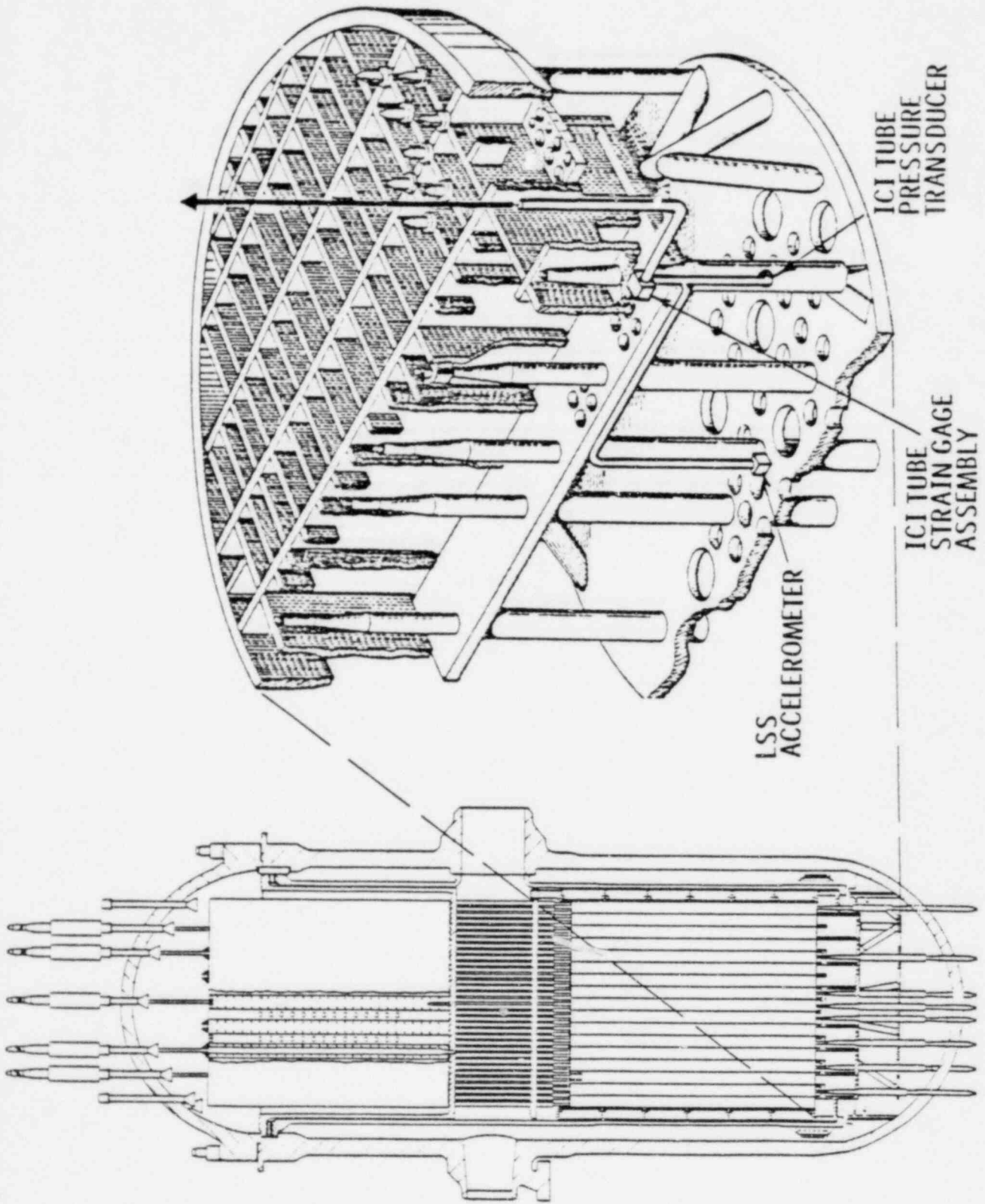
SYSTEM 80 VERTICAL ARRANGEMENT SHOWING ASSEMBLIES
INSTRUMENTED FOR CVAP
FIGURE I

CORE SUPPORT BARREL INSTRUMENTATION
FIGURE II



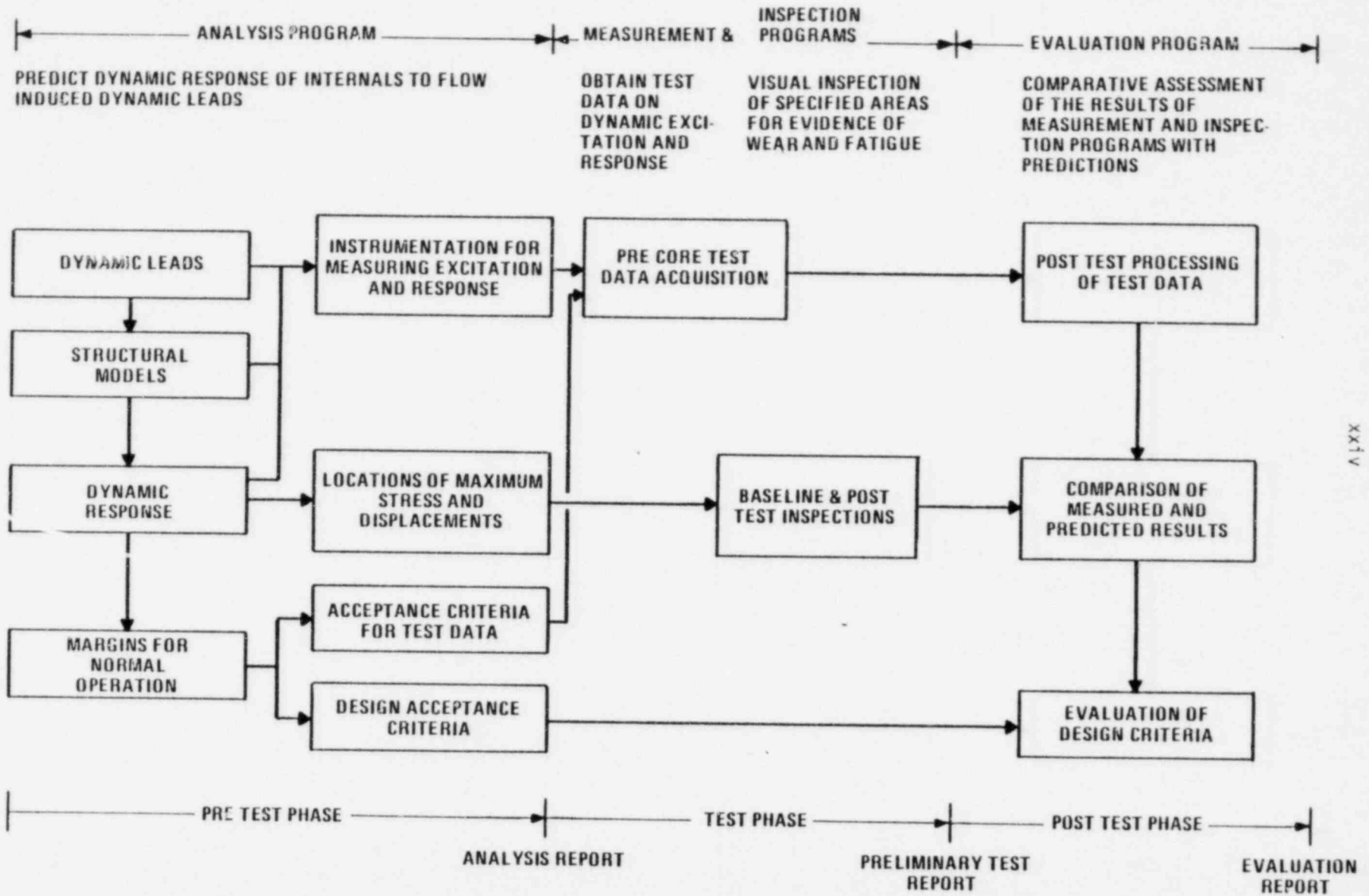
UPPER GUIDE STRUCTURE INSTRUMENTATION
FIGURE III





LOWER SUPPORT STRUCTURE INSTRUMENTATION
FIGURE IV

FIGURE V
COMPREHENSIVE VIBRATION ASSESSMENT PROGRAM



1.0 SYSTEM 80 PROTOTYPE COMPREHENSIVE VIBRATION ASSESSMENT PROGRAM

1.1 Introduction

A comprehensive vibration assessment program (CVAP) has been developed for the Palo Verde Nuclear Generating Station Unit 1, in accordance with NRC Regulatory Guide 1.20, Rev. 2 (Ref. 1). This reactor is classified as the prototype for Combustion Engineering's System 80 NSSS design. Therefore, this program, is intended to satisfy the requirements of a CVAP for a prototype reactor as defined in Ref. 1. Reactor vessel arrangement is shown in Figure 1.1-1.

The purpose of the CVAP is to verify the structural integrity of the reactor internals to flow induced vibrations prior to commercial operation. This program is to be implemented during pre-operational and initial start-up testing of Palo Verde Unit 1.

The comprehensive program includes four separate, yet complementary, programs. These programs include; an analysis program to predict the dynamic excitation and response of the internals from flow induced dynamic loads, a measurement program to obtain experimental data with which to compare these to predictions, a visual inspection of specific areas for evidence of wear and, finally, a comprehensive evaluation of the results of the analysis, measurement, and inspection programs to judge the adequacy of the predictive methodology.

The reactor internals related to safety are designed to accommodate both static and dynamic design loads. These design loads include both static and dynamic flow induced loads related to normal operating and anticipated transients and mechanical excitation due to the operating base earthquake (OBE). Stresses due to these loads must, at design conditions, satisfy limits based on preventing overstressed conditions due to static loads and fatigue damage due

to dynamic loads. A design margin of safety for static loads is defined on the basis of the ratio of maximum allowable stresses, as defined in the ASME Code, to predicted stresses being greater than one. For dynamic loads, margin is defined in terms of a usage, or cumulative damage, factor which must be less than one. A summary of these design calculations for System 80 are given in Ref. 2.

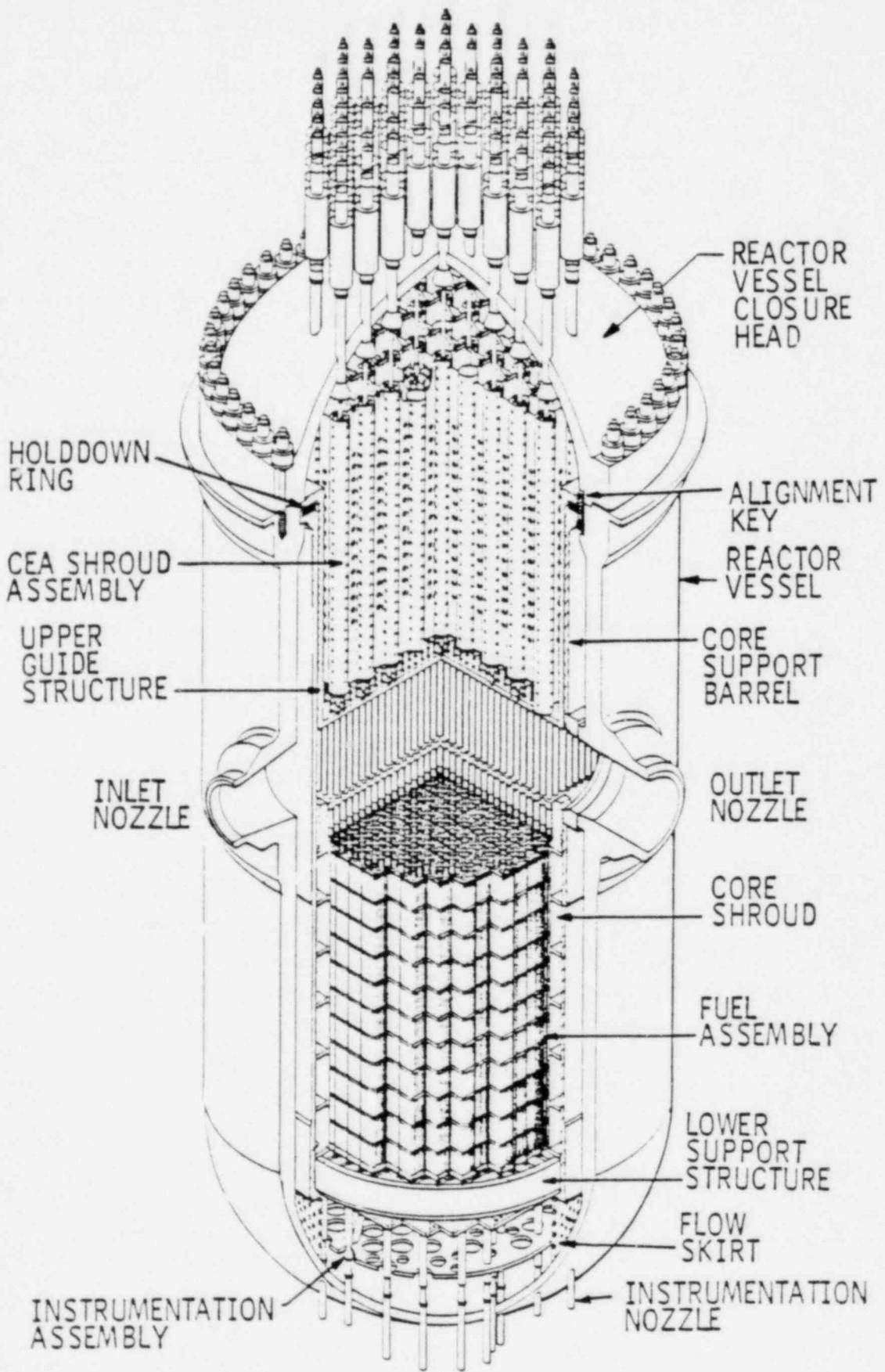
Intent of the CVAP is to show that the internals will not suffer damage due to fatigue caused by flow induced excitation. Thus, the measured response e.g., stress should be below the design values and in agreement with the predictions.

The objective of the CVAP is to compare the measured hydraulic excitation and dynamic response with the predicted values. These predictions are based on expected, or best estimate flow rates. The best estimate flow with the core is less than without the core, and flow induced loads are higher for pre-core conditions than post-core. Thus flow induced loads for the CVAP are conservative with regards to the loads the internals are subjected to under best estimate conditions for long term normal operation.

Since CVAP testing is required for a minimum of 10^6 cycles of structural vibration a criteria for fatigue damage can be defined on the basis of the endurance limit for the material. This limit is the value of stress for the material at 10^6 cycles. If for a specific class of transients the peak stress (stress concentration factor times maximum alternating stress) is less than the endurance limit, the structure can undergo an infinite number of cycles. The usage factor, defined as,

$$\text{Usage Factor} = \frac{\text{Cycles for Specific Transient}}{\text{Maximum Number of Cycles}}$$

is then zero. Hence a margin of safety for flow induced loads, for the CVAP, can be defined on the basis of the ratio of the endurance limit divided by the peak alternating stress.



REACTOR VESSEL ARRANGEMENT

FIGURE 1.1-1

1.2

CVAP Program

The CVAP consists of four separate programs (a) analysis program, (b) measurement program, (c) inspection program, (d) evaluation program.

This report documents results of the analysis program and describes the measurement and inspection programs.

These programs include:

(a) Analysis Program

Analytical and empirical methods are used to predict the steady state and transient flow induced loads or forcing functions. Dynamic response of the reactor internals components are then analytically determined for those forcing functions which correspond to pre-operational and initial start-up, test, and normal operating conditions. A description of the internals is given in Section 2.0. The methods employed in these analyses are described in Section 3.0.

This program includes theoretical predictions of the forcing functions and associated structural responses, definition of test acceptance criteria, and the basis for the establishment of the criteria. Results of this program are summarized in Sections 4.0 through 5.0.

(b) Measurement Program

This program includes an experimental program incorporating accelerometers, pressure transducers, and strain gages, which will permit the recording of time dependent accelerations, pressures, and strains at specific locations. The type, number, and position of the instruments are based upon the results of the analysis program. These measurements will be made during pre-core,

pre-critical, testing. General locations of the measurement program instrumentation are shown in Figure 1.2-1. Details of this program are presented in Section 6.0.

Data are recorded on magnetic tape, on a time history basis, for subsequent reduction using methods of random data analysis. In addition on-line evaluation of the data is done at each test condition. This evaluation includes an assessment of the spectral content of the signals and a comparison of the RMS values of the structural response with the acceptance criterion, discussed in Section 7.0.

(c) Inspection Program

A visual inspection program, including photographic documentation, is to be implemented at both the start and conclusion of the vibration measurement program. Specific locations will be inspected for evidence of contact and wear and for effects of vibration. These locations include contact and potential contact surfaces between all major load bearing reactor internal components, highly stressed locations identified in the analysis program, lateral, vertical, and torsional restraints, locking and bolting components, specific welds, and CVAP instrumentation housings, mountings, and conduits.

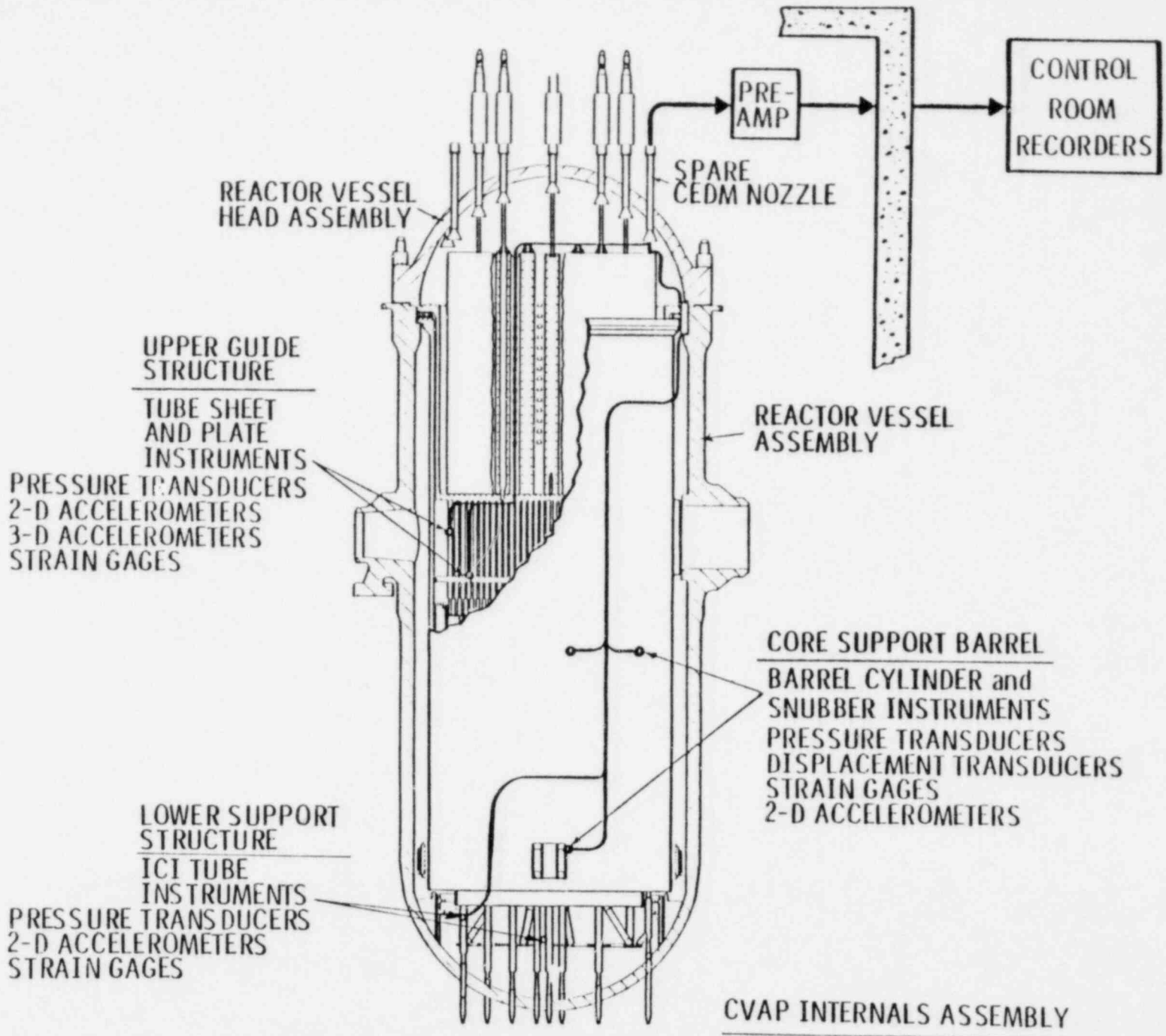
Testing will be of sufficient duration to assure satisfaction of the requirement that critical components be subjected to a minimum of 10^6 cycles of vibration before post test inspection. Description of the inspection program is given in Section 8.0.

(d) Evaluation Program

A report will be issued following completion of pre-critical testing to document and evaluate results of the measurement and inspection programs. This report will include a comparison between the measured and analytically

INTERNALS ASSEMBLIES WITH CVAP INSTRUMENTATION

FIGURE 1.2-1



determined responses and excitations to demonstrate the validity of the analytical techniques. An evaluation of the CVAP results with respect to design and test acceptance criteria will also be made to verify the margin of safety associated with normal steady-state and anticipated transient operation over the service life of the reactor.

1.3 Test Conditions

Reference 1 states that CVAP testing be done under conditions of normal operation (e.g. steady state, four pump operation) and anticipated transients (e.g. pump start-up and shutdown).

Part loop operation at temperatures less than hot standby (564°F) is not considered to be normal operation. However, flow related loads are proportional to both flow velocities and temperature e.g. turbulence levels are related to kinetic head ($1/2 \rho v^2$) while pump related periodic pressure pulsations are acoustic in nature and are related to the speed of sound in the coolant. Thus dynamic loads and the resulting dynamic response may change at conditions of flow and temperature different from normal operation. Conditions of both flow and temperature must be varied to verify the relationships for the flow induced excitations used in the analysis.

Consequently, test conditions, in addition to those at normal operation, have been specified that correspond to points in the pre-core hot functional test procedure (Ref. 41) at which information on system operation is to be recorded. Test conditions at which data will be recorded and for which flow induced loads and forced response have been predicted are listed in Table 1.3-1.

1.4 Pre-Core and Post-Core Testing

CVAP testing can be done without the core if it can be shown that this condition results in higher response as compared to the post-core conditions. Dynamic response, due to flow induced loads, is a function of the magnitude, frequency and distribution of the load

TABLE 1.3-1

SUMMARY OF TEST CONDITIONS

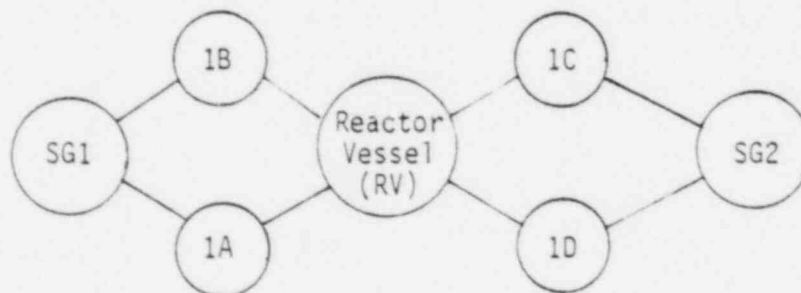
<u>Test Condition</u>	<u>Temperature</u>	<u>SG1</u>		<u>SG2</u>		<u>Test</u>
		<u>RCP 1A</u>	<u>RCP 1B</u>	<u>RCP 1C</u>	<u>RCP 1D</u>	
Pump Startup	<200°F	NO	NO	S	NO	Transient
Pump Startup	200°F	S	NO	O	NO	Transient
Pump Startup	200°F	O	NO	O	S	Transient
Pump Shutdown	260°F	O	NO	Sp	O	Transient
Hot Shutdown	260°F	O	NO	NO	O	Steady State
Hot Shutdown	260°F	O	NO	O	O	Steady State
Part-Loop	500°F	O	NO	NO	O	Steady State
Part-Loop	500°F	O	O	NO	O	Steady State
Pump Startup	500°F	O	O	S	O	Transient
Max Flow	500°F	O	O	O	O	Steady State
Hot Standby	564°F	O	O	O	O	Steady State
Pump Shutdown	564°F	O	O	Sp	O	Transient
Part-Loop	564°F	O	O	NO	O	Steady State
Part-Loop	564°F	O	NO	NO	O	Steady State
Part-Loop	564°F	NO	NO	O	O	Steady State

NO - Not Operating

O - Operating

S - Start

Sp - Stop



and the response characteristics, e.g., modal frequency and mode shapes of the structure. A condition that results in a larger magnitude for the flow related load and a frequency of the load close to a modal frequency of the structure will, in general, produce a larger response. In this section, the effects of the core on the vibration characteristics of the components and the hydraulic loading are discussed to determine the more conservative test condition.

The presence of the core has two main effects; (a) change in the coolant velocity in the various regions of the reactor, mainly due to the increased hydraulic resistance, (b) changes in the natural frequencies of some structures due to the additional mass of the core.

The effects of these changes on the loading and response of each component are discussed as follows.

1.4.1 Core Support Barrel

1.4.1.1 Hydraulic Loads

Due to the larger pre-core system flow, the velocities in the downcomer annulus are higher (Table 1.4-2). Random pressure fluctuations due to turbulence are proportional to the kinetic head. Kinetic head being higher for pre-core than post-core conditions, the random excitation is higher for the pre-core conditions.

Since the pump induced pressure pulsations are acoustic in nature, they are independent of the coolant flow and are a function of temperature only. The pre- and post-core conditions are equivalent in this case.

1.4.1.2 Natural Frequencies

Beam and shell mode frequencies of the core barrel with and without the core are given in Table 1.4-1. The presence of the core is accounted for by considering it as a lumped mass located at the bottom of the CSB. This additional mass has the effect of reducing the beam mode ($m=1, n=1$) frequency as shown in Table 1.4-1. For the shell modes ($m \geq 2$), however, the situation is complicated because of hydrodynamic mass effects. Because of the absence of the core in the pre-core conditions, the hydrodynamic mass is larger than for the post-core conditions. This is the reason why certain shell mode frequencies are lower for the pre-core conditions (see Table 1.4-1.)

Turbulence related pressures are broad band in nature, though there are indications (Ref. 33) that the energy is concentrated within a frequency band related to the downcomer velocity. Even so, the core barrel fundamental frequency falls within this frequency band both with and without core (Table 1.4-1). Therefore, the lowering of the fundamental frequency has little effect on the random response.

The periodic pressure pulsations occur at multiples of the pump rotor (20 Hz) and blade passing frequencies (120 Hz). These frequencies are above the beam mode frequency of the core barrel, with or without core. However, the beam mode frequency is higher at pre-core conditions thus closer to the 20Hz rotor frequency. The more easily excited lower shell mode frequencies are, in addition, closer to the excitation frequencies for the pre-core conditions.

1.4.2 Lower Support Structure

1.4.2.1 Hydraulic Loads

The hydraulic loads considered here are pump induced periodic pulsations, vortex shedding, and random pressures due to turbulence.

As stated earlier, pump induced pressure loads are not affected by the core.

The vortex shedding periodic loads on the ICI tubes are a function of crossflow velocity and velocity head. Therefore, the vortex shedding loads are a function of system primary flow and velocity distribution in the lower plenum. The increased primary system flow (Table 1.4-3) during pre-core operating conditions would tend to maximize the vortex shedding loads. The lower plenum velocity distribution, discussed below, would also tend to maximize the ICI tube crossflow velocity at pre-core operating conditions. Therefore the ICI tube vortex shedding periodic loads would be at a maximum at pre-core operating conditions.

The random loads on the ICI tubes are due to turbulent buffeting caused by jets formed by the coolant passing through the flow skirt flow holes. These random loads are thus a function of the crossflow velocity in the lower plenum.

The absence of the reactor core does have an effect on the lower plenum flow distribution. Flow model tests (Ref. 14) indicate removal of the core results in higher flow into the central region of the lower plenum. This results in higher crossflow velocity past the ICI tubes during the pre-core operating conditions.

The increased flow and higher flow skirt jet velocities at pre-core conditions results in larger hydraulic loading on the ICI tubes than at post-core conditions.

1.4.2.2 Natural Frequencies

The presence of core has minimal effect on the natural frequencies associated with the ICI tubes and their support structure. Thus its frequency response characteristics should be identical for both pre- and post-core conditions.

1.4.3 Upper Guide Structure Assembly

1.4.3.1 Hydraulic Loads

Pump induced periodic pressure pulsations and turbulence related random pressures are considered here.

The periodic loads are not significantly altered due to the change in the flow velocities because of the removal of the core. However, the pump induced periodic loads are attenuated as they pass through the core region and thus should be higher without than with the core.

The random loads on the CEA shroud tubes are caused by turbulent buffeting related to crossflow velocity. Test data from flow tests on a 1/4 scale model of the CEA shroud tube region indicates that dynamic response is a function of the crossflow velocity and the velocity head. The factors which affect these parameters are the primary system flow rate and the upper plenum flow distribution. The flow distribution approaching the fuel alignment plate is essentially identical for pre-core and post-core operating conditions. Therefore, at pre-critical conditions, the pre-core operating conditions are more severe due to the larger primary system flow rate.

As shown in Table 1.4-4, at post-core full power conditions velocities in the CEA shroud tube region are higher than those achieved at pre-core conditions. This is because the increase in coolant specific volume that results from the coolant temperature rise through the core is greater than the decrease in primary system mass flow rate between pre-core and post-core conditions.

Differences in the coolant velocity could have an effect on flow induced response of the shroud tubes. A group of cylindrical tubes, subject to crossflow, can experience large amplitude motions at a velocity above some threshold value. The fluid-elastic mechanism by which this occurs is distinct from periodic vortex shedding (Ref. 30). This threshold, or critical velocity is a function

of tube frequency, damping, fluid density, and tube mass, diameter and spacing. Extensive tests have been done at C-E on both a reduced number of full size tubes (Ref. 22) and a 1/4 scale model of the CEA shroud tube region (Ref. 31). These latter tests indicate this threshold velocity to be 80 ft/sec. This results in a calculated margin of [] between the threshold and the design velocity. This threshold velocity is larger than the crossflow velocity at either the pre- or post-core conditions (Table 1.4-4). Pre-core velocities being higher than post-core values, pre-core conditions are conservative with respect to being closer to the threshold velocity for fluid-elastic motion.

1.4.3.2 Natural Frequencies

The presence of the core results in a compressive load on the CEA shroud tubes. This compressive load being substantially less the buckling load, the effect on the frequency is minimal. Hence the natural frequencies are virtually equal for both pre- and post-core conditions.

1.4.4 Summary

Based on this evaluation it is concluded that:

1. Pre-core flow rate being higher than post-core, the random loads, which are proportional to kinetic head, are larger at pre-core conditions, while the frequency bands for the random loads are unchanged.
2. While the core may reduce the magnitude of the pump induced periodic loads (e.g. on the CEA tubes) their frequencies are unchanged by the presence of the core.
3. Periodic forces related to fluid velocity (e.g. vortex shedding) are higher in magnitude and closer to a modal frequency of the ICI tubes for pre-core conditions.
4. CEA shroud tube frequencies are unchanged by the core. Thus the higher pre-core flow results in cross flow velocities closer to the threshold value for fluid elastic motion.

5. Except for the core barrel, the modal frequencies of the structures are unaffected by the core. For the core barrel, modal frequencies are higher without the core and closer to those of the pump rotor and blade passing frequencies.

Thus pre-core conditions will result in higher response than post-core conditions.

TABLE 1.4-1
IN WATER (564°F)
FREQUENCIES OF CSB WITHOUT AND WITH CORE

N	M	Pre-Core	Post-Core
1	1	[]
	2		
	3		
	4		
2	1		
	2		
	3		
	4		
3	1		
	2		
	3		
	4		

N = Axial Mode Number
M = Circumferential Mode Number

TABLE 1.4-2
PRE- AND POST-CORE FLOW PARAMETERS RELATED TO CSB RESPONSE

Condition	Pumps	Temperature	V	$\rho V^2/2$	$f_t^{(1)}$
Pre-Core	4	564	[]	[]	[]
Post-Core	4	564	[]	[]	[]
Post-Core (100% Power)	4	564	[]	[]	[]
		°F	ft/sec	psi	Hz

(1) Characteristic frequency for turbulence, assuming a coherence length equal to the RV to CSB clearance (Ref. 33), is approximated as $f_t \sim V/CLR$.

V = Axial Velocity in CSB/RV Annulus

ρ = Fluid Density

CLR = Radial Clearance RV/CSB

TABLE 1.4-3
PRE- AND POST-CORE FLOW PARAMETERS RELATED TO ICI RESPONSE

Condition	Pumps	Temperature	V	$\rho V^2/2$	$f_{vs}^{(1)}$
Pre-Core	4	564	[]	[]	[]
Post-Core	4	564	[]	[]	[]
Post-Core (100% Power)	4	564	[]	[]	[]
		°F	ft/sec	psi	Hz

(1) Range of Vortex Shedding Frequencies $f_{vs} = St (V/D)$,
 $.20 \leq St \leq .45$ (Ref. 21).

V = Crossflow Velocity

ρ = Fluid Density

St = Strouhal Number

f_1 = First Mode Frequency [].

TABLE 1.4-4

PRE- AND POST-CORE FLOW PARAMETERS RELEASED TO CEA TUBE RESPONSE

Conditions	Pumps	Temperature	V	$\rho V^2/2$	$f_t^{(1)}$	$V_c^{(2)}$
Pre-Core	4	564	[]	[]	[]	[]
Post-Core	4	564	[]	[]	[]	[]
Post-Core (100% Power)	4	618	[]	[]	[]	[]
		°F	ft/sec	psi	Hz	ft/sec

(1) Dominant Frequency for Turbulent Buffetting

$$f_t = .20 V/D \text{ (Ref. 31)}$$

(2) Based on Critical Value of .4 for the Reduced Velocity ($f_n D/V_c$)

(Ref. 31)

V = Intertube Crossflow Density

D = Tube Diameter

ρ = Fluid Density

f_1 = First Mode Frequency []

1.5 Stress Margins

General design methodology requires calculation of structural response e.g. stresses, to both static and dynamic loads. The design stress values, expressed as stress intensities, are then compared to material stress limits tabulated in the ASME Code (Ref. 5). These design stresses must be less than the limits specified to demonstrate that the design is adequate for its design life.

Structures are designed to prevent total component failure as well as localized fatigue failure. To assure the former, the ASME Code requires that the values of primary membrane (P_m), bending (P_b) and secondary (Q) (e.g. thermal) stress intensities must meet the following criteria at the design condition:

Primary Membrane; $P_m \leq S_m$

Primary Membrane + Bending; $P_m + P_b \leq 1.5 S_m$

Primary Membrane + Bending + Secondary; $P_m + P_b + Q \leq 3 S_m$

where S_m is the design stress intensity for the particular material (Figure 1.5-1A).

The ratio of ASME Code allowable stress divided by the design stress intensity can be defined as the design margin. This margin must be greater than or equal to one for all three of the above conditions.

Dynamic loading conditions, result in cyclical stresses, for which the ASME Code requires a fatigue analysis. A comparison is made of the value of peak alternating stress with limits dictated by an allowable alternating stress versus maximum number of cycles (S-N curve) for the material (Figure 1.5-1B). The ratio of actual cycles for the event producing these loads to the maximum number of cycles defines the usage factor. The cumulative damage, or sum of usage factors for all dynamic events, must, by the Code be less than one.

The reactor internals are designed to meet both the total component and fatigue limits; the ratios of maximum allowable to calculated design stresses are greater than one and the sum of the usage factors are less than one.

1.5.1 Design Conditions

The System 80 core support structures are designed to meet ASME Code criteria for both normal operation and faulted conditions (Ref. 2).

For normal operation the loads are based on a summation of conservative values for the mechanical, thermal, and hydraulic loads, determined at 4 pump, 100% power conditions plus the Operational Base Earthquake (OBE).

These design loads are calculated at the steady state conditions of;

Design Pressure	2,500 psi
Design Temperature	650°F
Design Flow	516,900 GPM (116% of best estimate flow)

and for the following transient events;

<u>Event</u>	<u>Lifetime Cycles</u>
Plan Heatup - 100°F/hr.	500
Plant Cooldown - 100°F/hr.	500
Plant Loading - 5%/min.	15,000
Plant Unloading - 5%/min.	15,000
Normal Plant Variations	
10% Step Load Increase	} 10 ⁶
10% Step Load Decrease	
Pressure, Temperature Variations	
Reactor Trip	400
Loss of Reactor Coolant Flow	40
Loss of Load	40
Operational Basis Earthquake (OBE)	200
Flow Induced Dynamic Loading (Periodic and Random)	(40 years) x f_n^*

Results for the design conditions at normal operation are summarized in Tables 1.5-1 and 1.5-2 from Ref. 2.

* f_n is the frequency of component at which the response is a maximum.

1.5.2 CVAP Test Conditions

Distinction must be made between design conditions for normal operation and actual, or expected, normal operating conditions. Design conditions for normal operation include conservative assumptions regarding both static and dynamic thermal and hydraulic loads in addition to including OBE loads. Normal operating conditions as used in this report, refer to the best estimate conditions of flow and inlet temperature corresponding to four pumps operating at 100% power.

CVAP test conditions are representative of the normal operating conditions of flow and temperature the internals will be subjected to over the design life of the reactor. These best estimate conditions will result in both static and dynamic loads significantly lower than the design values. Main emphasis of the CVAP is to predict and verify that the core support structures will not be subject to fatigue damage caused by flow induced dynamic loads over their design life. Thus any valid comparison between predictions and test can only be made on the basis of best estimate values of flow.

Regulatory Guide 1.20 requires that the internals be subjected to a minimum of 10^6 cycles of flow induced loading. The value of 10^6 is based on the definition of endurance limit as the value of alternating stress at 10^6 cycles on the S-N curves for a material (Ref. 5). If the alternating stress is below this limit, fatigue damage will be zero for the structure.

Hence in addition to the commonly used measures of fatigue, usage factor and cumulative damage, a margin based on the endurance limit can be defined as,

$$\text{Fatigue Margin} = \frac{\text{Endurance Limit}}{\text{Peak Alternating Stress}}$$

A summary of the fatigue margins for the design values of flow induced excitation are given in Table 1.5-3.

This margin for CVAP conditions will be evaluated in section 5.4 of this report.

TABLE 1.5-1
DESIGN STRESSES; CSB ASSEMBLY

ASME Allowable Stress (psi)	Design Stresses (psi) (Fig. 1.5-2)		
	Upper Flange	Lower Flange	LSS Assembly
Pm 16,100	[]
Pm + Pb 24,150			
Pm + Pb + Q 48,300			
Fatigue (Usage Factor) <1.0			

Pm = Primary Membrane

Pb = Primary Bending

Q = Secondary

TABLE 1.5-2

DESIGN STRESSES; UGS ASSEMBLY

ASME Allowable Stress (psi)	Design Stresses (psi) (Fig. 1.5-3)		
	Upper Flange	Lower Flange	CEA Shroud Tubes
Pm 16,100	[]
Pm + Pb 24,150			
Pm + Pb + Q 48,300			
Fatigue (Usage Factor) <1.0			

Pm = Primary Membrane

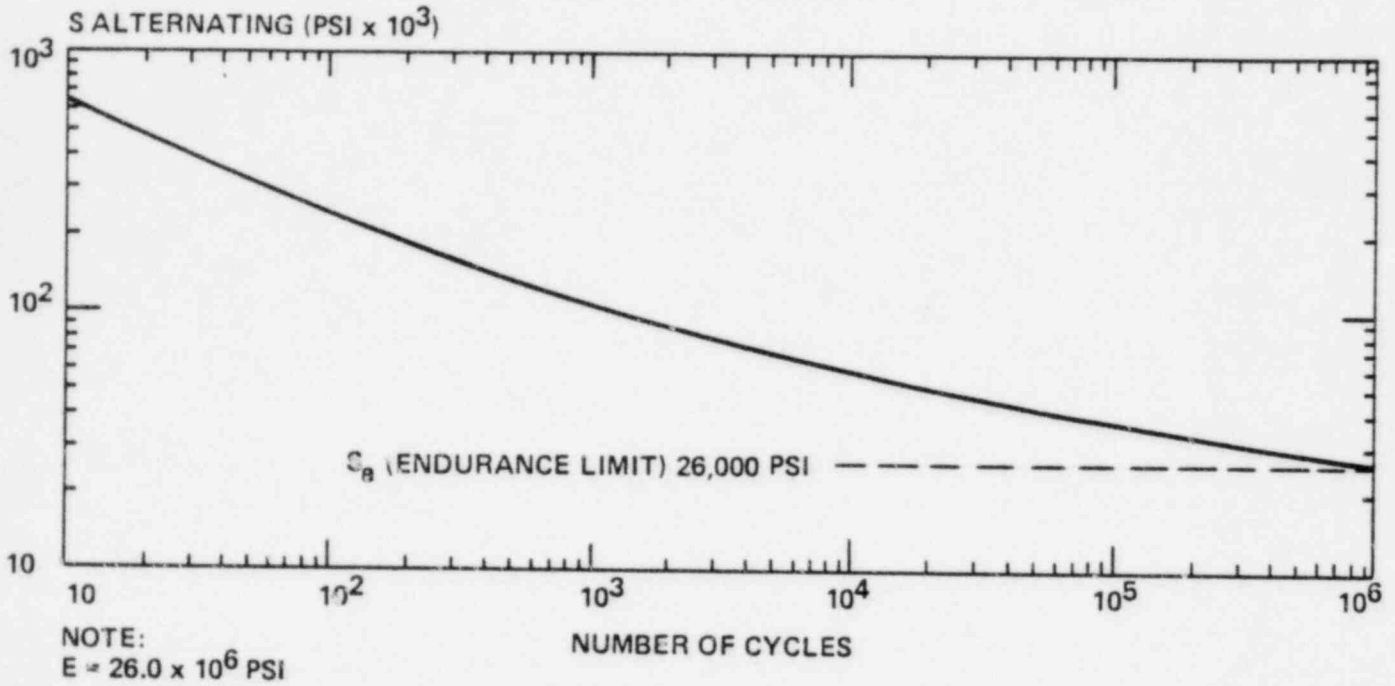
Pb = Primary Bending

Q = Secondary

TABLE 1.5-3

DESIGN MARGIN FOR FATIGUE DAMAGE
DUE TO FLOW INDUCED LOADS AT DESIGN CONDITIONS FOR NORMAL OPERATION

Component	Location	Peak Alternating Stress (psi)	Design Margin
CSB (Fig. 1.5-2)	1	[]
	2		
	3		
LSS (Fig. 1.5-2)	1	[]
	2		
	3		
UGS (Fig. 1.5-3)	1	[]
	2		
	3		



B. DESIGN FATIGUE CURVE FOR AUSTENITIC STEELS, NICKEL-CHROMIUM-IRON ALLOY, NICKEL-IRON-CHROMIUM ALLOY, AND NICKEL-COPPER ALLOY (ASME CODE)

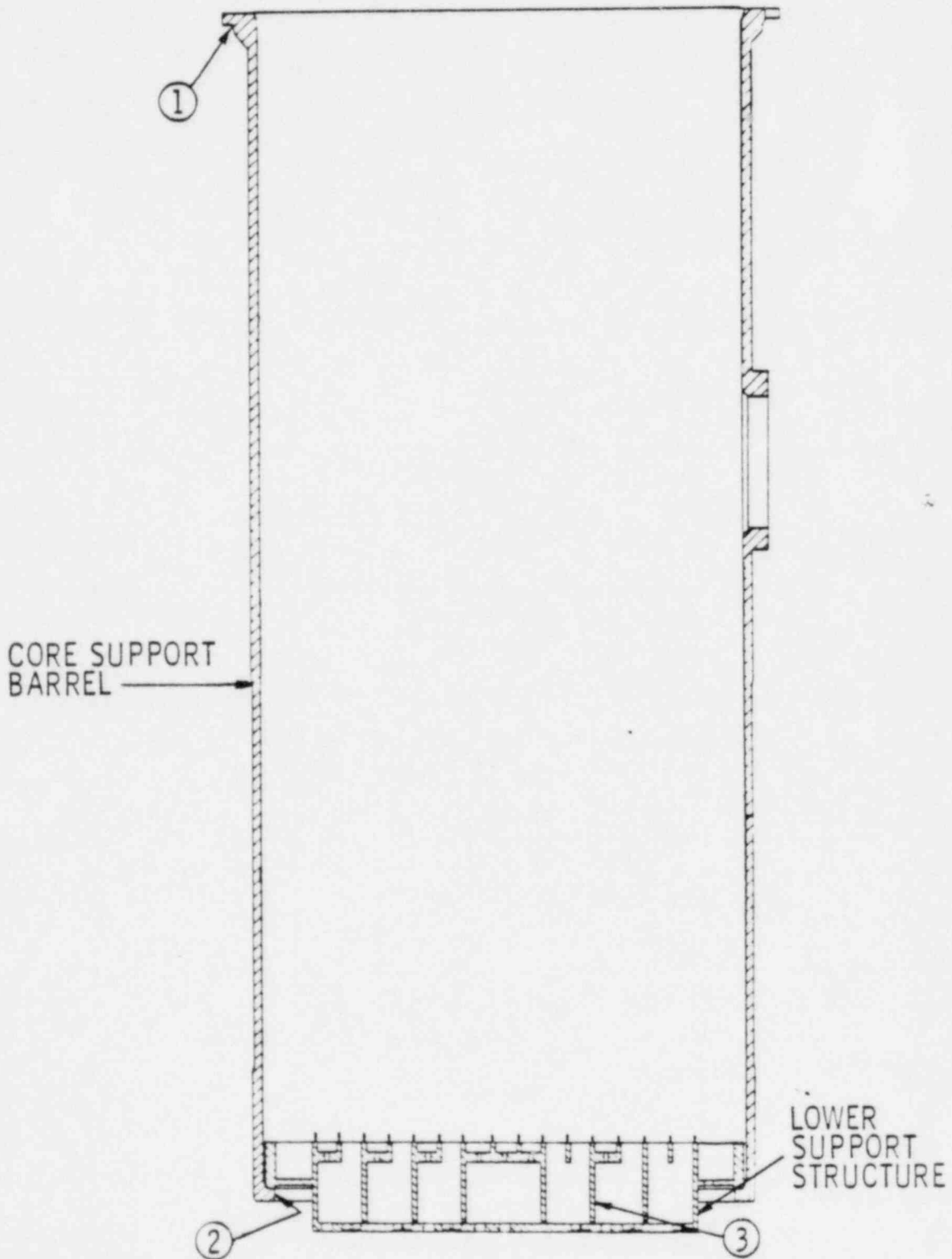
TYPE 304 STAINLESS STEEL AT 650°F;

E (PSI) YOUNG'S MODULUS	25.1 x 10 ⁶
S _m (PSI) MATERIAL ALLOWABLE	16,100
S _y (PSI) YIELD STRENGTH	17,900
S _u (PSI) TENSILE STRENGTH	63,500

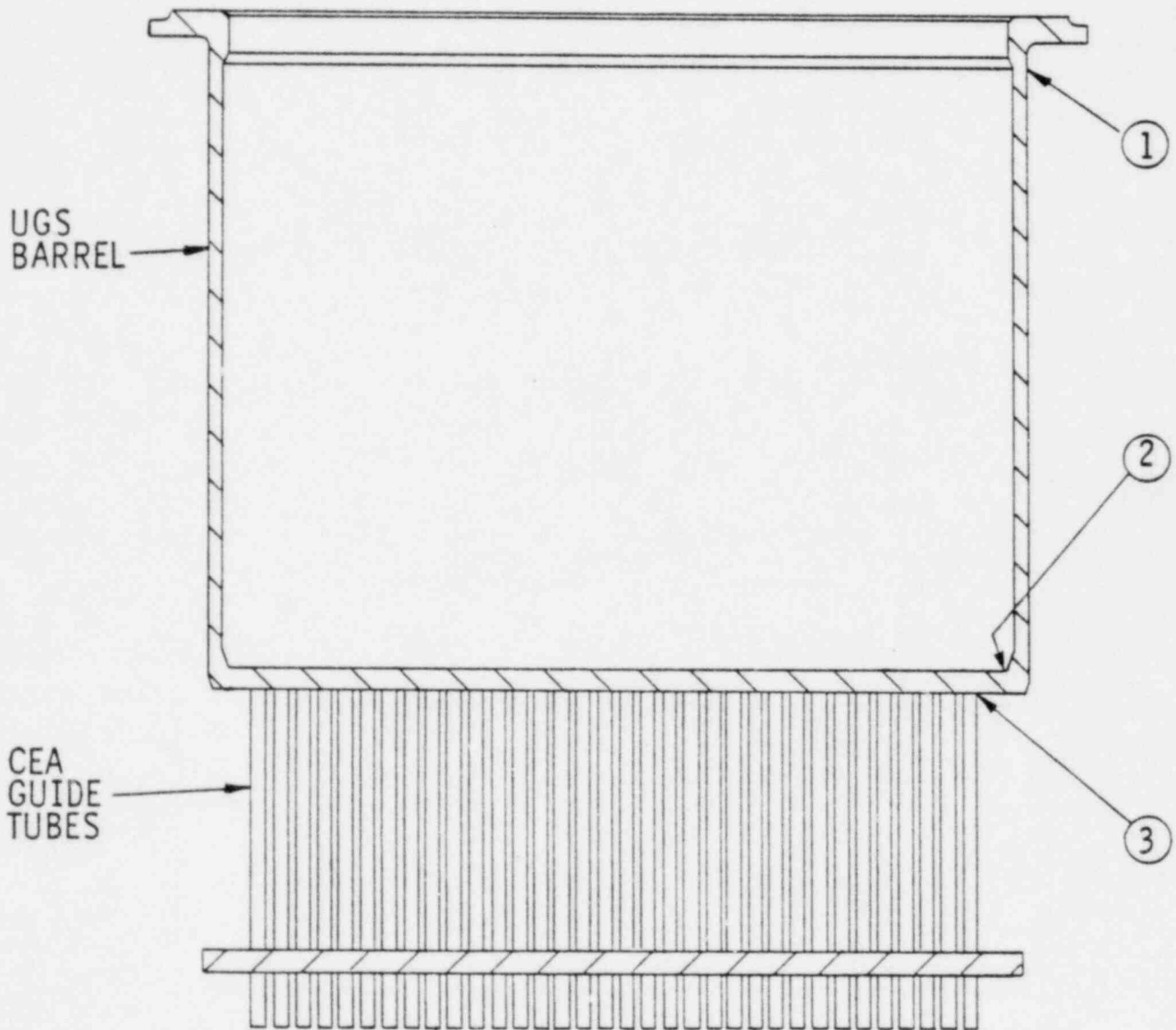
A. ELASTIC PROPERTIES (ASME CODE)

MATERIAL PROPERTIES

FIGURE 1.5-1



MAXIMUM STRESS REGIONS-CSB ASSEMBLY
FIGURE 1.5-2



MAXIMUM STRESS REGIONS-UGS ASSEMBLY

FIGURE 1.5-3

1.6 Test Duration

Reference (1) states that the internals must accumulate a minimum of 10^6 cycles of vibration prior to inspection. Based on a frequency of [] Hz for the core support barrel, the lowest frequency component with a significant response, this requires a minimum of [] hours of flow testing. The pre-core test program has been planned to accumulate, as a minimum, the required number of cycles.

2.0 DESCRIPTION OF THE STRUCTURAL ASSEMBLIES

This section describes briefly the reactor internals of a typical 3800 Mwt System 80 reactor. The structural assemblies that are of interest here are the ones that relate to the safety of the core; the Core Support Barrel Assembly, which includes the core support barrel and lower support structure, and the Upper Guide Structure Assembly (Figure 2.0-1).

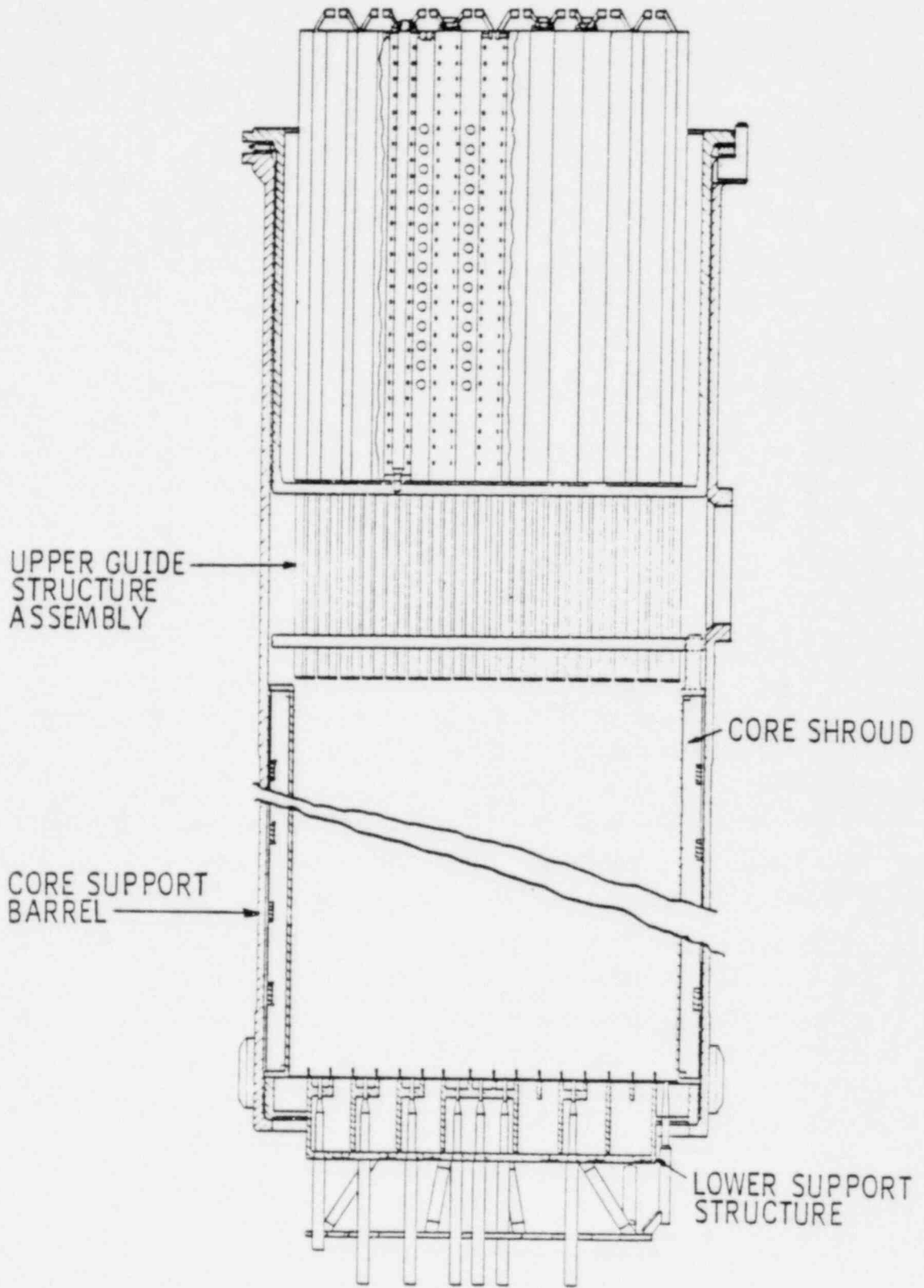
2.1 Core Support Barrel Assembly

The major member of the reactor core support structures for all C-E designs is the core support barrel assembly which includes the core support barrel, and the lower support structure. The material for the assembly is Type 304 stainless steel.

The core support barrel assembly is supported at its upper end by the upper flange of the core support barrel, which rests on a ledge at the top of the reactor vessel. Alignment is accomplished by means of four equally spaced keys in the flange which fit into keyways in the vessel ledge and closure head. The lower flange of the core support barrel support and positions the lower support structure and is attached to the lower support structure by means of a welded flexural type connection. The lower support structure provides support for the core as well as orientation for the lower ends of the fuel assemblies. The core shroud, which provides a flow path for the coolant, is also supported and positioned by the lower support structure. The lower end of the core support barrel is restricted from radial and torsional movement by six snubbers which interface with the reactor vessel wall.

2.1.1 Core Support Barrel

The core support barrel is a right circular cylinder including a heavy ring flange at the top end and an internal ring flange at the lower end. The core support barrel is supported from a ledge on the



REACTOR INTERNALS AS SEMBLY

FIGURE 2.0-1

reactor vessel. The core support barrel, in turn, supports the lower support structure upon which the fuel assemblies rest. Press-fitted into the flange of the core support barrel are four alignment keys located 90 degrees apart. The reactor vessel, closure head, and upper guide structure assembly flange are slotted in locations corresponding to the alignment key location to provide proper alignment between these components in the vessel flange region.

2.1.2 Lower Support Structure

In the System 80 design, the lower support structure is a welded assembly consisting of a short cylinder, support beams, a bottom plate, in core instrumentation (ICI) nozzles, and an ICI nozzle support plate. The short cylinder, which rests on the lower flange of the core support barrel, encloses a number of grid beams arranged in egg-crate fashion. The outer ends of these beams are welded to the cylinder.

Fuel assembly locating pins are attached to the beams. The bottoms of the parallel beams in one direction are welded to plates which contain flow holes to provide proper flow distribution. These plates also provide support for the ICI nozzles and, through support columns, the ICI nozzle support plate. The cylinder guides the main coolant flow and limits the core shroud bypass flow by means of holes located near the base of the cylinder. The ICI nozzle support plate provides lateral support for the nozzles. This plate is provided with flow holes for the requisite flow distribution.

2.2 Upper Guide Structure Assembly

The Upper Guide Structure (UGS) assembly aligns and laterally supports the upper end of the fuel assemblies, maintains the control element spacing, holds down the fuel assemblies during operation, prevents fuel assemblies from being lifted out of position during a severe accident condition and protects the control elements from the effects of coolant cross flow in the upper plenum.

The UGS assembly consists of the UGS support barrel assembly and the CEA shroud assembly. The UGS assembly consists of the UGS support barrel, fuel alignment plate, UGS base plate and control element shroud tubes. The UGS support barrel is a right circular cylinder welded to a ring flange at the upper end and to a circular plate (UGS base plate) at the lower end. The upper side of this flange, which is the supporting member for the entire UGS assembly, seats against the pressure vessel head during operation. The lower side of the flange is supported by the holdown ring, which seats on the core support barrel upper flange. The UGS flange and the holdown ring engage the core support barrel alignment keys by means of four keyways. The fuel alignment plate is positioned below the UGS base plate by cylindrical control element shroud tubes. These tubes are attached to the UGS base plate and the fuel alignment plate by rolling the tubes into the plates and welding. The fuel alignment plate aligns the lower ends of the control element shroud tubes, which in turn locate the upper ends of the fuel assemblies. The fuel alignment plate also has four equally spaced slots on its outer edge which engage with Stellite hardfaced lugs protruding from the core shroud to provide alignment. The control element shroud tubes bears the upward force from the fuel assembly holdown devices. This force is transmitted through the control element shroud tubes to the UGS barrel base plate. The CEA shroud assembly limits cross-flow and provides separation of the CEA assemblies. The assembly consists of an array of large vertical tubes connected by vertical plates in a grid pattern. The shroud assembly is mounted on the UGS base plate and is held in position by eight tie

rod tube assemblies which are threaded into the UGS base plate at their lower end. The tie rods are bolted against plates located at the top of the CEA shroud assembly and are pretensioned. Guides for the CEA extension shafts are provided at the tops of the tubes.

The holddown ring provides axial force on the flanges of the upper guide structure assembly and the core support barrel assembly in order to prevent movement of the structures under hydraulic forces. The holddown ring is designed to accommodate the differential thermal expansion between the pressure vessel and the internals in the vessel ledge region.

3.0 STRUCTURAL RESPONSE OF THE CORE SUPPORT ASSEMBLIES TO DETERMINISTIC AND RANDOM HYDRAULIC LOADS

The methodology used to calculate the dynamic response of the core support structures to flow induced loads is divided into three parts; calculation of the hydraulic loads, or forcing functions, analysis of the structures to determine their modal characteristics, e.g. frequencies and mode shapes, and finally, calculation of the response e.g. displacement, strain, and stress.

3.1 General Methodology

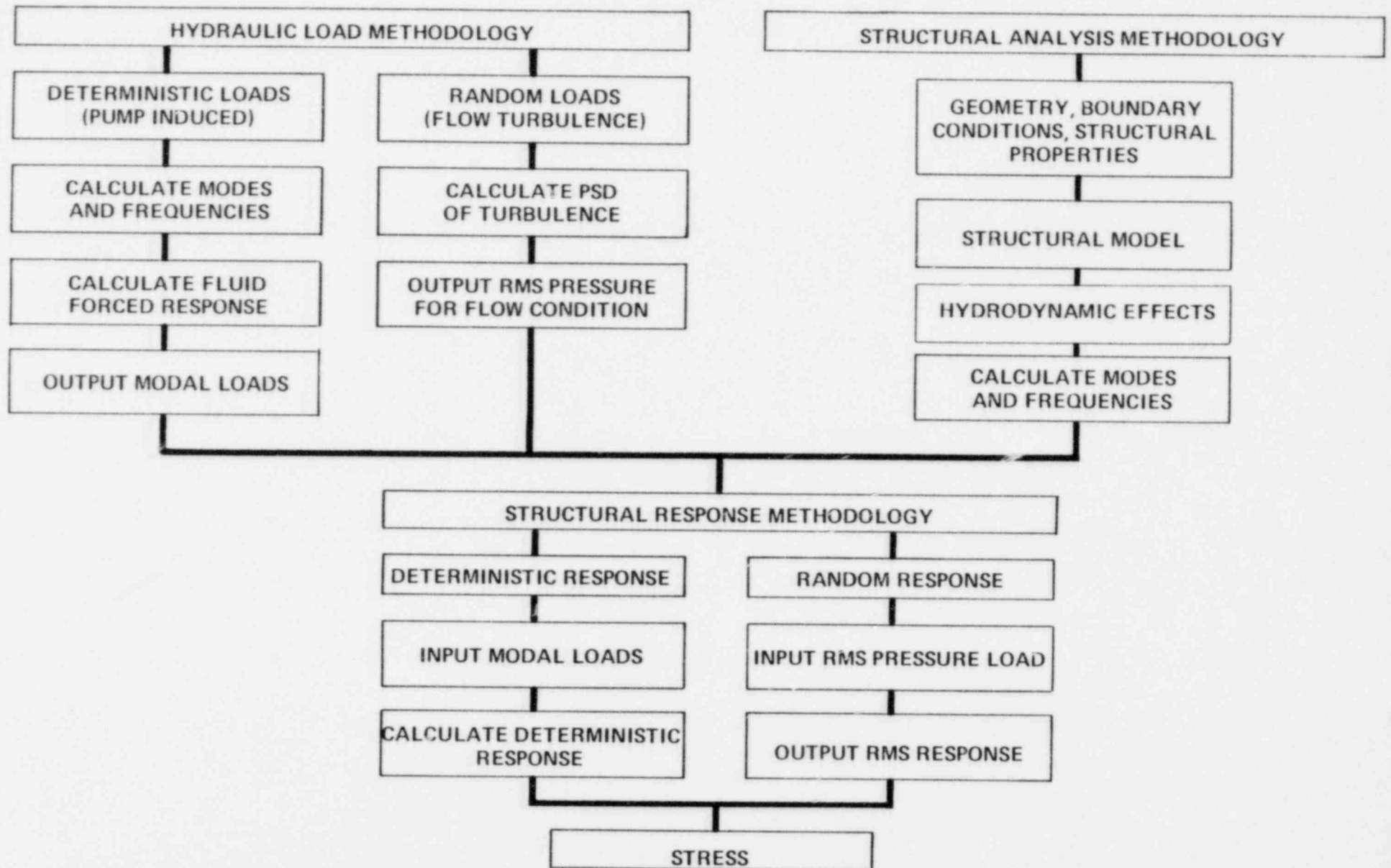
Dynamic response of the core support structure assemblies is a function of the magnitude, frequency, and spatial distribution of the flow induced loads and the modal frequencies and mode shapes of the assemblies. The procedures used to compute this response are shown in Figure 3.1-1.

The flow induced dynamic loads are classified as either deterministic or random according to their variation with time. The deterministic and random components are assumed to be uncorrelated; caused by independent sources. The hydraulic loads can thus be calculated separately for the deterministic and random sources of excitation. The methodologies used to compute these loads are shown in the left side of Figure 3.1-1.

The fluid and each assembly are dynamically coupled, the dynamic response of the structure influencing the fluid pressure distribution on the structure. This coupling results in an additional inertial force on the structure. This added force appears analytically as a mass, proportional to fluid density, added to the mass of the structure, and the sum multiplied times the acceleration of the structure. With the use of this "hydrodynamic mass" the calculation of the hydraulic load can be uncoupled from calculation of the response. The modal characteristics of the structure in the fluid can then be found by including this

FIGURE 3.1-1

SUMMARY OF ANALYTICAL METHODOLOGY



hydrodynamic or added mass and solving the set of equations that describe the free vibration force balance on the structure. The structural analysis methodology for solving for these modal characteristics is shown in the right side of Figure 3.1-1.

The response of a structure to a dynamic hydraulic load is a function of both the type of load (deterministic or random), its magnitude, frequency and spatial distribution and the modal characteristics of the structure. This response is the sum of the separate responses due to deterministic and random loads, and is calculated by the procedure shown in the lower portion of Figure 3.1-1.

3.1.1 Methods for Calculating Hydraulic Loads

A complete description of either the deterministic or random loads includes information on their magnitudes, frequencies, and spatial distributions.

Two types of deterministic loads are considered in the analysis. The first caused by pump induced variations in the coolant pressure and the second, vortex shedding, related to local cross flow velocities.

Pump pulsation loads are due to harmonic variations in fluid pressure caused by the reactor circulating pumps. These pulsations propagate throughout the system as acoustic waves, independent of fluid velocity. These pulsations occur at multiples of the pump rotor (20 Hz) and blade passing (120 Hz) frequencies. The magnitude and spatial distribution of these pressures are dependent on variations in the amplitude of the pump discharge pressure, phase difference between pumps, the number of pumps operating and in which of the four loops, geometry of the flow paths and the temperature dependent speed of sound in the liquid. A combination of

mathematical analysis, semi-empirical and empirical correlations are used to compute the magnitude, frequencies, and distributions of the deterministic loads caused by these pulsations.

Loads caused by vortex shedding are a function of local cross flow velocities, geometry and orientation of the structure, intensity of the turbulence and Reynolds Number. Their magnitudes, frequencies, and distributions are computed from correlations in the literature and developed from test results at Combustion Engineering.

Random loads are generated by flow turbulence. These loads include turbulent buffeting of the structures, which is a function of cross flow velocity, and turbulence induced variations in surface pressure, related to flow parallel to the surface. Because of their random nature, statistical methods are used to define both their magnitude and frequency content in the form of power spectral densities (PSD). Spatial distributions are described by specifying areas and/or lengths over which these loads can be considered coherent. All random loads are assumed to be stationary and ergodic. The PSD representations, in the form of pressure or force squared, per unit frequency versus frequency, are taken from test data and analytical predictions. The analytically derived distributions are assumed to be of constant amplitude (white noise) versus frequency.

3.1.2 Structural Analysis Method

The free-vibration frequencies and mode shapes of the assemblies, in air and water, are found using a variety of methods. These methods include finite element models, multiple degree-of-freedom lumped mass models and experimental data from both full size and scale models. The choice of particular method depends on the complexity of the structure and the nature of the hydraulic load.

Dynamic equilibrium of the structure is described by a force balance which includes mass dependent inertial forces, resistive forces due to velocity dependent damping, and restoring forces, related to the structural stiffness and the displacement. Inertial forces are described by mass times the unknown accelerations. In air the mass is the structural mass, while for the in-water case a hydrodynamic mass is added to the structural mass. This hydrodynamic mass is determined, in the case of the core support barrel, by analytical means, and for the lower support and upper guide structures, from test data and equations in the literature for calculating hydrodynamic mass. The hydrodynamic mass, being dependent on fluid density, varies with temperature resulting in variations in structural frequency with coolant temperature. Damping ratios, in both air and water, are based on experimental data from tests at Combustion Engineering and data in the literature. Structural stiffness depends on material properties, geometry, and boundary conditions.

The resulting set of equations are solved for the modal frequencies and corresponding mode shapes.

3.1.3 Methods for Calculating Structural Response

The dynamic response of any particular assembly is the sum of the separate responses due to the deterministic and random loads. In either case, the response is a function of the magnitude of the load, its frequency and spatial distribution, and the modal frequency and corresponding mode shapes of the assembly. The functional relationships between the response and these factors are different depending whether the excitation is deterministic or random.

For deterministic loads, the steady state response and load have the same harmonic variation with time. The amplitude of the response, for any particular mode, is inversely proportional to the difference between the squares of the modal and forcing frequencies, and

directly proportional to a modal participation factor. The method of mode superposition is used to compute the total response when the structure has significant response at more than one mode. The response, being harmonic, is expressed as either the maximum or root mean square value.

The response to random loading is calculated using statistical methods developed for analyzing random vibrations. The product of the load, expressed as a PSD, and the frequency response characteristics, or transfer function, is integrated over a frequency range to obtain the mean square value (RMS value squared) of the response. Spatial variations in the load are accounted for by performing this integration over the area on which the load is assumed coherent.

The total response is the sum of the deterministic and random contributions. In cases where the response is calculated using a finite element model, values of strain, displacement, and stress are obtained directly. Where lumped mass models are used, displacements assuming elastic behavior, are converted to strain and then to stress.

3.2

Summary

Summaries of the loads considered for each assembly, types of models used in the frequency analysis and structural response calculations for each assembly are listed in Table 3.2-1. Computer codes (Appendix B) used in each of the analyses are identified in this Table. Also noted in the Table are the sections of the CVAP report related to specific portions of the analyses for each of the assemblies.

TABLE 3.2-1
SUMMARY OF HYDRAULIC LOADS, STRUCTURAL
ANALYSIS, AND STRUCTURAL RESPONSE ANALYSES

Assembly	Hydraulic Loads		Structural Analysis	Structural Response	
	Deterministic	Random		Deterministic	Random
Core Support Barrel	Pump pulsations (DPVIB)*	Wall turbulence, white noise.	Finite element (ASHSD), hydrodynamic mass (HYDRO)	Modal superposition (STEADY STATE, SS POST)	Lumped mass, single degree of freedom
Section	4.2.1.1	4.2.1.2	5.2.1	5.2.1.2	5.2.1.3
Lower Support Structure	Pump pulsations and vortex shedding	Turbulent buffeting, band limited	Finite element (STARDYNE, STRUDL) Full size tests in air	Modal superposition	Modal superposition
Section	4.2.2.1	4.2.2.2	5.2.2.1	5.2.2.2	5.2.2.3
Upper Guide Structure	Pump pulsations test data full size CEA tubes	Turbulent buffeting, scale model test data	Lateral motion; finite element (STARDYNE) and test data from scale model and full size tubes Vertical motion; two-degree-of-freedom lumped mass model	Lateral; Modal superposition. Vertical; lumped mass model	Test data, scale model Lumped mass model
Section	4.3.1	4.3.2	5.3.1	5.3.2	5.3.3

* Computer (CODE) used in the calculation, see Appendix B.

4.0 CALCULATION OF THE FORCING FUNCTION

4.1 General Methodology

The analytical method employed assumes the hydraulic forcing functions, associated with the steady and transient operating conditions, can be separated into deterministic and random components.

Periodic loads of primary interest are those caused by pump induced pressure fluctuations. The forces are acoustic in nature, occurring at the harmonics of the pump rotor and blade passing frequencies (BPF), independent of flow rate. In addition, some structures are subjected to flow induced forces related in frequency to cross flow velocity and magnitude to kinetic head ($1/2 \rho V^2$).

Flow induced random loads are primarily due to turbulence. The magnitude of these forces are normally proportional to the kinetic head, and occur over a broad range of frequencies.

Methods for developing the deterministic and random components of the hydraulic forcing function are discussed in this section. Where complex flow path configurations or wide variations in pressure distribution are involved, the hydraulic forcing functions are formulated using a combination of both analytical and empirical methods. The empirical methods utilize data obtained from plant tests and/or scaled model tests.

4.1.1 Transient Conditions

Forced response analyses are done for each of the thermal and hydraulic conditions listed in Table 1.3-1. These conditions cover both steady state and transient operation in addition to intermediate conditions needed to verify the models related to flow induced loads.

For the CVAP, the only transients considered important are due to pump startup and shutdown. These transients cause variations, with time, in flow rate and pump rotor and blade passing frequencies which could affect both the magnitude and frequency of the flow induced loads and the structural response.

The magnitude and frequency of the deterministic loads caused by pump pressure pulsations are independent of fluid velocity and thus unaffected by transient variations in flow rate. The increase or decrease in pump rotational frequency with time will, however, cause changes in the frequency of propagation of these pulsations. As discussed in Section 5.1.1, this will, in some cases, result in a momentary resonance condition between the force and the structure. However, the duration of this resonance should be short compared to the response time of the structure and not result in any significant amplification of the response.

Both the magnitude and frequency of the deterministic loads due to vortex shedding are functions of flow rate. However, the natural frequencies of the assemblies for which these loads are considered are higher than the vortex shedding frequencies. Thus resonance between the structure and the vortex shedding load will not occur for any of the CVAP test condition flow rates. Consequently transient variations in flow will not effect the response.

The magnitude of the random forces is proportional to kinetic head while its frequency content depends, to some extent, on flow velocity. The magnitude can conservatively be calculated based on the steady state value of kinetic head, either before or after the transient, depending which condition results in the largest value. The power spectral densities for the random loads are in general wide band, with maximum frequency at least equal to the maximum frequency at which structure has a significant response. Thus any minor variations in frequency content will not change the response.

Based on this evaluation, any differences in the magnitudes and frequencies of the flow induced loads from their steady state values, due to transient changes in flow rate and pump rotational frequencies, should have no significant effects on the structural response. Consequently the magnitudes of the transient flow induced loads are assumed to be equal to their steady state values, either before or after the transient, and to occur at frequencies equal to their steady state values.

4.2 Core Support Barrel Assembly

4.2.1 Core Support Barrel

4.2.1.1 Deterministic Forcing Function

An analysis based on an idealized hydrodynamic model (Ref. 6, 7, 36) is employed to obtain the relationship between reactor coolant pump pulsation in the inlet ducts and the periodic pressure fluctuations on the core support barrel. The model represents the annulus of coolant between the core support barrel and the reactor vessel. In deriving the governing hydrodynamic differential equation for the above model, the fluid is taken to be compressible and inviscid. Linearized versions of the equations of motion and continuity are used. The excitation on the hydraulic model is harmonic with the frequencies of excitation corresponding to pump rotational speeds and blade passing frequencies. The result of the hydraulic analysis is a system of equations which define the forced response, natural frequencies and natural modes of the hydrodynamic model. The forced response equations define the spatial distributions of pressure on the core support barrel as a function of time. The details of this analysis are given in Appendix

A.1.1.1.

4.2.1.2 Random Forcing Function

The random hydraulic forcing function is developed by analytical and experimental methods. An analytical expression is developed to define the turbulent pressure fluctuation for fully developed flow (Ref. 13). This expression is modified, based upon the result of scale model testing (Ref. 14, 15) to account for the fact that flow in the downcomer is not fully developed. Based upon test results, an expression is developed to define the spatial dependency of the turbulent pressure fluctuations. In addition, experimentally adjusted analytical expressions are developed to define the peak value of the pressure spectral density associated with the turbulence and the maximum area of coherence, in terms of the boundary layer displacement, across which the random pressure fluctuations are in phase (Ref. 13, 14, 15). The transient behavior of the random fluctuations during pump startup and shutdown is assumed to be identical to that at steady state conditions. Details of the analysis are given in Appendix A.1.1.2.

4.2.2 Lower Support Structure Assembly

The ICI nozzles and the skewed beam supports for the ICI support plate are excited by periodic and/or random, flow induced forces.

4.2.2.1 Deterministic Forcing Function

The periodic component of this loading is due to pump related pressure fluctuations and vortex shedding due to crossflow. High intensity turbulence, caused by jetting through the flow skirt, makes it unlikely that regular vortex shedding will occur (Ref. 18). In spite of the high intensity turbulence, for conservatism, vortex shedding is assumed to occur. The maximum shedding frequency is below the lowest structural frequency for both the ICI nozzles and skewed beams. The magnitude and frequency of this periodic

force are accounted for based on data in the literature for crossflow over both vertical (Ref. 21) and skewed (Ref. 20) isolated tubes.

Derivation of pump frequency related loads is accomplished by assuming that these periodic pressure variations are propagated unchanged through the flow skirt from the lower portion of the core barrel - reactor vessel annulus. The magnitude of these pulsations is based on a combination of analytical predictions, based on Reference 6, and data from previous pre-critical vibration monitoring programs (Ref. 8, 9). See Appendix A.1.2.1.

4.2.2.2 Random Forcing Function

The ICI nozzles and ICI support plate support beams are both subjected to turbulent buffeting by the flow skirt jets. The outermost ICI nozzles and beams receive full impact of the jets before the jets decay due to fluid entrainment and the presence of inner tube rows. The force spectrum of these jets is assumed to be represented as wide band white noise. The magnitude of this spectrum is based on data in the literature for impingement of turbulent jets (Ref. 19, 25). This velocity dependent magnitude is applied to each tube, assuming no change in jet characteristics, between the outermost and inner tubes. The approach velocity for each tube is calculated from an analytical expression based on experimental data on the velocity distribution in the lower portion of the reactor vessel-core barrel annulus and the flow skirt. See Appendix A.1.2.2 for details.

4.3 Upper Guide Structure

The dynamic force on the upper guide structure assembly is mainly due to flow induced forces on the CEA shroud tubes.

4.3.1 Deterministic Forcing Function

The periodic components of these forces can be caused by pressure pulsations at harmonics of the pump rotor and blade passing frequencies, and vortex shedding due to crossflow over the tubes.

A series of tests on full size tubes, at reactor pressure and temperature, indicated no evidence of periodic vortex shedding at the Reynolds Number and turbulence levels expected in the tube bank (Ref. 22). Thus, the only significant periodic force expected is that due to pump pulsations. Reactor pre-critical vibration monitoring test results (Ref. 27) were utilized to determine the magnitude of these pulsations at the pump rotor, twice the rotor, blade passing, and twice blade passing frequencies. See Appendix A.2.1.

4.3.2 Random Forcing Function

Results of the full size tube tests (Ref.22) showed that at normal operating conditions the control element shroud tubes are excited by upstream and wake produced turbulent buffeting (Ref. 22, 23, 24, 31). The forcing function for this type of loading can be represented as a band limited white noise power spectrum (Ref. 22). The magnitude of this spectrum is computed based on data from tests on the quarter-scale tube bank model (Ref. 31). The resultant velocity dependent forces are used to compute the amplitude of the response and resulting stress levels. See Appendix A.2.2.

5.0 CALCULATION OF THE STRUCTURAL RESPONSE

5.1 General Methodology

A variety of mathematical models (finite element or multiple degrees-of-freedom lumped mass models), which describe the structural assemblies, are employed to obtain the structural response to different loading conditions. Classical modal analysis methods are used to obtain the dynamic response. These require determination of the natural vibration modes and the frequencies. The effect of fluid on these characteristic parameters is accounted for by either solution of the coupled fluid-structure problem or utilizing an added, or hydrodynamic, mass. Forced response to deterministic and random excitations is obtained using the method of mode superposition. Subsequent sections describe in detail the analyses for different assemblies.

5.1.1 Transient Conditions

It is recognized that during pump start up or shutdown, pump speed, and thus the frequencies of the periodic pressure pulsations, will vary. These variations will result in forcing frequencies that pass through the natural frequencies of the structures. When this occurs peak amplitudes could be obtained that momentarily exceed those calculated for the steady state response. Based on a mechanically excited, lumped parameter, single degree-of-freedom analysis (Ref. 29), this transient response is inversely proportional to the rate of change of the forcing frequency and directly proportional to the modal frequency of the structure, squared. Thus, structures with low first mode frequencies like the core support barrel, will experience lower amplification than stiffer structures; eg CEA shroud tubes. This has been verified by measurements taken during reactor coolant pump startup and shutdown transients, (Ref. 9) which showed no evidence of a resonance response for the core barrel.

No dynamic magnification has been assumed in the forced response analysis for the startup and shutdown transients. These transients have been analyzed applying the quasi-steady loads at the particular test condition (Section 4.1.2). Though this quasi-steady assumption is thought conservative, instrumentation has been provided to monitor the response of the internals during these transients.

5.2 Core Support Barrel Assembly

5.2.1 Core Support Barrel-Analysis

Procedure, including computer codes (Appendix B), for calculating dynamic response of the core support barrel are shown in Figure 5.2-1.

5.2.1.1 Natural Frequencies and Mode Shapes

The natural frequencies and mode shapes of the CSB assembly, which form the basis for the forced response analysis, were obtained through the use of an axisymmetric shell finite element computer program ASHSD (Appendix B.1). This computer program is capable of obtaining natural frequencies and mode shapes of complex axisymmetric shells; e.g., arbitrary meridional shape, varying thickness, branches, multi-materials, orthotropic material properties. An inverse iteration technique is utilized in the program to obtain solutions to the characteristic equation, which is based on a diagonalized form of consistent mass and stiffness matrices developed using the finite element method. Four degrees of freedom - radial displacement, circumferential displacement, vertical displacement, and meridional rotation - are taken into account in the analysis, giving rise to coupled mode shapes and corresponding frequencies. The core support barrel is modeled as shown in (Figure 5.2-2). The structure is fixed at the upper flange to determine the beam modes and frequencies. The shell modes and frequencies are found by considering the upper flange fixed and the

lower flange pinned. The frequencies in water are computed utilizing the computer code HYDRO. This code is based on a continuum approach to the hydrodynamic effects (Ref. 38).

5.2.1.2 Forced Response to Deterministic Loading

The normal mode method is used to obtain the structural response of the CSB assembly to deterministic forcing functions. Generalized masses, based on mode shapes and the mass matrix from the ASHSD finite element computer program, are calculated for each CSB mode of vibration. Modal participation factors, based on the mode shapes and the predicted periodic forcing functions, are calculated for each mode and forcing function. The generalized response for each mode is then obtained through solution of the corresponding set of uncoupled, second order, ordinary differential equations similar in form to single degree of freedom system equations. Utilizing displacement and stress mode shapes from the shell finite element computer program, the structural response of the CSB for each mode are obtained by means of the appropriate coordinate transformations. Response to any specific forcing function is obtained through summation of the component modes for that forcing function. The general methodology is shown schematically in Figure 5.2-1.

5.2.1.3 Response to Random Excitation

The random response analysis considers the response of the CSB assembly to the turbulent component of flow during steady-state operation. The random forcing function is assumed to be a wide-band stationary random process with force spectral density, S_f , measured in units of $(\text{force})^2/(\text{rad}/\text{sec})$. To obtain the root mean square (RMS) vibration level of the CSB assembly, the CSB assembly is taken to be a single degree of freedom system ("beam" mode). It follows that the RMS displacement level of the CSB assembly is given by (Ref. 8, 13);

$$\delta_{\text{RMS}} = \left[\frac{\pi}{4} \cdot \frac{S_f}{m^2 \zeta \omega^3} \right]^{1/2}$$

where: m = mass,
 ζ = damping factor,
 ω = natural frequency

If the RMS random pressure fluctuation is assumed spatially invariant, the force spectral density is given by:

$$S_f = A_s \cdot A_c^2 \cdot \bar{p}^2 \cdot \phi(\omega)$$

where: $\bar{p}^2 = C_1 K_E N^2$

A_s = surface area

A_c = max. area of coherence

$\phi(\omega)$ = peak of frequency spectrum associated with turbulence

C_1 = constant

K_E = average kinetic head of coolant per functioning loop in annulus

N = number of functioning loops

5.2.1.4 Core Support Barrel-Results of Analysis

5.2.1.4.1 Natural Frequencies and Mode Shapes

A free vibration analysis of the CSB assembly was performed, using the method previously described, to obtain the system's natural frequencies and associated mode shapes. The frequencies for the "beam" mode ($n=1$) and for the shell (ring) modes ($m=2,3,4$) are given in Table 5.2-1, 5.2-2. The pertinent beam mode shapes are plotted in Figure 5.2-3. CSB displacements appear as dotted lines in Figure 5.2-4. The shell modes are standard $\cos(m)$ ring distortions and as an example the first four mode shapes are shown in Figure 5.2-4. A summary of the frequencies are shown in Figure 5.2-5.

5.2.1.4.2 Response to Deterministic Loading

Deterministic loads on the CSB are caused by propagation of pump induced periodic variations in pressure through the reactor vessel-CSB annulus. The distribution, frequency and amplitude of these pulsations are discussed in Section 4.2.1.1 and developed in Appendix A.1.1.1. The in-water frequencies and mode shapes for the CSB are predicted by the methods discussed in Section 5.2.1.1. These pressure distributions and frequencies are used, with the response prediction methods in Section 5.2.1.2, to compute the forced vibration response of the CSB. Values of strains and corresponding stresses are summarized in Figure 5.2-6 to 5.2-11.

These regions correspond to instrument (strain gauge) locations described in Section 6.2.1.

The larger stress found for lower temperature is due to a circumferential mode being closer to resonance with the 20 Hz component of the pump pulsations. This shift in frequency caused by a larger hydrodynamic mass effect at the lower temperature.

5.2.1.4.3 Response to Random Excitation

The PSDs developed in Appendix A.1.1.2 and described in Section 5.2.1.3 are used to compute the response of the CSB to random excitation. The spectra is assumed to have a constant amplitude versus frequency (white noise). The beam mode will, as a result of it having the lowest value of frequency, be the mode most easily excited by the random excitation. Thus the PSDs are applied to a single degree-of-freedom lumped mass model of the CSB to calculate the RMS values of the random response.

The resulting response is found to be an order of magnitude less than the deterministic.

Values of stress in Figures 5.2-6 to 5.2-9 include both random and deterministic components. Strains corresponding to these stresses are found from the two dimensional stress-strain relationships, and are shown in Figures 5.2-10 to 5.2-11. Total displacement at the lower flange, including all modal contributions, is shown in Figure 5.2.-12.

The multiple pump response (N times the one pump results, $N = 2, 3, 4$) is found by a superposition of the one pump results. This conservatively assumes the phasing between pumps is such that the resulting pressure distribution is an N pump multiple of the one pump case (Appendix A.1.1). Thus the results presented in Figures 5.2-6 to 5.2-12 are all conservative upper bound values.

TABLE 5.2-1
 PRE-CORE CSB FREQUENCIES IN AIR
 AND IN WATER
 (564°)

$f(\text{Hz})$ air $f(\text{Hz})$ water	N = 1	N = 2	N = 3	N = 4
M = 1				
M = 2				
M = 3				
M = 4				

N = Circumferential Modes

M = Axial Mode

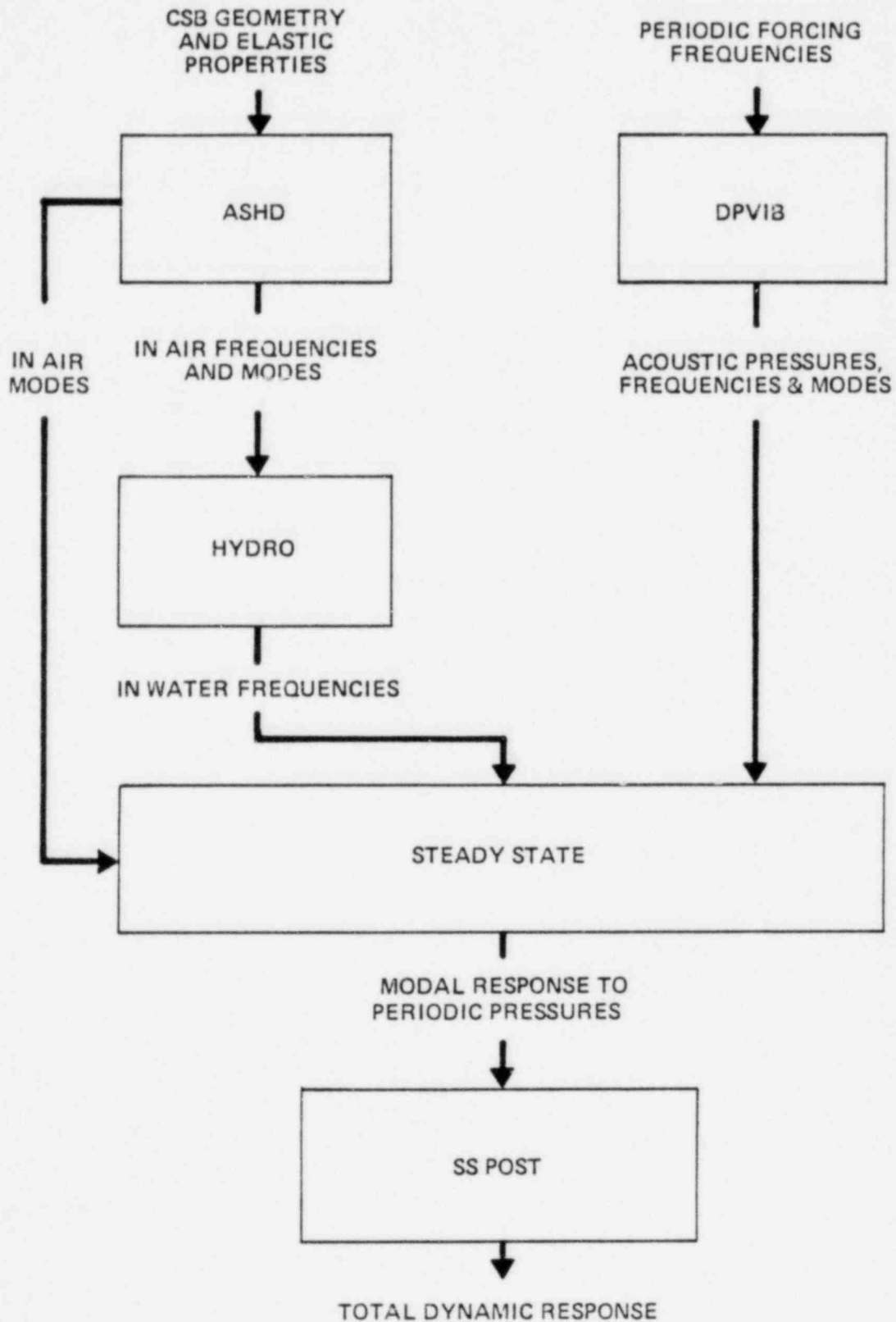
TABLE 5.2-2
LIQUID (564°F) NATURAL FREQUENCIES IN CSB ANNULUS

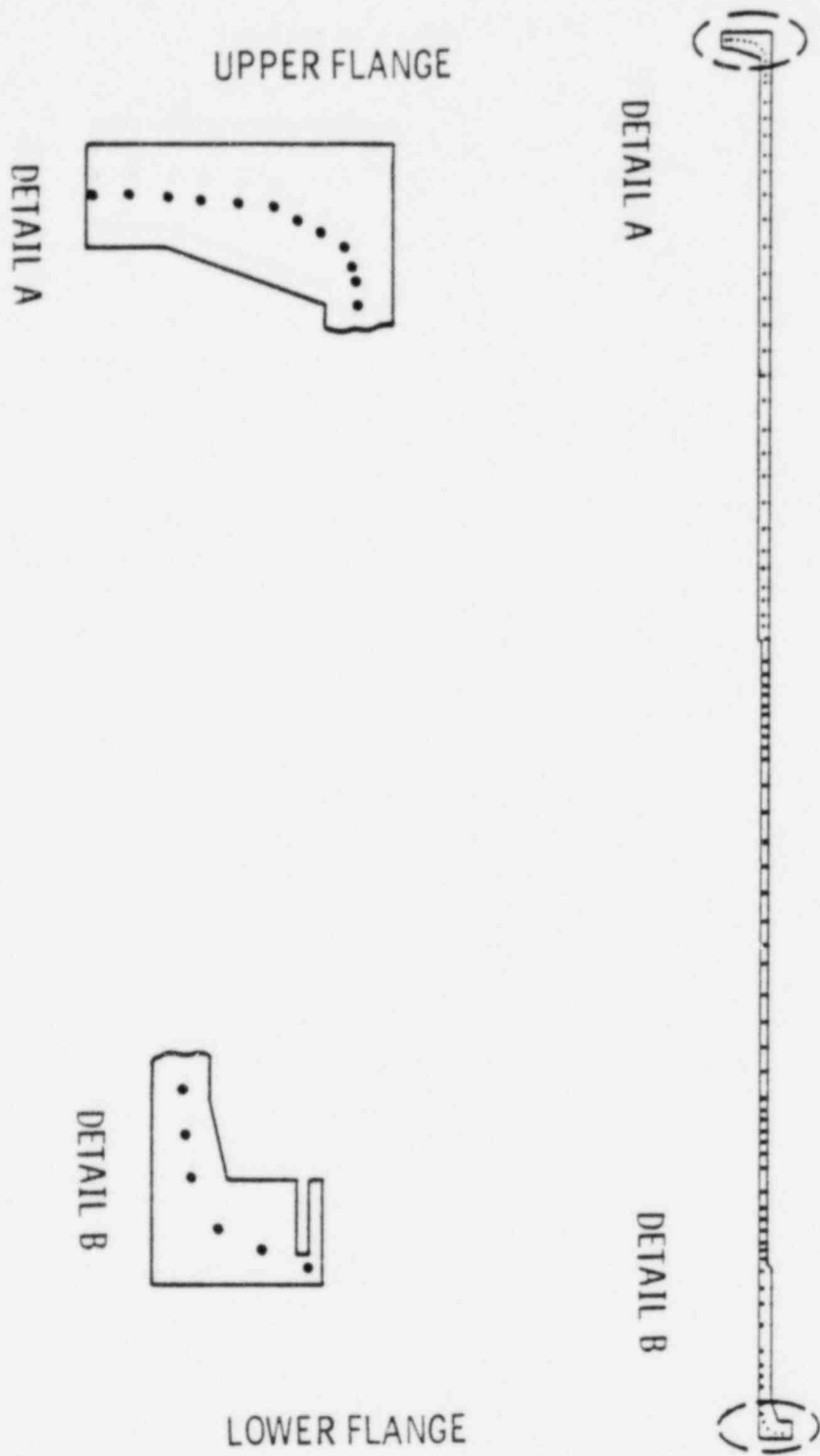
f (HZ)	N = 1	N = 2	N = 3	N = 4
M = 1]]
M = 2				
M = 3				
M = 4				

N = Circumferential Modes

M = Axial Modes

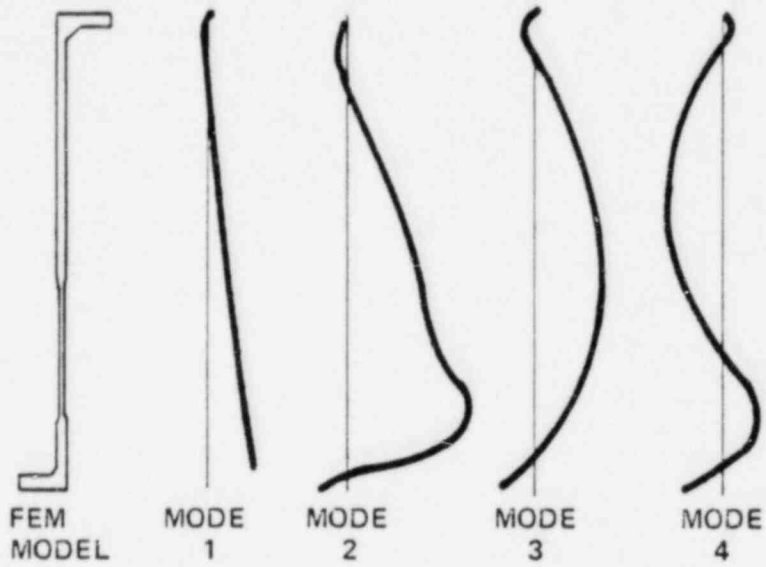
FIGURE 5.2-1
CALCULATION OF CSB DYNAMIC RESPONSE TO
PERIODIC PRESSURE FORCES





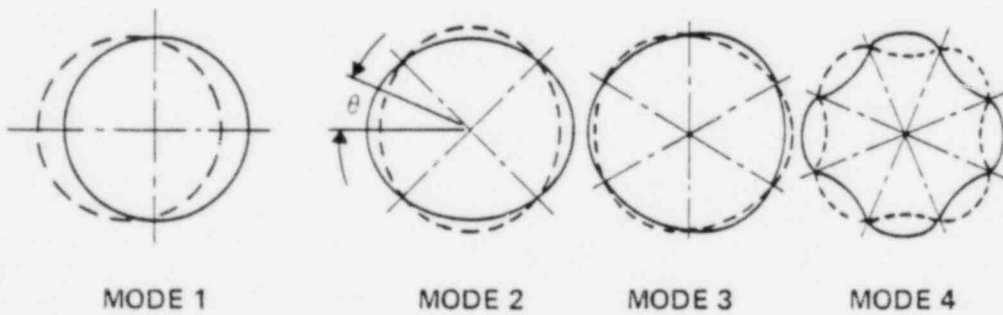
CSB FINITE ELEMENT MODEL

FIGURE 5.2-2



CSB BEAM MODESHAPES

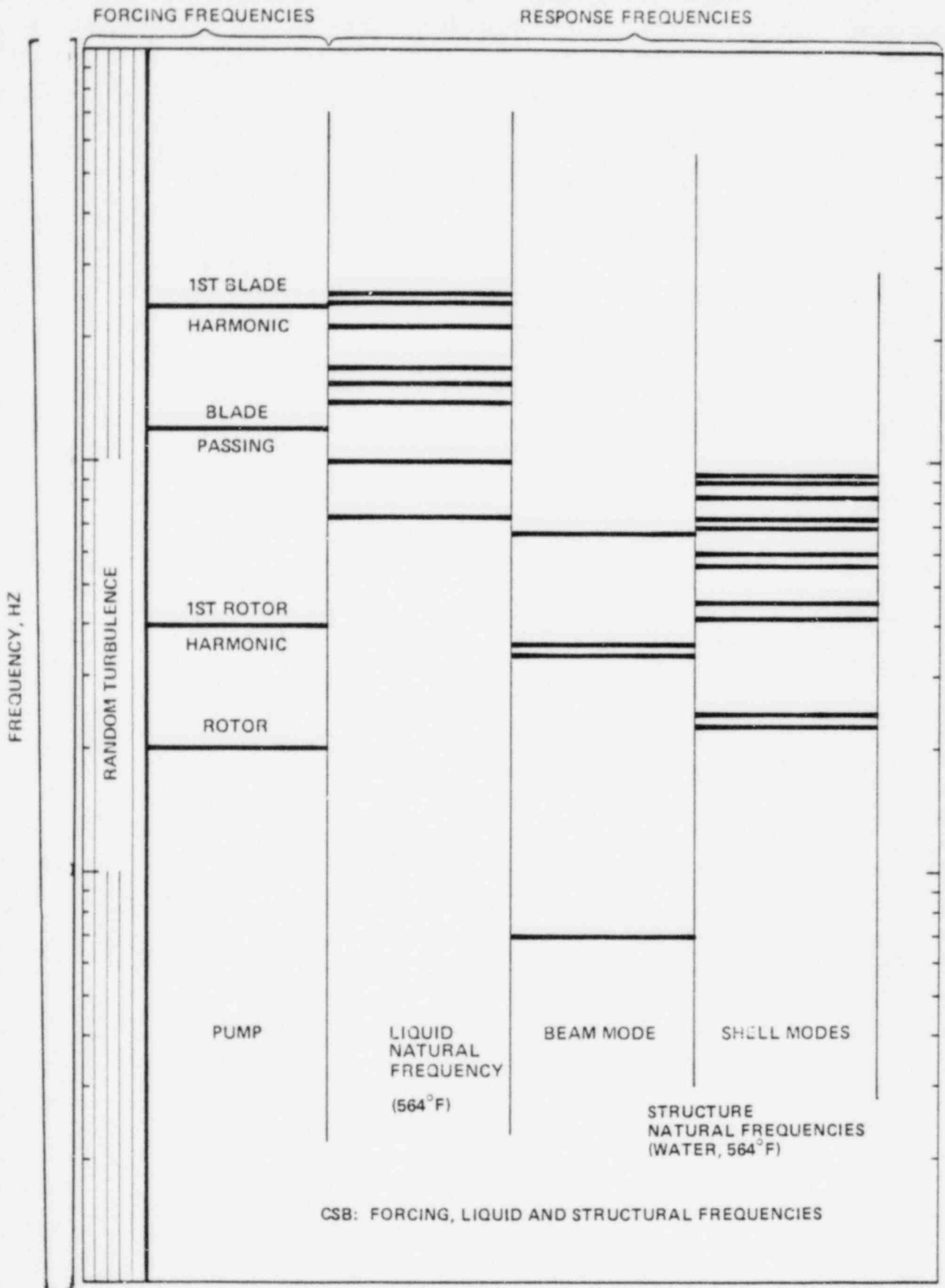
FIGURE 5.2-3



CSB SHELL MODESHAPES

FIGURE 5.2-4

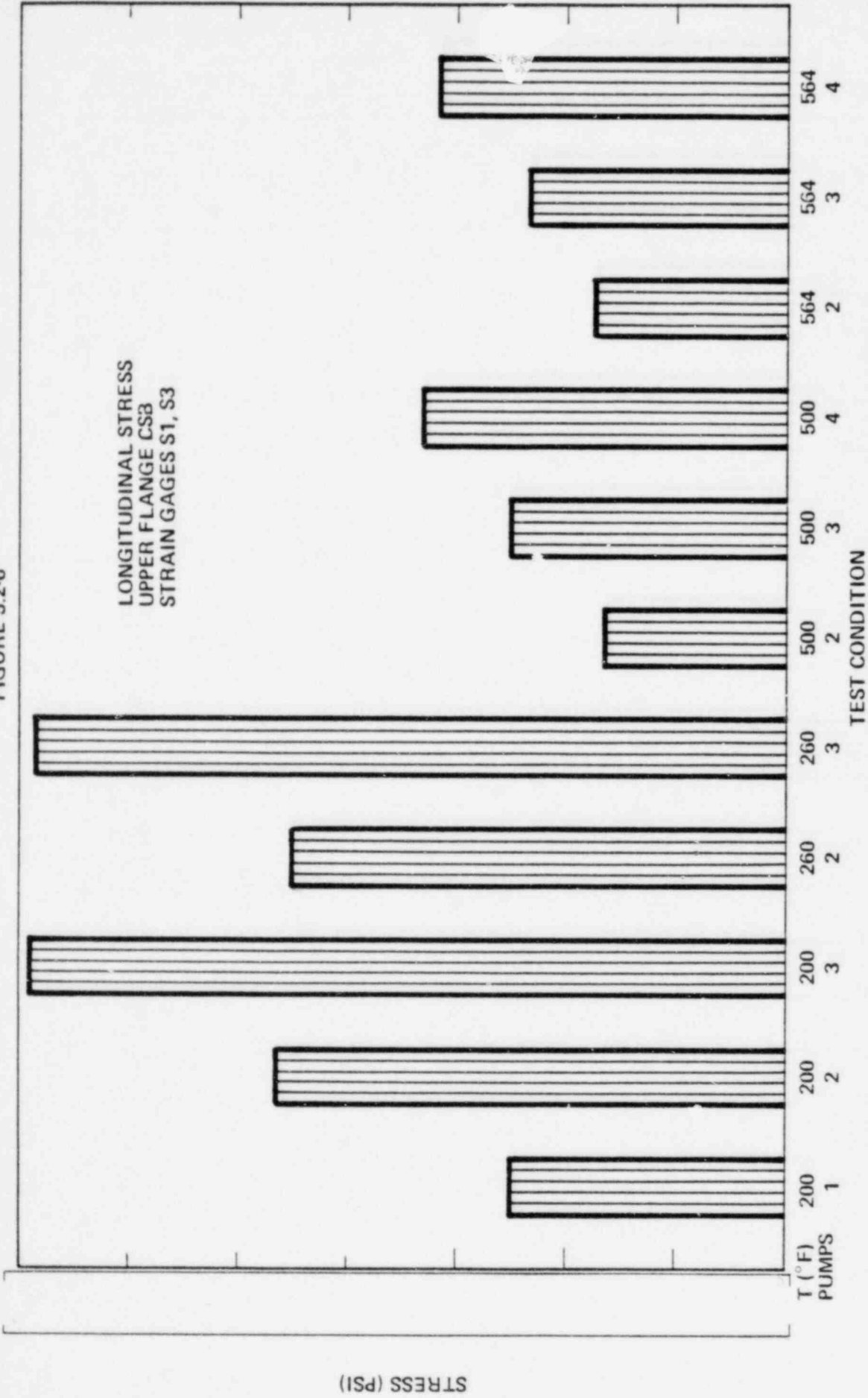
CSB ASSEMBLY



CSB: FORCING, LIQUID AND STRUCTURAL FREQUENCIES

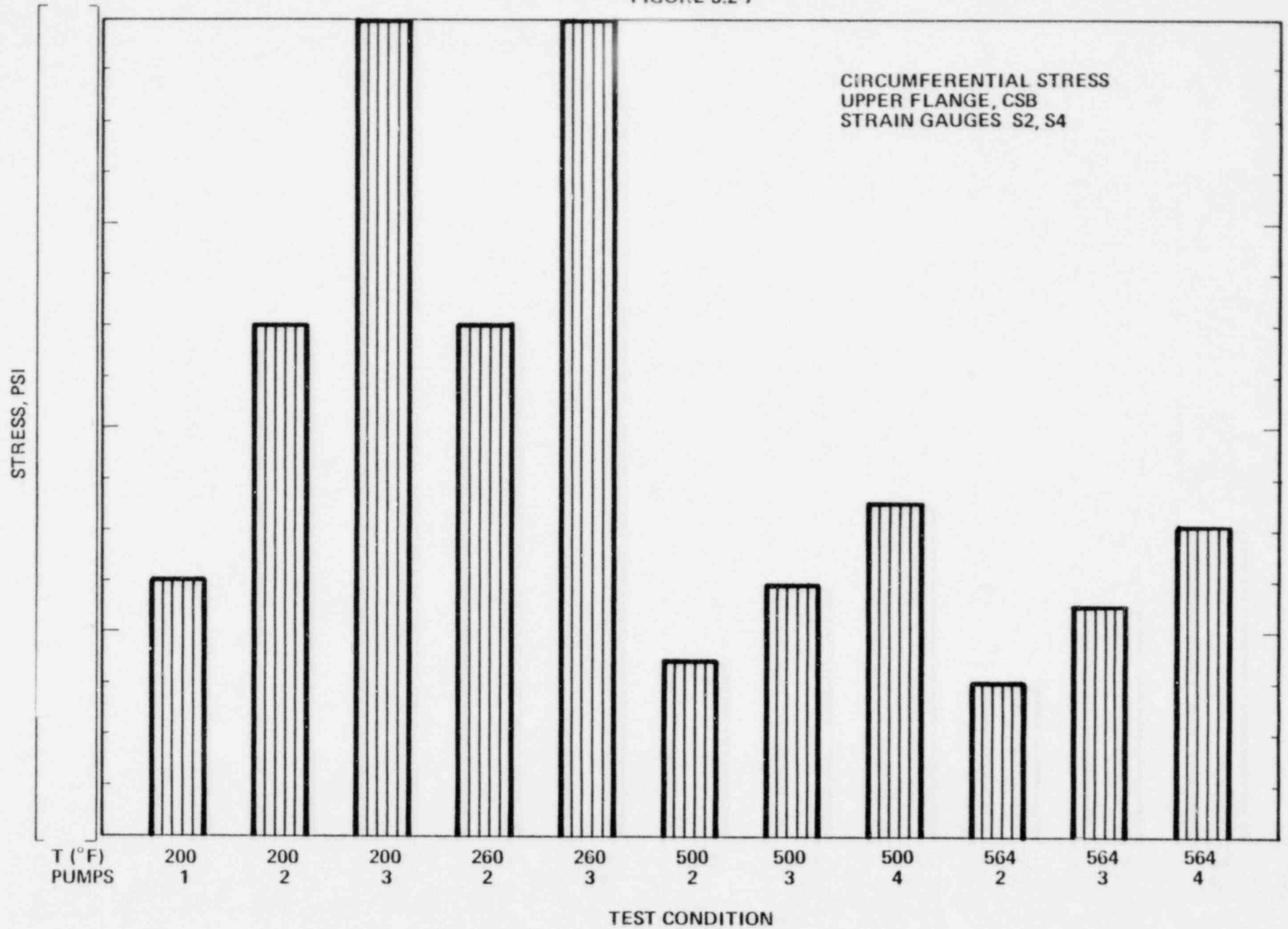
FIGURE 5.2-5

CSB: MAXIMUM STRESS - UPPER FLANGE, LONGITUDINAL; INSTRUMENTS S1, S3
FIGURE 5.2-6

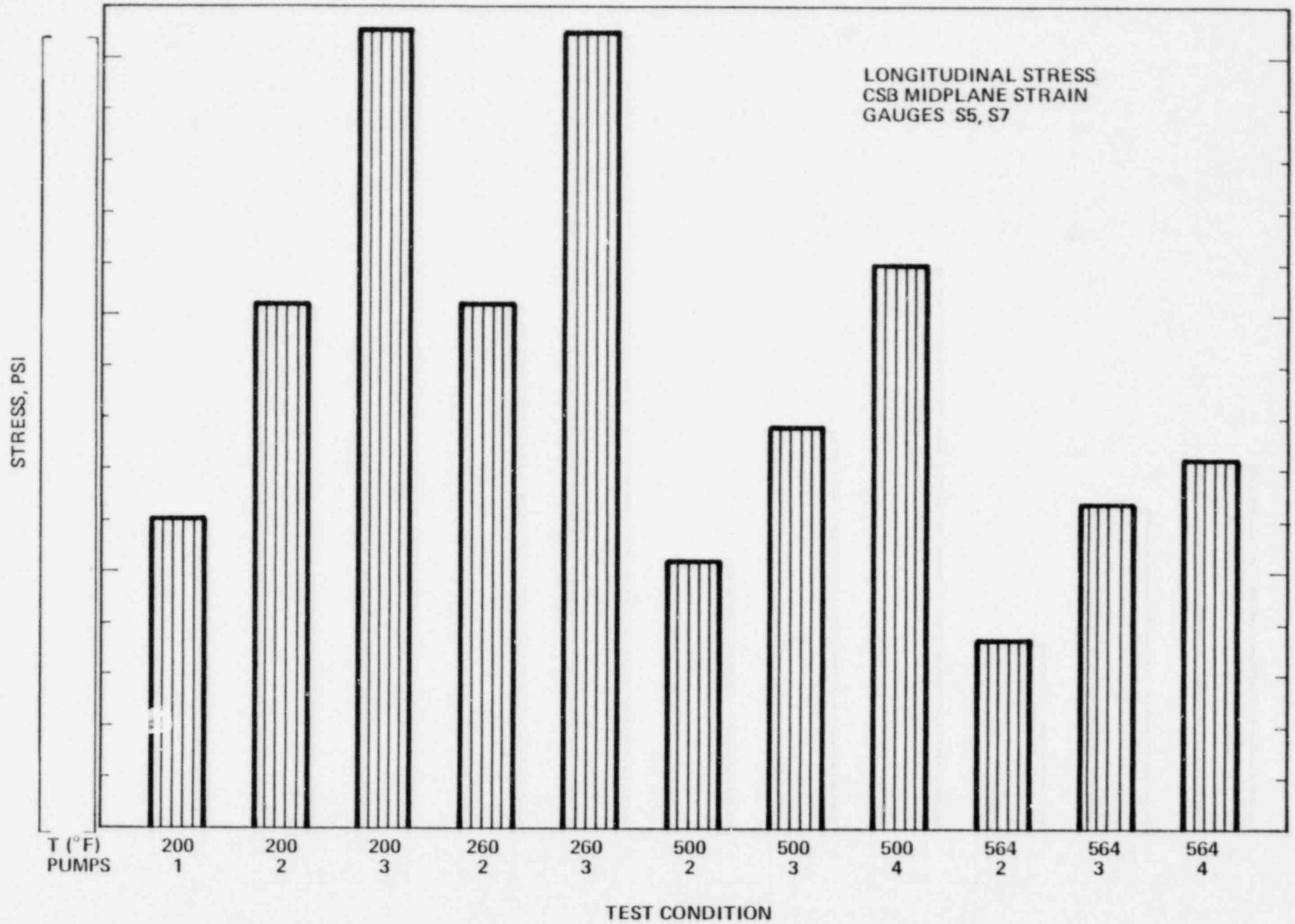


STRESS (PSI)

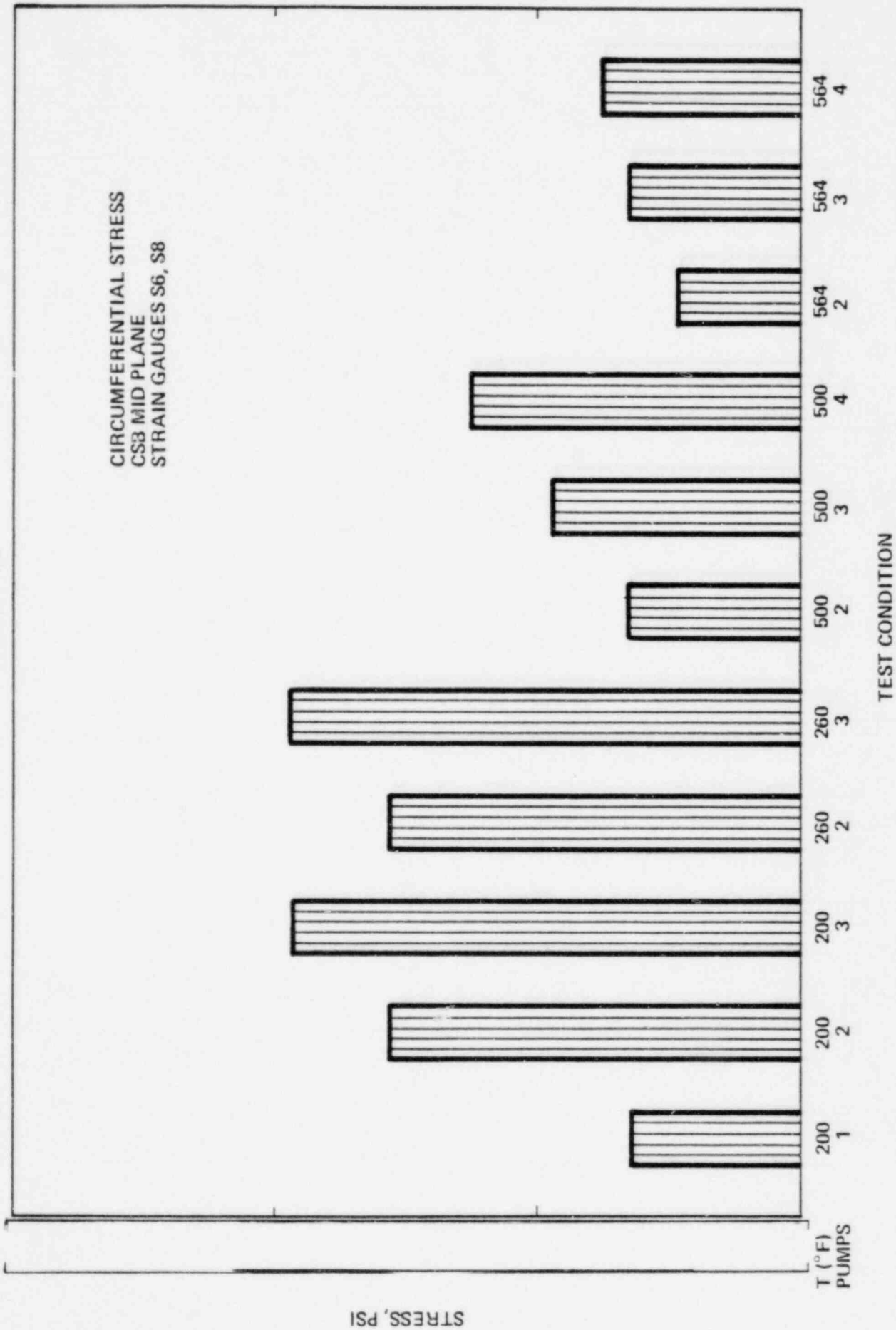
CSB: MAXIMUM CIRCUMFERENTIAL STRESS – UPPER FLANGE; INSTRUMENTS S2, S4
FIGURE 5.2-7



CSB: MAXIMUM LONGITUDINAL STRESS – MID PLANE; INSTRUMENTS S5, S7
FIGURE 5.2-8

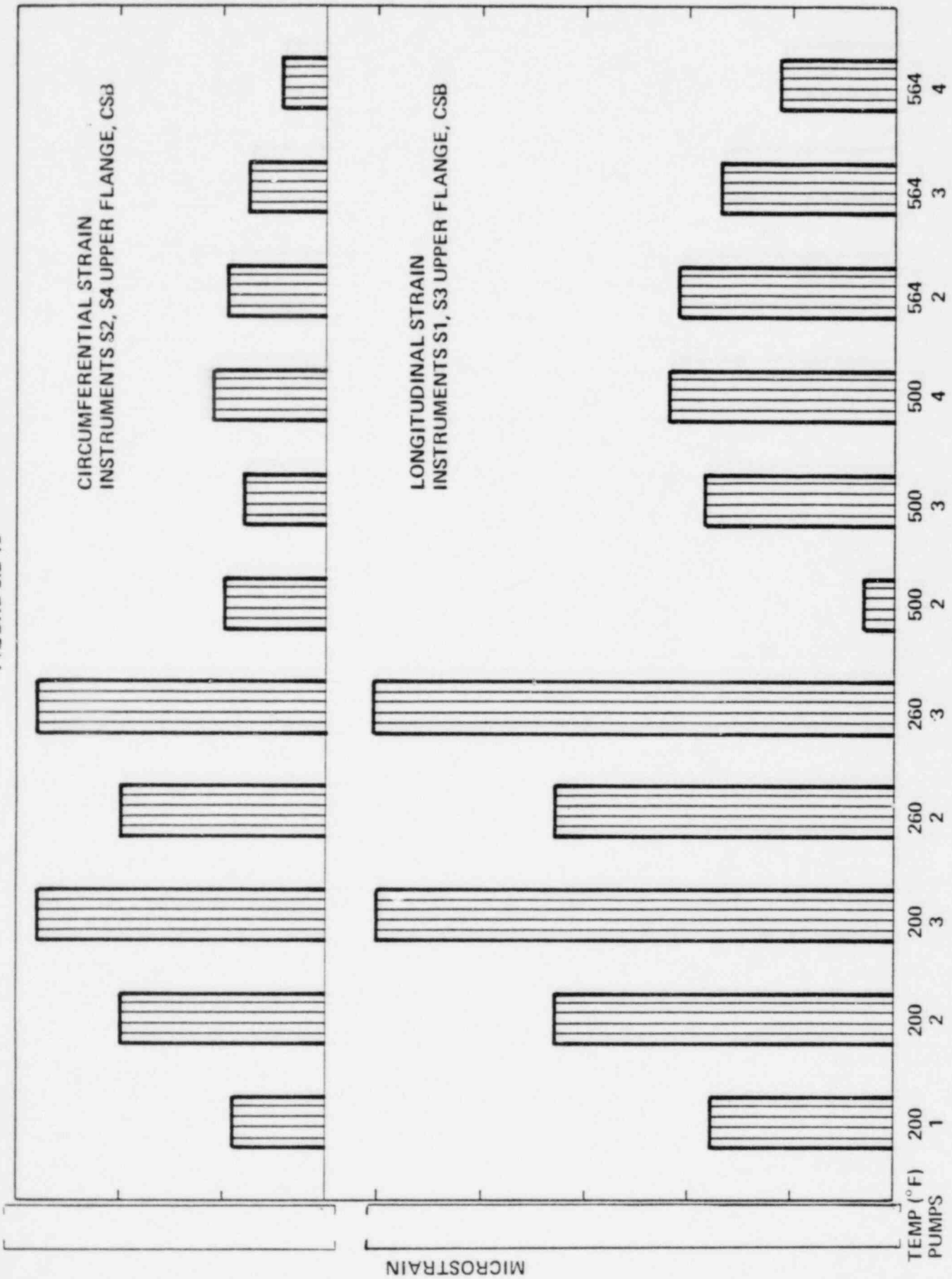


CS3: MAXIMUM CIRCUMFERENTIAL STRESS - MID PLANE; INSTRUMENTS S6, S8
FIGURE 5.2-9

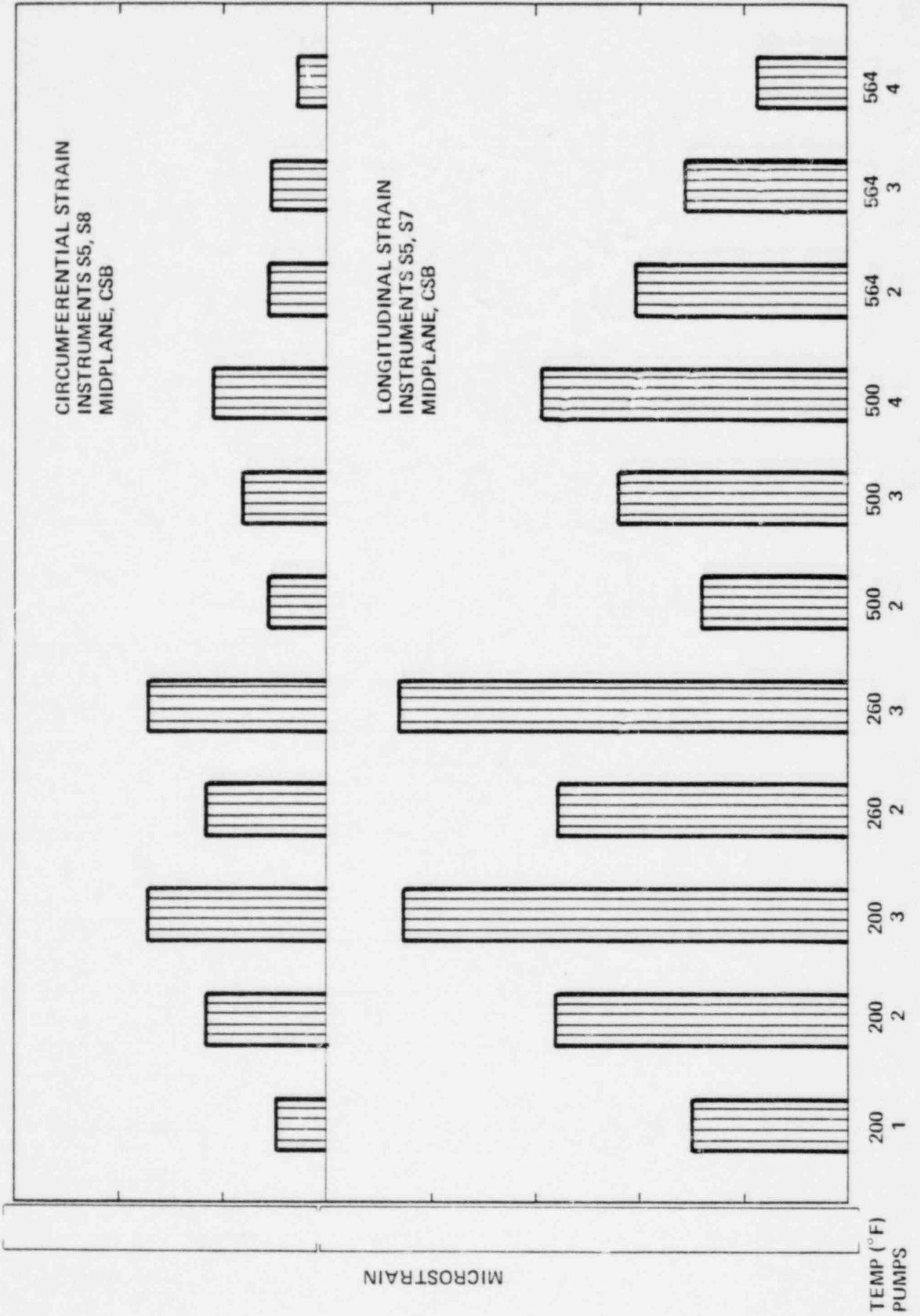


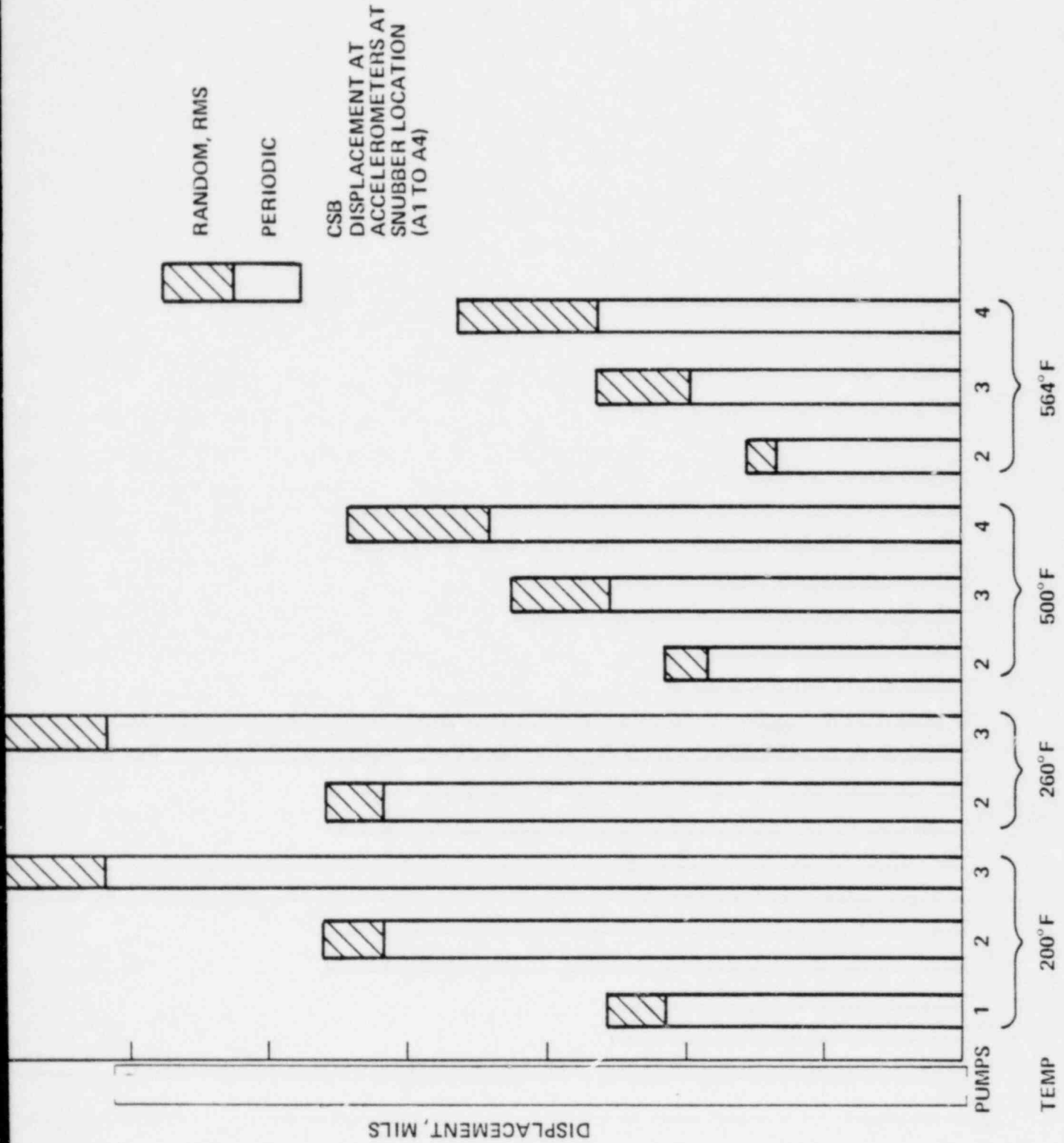
STRESS, PSI

CSB: MAXIMUM STRAIN - UPPER FLANGE
 FIGURE 5.2-10



CSB: MAXIMUM STRAIN - MID PLANE
FIGURE 5.2-11





CS3: MAXIMUM DISPLACEMENT AT BOTTOM OF BARREL: INSTRUMENTS A1-A4
 FIGURE 5.2.12

5.2.2 Lower Support Structure-Analysis

5.2.2.1 Natural Frequencies and Mode Shapes

Several models are used to analyze the lower support structure assembly. Beam and plate elements are used to model the entire instrument nozzle assembly (Figure 5.2-13). This representation of the structure is used with the STARDYNE computer code to determine the modes, frequencies, and response actions of the assembly as a system. The reaction points in this model are taken at the bottom plate level of the LSS assembly. Typical ICI nozzles (Figure 5.2-14) are modeled as fine mesh beam elements reacted at the support points by spring elements representing the surrounding structure flexibility. These component models are used with the STARDYNE computer code to provide the individual structural modes, frequencies, and responses within the system. The results of both individual and system analysis are combined to provide the total response. Coolant effects on the frequencies of these items are accounted for by the addition of "hydrodynamic mass" to the structural mass in the models.

Free vibration analyses of the instrument nozzle assembly and the ICI nozzles were performed using finite element techniques to obtain the structural mode shapes and frequencies in air and in water. Modal testing of the actual structure in air was performed to verify the analysis and obtain damping information. Test results compared well with the analytical predictions and were used to obtain damping values used in this analysis. The resulting modeshapes and frequencies for the instrument nozzle assembly and ICI nozzle are the outcome of the combined test and analysis effort. These are shown in Figures 5.2-15 and 5.2-16 and represent all those modes and frequencies considered to contribute significantly to the total response for the frequency range of excitation involved. A summary of the response and forcing frequencies are shown in Figure 5.2-17.

5.2.2.2 Response to Deterministic Loading

Deterministic loading (Appendix A.1.2) in this area causes a dynamic response of the entire instrument nozzle assembly as well as the individual ICI support tubes. Response of the entire assembly is found using the finite element model shown in Figure 5.2-13. This analysis provides deflections and accelerations of the assembly as well as loading carried by the individual tubes. The individual support tube is then analyzed using the more detailed model shown in Figure 5.2-14. This analysis determines the dynamic response of the single tubes to the deterministic loading using the modeshapes and frequencies found during modal analysis. The results of both system and individual analysis are combined to provide the total response.

Damping used in the response analysis of both the system and individual tubes is obtained from the modal testing done on the lower support structure.

5.2.2.3 Response to Random Excitation

The lower support structure will not respond to random excitation as a complete assembly but rather will experience local disturbances of individual components within the assembly. The modal analysis from the finite element model of the ICI support tube (Figure 5.2-14), already used for deterministic analysis, is again utilized to determine the random response by the normal mode method.

5.2.2.4 Lower Support Structure-Results of the Analysis

5.2.2.4.1 Response to Periodic Loading

The natural frequencies and mode shapes together with the periodic hydraulic forcing function are utilized to obtain the structural response of the LSS assembly.

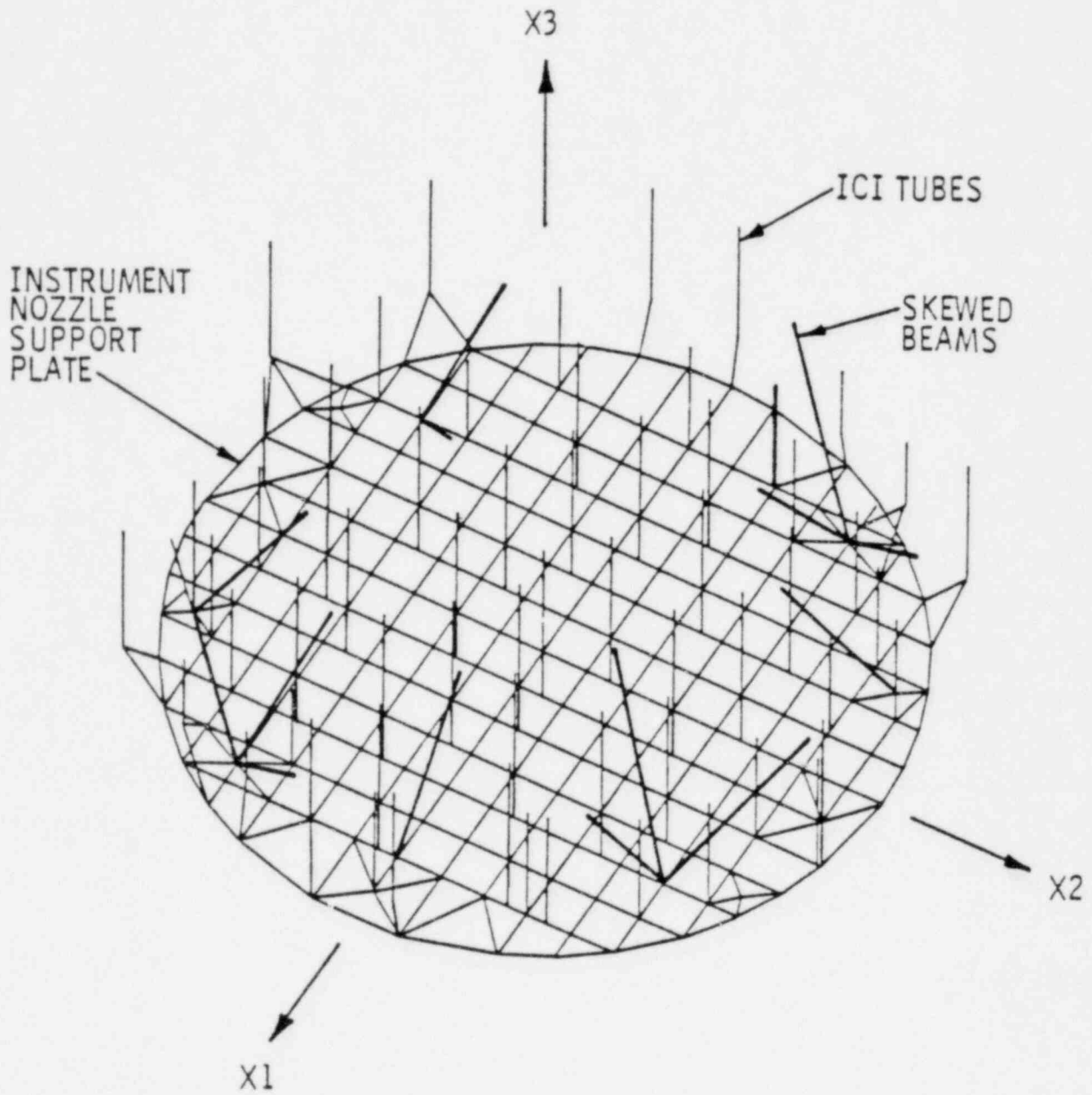
The design analysis (Ref. 2) for this assembly showed ICI tube 58 to be the mostly highly stressed member of the assembly. The response to pump induced and vortex shedding loads is calculated at the instrumented locations for this ICI tube using the models discussed in Section 5.2.2.2. The entire LSS assembly will respond to periodic crossflow induced loads on the support beams. A response analysis has also been done to predict motion of the assembly at the location of an accelerometer (A11) on the LSS.

The results of these analyses are presented in Figures 5.2-18 to -22. These figures indicate the maximum strain, stress acceleration response levels at the instrument locations for the noted operating conditions.

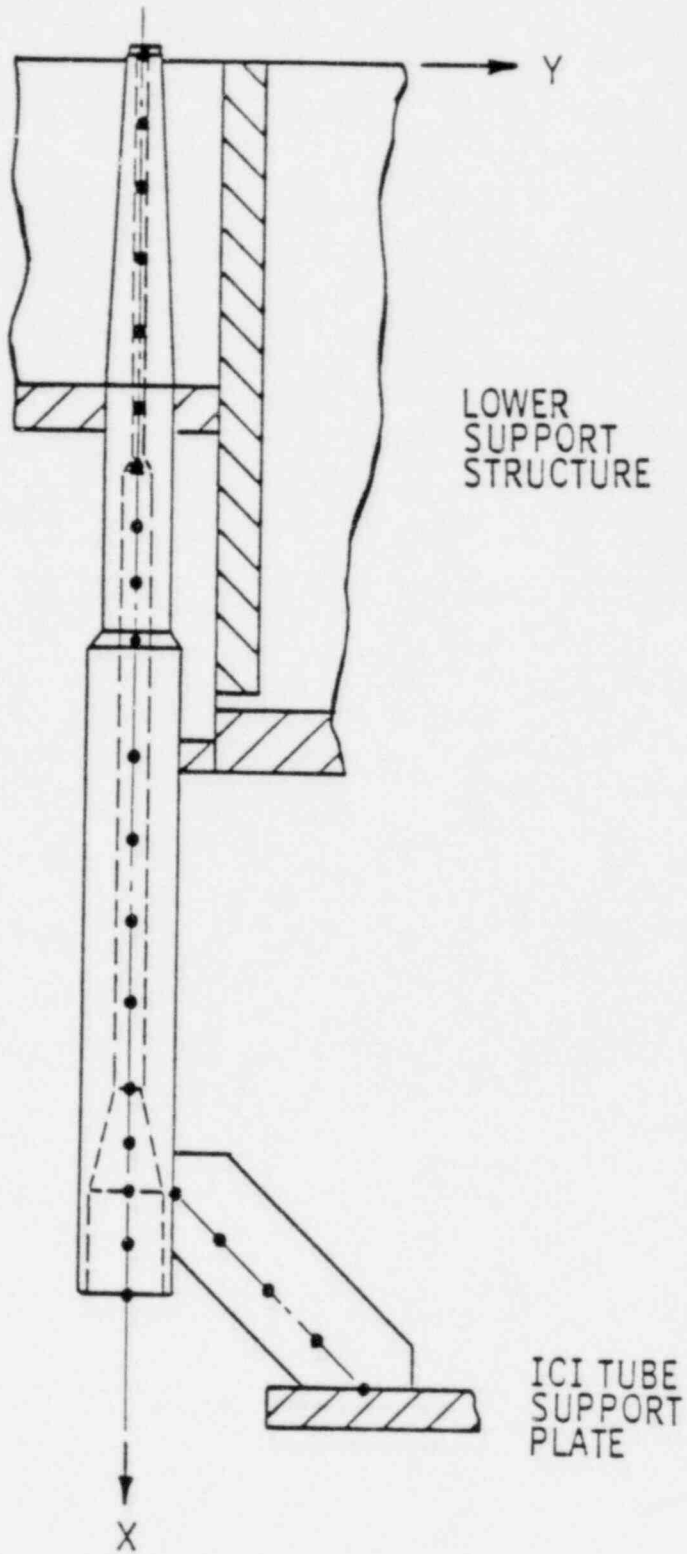
5.2.2.4.2 Response to Random Excitation

Per Section 4.2.2.2, random excitation of both the ICI tubes and support beams is caused by turbulent buffeting. The magnitude of the PSD for this excitation is assumed to be constant (white noise), as calculated in Appendix A.1.2. This spectra is used in conjunction with the finite element model, described in Section 5.2.2-3, to predict the random response at the location of instruments SB, S14 and A11.

The results of these analyses are shown in Figures 5.2-18 to 22. The random response in these figures has been plotted as an additional response over and above the deterministic levels. These are shown as both the one and three standard deviation level so as to be more useful in the evaluation of data. Response at instrument A11 under random loading is negligible.

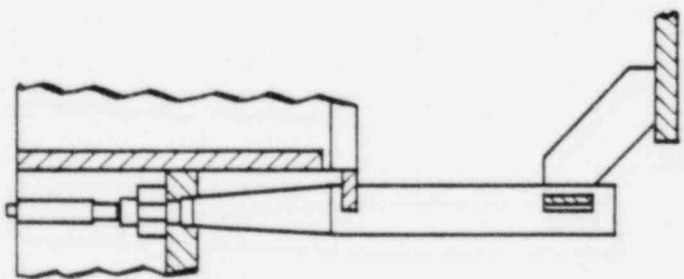
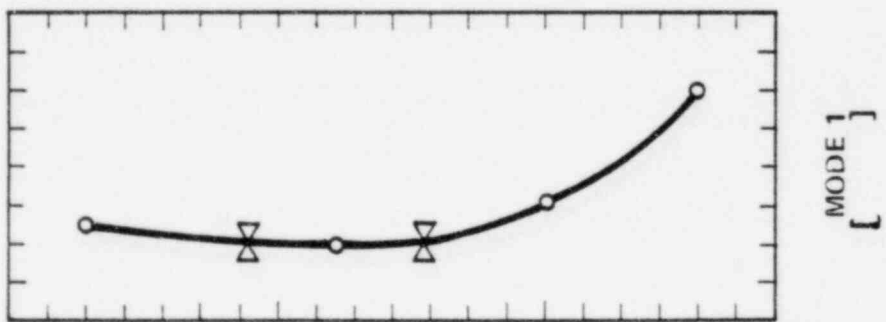
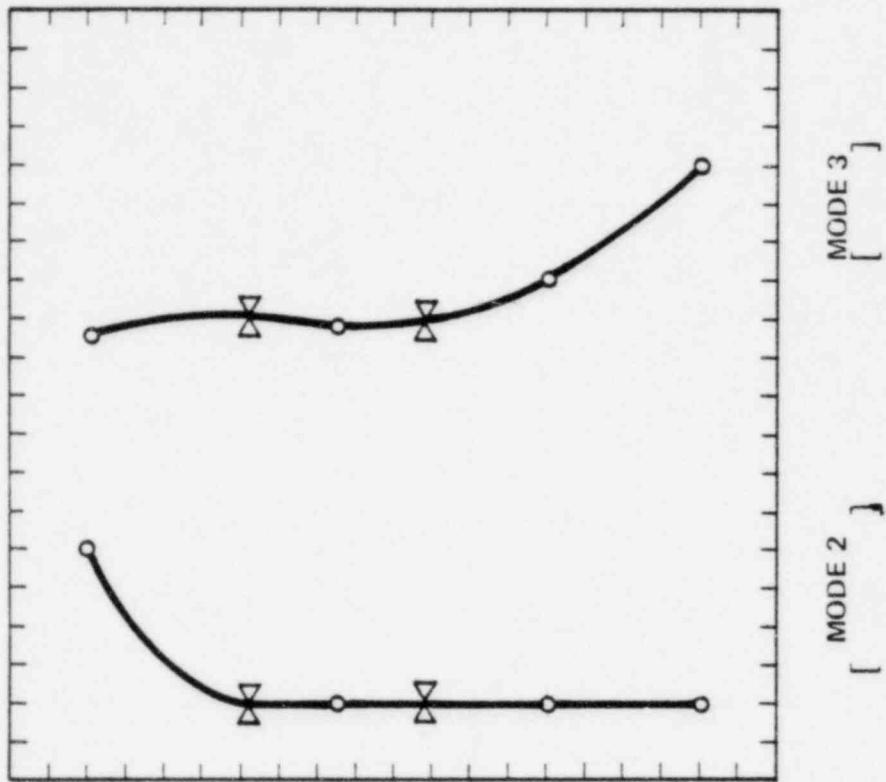


LOWER SUPPORT STRUCTURE INSTRUMENT NOZZLE ASSEMBLY;
FINITE ELEMENT MODEL
FIGURE 5.2-13



ICI SUPPORT TUBE: OUTER POSITION FINITE ELEMENT MODEL

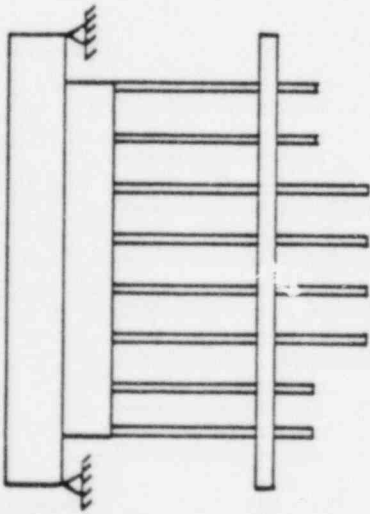
FIGURE 5.2-14



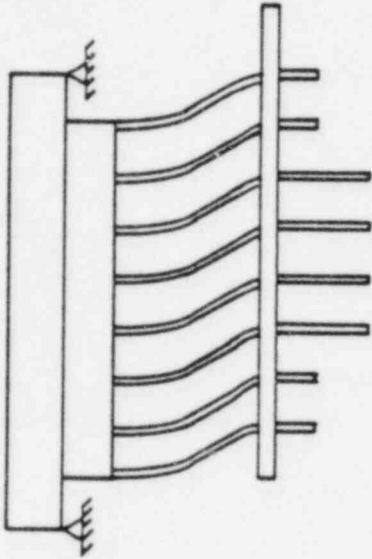
ICI NOZZLE
TYPE D

MODESHAPES AND FREQUENCIES

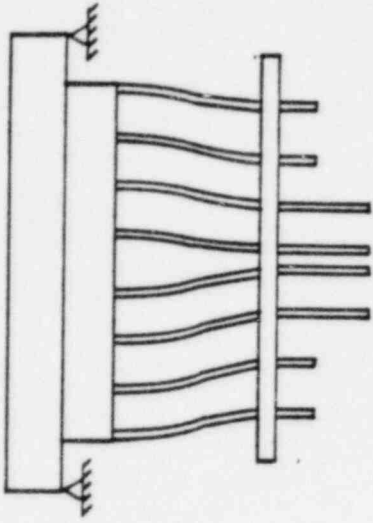
ICI NOZZLE MODE SHAPES AND FREQUENCIES
FIGURE 5.2.15



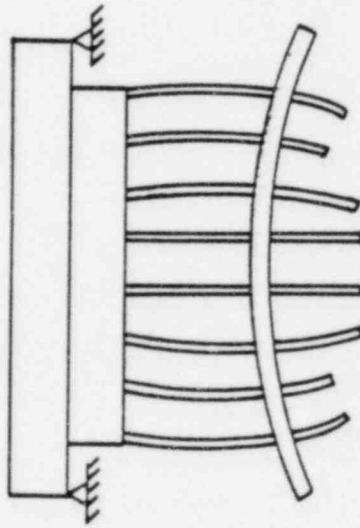
INSTRUMENT NOZZLE ASSEMBLY



MODE 1 - LATERAL



MODE 2 - LATERAL



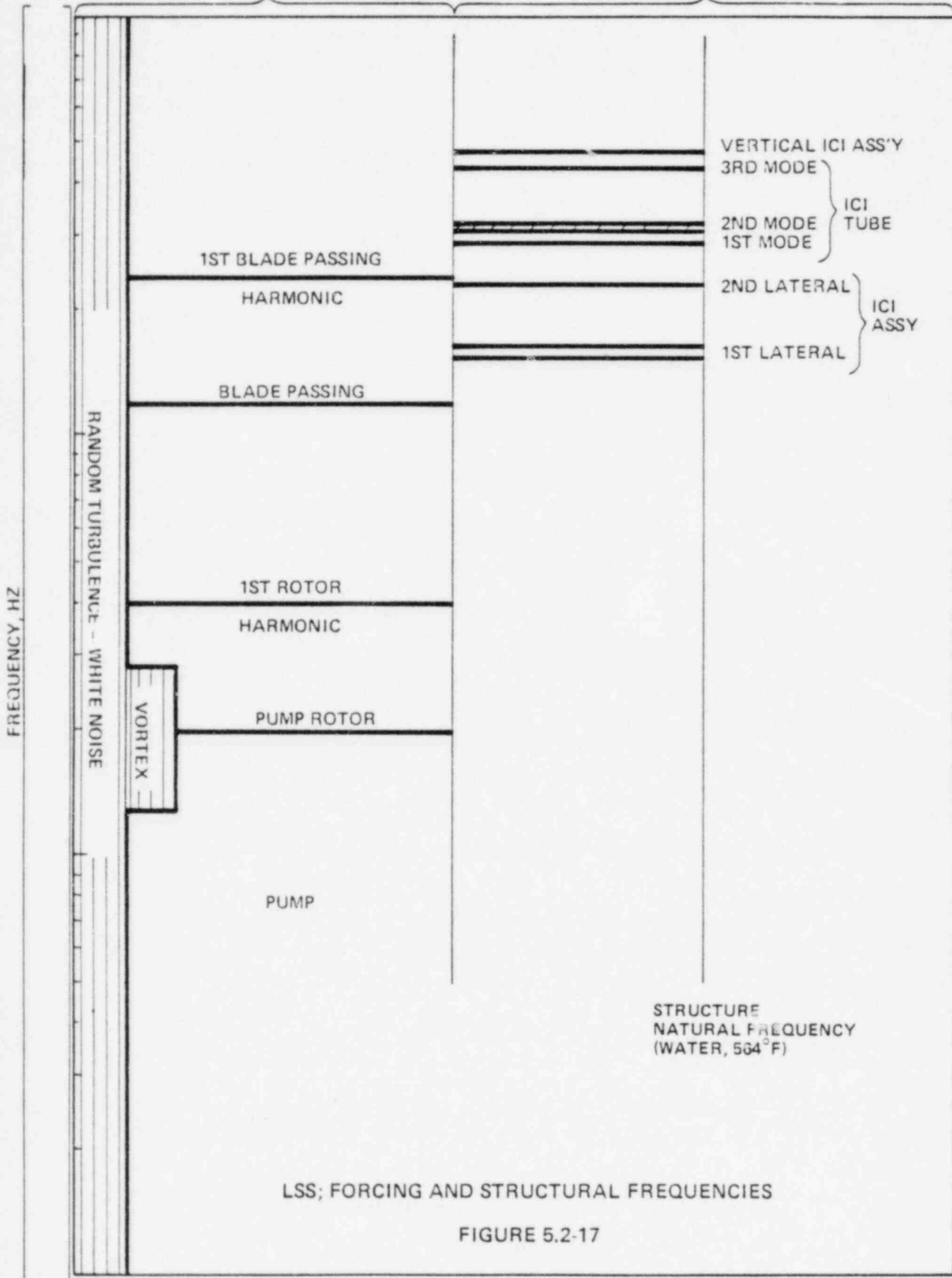
MODE 1 - VERTICAL

INSTRUMENT NOZZLE ASSEMBLY -
MODESHAPES AND FREQUENCIES
FIGURE 5.2-16

LOWER SUPPORT STRUCTURE

FORCING FREQUENCIES

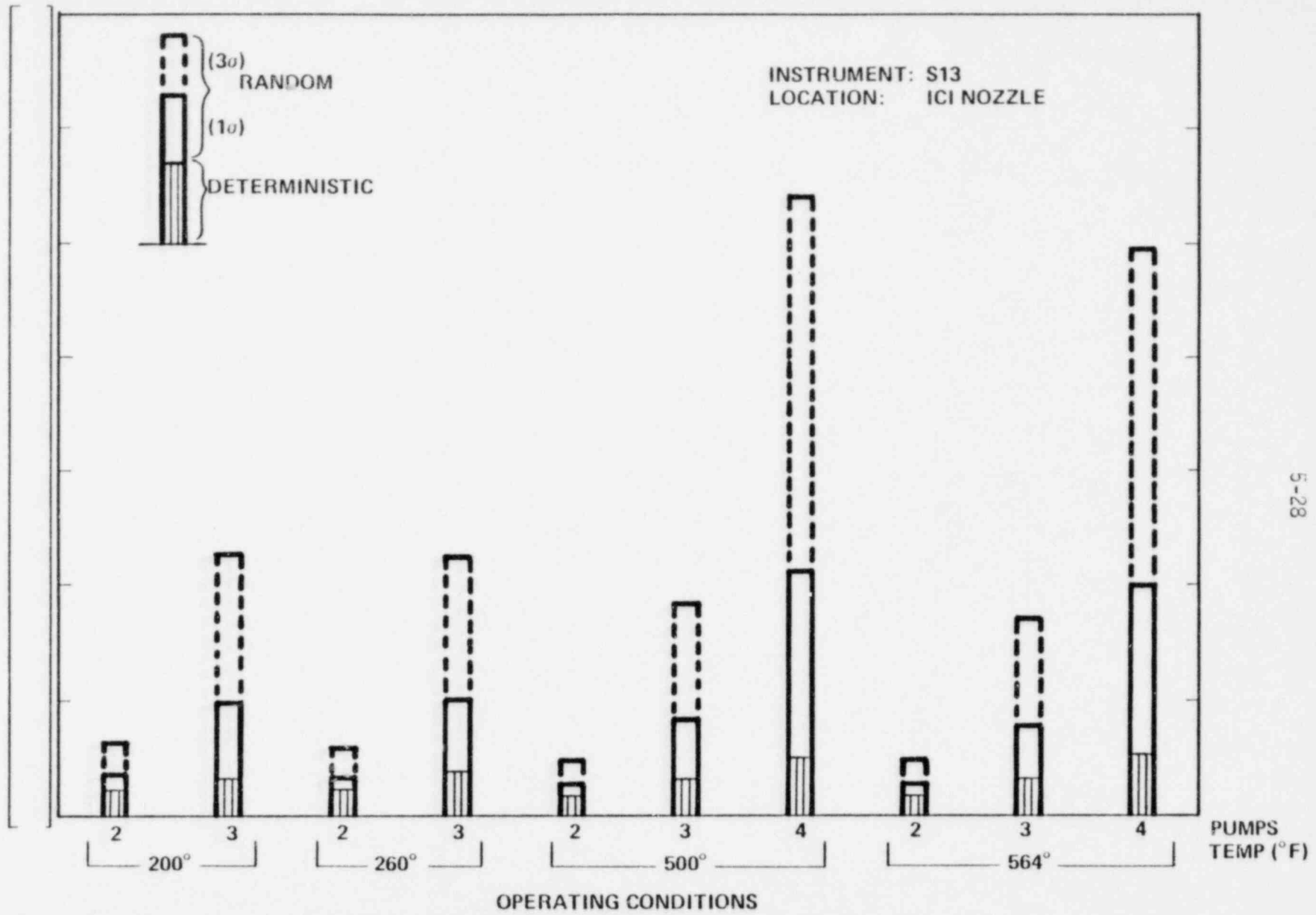
RESPONSE FREQUENCIES



LSS; FORCING AND STRUCTURAL FREQUENCIES

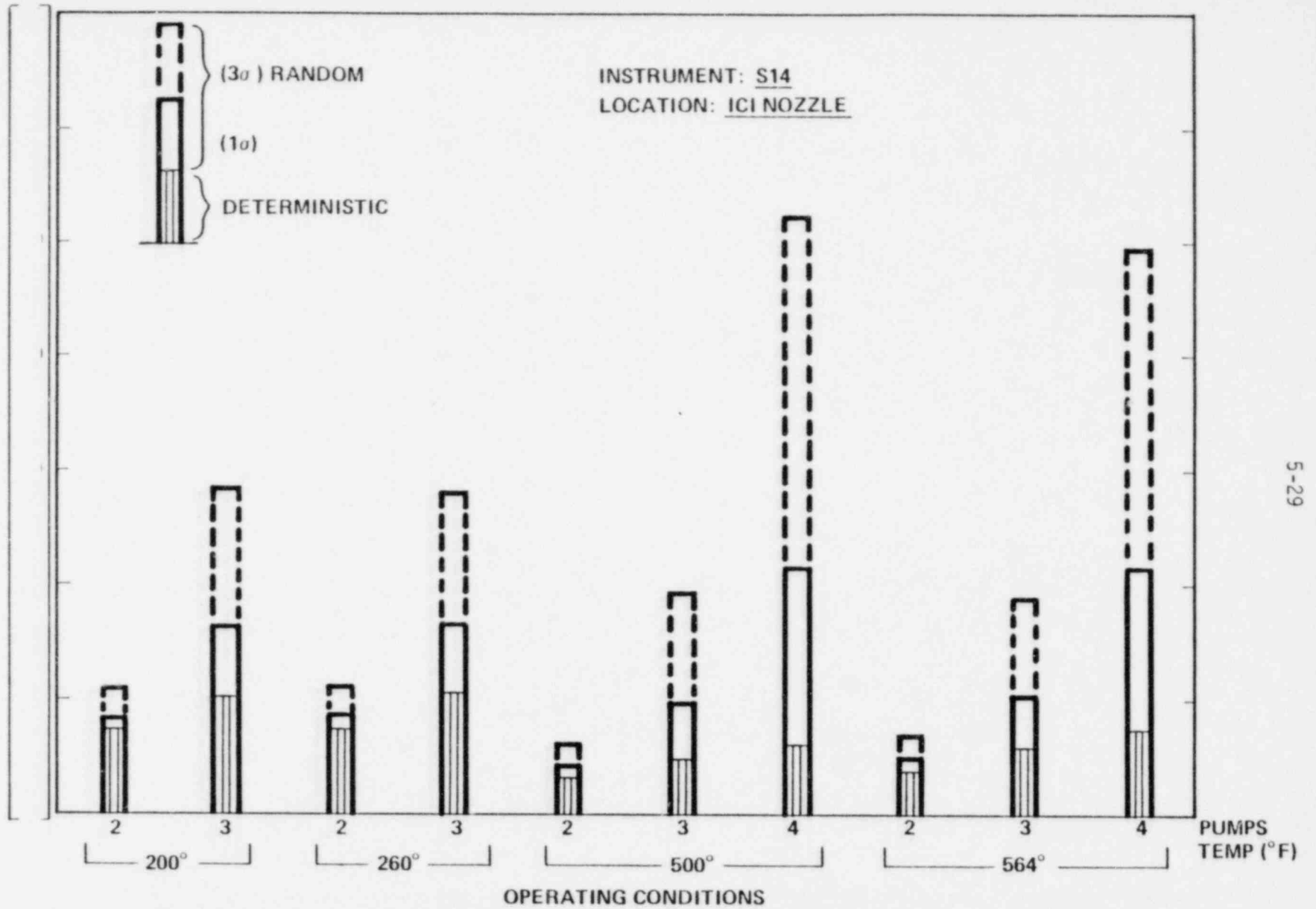
FIGURE 5.2-17

MICROSTRAIN $\sim \mu\epsilon$

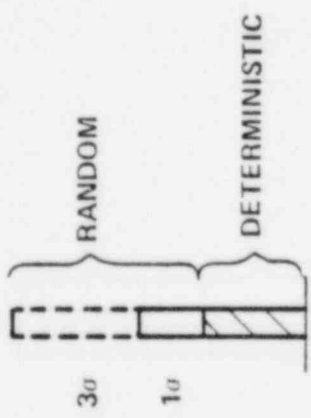


ICI NOZZLE; STRAIN; INSTRUMENT S13
FIGURE 5.2-18

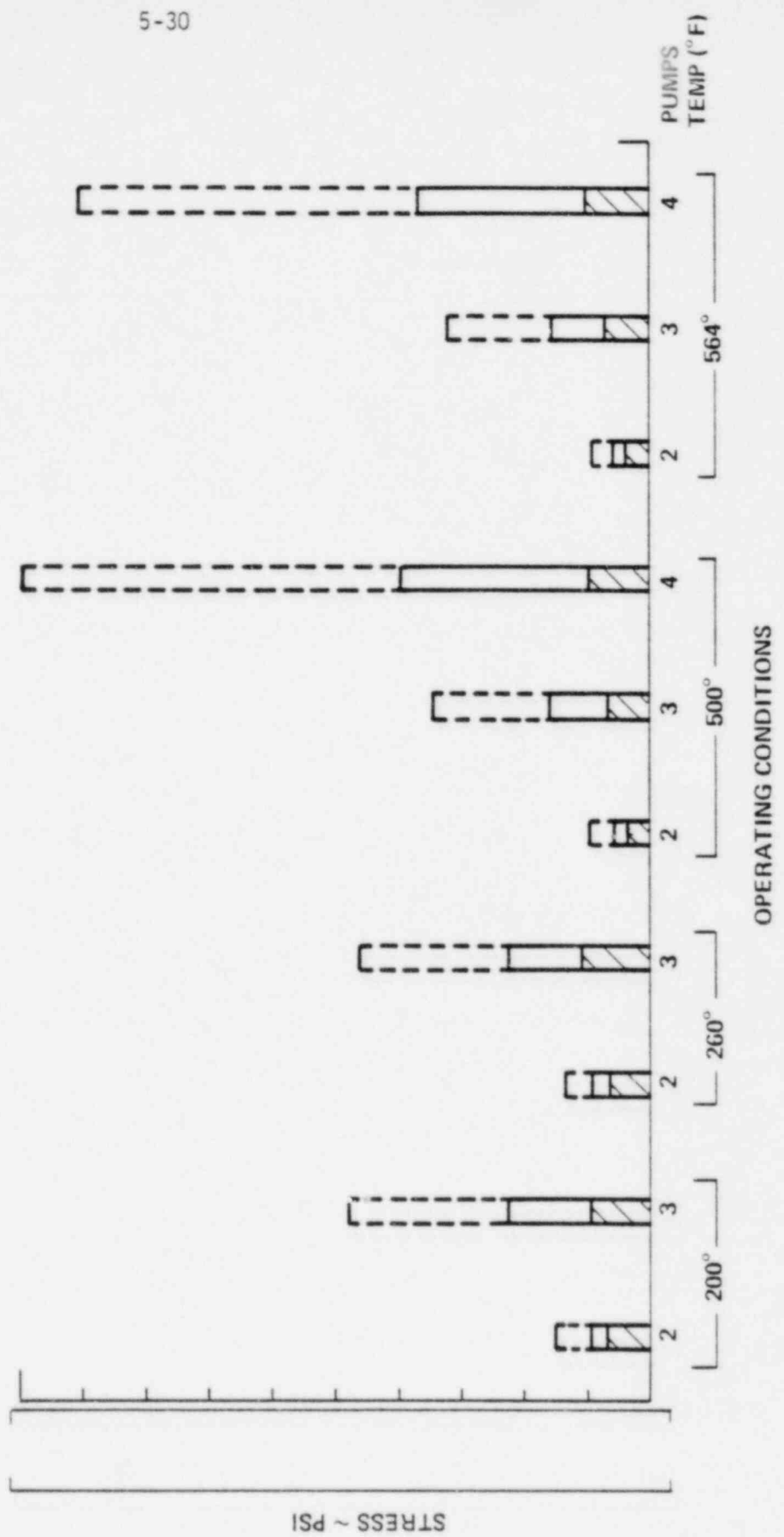
MICROSTRAIN $\sim \mu\epsilon$



ICI NOZZLE; STRAIN; INSTRUMENT S14
FIGURE 5.2-19

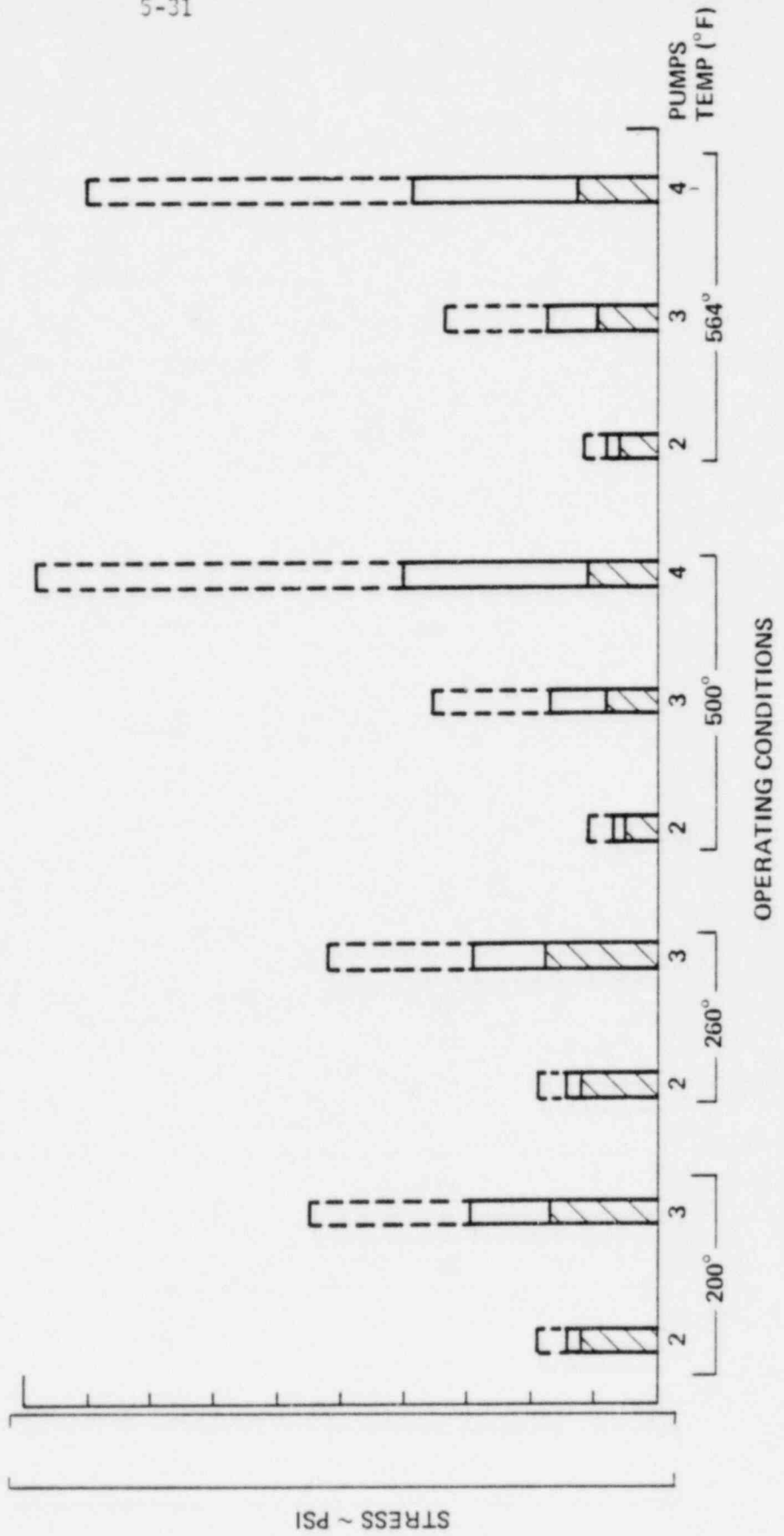
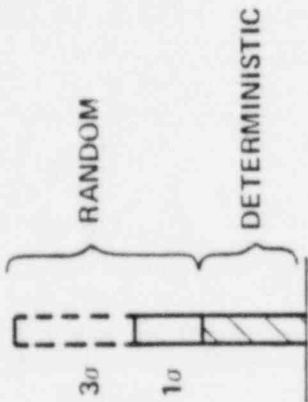


INSTRUMENTS S13
 LOCATION ICI NOZZLE

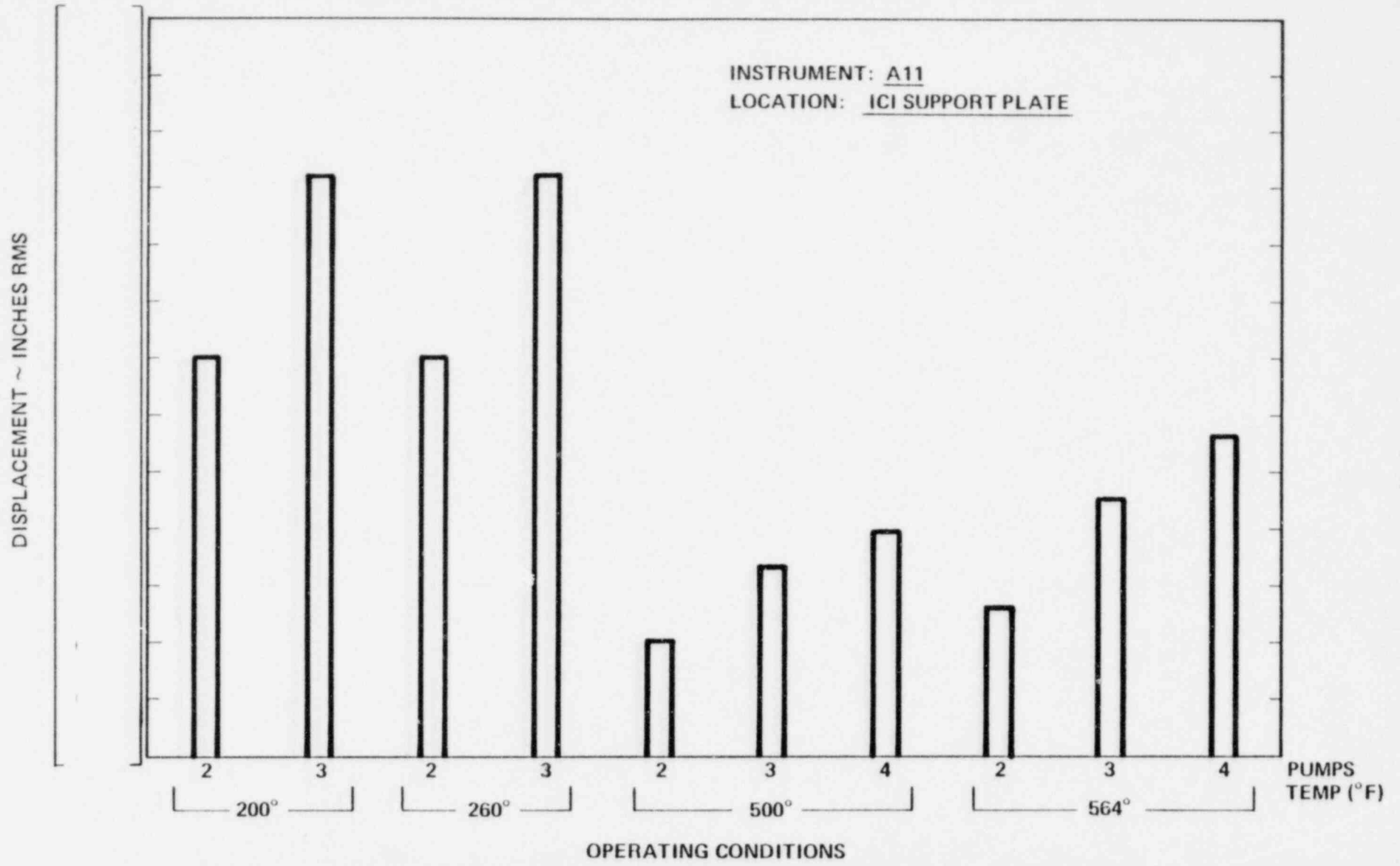


ICI NOZZLE; STRESS; INSTRUMENT S13
 FIGURE 5.2-20

INSTRUMENT: S14
 LOCATION: ICI NOZZLE



ICI NOZZLE; STRESS; INSTRUMENT S14
 FIGURE 5.2-21



ICI SUPPORT PLATE; DISPLACEMENT; INSTRUMENT ALL
 FIGURE 5.2-22

5.3 Upper Guide Structure Assembly-Analysis

5.3.1 Natural Frequencies and Mode Shapes

Mode shapes and frequencies of the various components in this assembly are found using both finite element methods and lumped mass models. Fluid effects are accounted for by adding hydrodynamic mass to the structural mass, as described in Section 5.2.2.1.

The control element shroud tubes in the upper guide structure assembly are modeled as beams supported at the ends by plate elements. The end plates are in turn supported by spring elements which represent the stiffness of the surrounding structure. A typical model of this configuration is shown in Figure 5.3-1. The STARDYNE computer code (Appendix B.2) is employed to allow the same models to be utilized for modal analysis as well as deterministic and random response analysis.

The control element shroud tube assembly, including support plate and fuel alignment plate, is modeled as a lumped mass system for a guided cantilever beam to determine of the lateral response mode. The support plate end of the assembly is considered fixed and the tubes are assumed to respond as springs in parallel. Frequency for the vertical motion of the shroud tube assembly is found using a lumped mass model with the assembly modeled as a coupled plate structure.

The barrel assembly lateral and vertical frequencies are found assuming the structure to behave as a spring and lumped mass system in the form of a cantilever shear beam fixed at the upper flange. The hydrodynamic effects of the coolant entrained in the gap between the core support barrel and the upper guide structure barrel are considered in this model.

5.3.2 Response to Periodic Loading

Response to deterministic forcing functions will result in structural response of the entire shroud tube assembly as well as of the individual tubes. Dynamic coupling between the UGS barrel assembly and CEA tube assembly is accounted for by the use of a two degree-of-freedom lumped mass model as shown in Figure 5.3-2. The mathematical solution to the second order equations for this system is programmed such that the response of the shroud tube assembly to its own excitation and that of the UGS barrel is determined. Individual tube response, to deterministic excitation, is found using the finite element model in Figure 5.3-1. This response is added to that of the shroud tube assembly to determine the total tube response.

5.3.3 Response to Random Excitation

The upper guide structure will not respond to random excitation as a complete assembly but rather will experience local disturbances of individual components within the assembly. The results of flow testing conducted on a 1/4 scale shroud tube assembly model (Ref. 31) are utilized here to determine the random responses of the shroud tubes and support plates. The model used in the testing was designed so that the resulting dynamic strains could be scaled directly to prototype levels of loading. Data reduction techniques used in this testing allowed for the separation of the random response from the deterministic response over the range of thermal and hydraulic test conditions. The test results allow midspan displacement of the tubes at various flow conditions to be found as a function of the recorded dynamic strains. This is utilized to predict the response of levels at all CVAP test conditions.

5.3.4 Upper Guide Structure-Results of the Analysis

5.3.4.1 Natural Frequencies and Mode Shapes

Free vibration analyses of the control element shroud tubes, shroud tube assembly, UGS barrel assembly and complete upper guide structure assembly were performed using the methods previously described to obtain the system natural frequencies and mode shapes.

The frequency of lateral motion of any individual CEA shroud tube is a function, through hydrodynamic coupling, of the number of surrounding tubes (Ref. 32, 34). The hydrodynamic mass effect, associated with this coupling, is a function of the relative motion between tubes. The hydrodynamic mass will be greater with the relative motion out-of-phase and smallest for the motion in-phase. The result is a range in values of frequency for an individual tube. The maximum (out-of-phase) and minimum (in-phase) frequencies are found for the first four lateral modes. Modes higher than the fourth are not calculated since they are out of the forcing frequency range. The first four mode shapes and their frequencies are shown in Figure 5.3-3.

The shroud tube assembly is represented by a single degree of freedom model in both lateral and vertical directions. As such, only the first mode is computed in each direction. These mode-shapes and frequencies are shown in Figure 5.3-4.

The UGS barrel assembly lateral and vertical modes are representative of those for a cantilevered shear beam. The first mode in each direction is chosen as being the most significant and these are illustrated in Figure 5.3-5.

The complete UGS assembly, which includes both the shroud tubes and barrel assembly, has been treated as a two degree of freedom system in both the lateral and vertical directions. The resulting mode

shapes and resonant frequencies are shown in Figure 5.3-6. A summary of the predicted frequencies for this assembly are shown in Table 5.3-1.

5.3.4.2 Response to Periodic Loading

Utilizing the structural natural frequencies and mode shapes obtained from the analysis in Section 5.3.4.1, together with the periodic hydraulic forcing functions (Appendix A.2.2), the methods of Section 4.3 were used to obtain the structural response of the UGS assembly. Flow testing performed on a 1/4 scale, one quadrant model of the CEA shroud tube region indicated the most adversely loaded portions of the assembly to be the shroud tubes located near the outlet nozzle. The response analysis of these tubes has been done to predict the instrument readings at these locations for all CVAP test conditions.

The results of the analyses are presented in Figures 5.3-7 to -13. These figures indicate the expected strain and acceleration response levels at the instrument locations noted on the respective figures for the various test conditions discussed in Section 1.3.

5.3.4.3 Response to Random Excitation

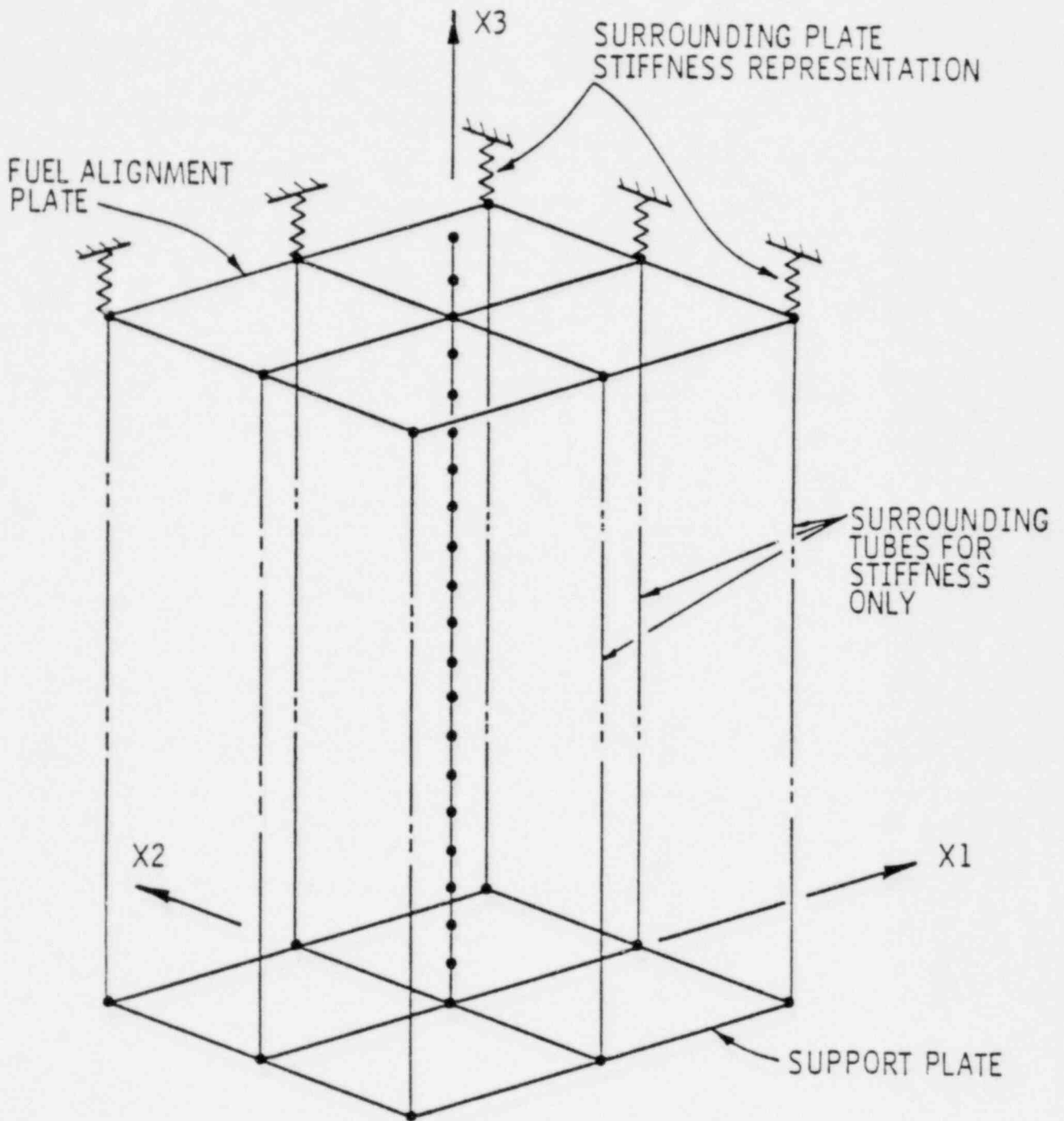
Power spectral density levels of random excitation are based on response values recorded during scale model development tests. Using these data (Appendix A.2.2) and the methodology of Section 5.3.3 the random responses of the UGS assembly at the various instrument locations are determined for the test conditions noted in Section 1.3.

The results of the analyses are presented in Figures 5.3-7 to -13.

TABLE 5.3-1

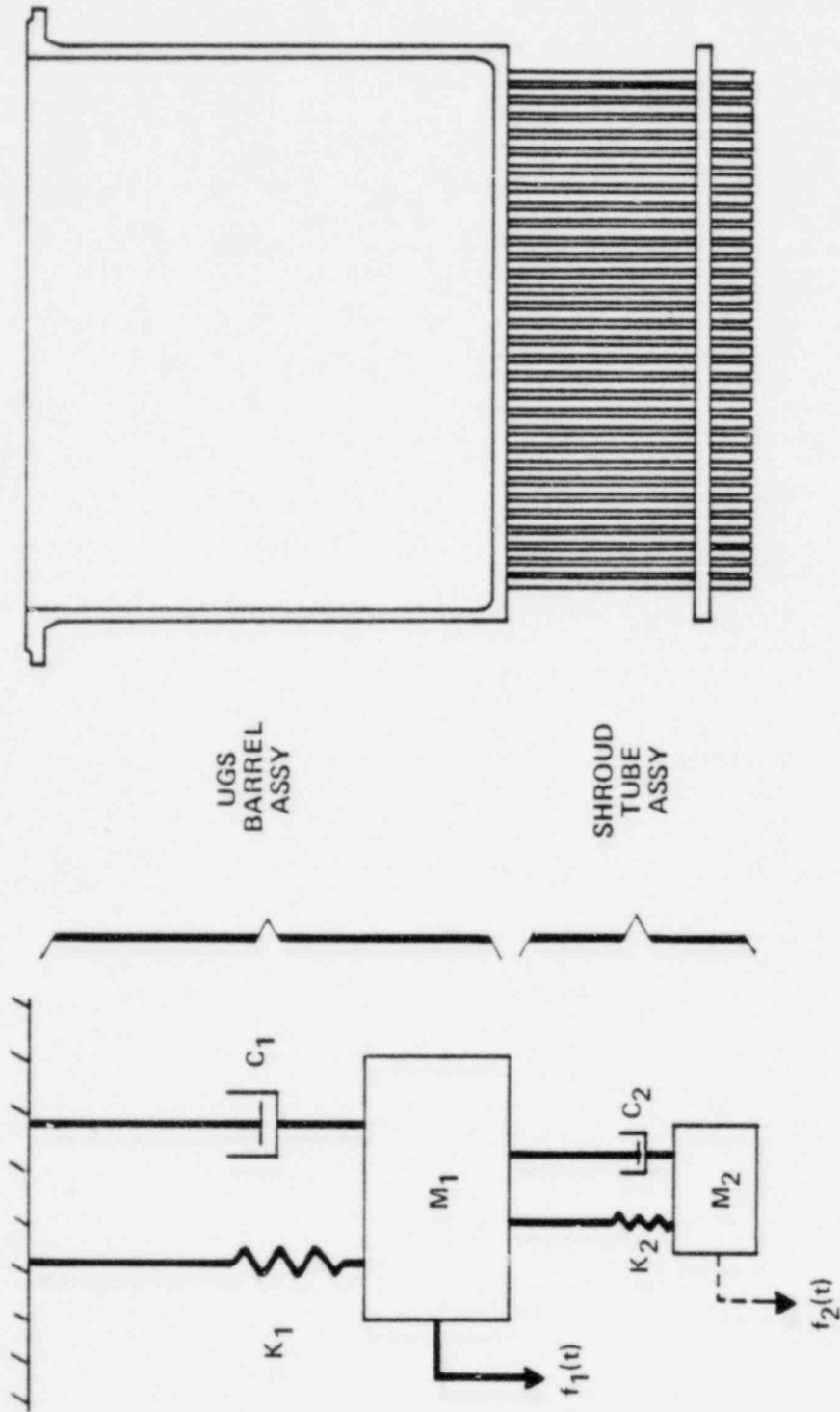
UGS IN WATER (564°F) FREQUENCY SUMMARY

COMPONENT	NATURAL FREQUENCIES (HZ)				
	LATERAL			VERTICAL	
	1	2	3	1	2
CEA Shroud Tubes Shroud Tube Assembly UGS Barrel Assembly UGS Complete Assembly					



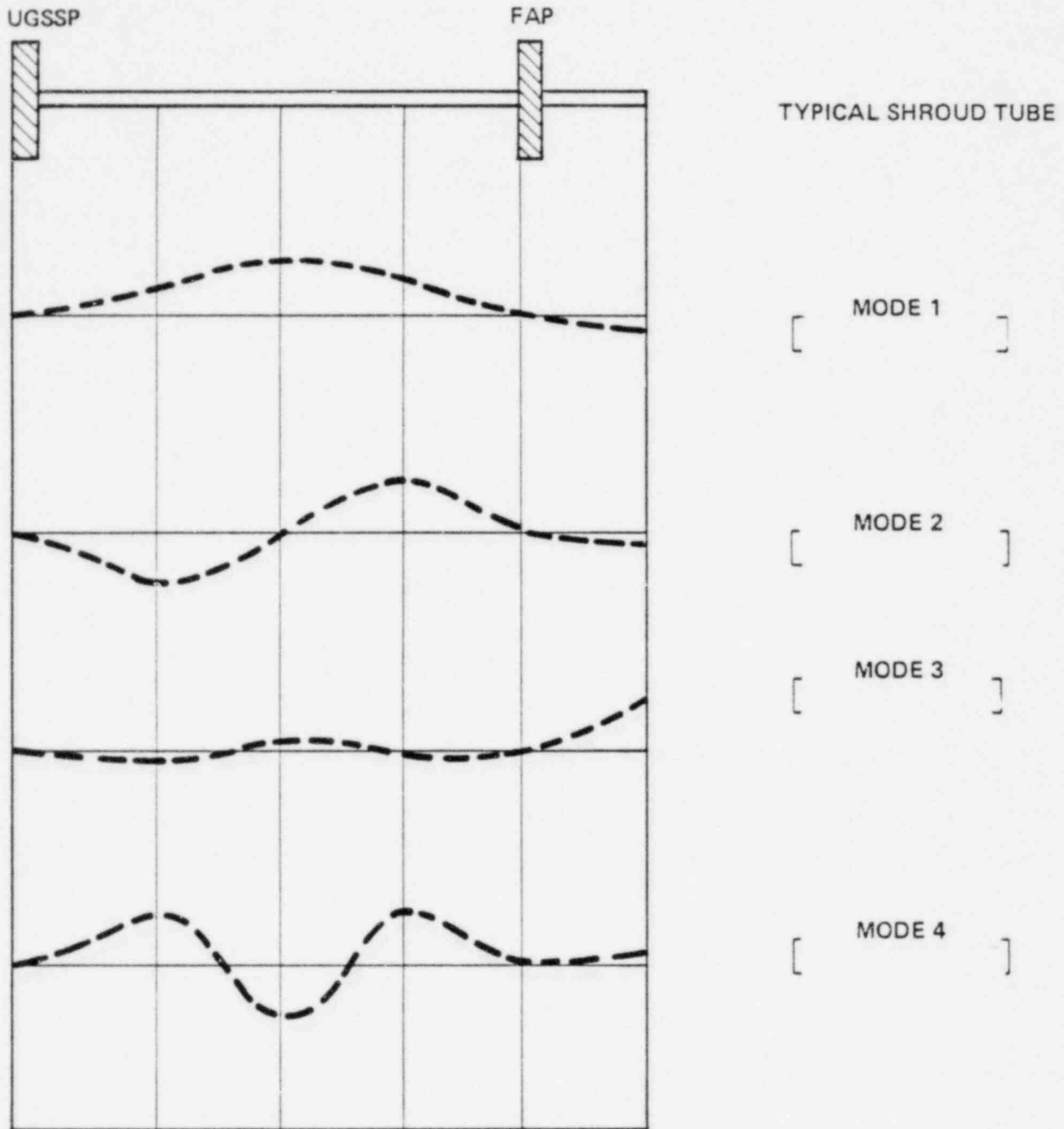
CONTROL ELEMENT SHROUD TUBE;
FINITE ELEMENT MODEL

FIGURE 5.3-1

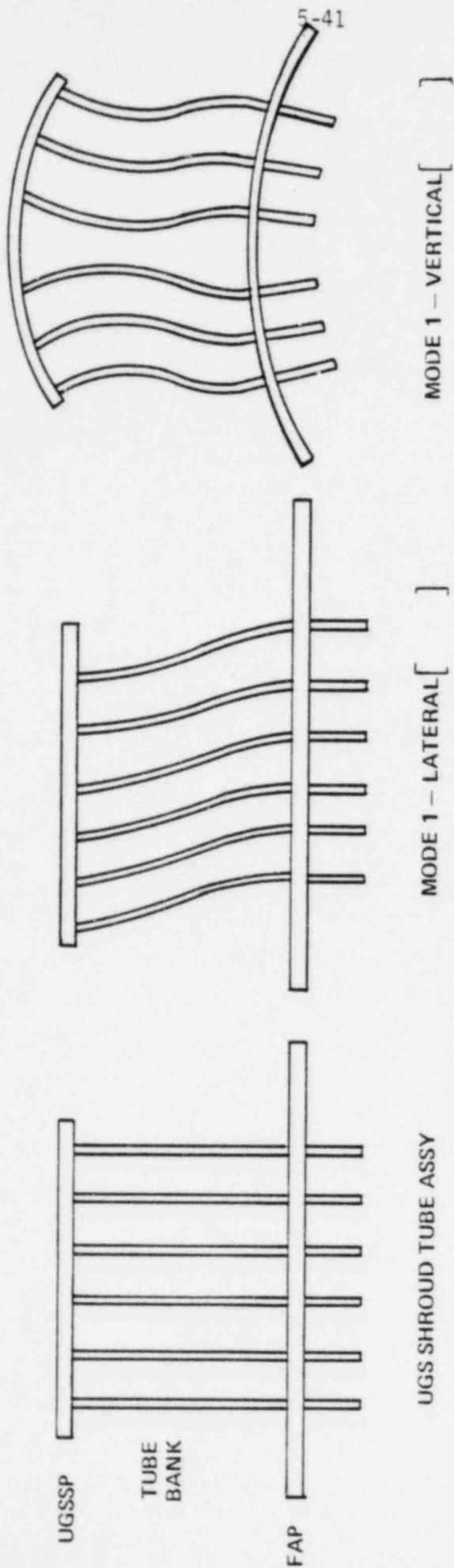


DYNAMIC RESPONSE MODEL OF UGS ASSY

FIGURE 5.3-2



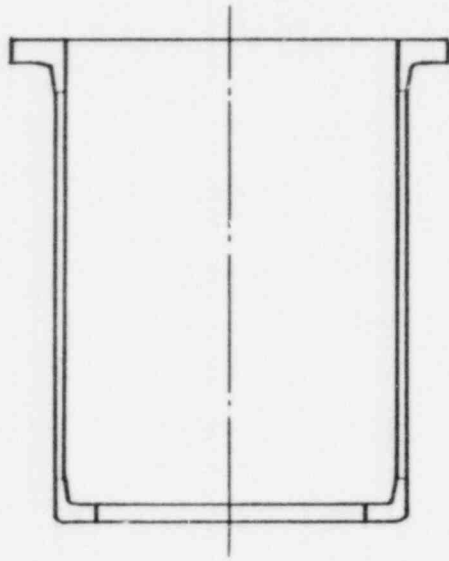
CEA SHROUD TUBE
 NATURAL FREQUENCIES & MODESHAPES
 FIGURE 5.3-3



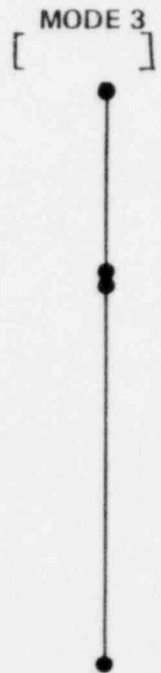
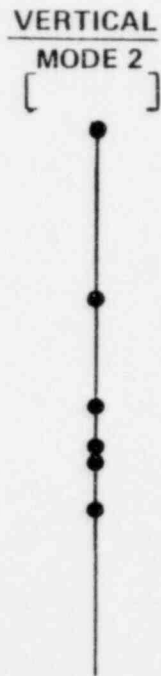
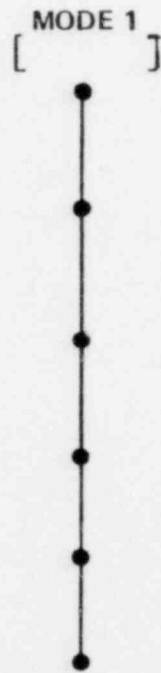
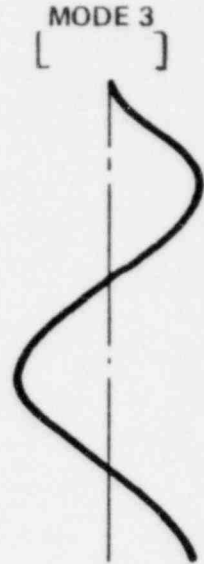
UGS SHROUD TUBE ASSY NATURAL FREQUENCIES & MODES: APES

FIGURE 5.3-4

MODESHAPES AND FREQUENCIES

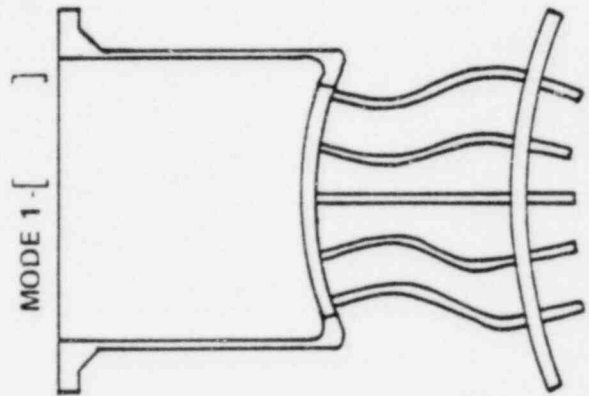
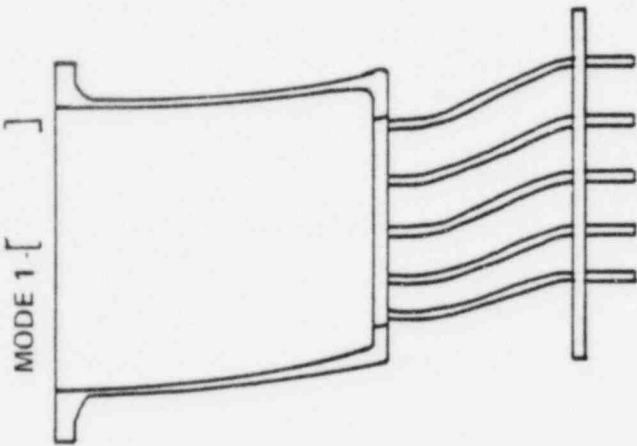
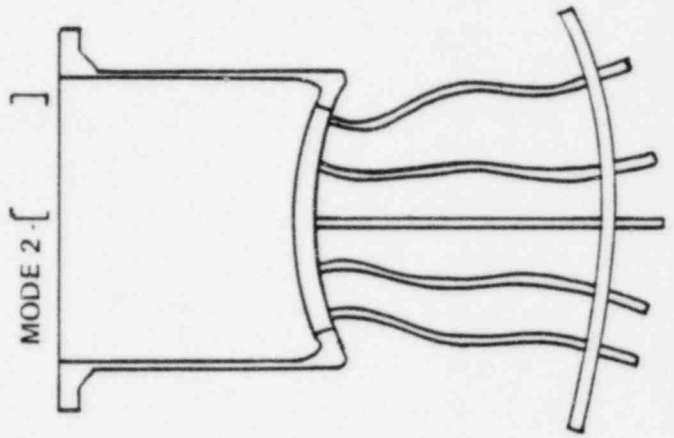
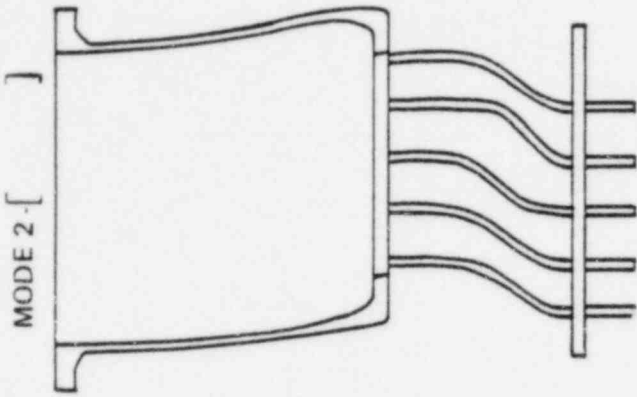


UGS BARREL ASSEMBLY

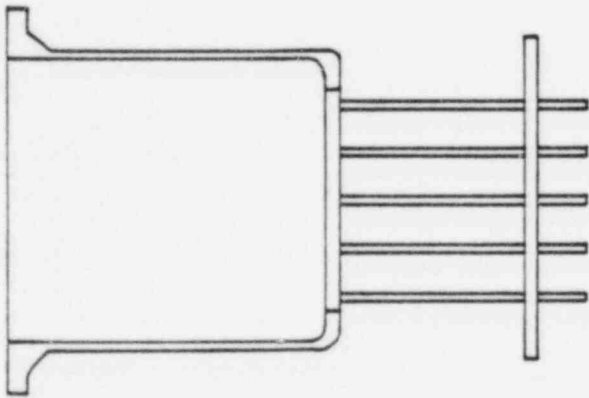


UGS BARREL ASSEMBLY; MODE SHAPES AND FREQUENCIES
FIGURE 5.3-5

LATERAL



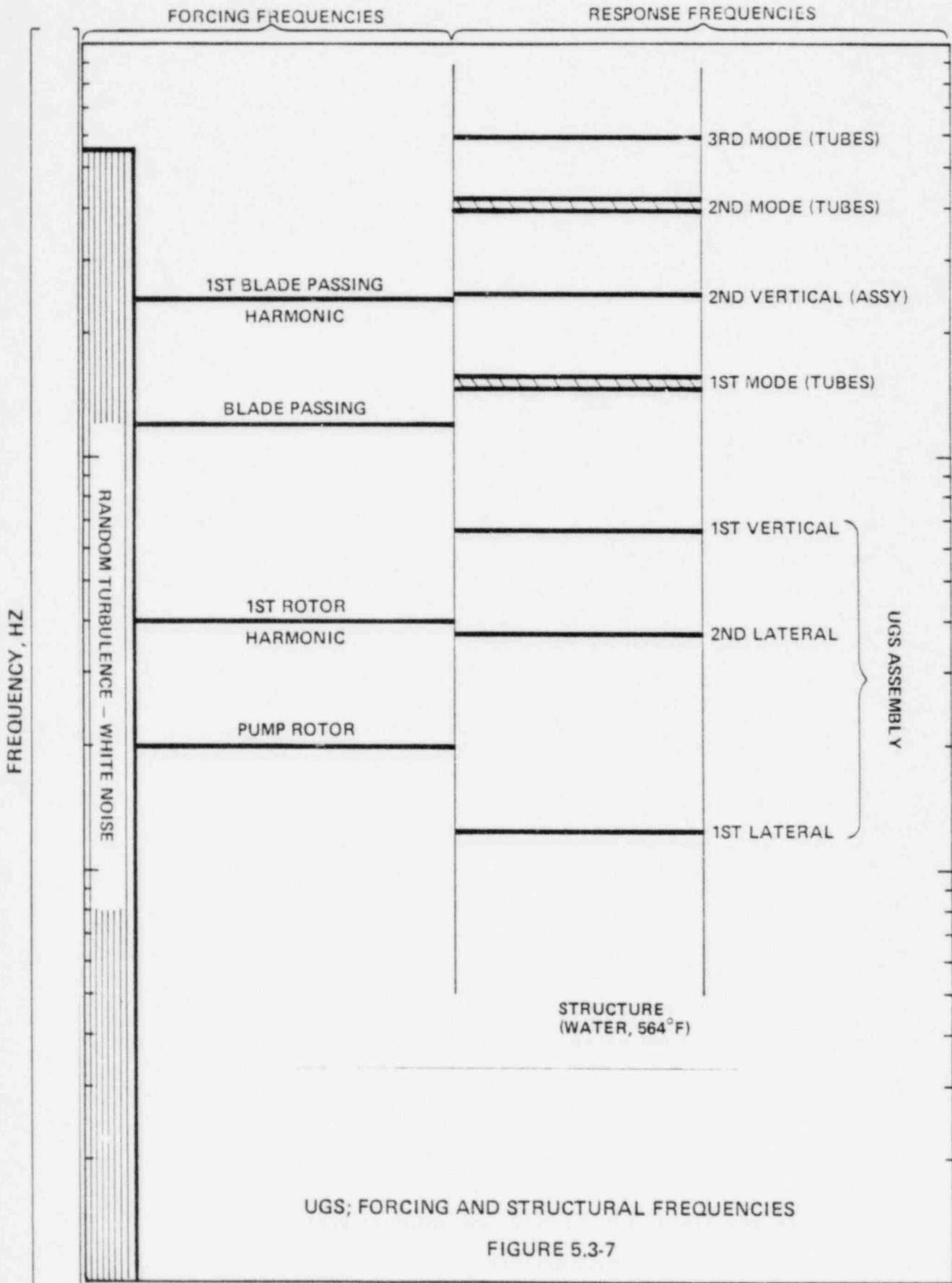
VERTICAL



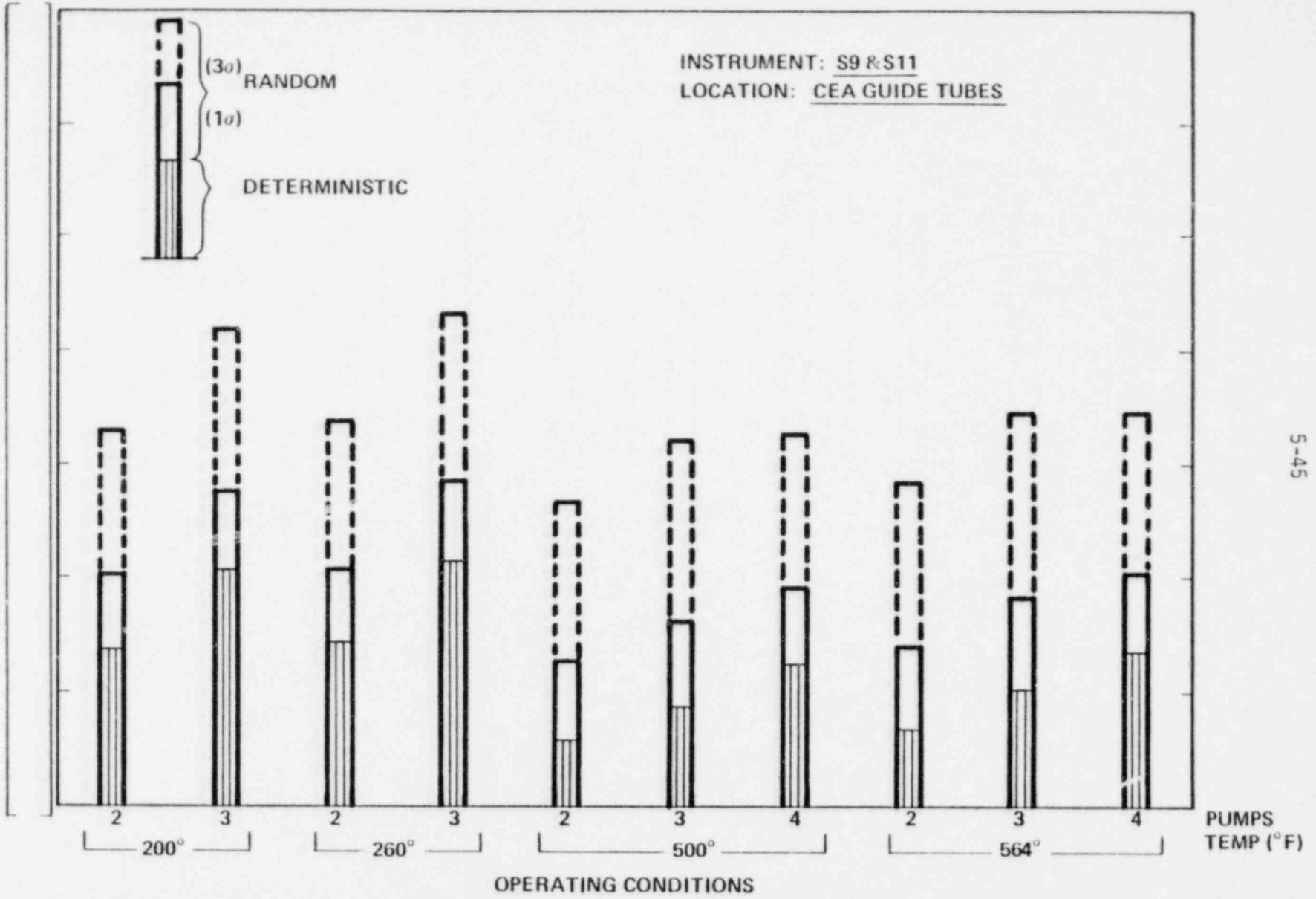
UGS ASSY
MODE SHAPES AND
FREQUENCIES

UGS ASSEMBLY; MODE SHAPES AND FREQUENCIES
FIGURE 5.3-6

UPPER GUIDE STRUCTURE ASSY

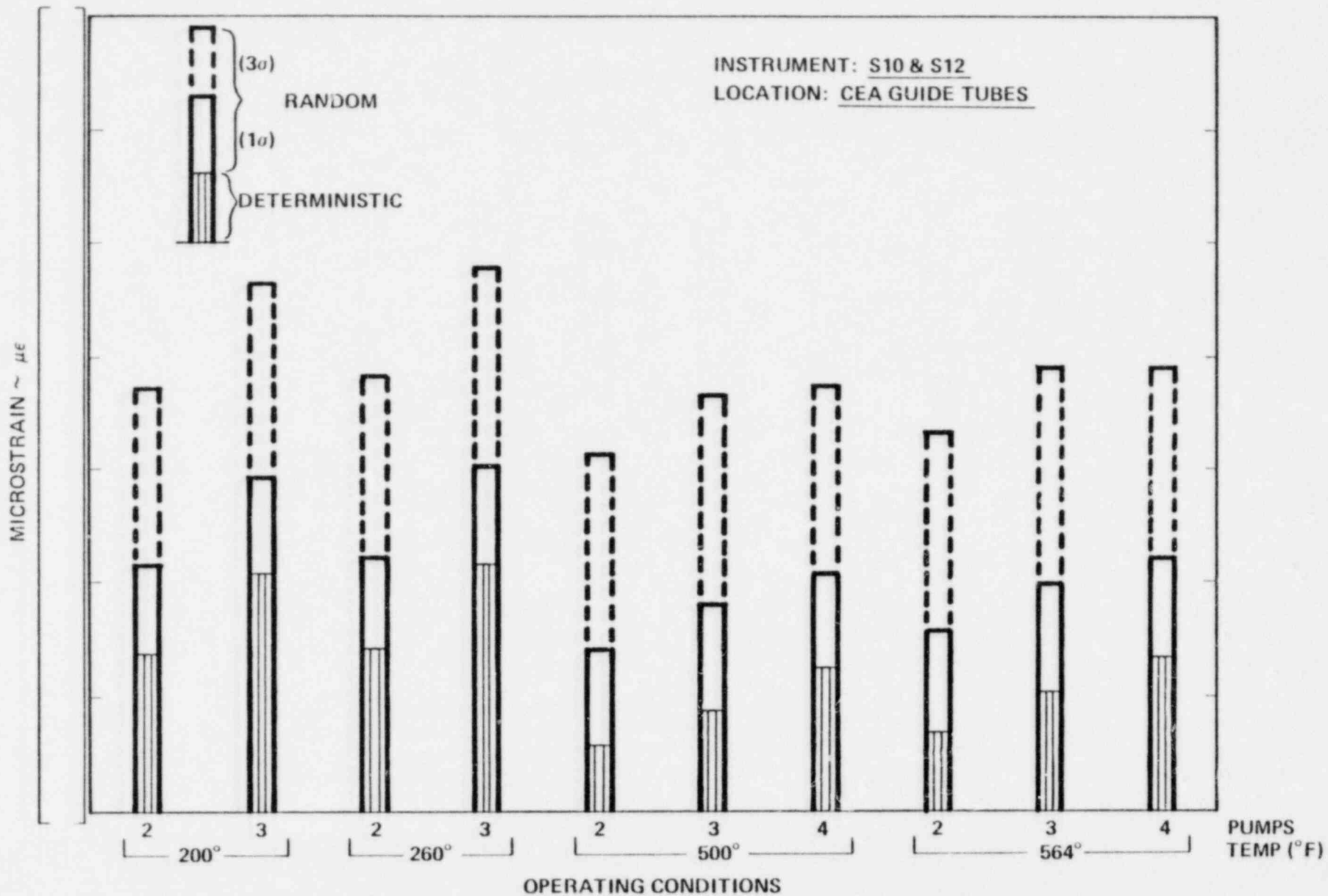


MICROSTRAIN $\sim \mu\epsilon$



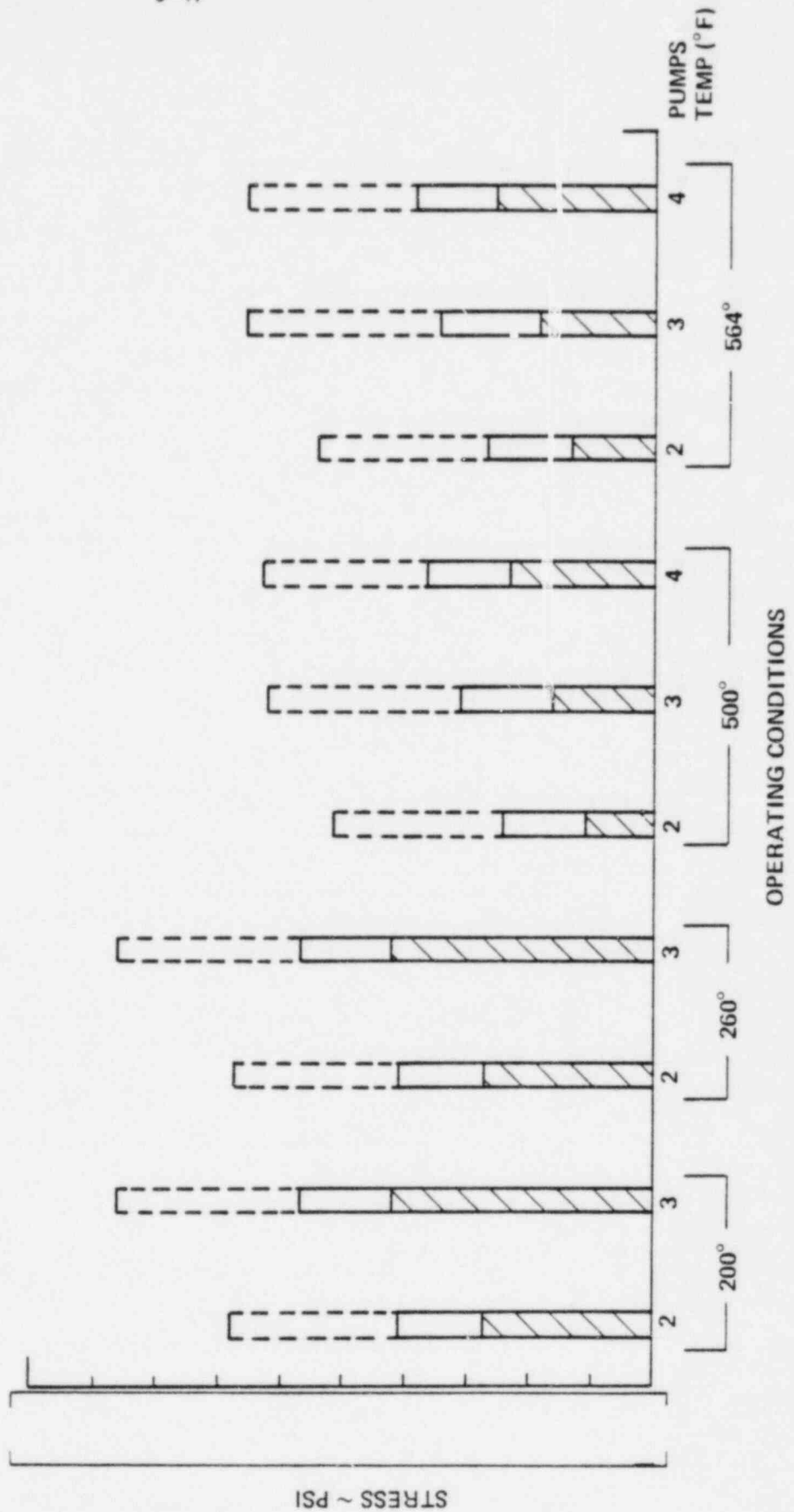
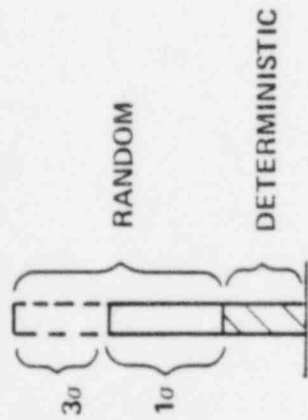
5-45

CEA GUIDE TUBES; STRAIN; INSTRUMENTS S9, S11
FIGURE 5.3-8



CEA GUIDE TUBES; STRAIN; INSTRUMENTS S10, S12
FIGURE 5.3-9

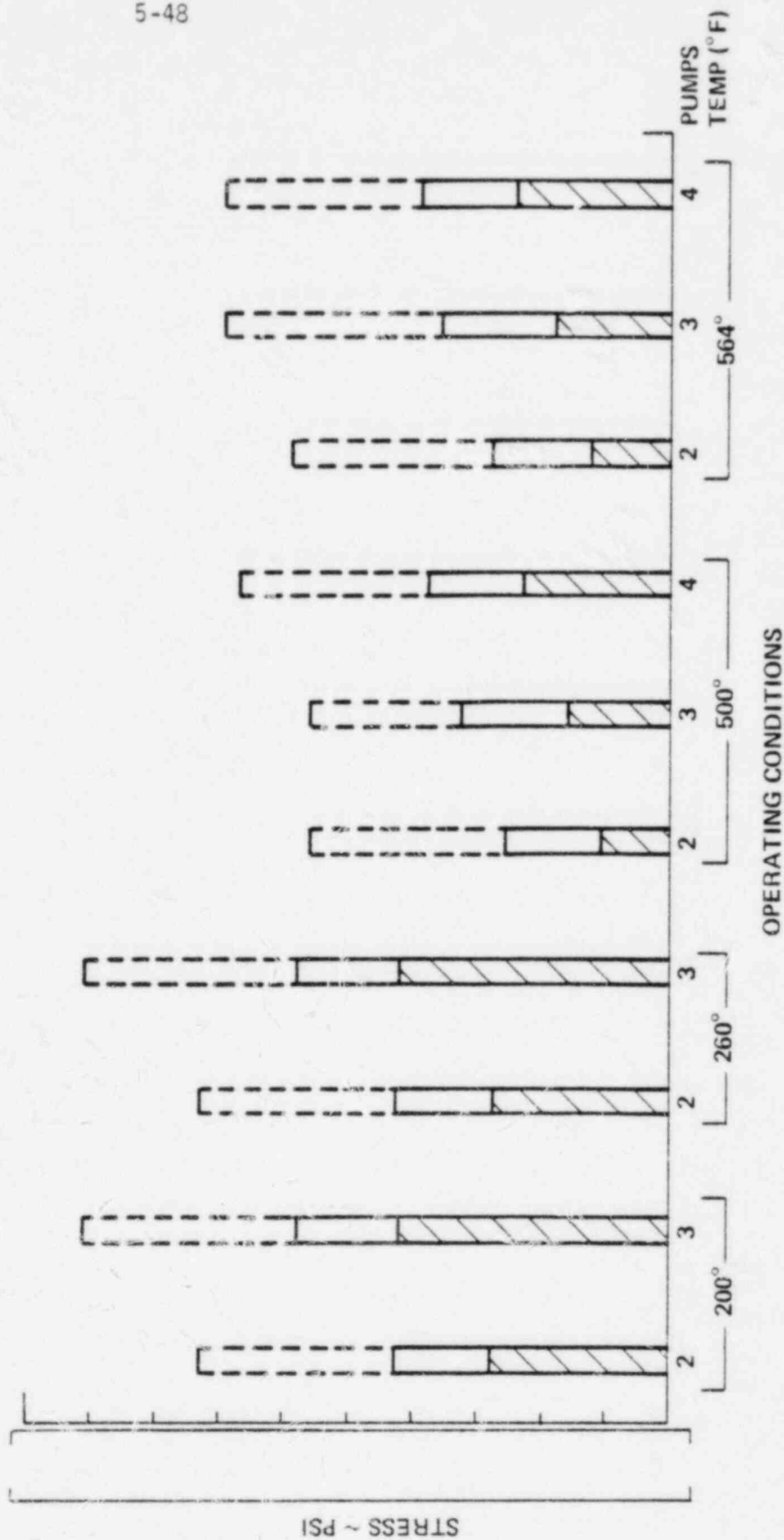
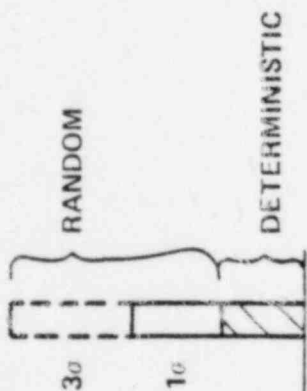
INSTRUMENTS S9 & S11
 LOCATION CEA GUIDE TUBES



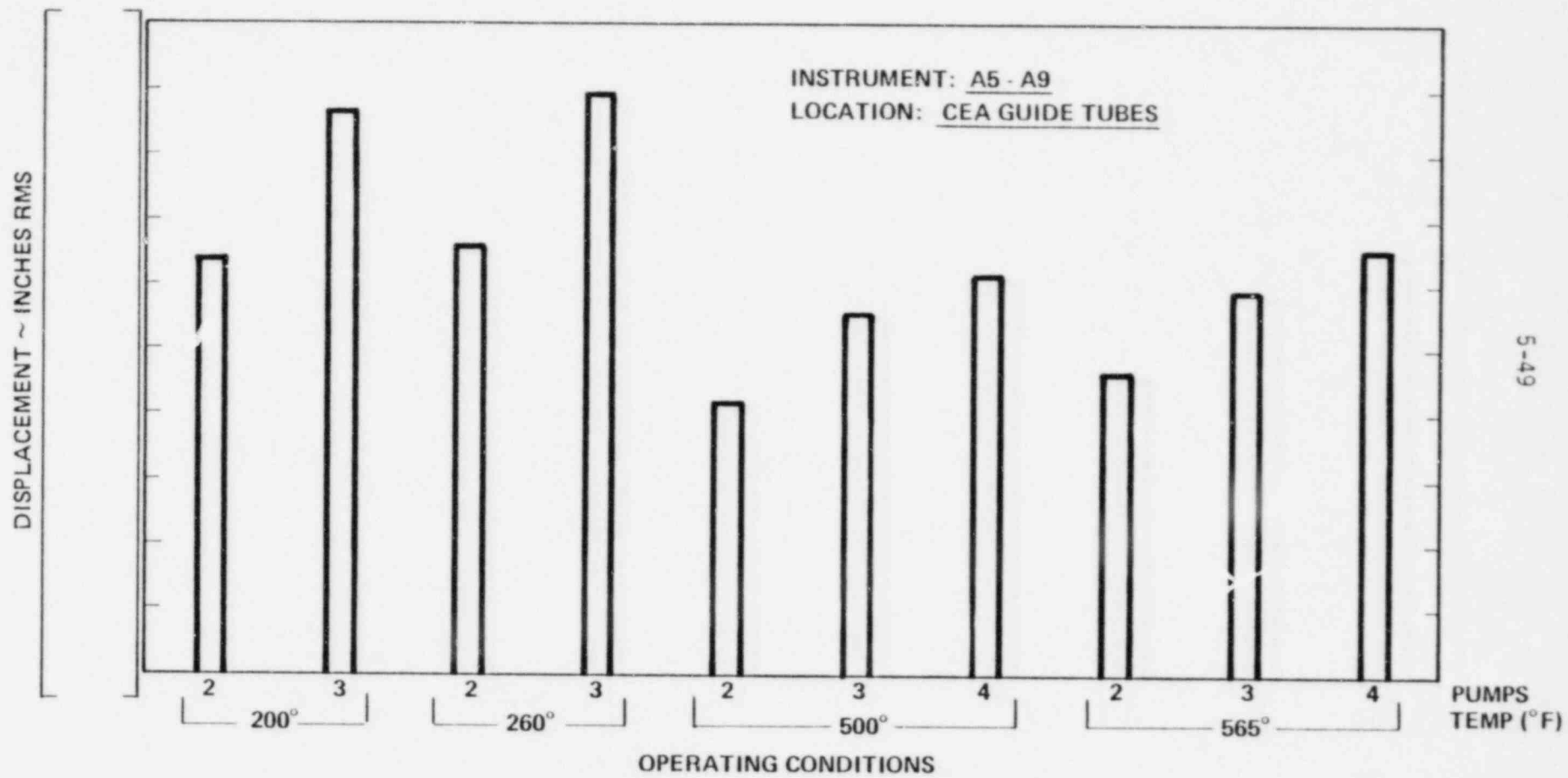
CEA GUIDE TUBES; STRESS; INSTRUMENTS S9, S11

FIGURE 5.3-10

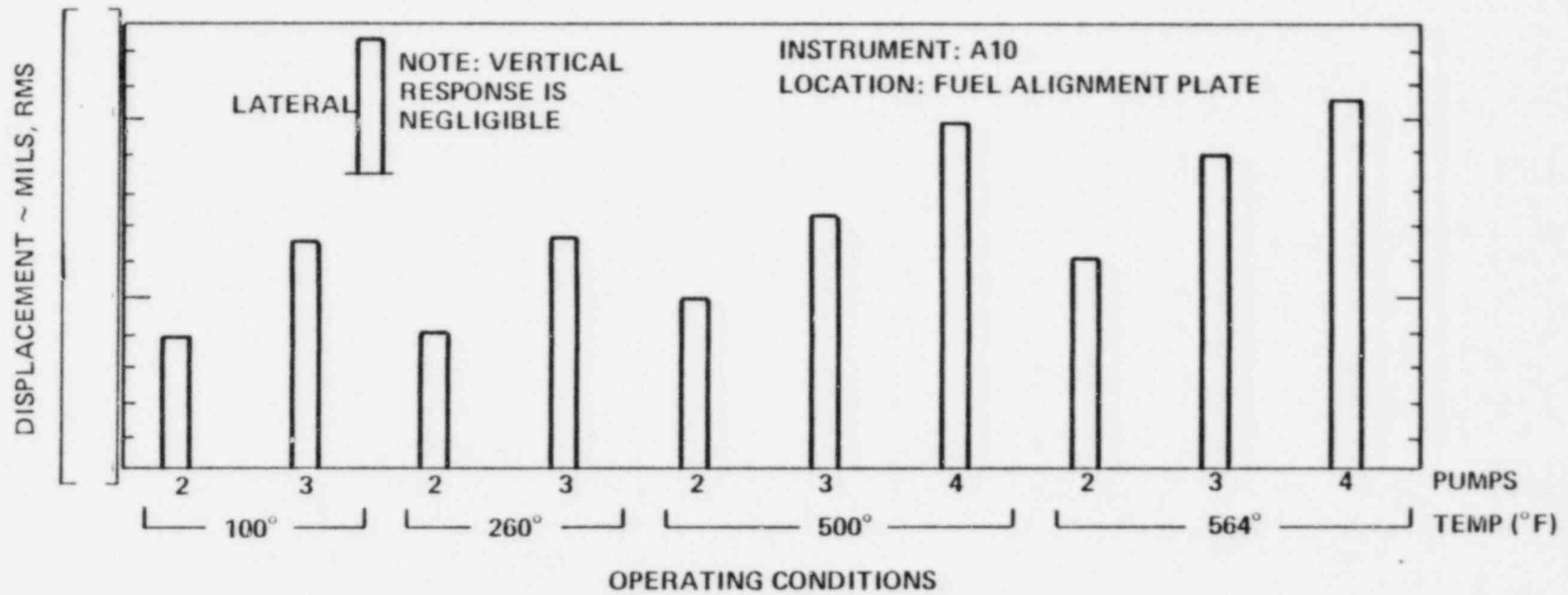
INSTRUMENT: S10 & S12
 LOCATION: CEA GUIDE TUBES



CEA GUIDE TUBES; STRESS; INSTRUMENTS S10, S12
 FIGURE 5.3-1



CEA GUIDE TUBES; DISPLACEMENT; INSTRUMENTS A5 TO A9
 FIGURE 5.3-12



5-50

FUEL ALIGNMENT PLATE DISPLACEMENT; INSTRUMENT A10
FIGURE 5.3-13

5.4 Maximum Values of Stress and Values of Stress Margin

5.4.1 Primary Stresses

As summarized in Section 1.5, the ASME Code requires that core support structures meet stress limits based on elastic behavior and fatigue damage. The elastic limit is based on the maximum stress intensities, considering primary membrane, bending and secondary stresses, being less than some multiple of the S_m value for the material (16,100 psi). CVAP test conditions being isothermal there are no secondary stresses due to thermal growth. The maximum values of alternating stress are thus equal to the primary membrane plus bending stress intensity which can then be compared to the Code Limit of $1.5 S_m$. These are summarized in Table 5.4-1, both for test conditions corresponding to normal operation and test conditions at which the maximum stress occurs. The table also lists margins for the design values of membrane plus bending stresses listed in Tables 1.5-1 and 1.5-2. The design margins are larger by an order of magnitude than the CVAP margins.

5.4.2 Fatigue

Per section 1.5.2, margin for fatigue can be defined as

$$\text{Fatigue Margin} = \frac{\text{Endurance Limit}}{\text{Maximum Value of Peak Alternating Stress}}$$

where the endurance limit (Fig. 1.5-1) is 26,000 psi. The maximum peak alternating stress is defined as the maximum value of alternating stress intensity multiplied by the stress concentration factor at the maximum stress location. The maximum stress, thus minimum margin, does not necessarily occur at the test condition

corresponding to normal operation. Margins for these conditions, and conditions at which the maximum peak stress does occur, are summarized in Table 5.4-2.

Since peak stress intensities are all less than the endurance limit, the usage factors, for all CVAP conditions are zero.

TABLE 5.4-1

SUMMARY OF MAXIMUM PRIMARY STRESSES AND MARGINS

Component	Location (Instrument)	CVAP Test Condition; Maximum <u>Stress</u> Normal Operation	Stress (psi)	CVAP Margin	Design Margin (at normal operation)
CSB	Upper Flange (S2-S4)	3 pumps, <u>200°F</u> 4 pumps, 564°F	[]
LSS	ICI Nozzle (S13,S14)	4 pumps, <u>500°F</u> 4 pumps, 564°F			
UGS	CEA Shroud Tubes (S9-S12)	3 pumps, <u>200°F</u> 4 pumps 564°F	[]

Stress = Stress Intensity due to Primary Membrane + Bending

$$\text{Margin} = \frac{\text{ASME Code Allowable}}{\text{Stress}}$$

ASME Code Allowable = $1.5 S_m = (24,150 \text{ psi})$

TABLE 5.4-2

SUMMARY OF PEAK STRESSES AND FATIGUE MARGINS

Component	Stress Concentration Factor	Peak Stress (psi)	Location (Instrument)	CVAP Test Condition; Maximum Stress Normal Op.	Fatigue Margin
CSB	3.4	[]	Upper Flange (S2-S4)	3 Pumps, 200°F <hr/> 4 Pumps, 564°F	[]
LSS	1.7		ICI Nozzle (S13, S14)	4 Pumps, 500°F <hr/> 4 Pumps, 564°F	
UGS	2.0		CEA Shroud Tubes (S10-S12) 564°F	3 Pumps 200°F <hr/> 4 Pumps	

Peak Stress = Stress x Stress Concentration Factor

Fatigue Margin = $\frac{\text{Endurance Limit}}{\text{Peak Stress}}$

Endurance Limit = 26,000 psi

6.0

MEASUREMENT OF HYDRAULIC FORCING FUNCTIONS AND STRUCTURAL RESPONSE

The objective of the measurements program is to obtain sufficient data to confirm predictions for the margin of safety at operating conditions of steady state and transient normal operation. This confirmation requires data related to both the flow induced hydraulic loads (forcing functions) and the dynamic response of the structural components. Hence instrumentation is necessary to measure flow and response data. This measurements program has been planned with adequate instrumentation to record the information necessary, with appropriate data reduction, to compare predicted and measured values of response and verify the margin of safety for long term operation.

Hydraulic loads are the instantaneous value of pressure on the surface of the components. Pressure transducers are used to record these pressures as a function of time. The recorded time histories of these pressures include both random and periodic components. Thus spectral analyses of the data, as power spectral densities, are required to obtain information on magnitude and frequency. Comparison of the power spectral densities at various locations will then yield information on mode shape.

Likewise, response (e.g. strain, displacement, acceleration) are characterized by modal frequency and amplitude. Transducers, consisting of strain gauges, eddy type displacement gauges and accelerometers are used to measure time histories of these quantities. Processing of these data, utilizing spectral analysis techniques, results in the required modal information.

Values of flow velocity will be calculated from measurements of system flow rate (Ref. 42) and data on flow distributions obtained from scale model tests.

6.1 Operating Requirements Conditions:

Steady State (dynamic)

Transient

Environment :

Temperature (Max) 565°F

Pressure (Max) 2250 psig

Parameters:

Hydraulic Forcing Functions;	magnitude, frequency, character (random/periodic), spatial characteristics.
Structural Response;	displacement, strain, acceleration are measured to determine mode shapes, associated frequencies, and stress levels.

6.2 Instrument Locations

A detailed explanation of the instrumentation, on a component by component basis, for the System 80 comprehensive vibration assessment program (CVAP), is presented in this section. Axial and circumferential locations, referred to in the text for transducer positions, are shown in Figures 6.2-1 and 6.2-2.

6.2.1 Core Support Barrel Assembly

6.2.1.1 Core Support Barrel

6.2.1.1.1 Hydraulic Input Function Measurement

Objectives:

- a. Measure the magnitude and frequency of the periodic and random pressure fluctuations.

- b. Determine the axial and circumferential coherence length of the random pressure fluctuations.
- c. Determine the spatial distribution of pressure fluctuations.
- d. Record the pressure transients during startup and shutdown.

Pressure transducers, to record the fluctuations, are placed at selected locations and mounted flush with the surface.

The locations of transducers chosen to meet these objectives are listed in Table 6.2-1 below and shown in Figure 6.2-3.

6.2.1.1.2 System Response Measurements

Objectives:

- a. Measure the maximum stress in the CSB.
- b. Record significant values of modal response and their associated frequencies of the CSB-UGS-LSS system.
- c. Measure maximum displacement at snubber elevation.

The maximum stress for the CSB occurs at its upper flange and shell intersection, due to the beam mode response of the CSB UGS-LSS system, while maximum displacement occurs at the lower flange.

Strain gauges are located at the upper flange and at the CSB mid plane to record strain which will be used to compute stress and both axial and circumferential response modes. Accelerometers and eddy type displacement transducers are located at the lower flange to record amplitude response in the range of from .10 to 300 Hz.

The locations of transducers selected to meet these objectives are listed in Table 6.2-2 and shown in Figure 6.2-4.

6.2.1.2 Lower Support Structure:

6.2.1.2.1 Hydraulic Input Function Measurement

Objectives:

- a. Determine the magnitude of the maximum turbulent loading on the instrumentation tubes.

Because of its location close to the flow skirt, tube no. 58 is subjected to the highest level of turbulence present in the lower support structure region. The pressure transducer, selected to record the fluctuating pressure, is mounted flush with the outer surface of the tube-58, at its mid-elevation.

The location of the transducer selected to meet this objective is listed in Table 6.2-3 and shown in Figure 6.2-5.

6.2.1.2.2 Structural Response Measurements

Objective:

- a. Determine the significant responses and resulting stresses in the LSS components.

For reasons explained in Section 6.2.1.2.1, in addition to its low lateral stiffness, tube-58 is expected to have the highest response and resulting stress levels amongst the instrumentation tubes. The accelerometer chosen to record this response is placed inside the tube. Strain is measured by a group of strain gauges at the intersection of the tube and upper support plate.

The locations of the transducers selected to meet the above objectives are listed in Table 6.2-4 and shown in Figure 6.2-5.

6.2.2 Upper Guide Structure Assembly

Based on evaluation of the hydraulic flow test data and the System 80 tube bank vibration analysis, it was concluded that the tubes directly in front of the outlet nozzles will be subjected to the maximum hydraulic loading due to cross flow. In addition, these same peripheral tubes, having a lower stiffness as compared to the inner tubes, will therefore have the maximum response.

Based on flow model tests, in which tubes with high crossflow velocities were identified, six tubes were selected for instrumentation.

6.2.2.1 Hydraulic Input Function Measurement

Objectives:

- a. Measure the magnitude and frequency of the random and deterministic pressure pulsations on the CEA shroud tubes.

Pressure transducers to record the pressure fluctuations, are mounted flush with the tube wall.

The locations of transducers chosen to meet these objectives are listed in Table 6.2-5 and shown in Figure 6.2-6,7,8.

6.2.2.2 Structural Response Measurements

Objectives:

- a. Determine the significant responses and resulting stress in the upper guide structure components.
- b. Record the flow-induced vibration response in the CEA shroud tubes.

- c. Measure the vertical and lateral response of the upper guide structure, at the fuel alignment plate level, in the 5-300 Hz frequency range.

The CEA Shroud tubes directly opposite the outlet nozzles are instrumented for their significant modal response and resulting stresses, as a result of flow and pump induced vibrations in the tube bank.

Biaxial accelerometers, placed inside the tubes, at their midspan, so that the flow characteristics around these tubes is not altered, will be used to record amplitude response.

In addition, strain gauges, located at the tube-plate junction, will be used to record strain from which stress and mid plane displacement will be calculated.

The locations of transducers selected to meet the above objectives are listed in Table 6.2-6 and shown in Figure 6.2-6, 7, 8.

6.2.3 Summary of Instrumentation Requirements

Table 6.2-7 is a summary of the required instrumentation, arranged according to component to be monitored, parameter measured, type and number of instruments. Details of the installations and locations of the instrumentation are shown in the drawings listed in Reference 39.

TABLE 6.2-1
CSB FORCING FUNCTION INSTRUMENTATION

ID Number	Pressure Transducer		Location+		Comment
	Identifier-Type*		Axial	Circumferential	
1 2 3	P-1 P-2 P-3	PT-A	L-2 L-2 L-7	120° 300° 300°	These will measure the magnitude and be used to determine the axial relationship of the pressure fluctuations at the inlets and along the CSB.
4 5 6	P-4 P-5 P-6	PT-A	L-4 L-4 L-4	300° 292° 270°	This group will be used to determine the circumferential coherence length** and provide information on circumferential distribution of the random pressure loading.
7 8	P-7 P-8	PT-A	L-5 L-6	300° 300°	This group will be used to calculate the axial coherence length bounds and provide further information on the axial distribution.
9	P-9	PT-B	L-2	240°	These will follow the system slow pressure transients, down to DC levels, in both loops, during 4 pumps and part loop operation.

**By examining coherence between P.T.'s "4" through "8", placed at L/2 and L distances apart (L = annulus thickness), one could determine the bounds of the coherence length, of the random hydraulic loading function.

*Section 6.3

+See Figures 6.2-1 and 6.2-2

TABLE 6.2-2
CSB RESPONSE INSTRUMENTATION

ID Number	Transducer		Location+		Response Axis	Comments
	Identifier	Type*	Axial	Circumferential		
10	S-1	SG	L-1	180°	Axial Hoop Axial Hoop	This group will measure the bi-axial stress state at the CSB upper flange and shell intersection.
11	S-2	A	L-1	180°		
12	S-3		L-1	270°		
13	S-4		L-1	270°		
14	S-5	SG-A	L-4	180°	Axial Hoop Axial Hoop	This group, in conjunction with information from a modal analysis of the system, be used to determine the maximum values of the significant forced or natural shell modal response and their associated frequencies in the 5-300 Hz range.
15	S-6		L-4	180°		
16	S-7		L-4	270°		
17	S-8		L-4	270°		
18	A-1	AC-A	L-8	180°	Radial and Tangential	This group will measure the CSB's beam and shell mode response in the 0.1 to 300 Hz range. In the frequency range (0.1 to 10 Hz) the response will be relative to the snubbers and hence will account for the rocking mode response of the vessel in this frequency range.
19	A-5	EDD-A	L-8	0°	Radial	
20	A-3		L-8	120°		
21	A-4		L-8	240°		

+ See Figures 6.2-1 and 6.2-2

* Section 6.3.

TABLE 6.2-3
LSS FORCING FUNCTION INSTRUMENTATION

ID Number	Transducer	Location+	Comment
	Identifier Type*		
34	P-12 A	Tube mid span, radially facing the flow skirt, level L-82	This will measure the magnitude of the random and oscillatory pressure fluctuations on tube-58.

+ See Figure 6.2-1

* Section 6.3.

TABLE 6.2-4
LSS RESPONSE INSTRUMENTATION

ID Number	Transducer	Location+		Response Axis	Comment
	Identifier-Type*	Axial	Tube		
35	S-13 A	L-B1	58	Axial	This group will record the bi-axial stress state in instrumentation tube 58.
36	S-14	L-B1	58	Axial	
37	A-11 A	L-B3	Lower Plate	Radial	This will measure lateral response of the lower support structures.

+ See Figures 6.2-1 and 6.2-5

* Section 6.3

TABLE 6.2-5
UGS FORCING FUNCTION INSTRUMENTATION

ID Number	Pressure Transducer	Location+			Comments
	Identifier-Type*	Axial	Quadrant	Tube	
22	P-10 A	L-3	180°-270°	3	This group will measure the magnitude of random and oscillatory pressure fluctuations on the tubes directly in front of the outlet nozzle, for each of the coolant loops hence make available information on 4-pump and part loop operation.
23	P-11	L-3	180°-270°	6	
38	P-13	LA-2	180°-270°		Pressure fluctuations on UGS upper plate to be compared to values from scale model test.

+ See Figures 6.2-1, 6.2-6 and 6.2-7.

* Section 6.3.

TABLE 6.2-6
USG RESPONSE INSTRUMENTATION

ID Number	Transducers		Location+			Response	Comment
	Identifier	Type*	Axial	Quadrant	Tube	Axis	
24	S-9	A	L-A2	180-270	6	Axial	This group will measure the maximum biaxial stress state at the junction of the tube and UGS plate.
25	S-10		L-A2	180-270	6	Axial	
26	S-11		L-A2	0°-90°	6	Axial	
27	S-12		L-A2	0°-90°	6	Axial	
28	A-5	A	L-A3	180°-270°	3	Radial	This group will measure the significant modal response of the CEA shroud tubes that are expected to see crossflow velocities greater than 50 ft/sec. Tubes in an in-line and in staggered tube arrays have been selected since their respective Strouhal numbers vary. Data will be used to identify sources of flow induced vibration in the tubes.
29	A-6		L-A3	180°-270°	4	&	
30	A-7		L-A3	180°-270°	6	Tangen-	
31	A-8		L-A3	180°-270°	10	tial	
32	A-9		L-A3	180°-270°	37		
33	A-10	B	L-A4	180°-270°	187	Radial (0-180° and 90°-270° and Vertical	Accelerometer to record vertical and radial response of the F.A.P., in the 5-300 Hz range.

+ See Figures 6.2-1, 6.2-6 and 6.2-7.

* Section 6.3.

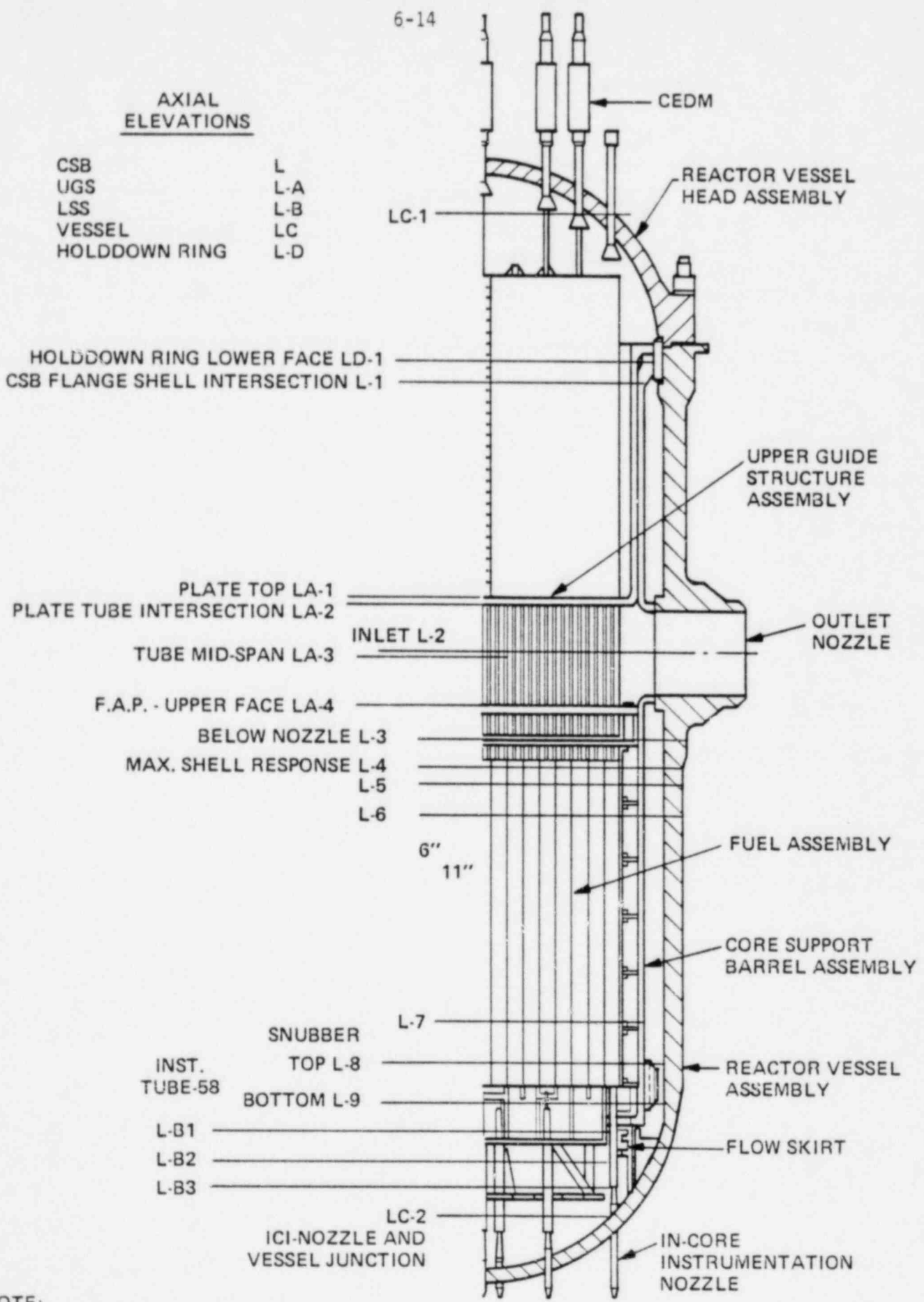
TABLE 6.2-7
CVAP INSTRUMENTATION

Assembly	Type	ID Number	Channels	Location
Core Support Barrel (Fig. 6.2-3 6.2-4)	1. Pressure Transducer	P1	1	CSB 120° Inlet
	2. Pressure Transducer	P2	1	CSB 300° Inlet
	3. Pressure Transducer	P3	1	CSB 300° Level 7
	4. Pressure Transducer	P4	1	CSB 300° Level 4
	5. Pressure Transducer	P5	1	CSB 270° Level 4
	6. Pressure Transducer	P6	1	CSB 270° Level 4
	7. Pressure Transducer	P7	1	CSB 300° Level 5
	8. Pressure Transducer	P8	1	CSB 300° Level 6
	9. Pressure Transducer	P9	1	CSB 240° Inlet
	10. Strain Gage	S1	1	CSB 180° Key Way
	11. Strain Gage	S2	1	
	12. Strain Gage	S3	1	CSB 270° Key Way
	13. Strain Gage	S4	1	
	14. Strain Gage	S5	1	CSB 180° Level 4
	15. Strain Gage	S6	1	
	16. Strain Gage	S7	1	CSB 270° Level 4
	17. Strain Gage	S8	1	
	18. Biaxial Accelerometer	A1	2	CSB 180 Snubber
	19. Displacement Transducer	A2	1	CSB 0° Snubber
	20. Displacement Transducer	A3	1	CSB 120° Snubber
	21. Displacement Transducer	A4	1	CSB 240° Snubber
Upper Guide Structure (Fig. 6.2-6 6.2-7)	22. Pressure Transducer	P10	1	UGS 180°-270° Tube 3
	23. Pressure Transducer	P11	1	UGS 180°-270° Tube 6
	38. Pressure Transducer	P13	1	UGS Plate
	24. Strain Gage	S9	1	UGS 180°-270° Tube 6
	25. Strain Gage	S10	1	
	26. Strain Gage	S11	1	UGS 0°-90° Tube 3
	27. Strain Gage	S12	1	
	28. Biaxial Accelerometer	A5	2	UGS 180°-270° Tube 3
	29. Biaxial Accelerometer	A6	2	UGS 180°-270° Tube 4
	30. Biaxial Accelerometer	A7	2	UGS 180°-270° Tube 6
	31. Biaxial Accelerometer	A8	2	UGS 180°-270° Tube 10
	32. Biaxial Accelerometer	A9	2	UGS 180°-270° Tube 37
	33. Triaxial Accelerometer	A10	3	UGS 180°-270° Tube 187
Lower Supprt Structure (Fig. 6.2-5)	34. Pressure Transducer	P12	1	LSS Ins. Guide Tube 58
	35. Strain Gage	S13	1	LSS Ins. Guide Tube 58
	36. Strain Gage	S14	1	
	37. Biaxial Accelerometer	A11	2	LSS ICI Support Plate
	Totals	38	47	

6-14

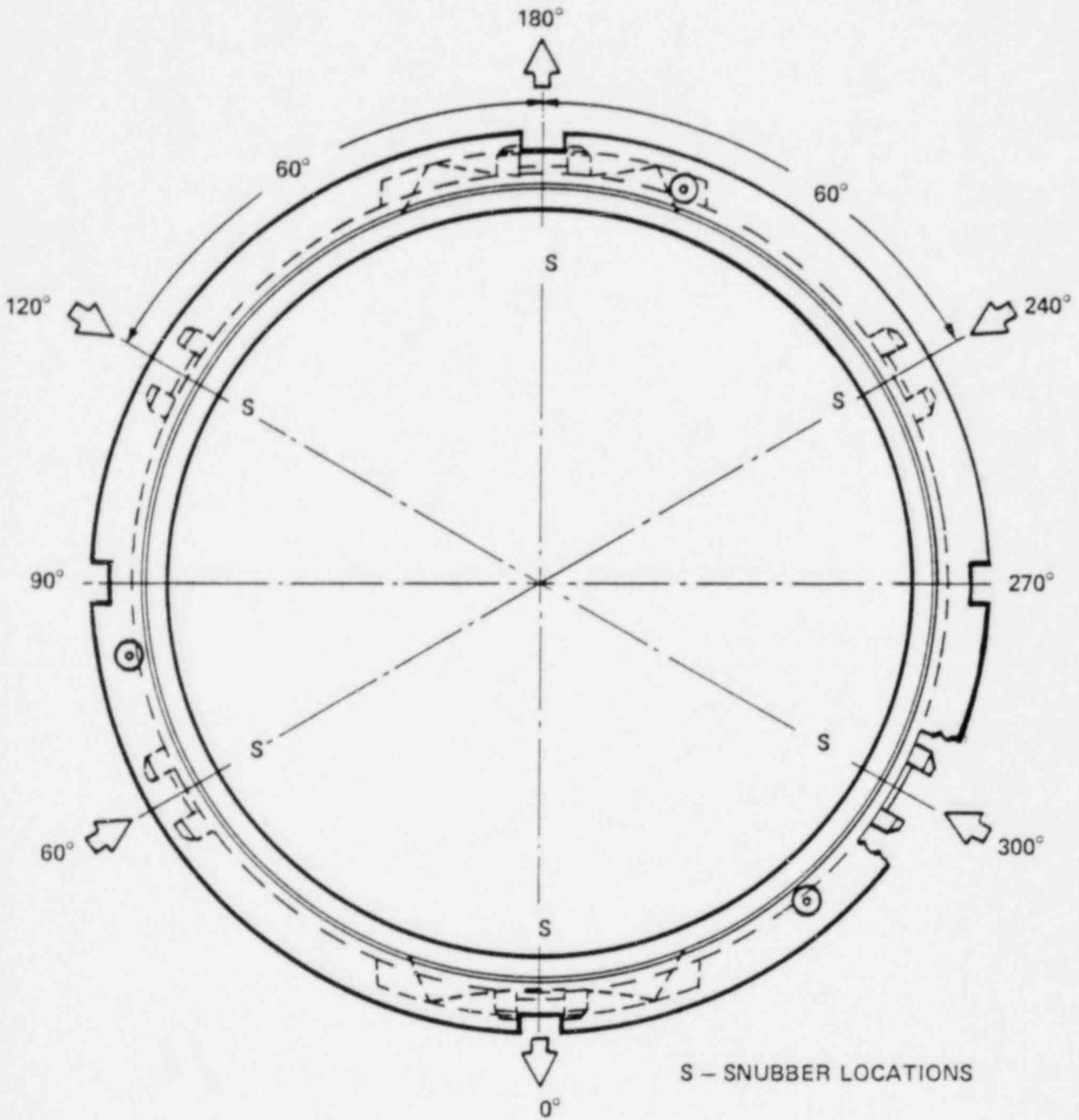
AXIAL ELEVATIONS

- | | |
|---------------|-----|
| CSB | L |
| UGS | L-A |
| LSS | L-B |
| VESSEL | LC |
| HOLDDOWN RING | L-D |



NOTE:
 L-4 = 237" FROM TOP OF CSB
 L-7 = 48" FROM BOTTOM OF CSB

TRANSDUCER AXIAL LOCATIONS
 FIGURE 6.2-1



CIRCUMFERENTIAL LOCATIONS
OF INLET AND OUTLET NOZZLES

FIGURE 6.2-2

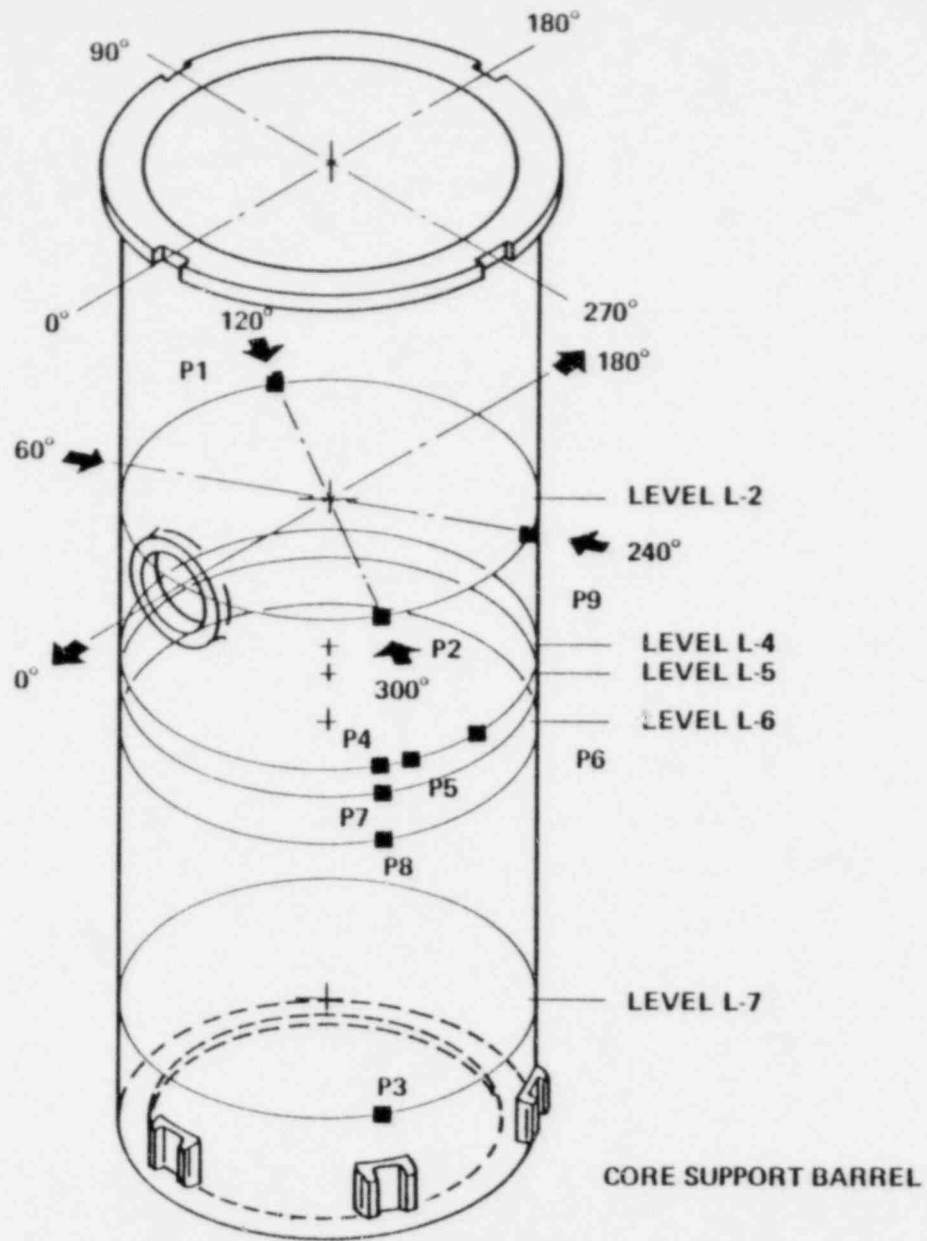


FIGURE 6.2.3
INPUT FUNCTION MEASUREMENT TRANSDUCERS
(■)

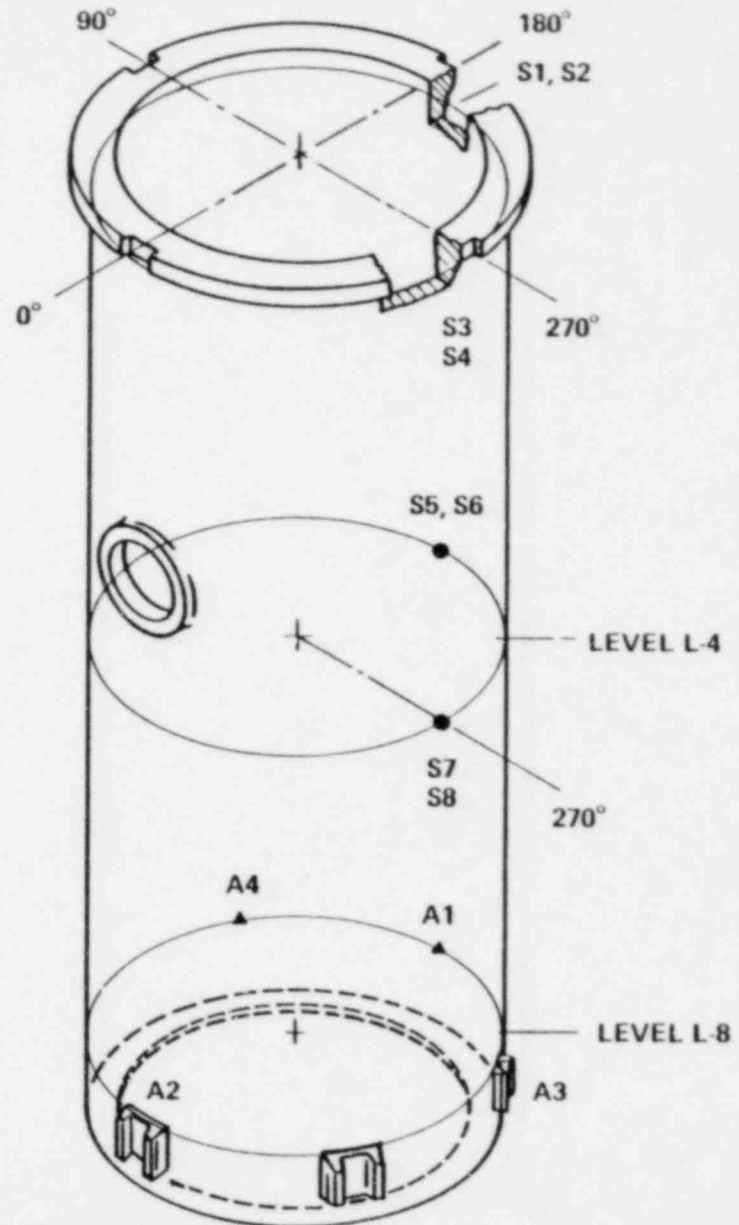
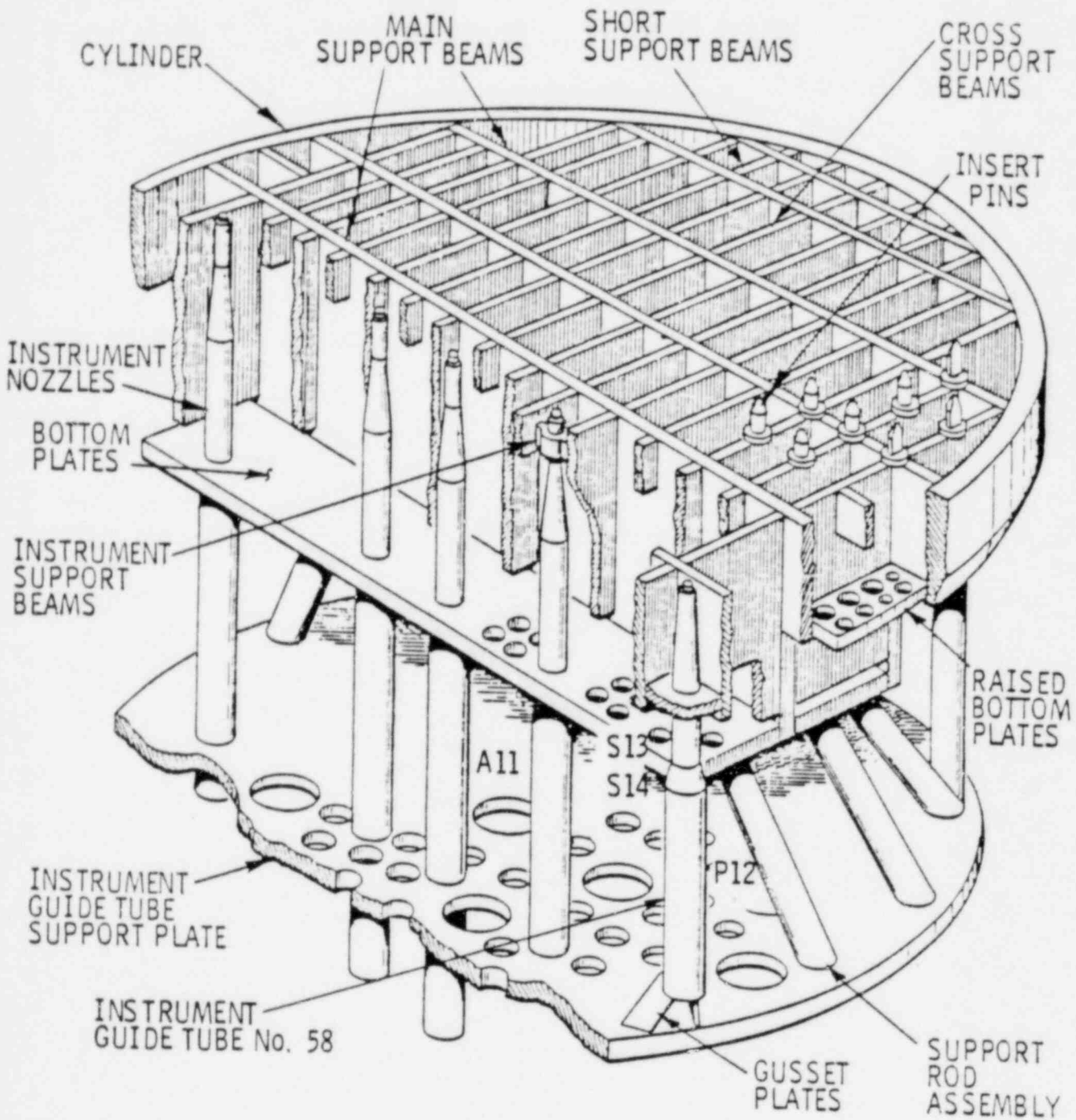
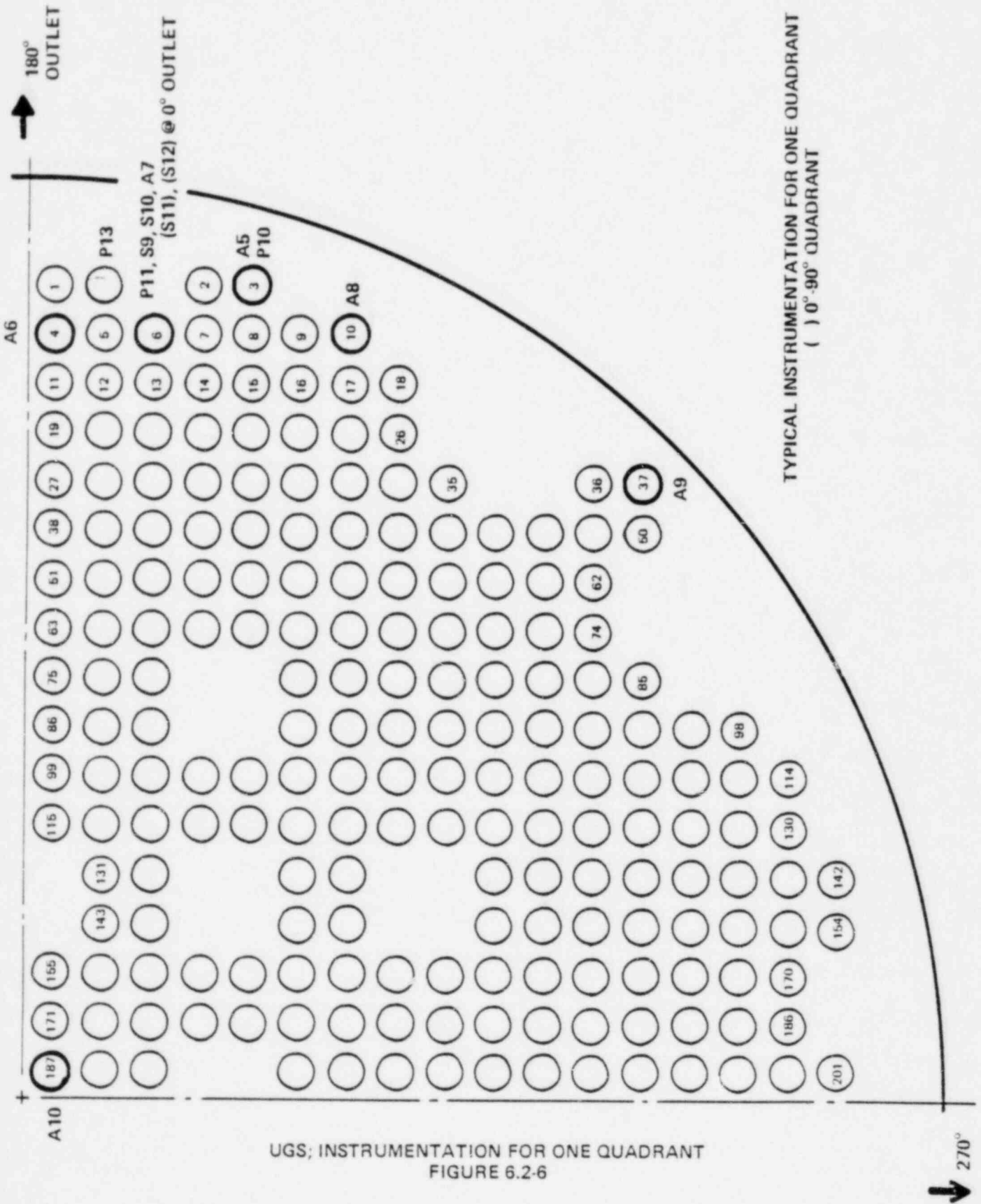


FIGURE 6.2.4
RESPONSE MEASUREMENT TRANSDUCERS
STRAIN GAUGE (●)
ACCELEROMETER & DISP. DEVICE (▲)

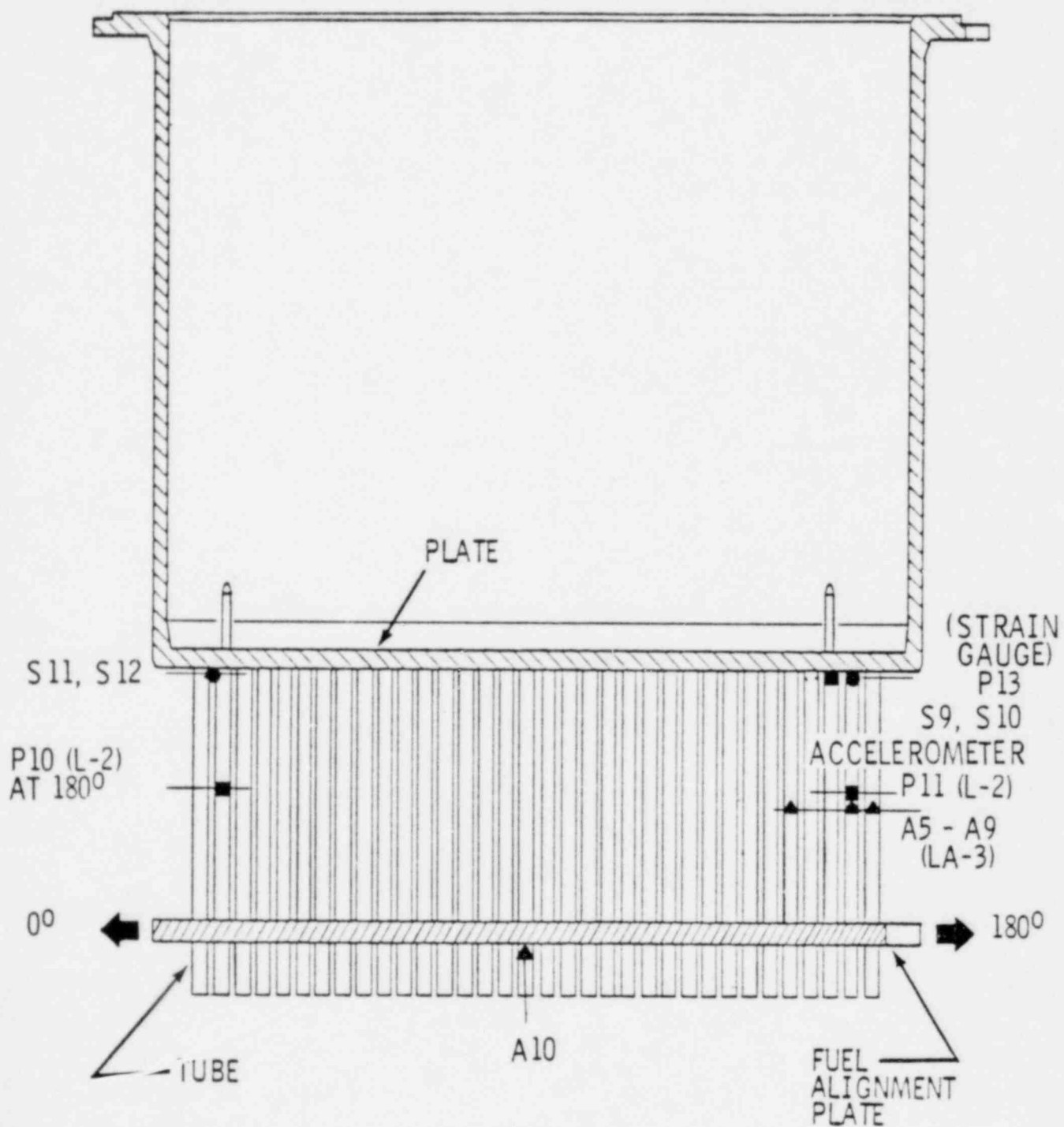


LOWER SUPPORT STRUCTURE & INSTRUMENT ASSEMBLY

FIGURE 6.2-5



UGS; INSTRUMENTATION FOR ONE QUADRANT
FIGURE 6.2-6



UGS; AXIAL LOCATIONS FOR INSTRUMENTATION

FIGURE 6.2-7

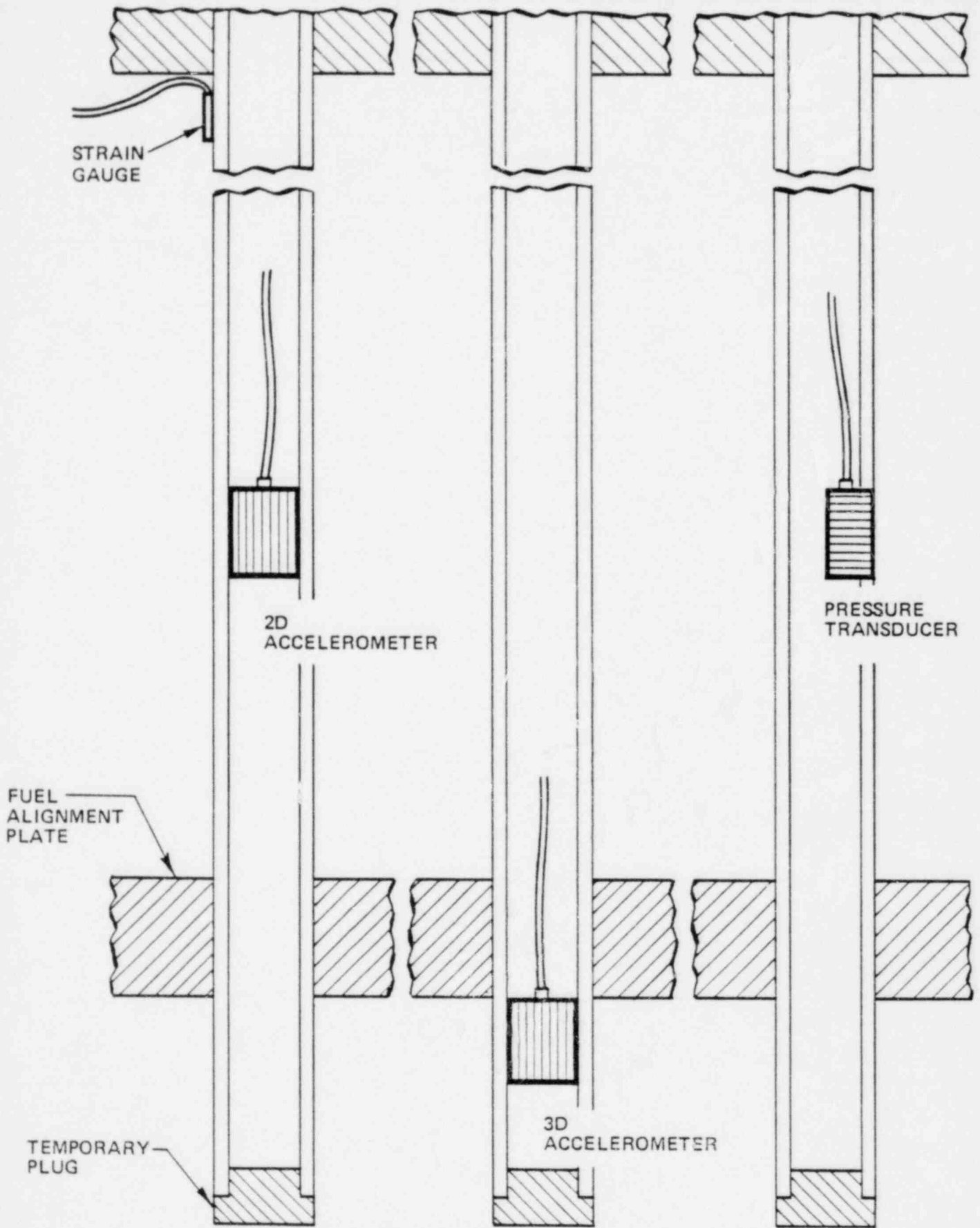


FIGURE 6.2-8

CEA SHROUD TUBE TYPICAL INSTRUMENTATION MOUNTING

6.3 Specifications for Instrumentation Systems

The instrumentation systems used in this program are listed as follows by sensor type and with operating specifications.

6.3.1 Pressure Transducer System Requirements (PT-A, B)

6.3.1.1 Sensors

Environment: Water at 2500 psi and 565°F

Types: (A) Dynamic Response only (0.5 to 500 Hz)
(B) Static and dynamic response (DC to 500 Hz)

Physical Description and Dimensions:

- (1) Type A: Columbia Research Lab. No. 774.
- (2) Type B: Kaman Model KP-1911 with 3000 psi full scale pressure range.

Leads: Stainless steel or inconel jacketed triaxial or twinaxial 1/8" OD mineral insulated integral cable. Only one lead per sensor.

Mounting: 0.625" flange on sensor is to be welded to one side of 0.505" diameter through hole in the structure.

6.3.1.2 Type A Sensor and Signal Conditioning

Performance: The following specifications apply to a pressure transducer with 40 ft. of "hard" cable, a remote charge converter, 500 ft. of "soft" cable (shielded twisted pair) and a local amplifier with range selector.

- (1) Frequency response: $\pm 5\%$ 0.5 Hz to 500 Hz

- (2) Full scale range (for $\pm 2.5V$ output): Switchable to 0.1, 0.3, 1, 3, 10, 30, 100 and 300 peak psi
- (3) Resolution $<10^{-3}$ psi on .10 to 3 psi range and typically better than $10^{-3} \times F.S.$ for ranges higher than 3 psi
- (4) Vibration sensitivity: $<.1\text{psi/g}$
- (5) Accuracy: (overall system when components are individually calibrated) $\pm 5\%$ of output value at 100 Hz

6.3.1.3 Type B Sensor and Signal Conditioning

Performance: The following specifications apply to a pressure transducer with 40 ft. of "hard" cable, a remote charge converter, 500 ft. of "soft" cable (shielded twisted pair) and a local amplifier with range selector.

- (1) Frequency response: $\pm 5\%$ DC to 500 Hz
- (2) Full scale range (for +5V) 3000 psi
- (3) Resolution: typically better than 2 psi
- (4) Vibration sensitivity: $<0.002\text{ psi/g}$
- (5) Accuracy: (overall system when components are individually calibrated) $\pm 5\%$ of output value at 100 Hz

6.3.2 Strain Gage System Requirements (SG-A)

6.3.2.1 Sensor

Environment: Water at 2500 psi and 565°F

- Type: "Ailtech" high-temperature weldable strain gage
(formerly called "Micro-dot")
- Dimensions: typically 1.5" x 0.5" x 0.125"
- Leads Stainless steel jacketed three conductor mineral insulated cable of 0.063" diameter. One cable per strain gage.
- Mounting: The gage is resistance spot welded to the structure. For structures with a curvature radius of less than 2 inches, the gages should be preformed by the manufacturer.

6.3.2.2 Sensor and Signal Conditioning

Performance: The following specifications apply to the strain gage with 40 ft. of hard cable, 100 ft. of soft shielded three-conductor cable and a Vishay BA-4 bridge amplifier.

- (1) Frequency response: $\pm 5\%$ 0 Hz to 10 KHz
- (2) Dynamic resolution: better than 5 microstrain
- (3) Full scale range: Switchable gain ranges yield full scale values of approximately 200, 400, 800 1600, 3200 and 6400 micro strain.
- (4) Dynamic accuracy: $< \pm 8\%$

6.3.3 Accelerometer System Requirements (AC-A,B)

6.3.3.1 Sensor

Environment: Water at 2500 psi and 565°F

- Types: (A) biaxial; Columbia Research Lab. No. 775
- (B) triaxial; Columbia Research Lab. No. 776
- Dimensions: (overall with suitable flange for welding to structure)
approximately 1.5" x 1.5" x 2.5" (except for tube mount)
- Leads: Stainless steel or inconel jacketed triaxial or
twinaxial 0.125" OD mineral insulated integral cables.
Two leads per biaxial accelerometer three leads per
triaxial accelerometer
- Mounting: (1) Transducer is to be welded to the structure.
- (2) Biaxial accelerometers shall also be capable of
spring mounting on the inside of tubes with an ID
of 1.562" and of approximately 3" ID.

6.3.3.2 Sensor and Signal Conditioning

Performance: The following specifications apply to an accelerometer with 40 ft. of "hard" cable, a remote charge converter, 500 ft. "soft" cable (shielded twisted pair) and a local amplifier with range selector.

- (1) Frequency response: $\pm 5\%$ 5 Hz to 500 Hz
- (2) Transverse sensitivity: <10%
- (3) Full scale range (for +5.0V output): Switchable to 0.1, 0.3, 1, 3, 10, 30, 100 and 300 pk g's

- (4) Resolution: $<10^{-3}$ g's on the .1 to 3 g range and typically better than 10^{-3} x F.S. for ranges higher than 3 g
- (5) Dynamic pressure sensitivity: $<10^{-2}$ g/psi
- (6) Accuracy: (overall system when components are individually calibrated) $\pm 5\%$ of output value at 100 Hz

6.3.4 Displacement Transducer System Requirements (EDD-A)

6.3.4.1 Sensor

Environment: Water at 2500 psi and 565°F

Type: Kaman Sciences KD-1901 displacement transducer, non-contacting eddy current sensing. The sensor indicates the displacement between it and a conductive target. A magnetic target is positioned 10 mils from the sensor. A total range of 100 mils is available.

Physical Description and Dimensions: Typically 750 in diam.

Leads: Single twin axial stainless steel sheathed mineral insulated cable. Cable diameter is 0.125 inches.

Mounting: Target shape and material type as well as mounting configuration including side loading materials and/or mounting ring materials is provided by Kaman Sciences for proper calibration of the instrument.

6.3.4.2 Sensor and Signal Conditioning

Performance: The following specifications apply to the displacement sensor, 40 ft. of hard cable and Kaman Sciences KD-2018 electronics.

- (1) Frequency response: 0. to 2.5 KHz (-3 dB)
- (2) Full scale range: 200 mils with non-magnetic target
- (3) Resolution (static): 0.2 mils
- (4) Errors: non-linearity: $\pm 2\%$ of full scale at any particular temperature

temperature coefficient: zero shift - $<0.01\%/^{\circ}\text{F}$
sensitivity shift -
 $<0.006\%/^{\circ}\text{F}$

6.4 Preparation and Installation of Instrumentation Systems

All transducers are tested prior to shipment to the site. This testing consists of; a helium leak test to check the housing welds, autoclave tests at 565°F and 2250 psig for 24 hours, after which the transducers are checked for resistance and capacitance. After the autoclave test another helium leak check is performed.

The sensor leads are protected from hydraulic forces by half round conduits which are welded to the CSB. These conduits are routed to spare CEDM nozzles where the leads penetrate the reactor vessel head. Sealing of the leads is accomplished by the use of "Conax-Lava Seal" in a GrayLoc hub assembly.

6.5 Data Acquisition

6.5.1 Recording Equipment

The CVAP data recording system is designed to record the electrical signals from transducers, mounted on the reactor internals, on magnetic tape. These tape recordings are the inputs used by various off line processing techniques. The recorded time histories are examined for both amplitude and frequency content.

6.5.1.1 Equipment Description

The transducers integral hard cable will be terminated at a junction box. The signal is then connected to the data acquisition system by means of a flexible shielded twisted pair cable. At the junction box the accelerometers and pressure transducers will be input to charge amplifiers to convert the charge signal to a voltage signal suitable for recording. The half-bridge strain gauges will be matched with completion resistors and connected to bridge amplifiers. Three displacement and one pressure (P9) transducers,

are eddy current type devices. An oscillator-demodulator system is used with these transducers. An additional D.C. amplifier will be used with the SC transducers to insure adequate recording levels.

The CVAP data acquisition system has the capability to simultaneously record 54 channels of conditioned transducer signals on a 14 single track one inch instrumentation grade analog tape recorder. The transducer signals are recorded on tape using a Pulse Code Modulation (PCM) technique. PCM involves frequency filtering and analog-to-digital (A/D) conversion of the continuous transducer time history prior to tape recording. Several transducer channels are then combined by an encoder into a serial bit stream. This data bit stream with necessary encoder framing information is then recorded on a single recorder track. The particular PCM scheme for CVAP uses nine tracks of the recorder. Each track has the encoded A/D values for six transducer signals. The PCM A/D rate and word length have been selected to allow a data channel frequency response of 0-500 Hertz and an amplitude resolution of ± 1.25 milivolts ($< \pm .03\%$ full scale). In order to achieve these operating specifications the PCM system requires a tape speed of 30 inches/second. The analog tape reels used during CVAP will accommodate 24 minutes of data recording. For data monitoring a PCM-decommutator (decom) system will be used during the test. This system will enable test personnel to monitor the recorded transducer signals, and verify the operation of the recording system.

The analog tape recorder, the PCM encoding and decom systems, signal conditioning and auxiliary test equipment are rack mounted in three standard electronic equipment cabinets. The cabinets are equipped with levelers, casters and lifting eye bolts to insure portability.

6.5.2 Data Acquisition Method

The three phases of CVAP data acquisition include: documentation, calibration, and data monitoring (Ref. 40).

6.5.2.1 Documentation

Each transducer and its associated cables are uniquely identified. The transducer and cables associated with a signal conditioner are logged in the transducer hook-up log. This identifies a signal path at every connection from the transducer to tape recorder. The accuracy of this hook up log is verified by acquisition personnel during instrumentation hook-up and checkout. Any deviations from the initial hook-up made during testing are noted and verified.

6.5.2.2 Calibration

The integrity of the transducers and connecting cables is monitored through leadwire insulation and transducer capacitance measurements. These checks are made and recorded in the transducer characteristics log. Additionally, twice a day, strain gauge transducers are shunt calibrated at the bridge amplifier and these shunt calibration voltages recorded on the characteristics log. Overall system calibration is performed at the start of each analog tape. All signal conditioners are switched into calibrate mode and a short tape recording is made. An entry for each system calibration is made in the CVAP data log.

6.5.2.3 Data Monitoring

When a test condition has been set and in the judgement of the acquisition engineer, the acquisition system is ready, a data recording will be made. The signal level of each transducer channel will be monitored while setting the signal conditioning amplifier gains for optimum output levels. The strain gauge amplifiers will be balanced and the sensitivity of all charge amplifiers verified. An entry is then made in the CVAP data log, a sequential test number is assigned, tape footage, and time of day noted and all signal conditioning gains are entered. The data log has space set aside for additional comments.

A recording session is started with a voice recording on tape detailing the test number, test conditions, data, time, and tape footage. Other pertinent information may also be included in the voice recording. As the recording proceeds the PCM-decom system is used to monitor the signals recorded on tape. Each signal is monitored to verify the recording process and the adequacy of the data signal level.

6.6 Data Reduction Methods

Reduction of the data will be done using methods of random data analysis (Ref. 37).

This includes both on-line and off-line evaluation of the data at the time of testing and post test reduction and evaluation.

6.6.1 Reduction During Tests

The purpose of data reduction during the tests is to determine if the response is within the acceptance limits. This reduction will include calculation of the RMS values for both the response and forcing function instrumentation. In addition, a spectrum analyzer will be used to examine the spectral characteristics of selected instruments.

6.6.2 Post Test Reduction

Complete reduction and evaluation of the data will be the subject of a separate evaluation report, as required by Regulatory Guide 1.20 (Ref. 1). It is not possible to define a complete program for post test reduction of the data without the actual response information. Tables 6.2-1 to 6.2-6 list the purpose of each instrument and its particular location. Based on this, a preliminary data reduction program has been formulated. This preliminary program is to obtain information on the overall and spectral characteristics of both the forcing functions (pressure) and response (strain, displacement, acceleration).

This program includes:

A. Identification of data characteristics through use of special software analysis. This will include:

1. RMS values for all transducers. The values will be broken

down into two categories: random and deterministic. The deterministic RMS will be the total RMS at all frequencies previously specified as deterministic. The random RMS will be what remains of the RMS after removing the deterministic.

2. Detected peaks for all transducers. The peaks will be broken down into two categories: deterministic and "others". Deterministic peaks will be those at frequencies previously specified as deterministic (i.e., pump rotational frequencies).
 3. For all transducers in a measurement group (strain, pressure, etc.), the overall RMS. Each transducer with an RMS significantly larger than either a reference transducer or the group mean RMS will be flagged for further investigation.
- B. Spectral analysis of the data for steady state and transient conditions.

Steady state; spectral analysis will include auto power spectral density (PSD) plots of all 47 channels. In addition cross PSD, coherence phase and amplitude probability distribution (APD) information will be obtained for selected pairs of instruments. A summary is given in Table 6.6-1.

Transient; peak spectrum analysis (PSA) will be done for all 47 channels to obtain information on the maximum response during a transient. In addition time history information will be obtained from the instruments capable of recording RMS levels versus time; all strain gages, displacement transducers, and pressure transducer, P9.

TABLE 6.6-1
SPECTRAL DENSITY DATA REDUCTION PLOTS

Assembly	Data Channel A	Data Channel B	Plot	Comment
CSB	P4	P5	XPSD	Axial & Circumferential coherence for random loading (2)
	P4	P6	XPSD	
	P4	P7	XPSD	
	P4	P8	XPSD	
	P2	P3	XPSD	Periodic load, axial & circumferential mode shape
	P2	P9	XPSD	
	A2	A3	XPSD	Displacement pattern & mode shape at CSB snubber level
	A2	A4	XPSD	
	A1	A2	(1)	
	S1	S5	XPSD	Axial & circumferential mode shapes between upper flange & midplane
S3	S7	XPSD		
S2	S6	XPSD		
S4	S8	XPSD		
UGS	P10	P11	XPSD	Attenuation, phase of random and periodic pulsations Response pattern of Tube 6
	S9	S10	XPSD	
	S11	S12	XPSD	
	A5	A5	(1)	Response pattern of tubes 3, 4, 6, 10, 37
	A6	A6	(1)	
	A7	A7	(1)	
	A8	A8	(1)	
	A9	A9	(1)	
	S9		APD	Determine tube response to random and flow induced forces.
	S10		APD	
	S22		APD	
	A5		APD	
	A6		APD	
	A7		APD	
A8		APD		
A9		APD		
LSS	S13	S14	XPSD	Response pattern relative vertical motion of LSS & FAP (core motion)
	A11	A10	XPSD	

(1) XPSD between radial and tangential directions.

(2) Coherence lengths obtained from cross correlation.

7.0 ACCEPTANCE CRITERIA FOR TEST DATA

Per Regulatory Guide 1.20 an acceptance criteria is defined for the measured stress*. The definition is based on ASME endurance limit stress for fatigue and includes deviations to account for measurement error and calculational uncertainty. The maximum allowable readings for the response instrumentation are specified based on this acceptance criteria.

7.1. Basis for the Acceptance Criteria

As discussed in Section 1.5, the design values of the flow induced loads on the core support assemblies are larger than the best estimate values used for the CVAP predictions. A comparison between stress intensities and fatigue margins for the design and CVAP flow induced loads, at the conditions corresponding to normal operation, are listed in Table 7.1-1.

The objective of the measurement program is to obtain values of the response i.e., stress, of the instrumented assemblies to flow induced loads. After suitable analysis of the data, measured response is then compared to the predicted values. This comparison includes consideration of both experimental error and calculational uncertainties in the predictions. The accuracy of the predict methods is related to the difference between the measured and predicted values. This accuracy is assumed to be the same for both the CVAP and design calculations.

*Since interest is in fatigue, stresses are peak values of alternating stress intensities, defined as,

$$\text{Peak Stress} = \text{Stress Concentration Factor} \times \text{Alternating Stress}$$

To be concise, these values are referred to as stress or stress intensity throughout this section.

The maximum difference between the measured and predicted stress is derived based on the requirement that the difference between the measured and predicted stress intensities for the CVAP conditions, be less than or equal to the difference in maximum allowable stress and the maximum predicted value of stress intensity for the design calculations. This is stated in equation form as,

$$(S_{a,cm} - S_{a,cp}) \leq (S_e - S_{a,d}) \quad (1)$$

where,

$S_{a,cm}$ stress measured for CVAP loads

$S_{a,cp}$ stress predicted for CVAP loads

S_e endurance limit stress (26,000 psi)

$S_{a,d}$ stress predicted for design loads

Per Appendix C.1 and equation 1, the maximum ratio of measured to predicted stress for the CVAP, is,

$$\left[\frac{S_{a,cm}}{S_{a,cp}} \right] = \left[\frac{S_{a,d}}{S_{a,cp}} \right] (\text{Fatigue Margin} - 1) + 1 \quad (2)$$

where the fatigue margin is defined as,

$$\text{Fatigue Margin} = S_e / S_{a,d} \quad (3)$$

Numerical values of this ratio for the three assemblies are listed in Table 7.1-1. Values of the maximum stress corresponding to this ratio are likewise listed in Table 7.1-1.

This ratio, shown in Figure 7.1-1 as a function of the differences in stresses, from equation 1,

$$\frac{\Delta m}{\Delta d} = \frac{(S_{a,cm} - S_{a,cp})}{(S_e - S_{a,d})} \leq 1 \quad (4)$$

defines the region of acceptable values of measured to calculated stress. The maximum values of this ratio forms the basis for defining the acceptance criteria.

7.1.2 Uncertainties

Limits on measured stress, listed in Table 7.1-1, are the maximum acceptable values. These values do not reflect the effect of calculational uncertainties in the predictions or uncertainties due to errors in the measured values.

Uncertainty in the measured values depends on the accuracy of both the acquisition and reduction of the data. The accuracy of the data acquisition is primarily a function of instrument error, which is on the order of magnitude of [_] The accuracy of the data reduction is a function of the number of data samples, the analysis bandwidth, etc. and has an upper limit of approximately [_] Consequently the measurement error is about [_]

Uncertainty in the predictions are substantially greater. Predictions for the loads on the CSB assumes that all pumps are in phase so that the loads and, therefore, the response for N pumps is N times the response for one pump. Data from previous precritical vibration monitoring programs (Ref. 12) show this is always conservative in predicting the maximum stress. Evaluation of these test results indicate an uncertainty on this calculation of [_] and [_] Calculation of the loads, thus the response of the LSS, is complicated by the complex distribution of flow in the lower plenum region. Because of approximations made with regard to the loads, the uncertainty is estimated to be within [_] For the UGS the prototype response has been scaled directly from the extensive tests on both full size and scale models. As a consequence of all the assemblies, the uncertainty is the lowest being approximately [_]

TABLE 7.1-1
 DESIGN, CVAP, AND MAXIMUM ACCEPTABLE MEASURED VALUES OF ALTERNATING STRESS

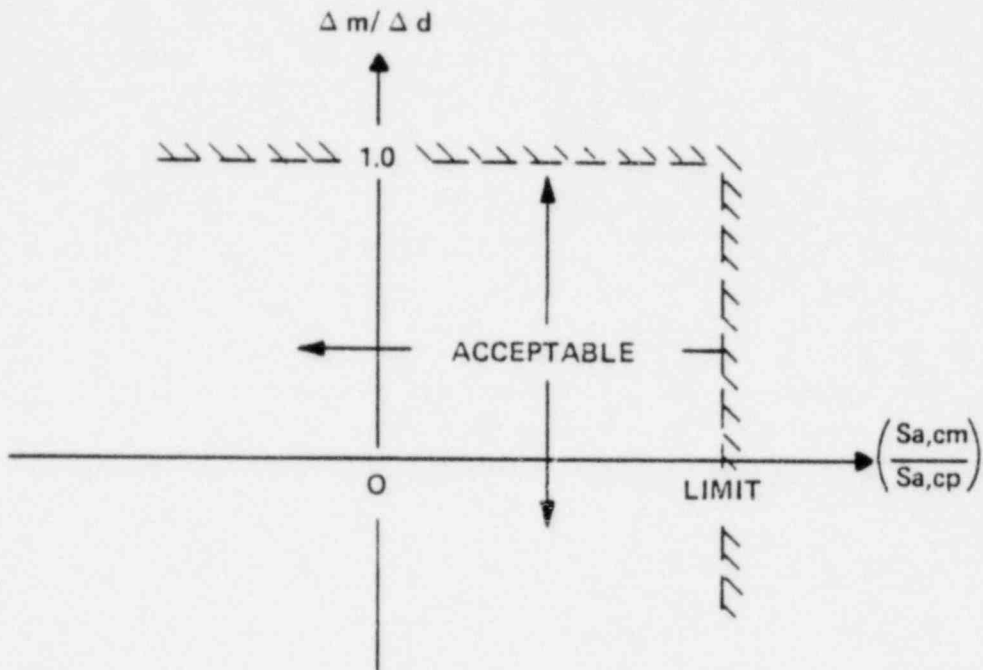
Component	Location	Peak Alternating Stress* (psi)		Fatigue Margin		Maximum Ratio of Measured to Calculated CVAP Stress	Maximum Acceptable Values of Measured Stress (psi)
		Design	CVAP	Design	CVAP		
CSB	upper flange	[]	[]	[]	[]	[]	[]
LSS	ICI nozzle	[]	[]	[]	[]	[]	[]
UGS	CEA shroud tubes	[]	[]	[]	[]	[]	[]

Fatigue Margin = Endurance limit (26,000 psi)/Peak Alternating Stress

* At conditions of Normal Operation (4 pumps, 564°F)

TABLE 7.1-2
RANGE FOR MEASURED STRESS AND VALUE FOR ACCEPTANCE CRITERION

Component	Measurement Plus Calculational Uncertainty		Limits on Acceptable Values of Measured Stress (psi)				Acceptance Criteria (psi) RMS Values	
	Plus	Minus	Peak		RMS		Minimum	Upper Limit
			Max	Min	Max	Min		
CSB	[]	[]	[]	[]	[]	[]	8,700	13,000
LSS	[]	[]	[]	[]	[]	[]	8,700	13,000
UGS	[]	[]	[]	[]	[]	[]	8,700	13,000



BASIS FOR ACCEPTANCE CRITERIA

FIGURE 7.1-1

The measurement and calculational uncertainties, being independent, are added as the square root of the sum of their squares. The results are summarized in Table 7.1-2. Corresponding values of maximum and minimum stress, and their RMS values, are also summarized in this table.

7.2 Acceptance Criterion

The measured response of the assemblies varies with time due to the dynamic nature of the flow induced loads. This response includes both deterministic and random contributions. It is convenient to define an acceptance criterion that is independent of both the statistical nature of the response and can be applied independent of the particular assembly. Furthermore, this criterion should be consistent with the limits on maximum values for measured stress listed in Table 7.1-2. Assume, as the basis for this criterion, that the deterministic as well as the random contribution to the measured stress are both the result of a random process. Then, on-line evaluation of the RMS values of the recorded data can be directly compared to the acceptance criterion.

As developed in Appendix C.2, the acceptance criterion is taken as equal to one third the endurance stress limit of 26,000 psi, or approximately 8,700 psi. This limit is conservative compared to the arithmetic average of the maximum and minimum values of the RMS stresses listed in Table 7.1-2. A permissible deviation of plus 50% is assumed for this criterion, resulting in an upper bound of one half the endurance limit, or 13,000 psi. This upper limit is less than the mean values for the RMS stresses listed in Table 7.1-2. The relationship between the acceptance criterion and the RMS values of the maximum measured acceptable values of stress for the assemblies is shown in Figure 7.2-1.

7.2.1 Acceptance Values for Response Instrumentation

The acceptance criterion, expressed for the response instrumentation in terms of strains, displacements, and accelerations, are listed in Table 7.2-1.

TABLE 7.2-1
RESPONSE INSTRUMENTATION
DATA ACCEPTANCE CRITERIA

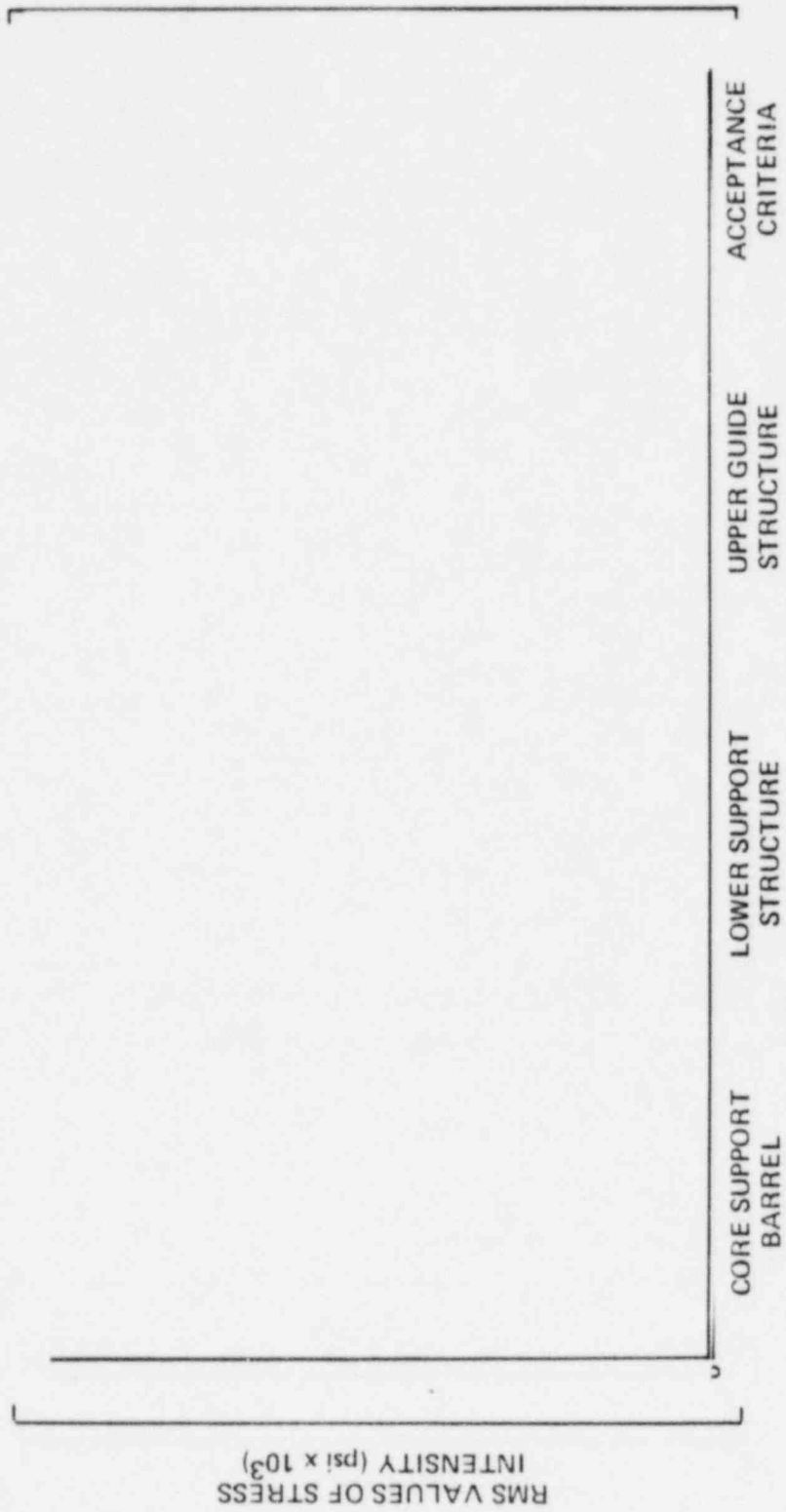
Assembly	Instrument		Criteria*
	Type	Number	
CSB	SG	S1 to S8	320 micro-in/in
	AC	A1	.030 in.
	DT	A2 to A4	.030 in.
UGS	SG	S9 to S12	320 micro-in/in
	AC	A5 to A9	.0185 in.
	AC	A10	.00167 in.
LSS	SG	S13, S14	320 micro-in/in
	AC	S11	.011 in.

*Limits are all based on 1/3 the endurance limit of 26,000 psi except for the CSB displacement (A1 to A4) which is based on the maximum clearance at the snubbers of ± 0.015 inches.

SG = Strain Guage

AC = Accelerometer

DT = Displacement Transducer



ACCEPTANCE CRITERION COMPARED TO MAXIMUM MEASURED
STRESS INTENSITIES FOR ASSEMBLIES
FIGURE 7.2-1

8.0

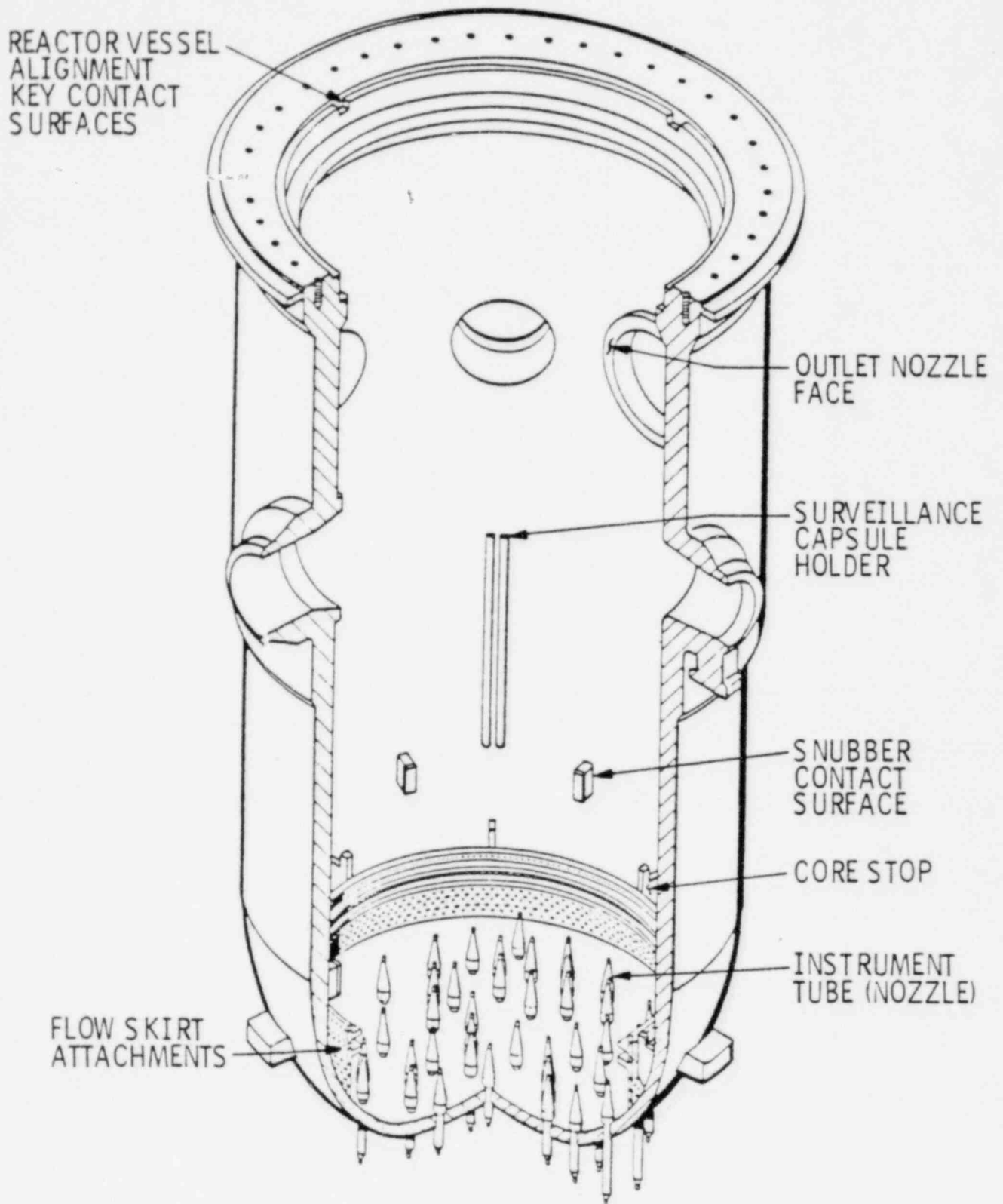
INSPECTION PROGRAM

The visual inspection of reactor vessel internals will be done in accordance with the requirements of NRC Regulatory Guide 1.20 (Ref. 1). Details of the inspection program procedure are given in Reference 3. Visual examination of the internals will be performed in two stages; a baseline review and a post hot functional precore test review. These examinations will be done under the conditions of lighting, distance, and angle specified in Section XI of the ASME Code (Ref. 4). The inspection program will include examination of all major load bearing surfaces, components to restrain motion of the internals and maximum stress locations predicted by the response analysis.

The CVAP inspection program will also include examination of welds, conduits and mountings associated with the CVAP instrumentation.

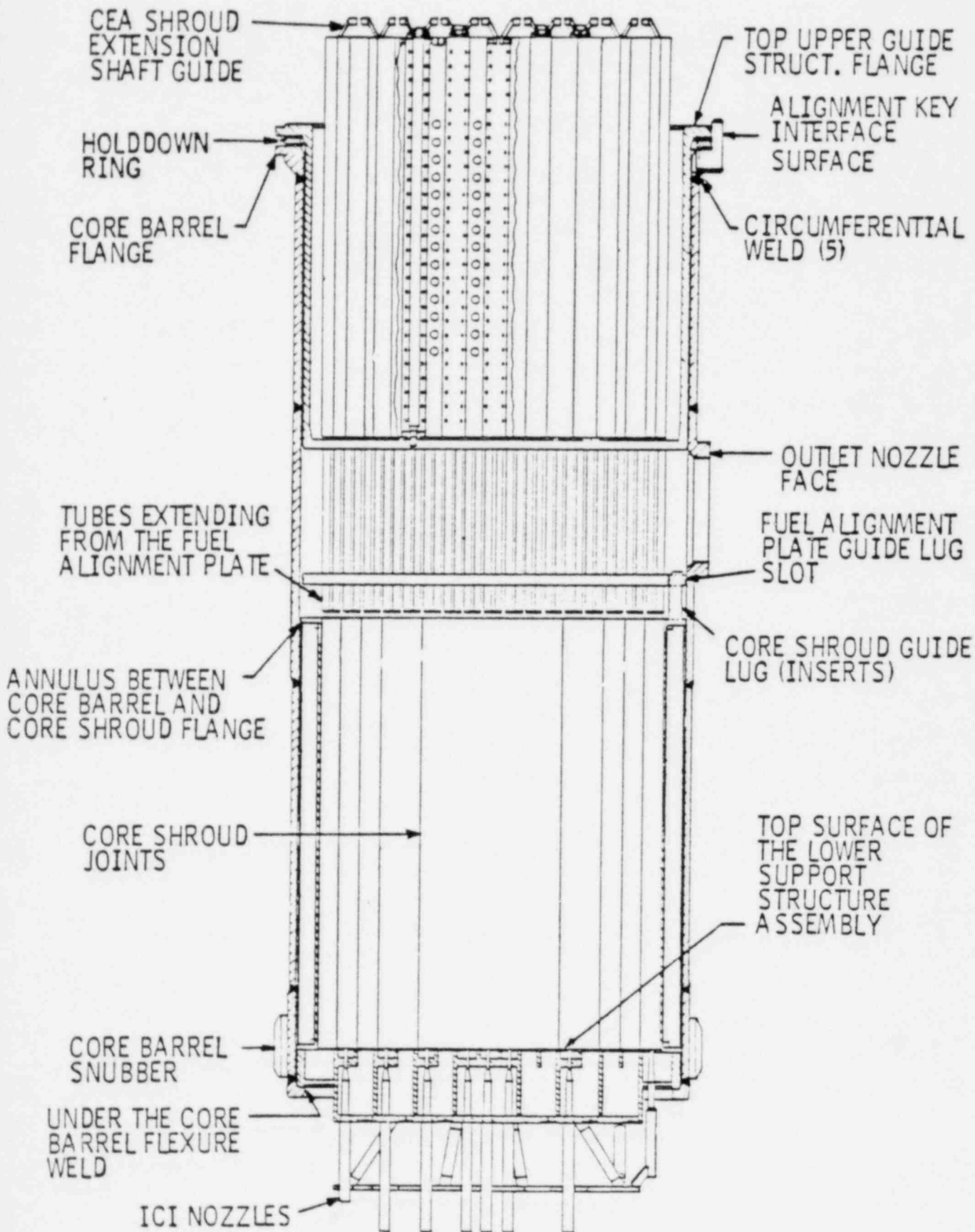
Results of the inspection will, in conjunction with the measurement program, be used to, where possible, verify predictions of the response analysis. For example, to correlate the beam mode displacement of the CSB with displacement transducer data and possible evidence of contact on the snubbers.

The inspection report will include a written description of all reportable conditions observed (e.g., scratches, wear, etc.). Photographic documentation of both the baseline and post hot functional test inspections will be conducted and included as part of this report.



REACTOR VESSEL CVAP INSPECTION

FIGURE 8.1-1



REACTOR INTERNALS ASSEMBLY
CVAP INSPECTION
FIGURE 8.1-2

8.1 Phases of Inspection Program

The inspection and documentation for the reactor internals will be completed in two stages. The first stage will take place prior to the cold hydraulic testing of the primary system and the second stage will take place after the hot functional pre-core testing of the internals is completed. The first inspection stage will compare the reactor internals components with design specifications, standards, and drawings. After the second inspection stage is completed, the data will be compared with the data from the first inspection stage. This comparison will determine the component performance and provide the basis for a comparison with the predicted behavior.

The components and areas to be inspected in both of these stages are enumerated in the following Sections and shown in Figures 8.1-1 and 2.

8.2 Inspection Procedure

8.2.1 Procedure - Baseline Inspection

8.2.1.1 Reactor Vessel

1. Inspect surface conditions of both side of the alignment key slots and the adjacent barrel seating surfaces.
2. Inspect surface conditions of the outlet nozzle faces in four quadrants.
3. Inspect the surface conditions of both wear faces of the six vessel snubbers and attachment bolt heads and lockbars.
4. Inspect the condition of the installed vessel surveillance capsule holder assemblies and attachment points.

5. Inspect the attachments of the flow skirt located in the bottom of the reactor vessel.
6. Inspect the condition of the instrumentation nozzles.

8.2.1.2 Core Barrel Exterior

1. Inspect the surface conditions of the five circumferential welds on the core barrel.
 - A. Between the upper flange and upper cylinder (located 16 inches below the top of the flange).
 - B. Between the upper cylinder and nozzle cylinder (located 85 in. below the top of the upper flange).
 - C. Between the nozzle cylinder and center cylinder (located 217 in. below the top of the upper flange).
 - D. Between the center cylinder and lower cylinder (located 44 in. above the bottom of the lower flange).
 - E. Between the lower cylinder and lower flange (located 9 in. above the bottom of the lower flange).
2. Inspect the surface conditions of both wear faces of the six core barrel snubbers.
3. Inspect the surface conditions of the core barrel, outlet nozzle faces in four quadrants.

8.2.1.3 Under the Core Support Barrel

1. Inspect the flexure weld located at the interface of the bottom of the lower support structure and the inside diameter of the bottom flange.

2. Inspect the surface conditions of the four core barrel alignment key interface surfaces both below and above the CSB flange, and the CSB flange bottom surfaces immediately adjacent to the alignment keys.
3. Above the flange at the Holddown Ring Interface surface.
4. Above the flange at UGS Interface Surface.
5. Above the flange at head interface surface.
6. Inspect the CSB Flange Surface which mates with the Holddown Ring.

8.2.1.4 Core Barrel Interior

1. Inspect the surface conditions of the eight guide lug insets (two for each lug), bolt, lockpins and lockwelds, located on the top surface of the core shroud.
2. Inspect the annulus between the core barrel and core shroud top flange for uniform width.
3. Inspect the fuel pins on the top surface of the lower support structure assy.
4. From inside of the core barrel, inspect the surface conditions of the two girth welds.
 - A. Between the upper flange and upper cylinder (located 16 inches below the top of the flange):
 - B. Between the upper cylinder and nozzle cylinder (located 85 inches below the top of the upper flange).

5. Inspect the inside joints of the core shroud

8.2.1.5 Under the Upper Guide Structure

1. Inspect the tubes extending from the fuel alignment plate.

8.2.1.6 The Outer Surface of the Upper Guide Structure

1. Inspect the surface conditions of both sides of the four guide lug slots located in the fuel alignment plate.
2. Inspect the surface conditions of both sides of the four alignment key slots located in the top UGS flange.
3. Inspect the holddown ring for uniform gap and concentricity with the alignment key slots.
4. Inspect the core shroud assy locking strap welds & the ext. shaft guide welds.

8.2.1.7 Holddown Ring

1. Inspect the holddown ring surface which mates with the UGS flange.

8.2.1.8 Reactor Vessel Closure Head

1. Inspect the surface conditions of the four alignment key slot faces.
2. Inspect the UGS mating surface.

8.2.1.9 CVAP Instrumentation

1. Inspect the surface condition of all instrumentation conduit and transducer assembly welds. Inspect for cracked welds and loose parts.
2. Inspect the instrumentation conduit housing on the top surface of the Lower Support Structure Assembly.
 - 3.1 View the bottom plates of the LSS Assembly from between the instrument nozzle support plate and the LSS Assembly. Inspect the flow hole sleeving in the bottom plates for loose sleeving.
 - 3.2 Near the 0° side of the CSB Assembly and under the LSS Assembly, inspect the surface condition of the instrumentation conduit and transducer assembly welds. Inspect for cracked welds and loose parts.
- 4.1 Inspect the flow hole sleeve inserts in the fuel alignment plate for any loosening.
- 4.2 Inspect the welded plugs in the flow hole sleeve inserts for cracked welds or loose parts.
- 5.1 On the 180° side of the UGS, inspect the surface condition of the instrumentation conduit and transducer assembly welds. Inspect for cracked welds and loose parts.
- 5.2 On the 0° side of the UGS inspect the surface condition of the instrumentation conduit and transducer assembly welds. Inspect for cracked welds and loose parts.
- 6.1 On the top of the CEA shroud assembly, inspect the surface condition of the instrumentation conduit welds. Inspect for cracked welds and loose parts.

- 6.2 On top of the CEA shroud assembly, inspect the support wings to support column and guide tube welds, also the support wing fasteners, and lockwelds.

8.2.2 Procedure - Post-Hot Functional (Pre-Core Test)

8.2.2.1 Reactor Vessel

1. Inspect surface conditions of both sides of the alignment key slots and the adjacent barrel seating surfaces.
2. Inspect surface conditions of the outlet nozzle faces in four quadrants.
3. Inspect the surface conditions of both wear faces of the six vessel snubbers and attachment bolt heads and lockbars:
4. Inspect the condition of the installed vessel surveillance capsule holder assemblies and attachment points.
5. Inspect the attachments of the flow skirt located in the bottom of the reactor vessel.
6. Inspect the condition of the instrumentation nozzles

8.2.2.2 Core Barrel Exterior

1. Inspect the surface conditions of the five circumferential welds on the core barrel.
 - A. Between the Upper Flange and Upper Cylinder (located 16 inches below the top of the flange).
 - B. Between the Upper Cylinder and Nozzle Cylinder (located 35 inches below the top of the Upper Flange).
 - C. Between the Nozzle Cylinder and Center Cylinder (located 217 inches below the top of the Upper Flange).

- D. Between the Center Cylinder and Lower Cylinder (located 44 inches above the bottom of the Lower Flange).
- E. Between the Lower Cylinder and Lower Flange (located 9 inches above the bottom of the Lower Flange).

- 2. Inspect the surface conditions of both wear faces of the six core barrel snubbers.
- 3. Inspect the surface conditions of the core barrel outlet nozzle faces in four quadrants.

8.2.2.3 Under the Core Support Barrel

- 1. Inspect the flexure weld located at the interface of the bottom of the lower support structure and the inside diameter of the bottom flange.
- 2. Inspect the surface conditions of the four core barrel alignment key interface surfaces both below and above the CSB flange, and the CSB flange bottom surface immediately adjacent to the alignment keys.
- 3. Inspect Above the flange at the holddown ring interface surface:
- 4. Inspect Above the flange at the UGS interface surface.
- 5. Inspect Above the flange at the head interface surface.
- 6. Inspect the CSB Flange Surface which mates with the Holddown Ring.

8.2.2.4 Core Barrel Interior

1. Inspect the surface conditions of the eight guide lug inserts (two of each lug), bolts, lockpins, and lockwelds, located on the top surface of the core shroud.
2. Inspect the annulus between the core barrel and core shroud top flange for uniform width.
3. Inspect the fuel pins on the core support plate.
4. From inside of the core barrel, inspect the surface conditions of the two girth welds at the following locations.
 - A. Between the upper flange and upper cylinder (located 16 inches below the top of the flange).
 - B. Between the upper cylinder and nozzle cylinder (located 85 inches below the top of the upper flange).
5. Inspect the inside joints of the core shroud

8.2.2.5 Under the Upper Guide Structure

1. Inspect the tubes extending from the fuel alignment plate.

8.2.2.6 The Outer surface of the Upper Guide Structure

1. Inspect the surface conditions of both sides of the four guide lug slots located in the fuel alignment plate.
2. Inspect the surface conditions of both sides of the four alignment key slots located in the top UGS flange.
3. Inspect the holdown ring for uniform gap and concentricity with the alignment key slots.

4. Inspect the CEA shroud assembly locking strap weld and the extension shaft guide welds.

8.2.2.7 Holddown Ring

1. Inspect the holddown ring surface which mates with the UGS flange, report any significant observations.

8.2.2.8 Reactor Vessel Closure Head

1. Inspect the surface conditions of the four alignment key slot faces.
2. Inspect the UGS mating surface.

8.2.2.9 CVAP Instrumentation

1. Inspect the surface condition of all instrumentation conduit and transducer assembly welds. Inspect for cracked welds and loose parts.
 - 2.1 View the bottom plates of the LSS Assembly from between the instrument nozzle support plate and the LSS Assembly. Inspect the flow hole sleeving in the bottom plates for loose sleeving.
 2. Near the 0° side of the CSB Assembly and under the LSS Assembly, inspect the surface condition of the instrumentation conduit and transducer assembly welds. Inspect for cracked welds and loose parts.
 3. Inspect the instrumentation conduit housing on the top surface of the Lower Support Assembly.
- 4.1. Inspect the flow hole sleeve inserts in the fuel alignment plate for any loosening.

- 4.2. Inspect the welded plugs in the flow hole sleeve inserts for cracked welds or loose parts.

- 5.1. On the 180° side of the UGS, inspect the surface condition of the instrumentation conduit and transducer assembly welds. Inspect for cracked welds and loose parts.

- 5.2. On the 0° side of the UGS inspect the surface condition of the instrumentation conduit and trnsducer assembly welds. Inspect for cracked welds and loose parts.

- 6.1. On the top of the CEA shroud assembly inspect the surface condition of the instrumentation conduit welds. Inspect for cracked welds and loose parts.

- 6.2. On top of the CEA shroud assembly inspect the support wings to support column and guide tube welds, also the support wing fasteners, and lockwelds.

8.3

INSPECTION REPORT

The inspection report will include a copy of the procedures (Ref. 3) along with completed data sheets and a summary of the significant findings of the engineering evaluations. If the post test inspection of the reactor internals reveals defects, evidence of unacceptable motion, excessive or undue wear, or deviation from the results of previously performed pre test inspections then the report will also include an evaluation and description of the modifications or actions planned to justify the acceptability of the reactor internals. The inspection report will contain data sheets with component descriptions, photographs of the inspected components, and a detailed comparison of the component's wear characteristics, as observed during the baseline and post-hot functional test inspections.

REFERENCES

1. Regulatory Guide 1.20, Rev. 2 "Comprehensive Vibration Assessment Program for Reactor Internals During Preoperational and Initial Startup Testing.
2. Combustion Engineering, "Evaluation of Core Support Structures for Arizona Nuclear Power Project Palo Verde Unit 1" Stress Report No. 14273-MD-001, June 17, 1981.
3. Combustion Engineering Specification No. 00000-RCE-457 "Comprehensive Vibration Assessment Program Standard Procedure for Visual Inspection of Reactor Vessel Internals for S80 Plants".

Combustion Engineering Specification No. 14273-RCE-457, Rev. 00 "Comprehensive Vibration Assessment Program Procedure for Visual Inspection of Reactor Vessel Internals for Arizona Unit 1".
4. ASME Boiler and Pressure Vessel Code, Section XI (Paragraph IS-211.1), 1977
5. ASME Boiler and Pressure Vessel Code, Section III, 1977
6. Penzes, L. E., "Theory of Pump Induced Pulsating Coolant Pressure in PWRs", 2nd Int. Conf. on Structural Mechanics in Reactor Technology, Vol. II, Part E-F, 1973.
7. Horvay, G., Bowers, G., "Forced Vibration of a Shell Inside a Narrow Water Annulus", Nuclear Engr. Design V34, 1975.
8. Maine Yankee Precritical Vibration Monitoring Program, Final Report, CENPD-93, February, 1973.
9. Omaha Precritical Vibration Monitoring Program, Final Report, CEN-7(0), May, 1974.

10. Calvert Cliffs Analysis of Flow-Induced Structural Response, CEN-4(B).
11. Comparison of Calvert Cliffs, Maine Yankee and Ft. Calhoun Design Parameters and Flow-Induced Structural Response, CEN-115, Supp. 1, April, 1974.
12. Comparison of ANO-2, Maine Yankee and Ft. Calhoun Reactor Internals Design Parameters and Flow-Induced Structural Response, CEN-8(A)-P Supp. 1, May 1975.
13. Mark, W. D., Chandiramani, K. L., Karnopp, R. L., Reactor Internals Vibration Study, BBN Report 151273, Oct. 1967.
14. Final Report on Studies of Flow in a 0.248 Scale Model of the Omaha PWR, H. L. Crawford and L. J. Flanigan, August, 1970, Battelle Memorial Institute, April, 1969.
15. Final Report on Studies of Flow in a 1/5-Scale Model of the Palisades PWR, CEND-358, L. A. Schultz, D. A. Trayser, L. J. Flanigan, Battelle Memorial Institute, April, 1969.
16. Chen, Y. N., "Properties of Karman Vortex Streets", Sulzer Technical Review, 1972.
17. Batham, J. P., "Pressure Distribution on Circular Cylinder at Critical Reynold Numbers", J1. Fluid. Mech. v57, pt 2, 1973.
18. Szecheny, I. E., "Supercritical Reynold Number Simulation for Two-Dimensional Flow Over Circular Cylinders", J. Fluid Mech., v70 pt 3 1975.
19. Donalson, C.D., et.al., "A Study of Free Jet Impingement", Part 2, J. Fluid Mech. 1971 V.45, Part 3, pg 477-512.

20. King, R., "Vortex Excited Oscillations of Yawed Circular Cylinders", ASME-76-WA/FE-16.
21. Chen, Y. N., "Fluctuating Life Forces of the Karman Vortex Streets on Single Circular Cylinders and in Tube Bundles", Part 1 (ASME-71-VIBR-11), Part 2 (ASME-71-VIBR-12), Part 3 (ASME-71-VIBR-13).
22. Lubin, B. T., "Response of a Tube Bank to Turbulent Crossflow Induced Excitation", ASME-77-DET-142.
23. Owen, P. R., "Buffeting Excitation of Boiler Tube Vibration", J1. of Mechanical Science, Vol. 7, N. 4, 1965.
24. Bruun, H. H., Davies, P. et al., "An Experimental Investigation of the Unsteady Pressure Forces on a Circular Cylinder in a Turbulent Cross Flow", J1. of Sound & Vibration, V40, N.4, 1975.
25. Gibson, M. M., "Spectra of Turbulence in a Round Jet", J. Fluid Mechanics V15, 1963.
26. Hurty, W. C., Rubinstein, M. F., Dynamics of Structures, Prentice-Hall, 1964.
27. L. Lee, S. Chandra, "Pump Induced Fluctuating Pressures in a Reactor Coolant Pipe", Int J. of Press Vess. & Piping, 8 (1980), 407-417.
28. Simpson, H. C., McCaskill, H. C., Clark, T. A., "Generation of Hydraulic Noise in Centrifugal Pumps", Paper 12, Session-4, Proc. of Symp. on Vib. in Hydraulic Pumps and Turbines, Manchester, U.K., 1966.
29. Panovko, Ya. Elements of the Applied Theory of Elastic Vibrations MIR Publishers, Moscow, USSR 1971.
30. Connors, H. J., "Fluid Elastic Vibration of Tube Array Excited by Cross Flow" Flow Induced Vibrations in Heat Exchangers, ASME, 1970.

31. Lubin, B. T., et.al "Response of a Tube Bank to Cross Flow-Induced Excitation at Transcritical and Supercritical Reynolds Numbers", Symposium on Practical Experiences with Flow Induced Vibrations, Karlsruhe, West Germany, Sept. 3, 1979.
32. Lubin, B.T., Hashlinger, K.H., "Frequency Response of a Tube Bundle in Water" J. of Fluids Engineering, ASME, June, 1977.
33. Au Yang, M. "A Computerized Method for Flow-Induced Random Vibration Analysis of Nuclear Reactor Internals", ASME-76-WA/PUP-12.
34. Chen, S. S., Chung, H., "Design Guide for Calculating Hydrodynamic Mass, Part I: Circular Cylindrical Structures", ANL-CT-76-45, June, 1976.

Chung, H., Chen, S. S., "Design Guide for Calculating Hydrodynamic Mass, Part II: Non-circular Cylindrical Structures", ANL-CT-78-49, Sept. 1978.
35. Simpson, A. C., Clark, J. A. "Noise Generation in a Centrifugal Pump", ASME 70-FE-37.
36. Cepkauskas, M. M. "Acoustic Pressure Pulsations in Pressurized Water Reactors" F4/2 5th Intl. Cong. on Structural Mechanics In Reactor Technology August, 1979.
37. Bendat, J., Piersol, A. G. Random Data: Analysis and Measurement Procedures, Wiley Interscience, New York 1971.
38. Penzes, L. E., Bhat, S. K., "Generalized Hydrodynamic Effects of a Double Annuli on a Vibrating Cylindrical Shell" 2nd Intl. Conf. on Structural Mechanics in Reactor Technology", Vol II, Part E-F, 1973.
39. Drawings Showing Instrument Locations.

- 39.1 Precritical Instrument Installation - Lower Support Structure E-14273-164-801-02.
- 39.2 Precritical Instrument Installation - Core Support Barrel E-14273-164-802-02.
- 39.3 Precritical Instrumentation Installation - Upper Guide Structure E-14273-164-803-02.
- 39.4 Precritical Instrumentation Installation - Upper Guide Structure E-14273-164-804-02.
- 39.5 Precritical Instrumentation Installation - Flange E-14273-164-805-02.
- 40. Palo Verde Nuclear Generating Station Manual. Procedure 92 HF-1RX01, Rev. A, "Pre-Ccore Reactor Internals Vibration Measurements".
- 41. Palo Verde Nuclear Generating Station Manual. Procedure 90HF-1ZZ-01, Rev. A, "Pre Core Hot Functional Test Controlling Document".
- 42. Palo Verde Nuclear Generating Station Manual. Procedure 91 HF-IRC03, Rev. A, "Pre Core RCS Flow Rate".

APPENDIX-A

HYDRAULIC LOADSA.1 Hydraulic Forcing Functions for CSB AssemblyA.1.1 Core Support Barrel

A.1.1.1 Deterministic Forcing Function

A hydrodynamic model was developed to obtain the pressure fluctuations on the core support barrel due to the operation of pumps. The idealized model (Figure A.1-1) represents the annulus of coolant between the core support barrel and the reactor vessel. The radii a_1 and a_2 correspond to the outer radius of the core support barrel and inner radius of the reactor vessel, respectively. The length, L , corresponds to the length of the core support barrel. The area bounded by z_1 and z_2 in the vertical direction and θ_1 and θ_2 in the circumferential direction corresponds to the area of the inlet duct, and is located at the position of an inlet duct.

In deriving the governing hydrodynamic differential equations for the above model, the fluid is taken to be compressible and inviscid. Linearized versions of the equations of motion and continuity are used. The equations of motion, continuity, and equation of state can be written:

$$\rho_0 \frac{\partial \tilde{V}}{\partial t} + \nabla P = 0 \quad (1)$$

$$\frac{\partial \tilde{\rho}}{\partial t} + \rho_C \nabla \cdot \tilde{V} = 0 \quad (2)$$

$$\tilde{P} = C_0^2 \tilde{\rho} \quad (3)$$

Where:

ρ_0 = reference density,

$\tilde{\rho}$ = fluctuating density,

\tilde{V} = fluctuating velocity,

\tilde{P} = fluctuating pressure,

C_0 = reference velocity of sound = $\left(\frac{\partial P_0}{\partial \rho}\right)^{\frac{1}{2}}$

P_0 = reference pressure,

t = time,

∇ = gradient vector operator

$\nabla \cdot$ = divergence operator

These equations are combined to produce the desired acoustic wave equation, the solution of which describes the pressure in the downcomer annulus as a function of space and time. In cylindrical coordinates, the wave equation can be written:

$$\frac{\partial^2 \tilde{P}}{\partial r^2} + \frac{1}{r} \frac{\partial \tilde{P}}{\partial r} + \frac{1}{r^2} \frac{\partial^2 \tilde{P}}{\partial \theta^2} + \frac{\partial^2 \tilde{P}}{\partial z^2} = \frac{1}{C_0^2} \frac{\partial^2 \tilde{P}}{\partial t^2} \quad (4)$$

To solve the wave equation, boundary conditions at $r = a_1$, $r = a_2$, $z = 0$, and $z = L$ are required.

1) $r = a_1$, The inner vertical wall is considered to be a rigid wall which is described by the expression:

$$\left. \frac{\partial \tilde{P}}{\partial r} \right|_{r=a_1} = 0 \quad (5)$$

- 2) $r = a_2$, The outer vertical wall is considered to be rigid except at the location of the pump inlets where the radial pressure gradient is

$$\left. \frac{\partial \tilde{P}}{\partial r} \right|_{r=a_2} = P_{op} A \cos \omega_p t \quad (6)$$

where P_{op} is the inlet pressure at the pump rotational frequency of ω_p and A is a constant.

Using the Heaviside step function, H , the boundary condition at $r = a_2$ can be written

$$\left. \frac{\partial \tilde{P}}{\partial r} \right|_{r=a_2} = h(z) h(\theta) P_{op} A \cos \omega_p t \quad (7)$$

Where:

$$h(z) = H(z-z_1) - H(z-z_2)$$

$$h(\theta) = H(\theta-\theta_1) - H(\theta-\theta_2)$$

- 3) $z = L$, The top of the cylinder is considered to be a rigid surface where the axial pressure gradient is

$$\left. \frac{\partial \tilde{P}}{\partial z} \right|_{z=L} = 0 \quad (8)$$

- 4) $z = 0$, The bottom of the cylinder is considered to be an open surface which is described by the expression:

$$\tilde{P} \Big|_{z=0} = 0 \quad (9)$$

The boundary conditions along with the wave equation give a complete description of the problem. Ref. 36 describes in detail the solution of this boundary value problem. The method of solution consists of transforming this problem to one with homogeneous boundary conditions and non-homogeneous differential equation. Usual modal analysis techniques are used to solve the transformed problem. The final solution which defines the spatial distribution of pressure on the core support barrel system as a function of time, space, excitation, and natural hydraulic frequencies is given as follows

$$\begin{aligned} \tilde{p}(r, \theta, z, t) = & \sum_{n=1}^{\infty} \sum_{m=0}^{\infty} \sum_{s=1}^{\infty} Q_{nms} P_{op} A C_0^2 A C_0^2 a_2 Q_s(a_2) \int_{\theta_1}^{\theta_2} Q_m(\theta) d\theta \int_{z_1}^{z_2} Q_n(z) dz \\ & \cdot \cos \omega_p t / (\omega_{nms}^2 - \omega_p^2) \int_0^L Q_n^2(z) dz \int_0^{2\pi} Q_m^2(\theta) d\theta \int_{a_1}^{a_2} Q_s^2(r) r dr \end{aligned} \quad (10)$$

where for the closed-open end conditions for the annulus

$$Q_n = \cos(n\pi z/2L) \quad n = 1, 3, 5, \dots$$

$$Q_m = \cos(m\theta) \quad m = 0, 1, 2, \dots$$

$$Q_s(r) = J_m(\lambda_{nms} r) + \eta_{nms} Y_m(\lambda_{nms} r)$$

$$\lambda_{nms} = (\omega_{nms}/C_0)^2 - (n\pi/2L)^2$$

$$\eta_{nms} = \frac{d}{dr} J_m(\lambda_{nms} r) \Big|_{r=a_1} / \frac{d}{dr} Y_m(\lambda_{nms} r) \Big|_{r=a_1}$$

ω_{nms} = liquid annulus natural frequencies

ω_p = pump rotational frequencies

a_2 = outer radius of annulus

P_{op} = inlet pressure at pump rotational frequency

A = constant-evaluated at inlet with known value of P_{op}

J_m, Y_m = Bessel functions of first and second kind of order m

To solve the expression for $p(r, \theta, z, t)$, the inlet pressure, P_{op}

or

$$\tilde{p}(r, \theta, z, t) \Big|_{\substack{r=a_2 \\ z=(z_1+z_2)/2 \\ \theta=(\theta_1+\theta_2)/2}}$$

is required. An analytical model and analysis was developed to obtain pump pressure pulsations at the System 80 inlet nozzle, Reference (27). The pump pressure pulsations originate at the pump discharge and propagate down the cold leg pipe to the inlet nozzle. An empirical relation for the pump discharge pressure pulsation (P_D) at the blade passing frequency (BPF) is (Ref. 35, 28);

$$\begin{aligned} \text{SPL})_{\text{BPF}} &= 20 \text{ Log}_{10} \left(\frac{P_D}{14.7 \times 10^{-6}} \right) \\ &= 222 + 20 \text{ Log}_{10} \left[\frac{\text{HP}}{N \cdot S \cdot R \cdot W} \right] \end{aligned} \quad (11)$$

where:

$\text{SPL})_{\text{BPF}}$	= sonic power level at BPF
HP	= pump horse power = $(\Delta p \cdot Q)$
Δp	= static pressure across pump
Q	= volumetric flow rate
N	= rotor speed
S	= pump specific speed = $(NQ^{1/2} / H^{3/4})$
H	= pump head = $\Delta p / \rho$
R	= average radius of impeller
W	= impeller exit width

To evaluate P_D at frequencies other than the blade passing frequency, an empirical formula which relates $P_D)_{\text{BPF}}$ to P_D at other frequencies is developed such that

$$\text{SPL})_i = \text{SPL})_{\text{BPF}} - K_i \quad (12)$$

Where K_i is a constant based on previous CVAP data (Ref.12),

$\text{SPL})_i$ = sonic power level for specific frequency

$$\text{SPL})_i = 20 \text{ Log}_{10} \left[\frac{P_{Di}}{14.7 \times 10^{-6}} \right] = \left[222 + 20 \text{ LOG}_{10} \left(\frac{\text{HP}}{N \cdot S \cdot R^2 \cdot W} \right) - K_i \right]$$

K_i	= 2.5 for rotor speed - 20 Hz
	= 10.2 for 2 x rotor speed - 40 Hz
	= -2.5 for 2 x BPF - 20 Hz

To develop a relationship between the pressure pulsation at the pump discharge and inlet nozzle, the fluid is assumed to be compressible and the pressure pulsations are considered to be plane waves. The momentum, continuity, and equation of state are used to develop the one-dimensional wave equation:

$$\frac{\partial^2 \tilde{p}}{\partial x^2} - \frac{1}{C_0^2} \frac{\partial^2 \tilde{p}}{\partial t^2} = 0 \quad (13)$$

where:

C_0 = sonic velocity

\tilde{p} = pressure fluctuation

x = distance along cold leg pipe from pump

Assuming boundary conditions

$$x = 0; \tilde{p} = P_D \cos \omega_p t$$

$$x = L; \frac{\partial \tilde{p}}{\partial x} - \frac{A_0}{k} \frac{\partial^2 \tilde{p}}{\partial t^2} = 0, \text{ piston - spring supported end} \quad (14)$$

where:

ρ = density of coolant

A = cross sectional area of cold leg pipe

k = empirically determined constant

ω_p = pump frequency

P_D = pressure pulsation at pump discharge

Test data from previous CVAP tests (Ref. 2, 3) indicate this boundary condition at $x=L$ best describes the measured results.

Solution of the boundary value problem defined by the governing equation (13) and the boundary conditions (14) (Ref. 27) yields the pressure fluctuation in the inlet pipe as,

$$\begin{aligned} \tilde{p}(x,t) = & - \sum_{n=1}^{\infty} \frac{I_3}{I_1} \left(\frac{\cos \omega_p t - \cos \omega_n t}{\omega_p^2 - \omega_n^2} \right) \sin \frac{\omega_n x}{C_0} \\ & + P_D \left(1 - \frac{x}{L + \frac{k}{\rho A C_0^2 (\omega_p)^2}} \right) \cos \omega_p t \end{aligned}$$

where:

$$I_3 = P_D \frac{\omega_p^2}{C_o^2} \left[- \frac{C_o}{\omega_n} \frac{1}{L + \frac{k}{\rho A C_o^2} \frac{C_o}{\omega_p}} \left[\frac{k}{\rho A C_o^2} \left(\left(\frac{C_o}{\omega_p} \right)^2 - \left(\frac{C_o}{\omega_{pn}} \right)^2 \right) \cos \frac{\omega_n L}{C_o} \right. \right. \\ \left. \left. - \left(L + \frac{k}{\rho A C_o^2} \left(\frac{C_o}{\omega_p} \right)^2 \right) \right] \right]$$

$$I_1 = \frac{1}{C_o^2} \left(\frac{L}{2} + \sin \frac{2 \omega_n L}{C_o} / \frac{4 \omega_n}{C_o} \right)$$

ω_p = pump related frequency

ω_n = liquid natural frequency

t = time

L = length of cold leg pipe

C_o = sonic velocity

A = pipe flow area

k = empirical factor based on test data - dependent on fluid temperature and geometry of annulus

ρ = liquid density

P_D = pressure pulsation at pump discharge

Values of $\tilde{P}(x,t)_{x=L}$ are used as input values for the solution of the pressure fluctuation expression in the downcomer annulus.

Predictions of periodic forcing functions by the analytical method are based on the inlet duct pressure pulsations given in Table A.1-1. Calculations were performed for all CVAP test condition temperatures. Results obtained were for one pump operation. Results for multiple pump operation were obtained by superposition of the one pump results and are presented as the maximum amplitude, P_{max} , of the ω_{pi} components of dynamic pressure where ω_{pi} is the pump rotor, twice the rotor, blade passing, and twice the blade passing frequencies. Values of P_{max} are presented in Table A.1-2. Plots for the

circumferential and axial variations of the pressure are presented in Figures A.1-2 and A.1-3 respectively for a typical one pump operation.

Data from previous pre-critical vibration monitoring programs (Ref. 8, 9) confirm that the pressure distributions for multiple pump can be obtained by superimposing various one pump pressure distributions; the peak pressure for N pumps ($N = 2,3,4$) is N times the pressure for one pump. The resulting pressure distribution is equivalent to N times that of a one pump pressure distribution.

Since superposition holds for multiple pumps and the phasing between pumps is unknown, the assumption that all pumps are in phase results in the maximum value of pressure. The structure being linear, the response for N pumps is that for a one pump case multiplied by N (Section 3.2.2.1).

A.1.1.2 Random Forcing Functions

The random hydraulic forcing function on the core support barrel assembly is developed from semi-empirical methods. An analytical expression is developed to define the turbulent pressure fluctuation for fully developed flow. This expression is modified, based upon results from scale model testing to account for the fact that the flow in the downcomer annulus is not fully developed. The experimentally adjusted analytical expressions are used to determine the peak value of the pressure spectral density associated with the turbulence and the maximum area of coherence. The resulting equation for the wide band white noise force power spectral density is expressed as:

$$S_F(\omega) = S_p(\omega) \cdot N \cdot A_C^2 \quad (1)$$

where:

- $S_p(\omega)$ = pressure power spectral density (psi²/Hz)
- A_C = coherence area of turbulent pressure fluctuations (in.²)
- N = ratio of total surface area to coherence area

Based on flow model test data, the turbulent pressure spectral density is defined as:

$$S_p(\omega) = (0.104 \frac{\rho V_{CSB}^2}{144 g_c})^2 [2 \phi(\omega)] \quad (2)$$

where:

- ρ = density of coolant in downcomer annulus (lbm/ft³)
- V_{CSB} = average coolant velocity in downcomer annulus (ft/sec)
- $(\phi)_\omega$ = normalized pressure spectral density = $0.3\delta^* / V_{CSB}$ (sec)
- δ^* = maximum boundary layer displacement thickness defined as $1/2 (R_{RV} - R_{CSB})$ (ft)
- R_{RV} = inside radius of reactor vessel (ft)
- R_{CSB} = outside radius of core support barrel (ft)

Based on flow model test data the coherence area is defined as:

$$A_c = (D_v - D_{CSB})^2 \quad (3)$$

where:

$$\begin{aligned} D_v &= \text{inside diameter of reactor vessel} \\ D_{CSB} &= \text{outside diameter of core support barrel} \end{aligned}$$

The ratio of total force contributing area to coherence area, N , is taken to be the ratio of total external surface area of the core support barrel, A_s , divided by A_c where

$$A_s = \pi D_{CSB} L \quad (4)$$

where:

$$L = \text{length of core support barrel}$$

Predictions of the random forcing pressure acting on the core support barrel are presented in Table A.1-3 in terms of the maximum pressure spectral density in units of psi^2/Hz . Predictions are made at both hot and cold conditions for a variety of multiple pump operating configurations. The coherence area in the core support barrel-reactor vessel annulus is

$$A_c = (D_v - D_{CSB})^2 = 2.64 \text{ ft}^2 \quad (5)$$

where:

$$\begin{aligned} D_v &= \text{inside diameter of reactor vessel} \\ D_{CSB} &= \text{outside diameter of core support barrel} \end{aligned}$$

The surface area of the core support barrel is:

$$A_s = \pi D_{CSB} L = 1346.6 \text{ ft}^2 \quad (6)$$

where:

L = length of core support barrel

Values of the force spectral density, $S_F(\omega)$, are calculated from the expression:

$$S_F(\omega) = S_p(\omega) N.A_C^2$$

where values of $S_p(\omega)$ are given in Table A.1-3

Upper bounds for the fluctuating pressures, including both random and periodic contributions, are shown in Figure A.1-4.

TABLE A.1-1

PUMP INDUCED PERIODIC PRESSURE AT INLET NOZZLE STATION (PSI)

Temperature °F	Rotor Speed 20 Hz	2 x RS 40 Hz	Blade Passing Frequency 120 Hz	2 x BPF 240 Hz
564	[
500				
250				
200				

TABLE A.1-2

MAXIMUM PUMP INDUCED PERIODIC PRESSURE
ON CORE SUPPORT BARREL AT PRESSURE
TRANSDUCER LOCATIONS (PSI)

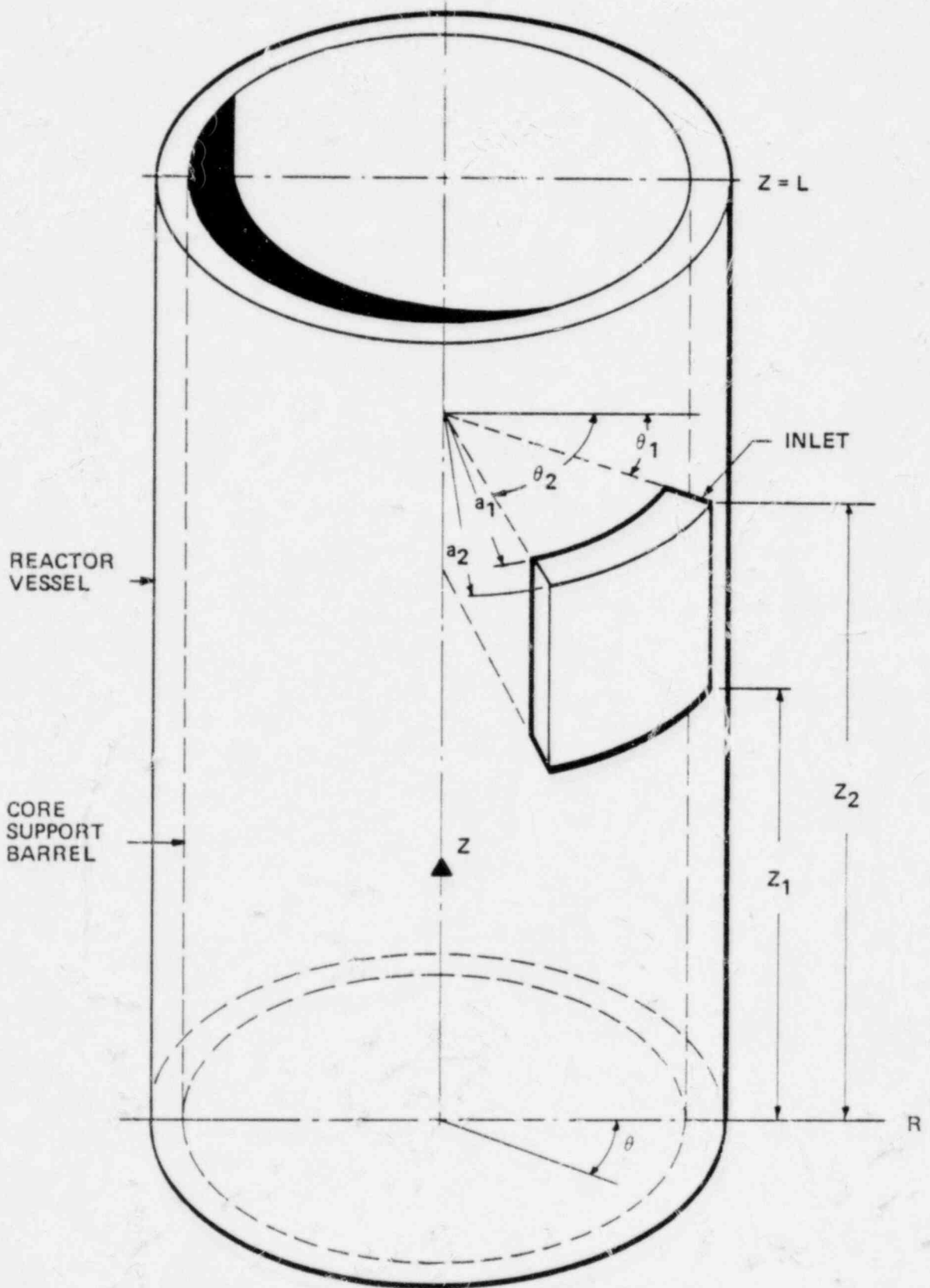
Temperature °F	No. Pumps	Rotor Speed		Blade Passing Frequency					
		20 Hz	40 Hz	120 Hz	240 Hz				
564	4	[
	3								
	2								
500	4								
	3								
	2								
260	3								
	2								
200	3]			
	2								

TABLE A.1-3

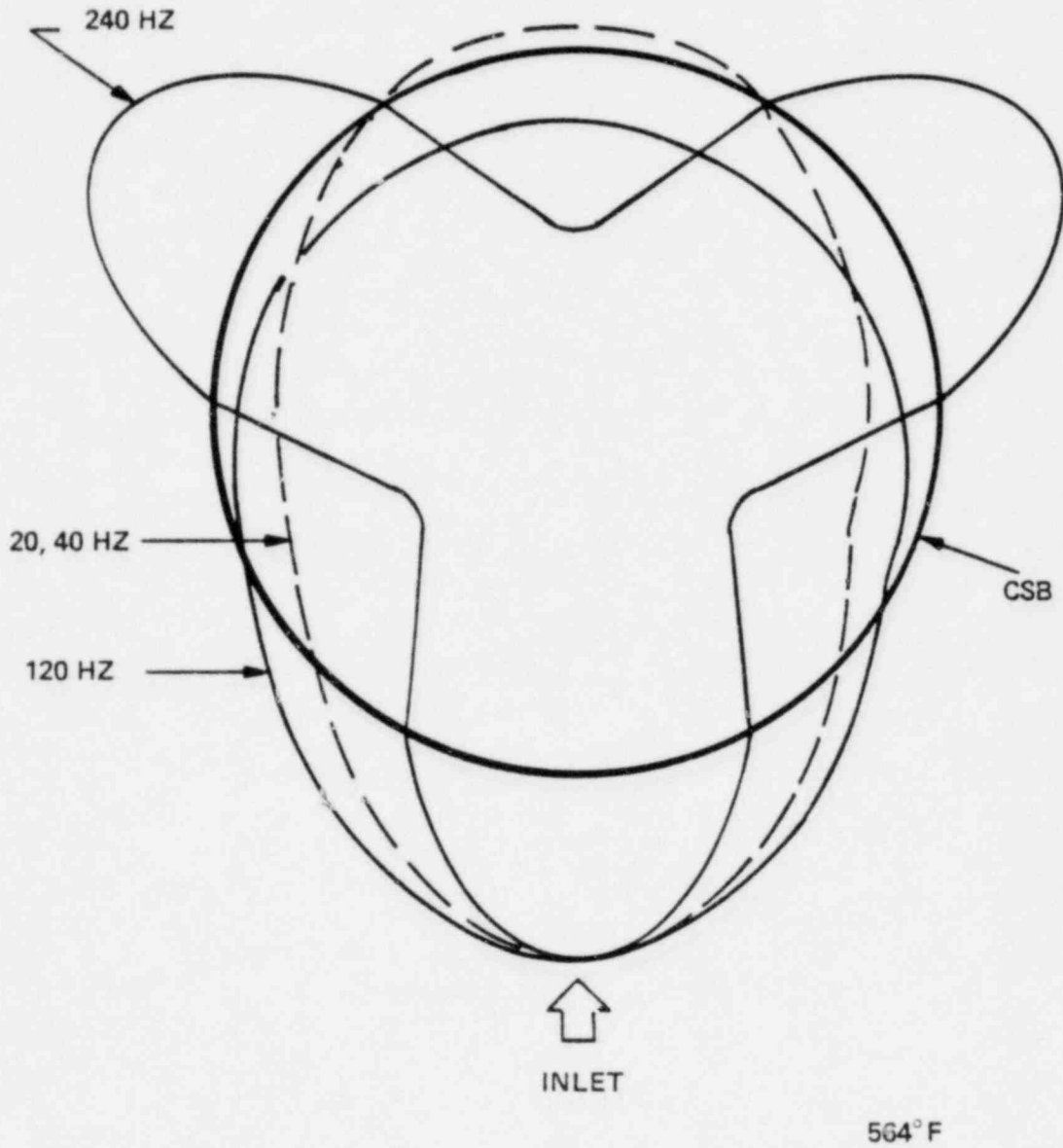
RANDOM FLUCTUATING PRESSURE ON CORE SUPPORT BARREL,
POWER SPECTRAL DENSITY (PSI²HZ)

Temperature °F	No. Pumps	Random Pressure PSD Psi ² /Hz
564	4	[]
	3	
	2	
500	4	
	3	
	2	
260	3	
	2	
200	3	
	2	

FIGURE A.1-1
 DETERMINISTIC HYDRAULIC MODEL

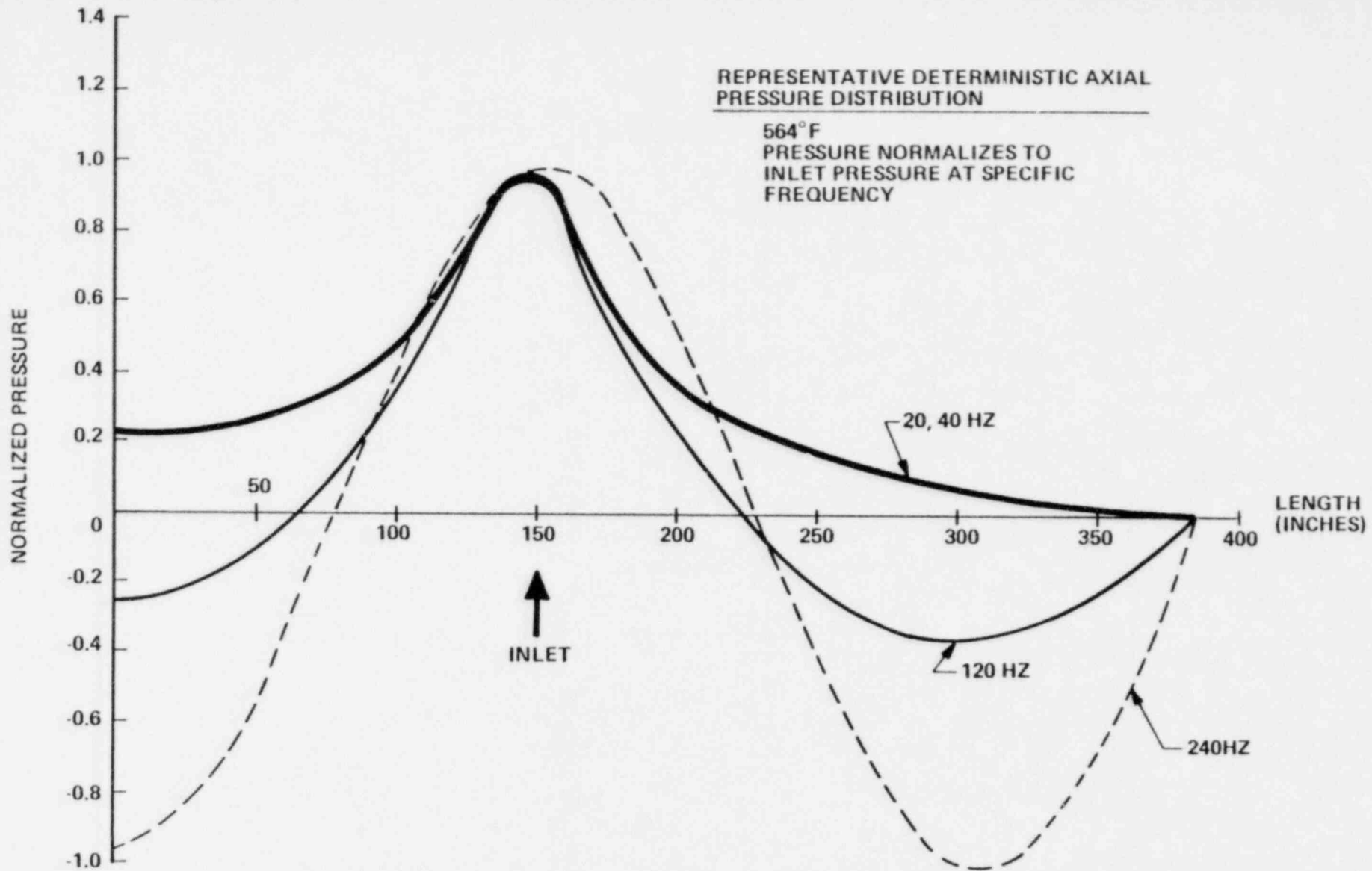


REPRESENTATIVE CIRCUMFERENTIAL DETERMINISTIC
PRESSURE DISTRIBUTION



CIRCUMFERENTIAL VARIATION IN PRESSURE

FIGURE A.1-2

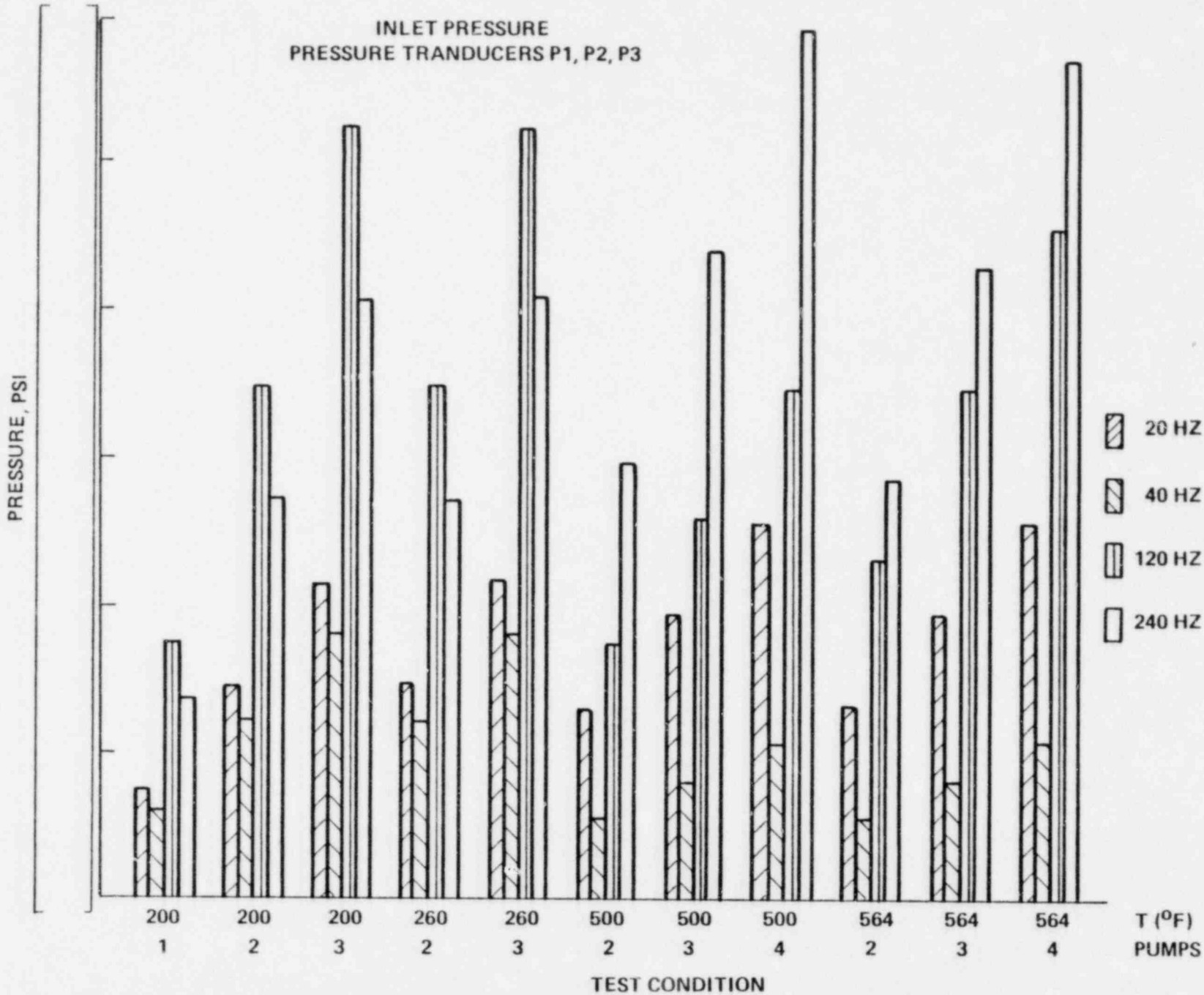


A-17

AXIAL VARIATION IN PRESSURE

FIGURE A.1-3

MAXIMUM VALUES OF PRESSURE PULSATIONS ON CSB
FIGURE A.14



A.1.2 Lower Support Structure

The most significant flow induced loading on the lower support structure is on the instrument tubes and the skewed beam supports for the instrument plate. These structures may be excited by periodic and/or random flow induced forces. The periodic component of this loading is due to pump related pressure fluctuations and vortex shedding due to crossflow.

A.1.2.1 Deterministic Forcing Function

Derivation of pump frequency related loads is accomplished by assuming that the periodic pressures calculated at the lower section of the downcomer annulus are propagated undiminished through the flow skirt. For operation with more than one pump, the principle of superposition is used which accounts for the pump azimuthal locations and the phasing between pumps. The phasing between pumps is chosen to provide the maximum pressure fluctuations acting on the LSS components. The rms pressure fluctuation acting on the LSS components is taken to be:

$$\bar{P}_{rms} = \bar{P}_{max} \sqrt{2} \quad (1)$$

The rms force exerted on the LSS components at the pump rotational frequency is then computed with the expression:

$$\bar{F}(\omega_p) = \bar{P}_{rms} \sin\left(\frac{\omega_p \Delta x}{C_0}\right) A_p \quad (2)$$

where:

- \bar{P}_{rms} = RMS pressure fluctuation at pump rotational frequency
- Δx = component diameter or thickness
- C_0 = speed of sound
- A_p = projected or frontal area of component

Forces are calculated at the pump rotor, twice rotor, blade passing, and twice blade passing frequencies.

Assuming that regular vortex shedding occurs, the maximum vortex shedding frequency is 30 Hz, well below the lowest structural frequency (230 Hz) for both the instrument tubes and skewed beams. The magnitude and frequency of this periodic force are accounted for based on data (Ref.20) for crossflow over both vertical and skewed isolated tubes. The lift and drag forces are expressed as:

$$F_{L,D} = C_{L,D} \frac{\rho v^2}{2} \sin(\omega_{vs} t) A_p \quad (3)$$

where:

- $C_{L,D}$ = Lift/Drag Coefficients
- v = Approach Velocity
- ρ = Density of Fluid
- ω_{vs} = Vortex shedding frequency = $2\pi \frac{V}{D} S_t$
- S_t = Strouhal number
- D = Tube diameter
- A_p = Projected or frontal area = DL
- L = Length of tube
- t = time

The magnitude of the drag coefficient and Strouhal number are taken from Reference 21. The lift coefficient is taken to be equal to the drag coefficient. The maximum force is computed for the maximum value of $\sin(\omega_{vs} t) = 1.0$

$$\bar{F}_{max} = C_{L,D} \frac{\rho v^2}{2} A_p \quad (4)$$

A.1.2.1.1 Results

Predictions of the pump periodic force on the LSS components are based upon the inlet duct pressure pulsations given in Table A.1-1 and the assumption that the periodic pressure variations are

propagated undiminished through the flow skirt from the lower portion of the core barrel-reactor vessel annulus. Predictions are made at both hot and cold conditions for a variety of multiple pump operating configurations. The pump pressure pulsation loads on the instrumentation tube 58 and instrumentation plate are given in Table A.1-4 at the blade passing and twice blade passing frequencies. Pump pulsation loads at the rotor and twice rotor frequencies are negligible. In addition, the maximum pressure amplitude, P_{max} , of the components of the dynamic pressure acting in the lower support region are provided in Table A.1-4.

Predictions of the vortex shedding frequencies and lift/drag force on the instrumentation tube 58 are provided in Table A.1-5. Predictions were made for an outermost ICI tube which is subjected to the full impact of the high approach velocities from the flow skirt, Figure A.1-5.

A.1.2.2 Random Forcing Function

The instrument tubes and instrument plate support beams are both subjected to direct impact and/or turbulent buffeting by the flow skirt flow jets. The force spectrum of these jets is assumed to be represented as wide band white noise. The magnitude of this spectrum is based on data in the literature for impingement of turbulent jets (Ref. 19). This velocity dependent magnitude is applied to an outside tube which receives the full impact of the flow skirt jets before they decay due to fluid entrainment and the presence of inner tube rows. For both direct jet impact and turbulent buffeting the wide band force power spectral density is approximated by:

$$S_F(\omega) = S_p(\omega) N A_c^2 \quad (1)$$

where:

$S_p(\omega)$ = Pressure power spectral density (psi^2/Hz)

A_c = coherence area

N = ratio of total force contributing area to A_c
taken to be the ratio of the total external area of the ICI tube, A_s , to A_c

$A_s = \pi D_{\text{ICI TUBE}} L_{\text{ICI TUBE}}$

The pressure power spectral density can be written as

$$S_p(\omega) = C_p^2 (1/2 \rho V^2)^2 [2\phi(\omega)] \quad (2)$$

where:

C_p^2 = squared fluctuating pressure coefficient

ρ = fluid density

V = mean velocity past ICI tube - stream velocity

$2\phi(\omega)$ = normalized pressure spectral density

Based upon data for an impinging jet (Ref. 19) C_p^2 , is conservatively taken to be 0.10 and the normalized pressure spectral density, $2 \phi(\omega)$, has a maximum value of .01. The pressure power spectral density can be written:

$$S_p(\omega) = .001 (1/2 \rho V^2)^2 \quad (3)$$

The velocity past the ICI tube is based upon experimental data on the velocity distribution in the lower head region.

The coherence area, A_c , is taken to be:

$$A_c = L_{c\theta} L_{cz} \quad (4)$$

where:

$L_{c\theta}$ = circumferential coherence length

L_{cz} = axial coherence length

Based on data from Reference 19, $L_{c\theta}$ is equal to $\pi D/4$ and L_{cz} is equal to $D/2$ where D is the outside diameter of the instrumentation tube.

Predictions of the random forcing functions acting on instrumentation tube 58 are presented in Table A.1-6 in terms of the maximum pressure spectral density in psi^2/Hz . Predictions computed at both hot and cold conditions at a variety of multiple pump operation configurations. Predictions are made on an ICI tube adjacent to the flow skirt which is subjected to the maximum approach velocities and loading. The coherence area of the instrumentation tube is:

$$A_c = \frac{\pi D^2}{8} = 6.28 \text{ in}^2 \quad (5)$$

where:

D = tube diameter

The surface area of the instrumentation tube is:

$$A_s = \pi D L \quad 307.9 \text{ in}^2$$

where:

L = tube length

Values of the force spectral density, $S_F(\omega)$, are calculated with the expression:

$$S_F(\omega) = S_p(\omega) A_c A_s$$

where values of $S_p(\omega)$ are given in Table A.1-6.

TABLE A.1-4

PUMP PULSATION LOADS
IN THE LOWER SUPPORT STRUCTURE REGION

Temperature °F	No. Pumps	Loads (Lbs.)				Maximum Pump Pulsation Pressures (psi)	
		ICI Tube 58		Instrument Support Plate		120Hz	240Hz
		120Hz	240Hz	120Hz	240Hz		
564	4						
	3						
	2						
500	4						
	3						
	2						
260	3						
	2						
200	3						
	2						

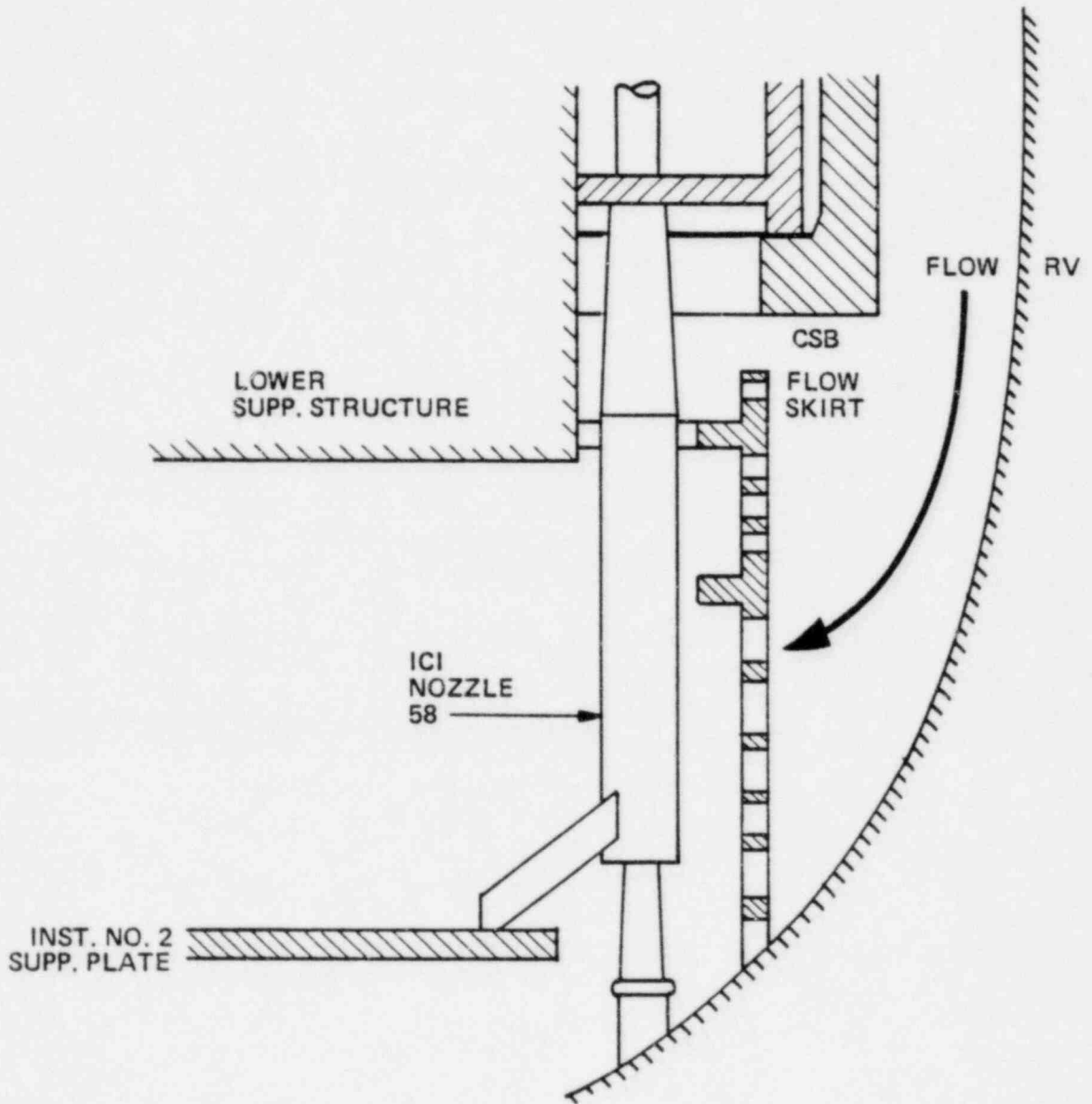
TABLE A.1-5

PERIODIC LIFT/DRAG FORCE ON ICI TUBE 58
DUE TO VORTEX SHEDDING (LBS)

<u>Temperature</u> °F	<u>No.</u> <u>Pumps</u>	<u>Vortex Shedding Frequency</u> Hz	<u>Lift Load</u> lbs	<u>Drag Load</u> lbs
564	4	[
	3			
	2			
500	4			
	3			
	2			
260	3			
	2			
200	3			
	2]		

TABLE A.1-6
RANDOM FLUCTUATING PRESSURE ON ICI
TUBE 58

Temperature °F	No. Pump	Random Pressure PSD Psi ² /Hz
564	4	[]
	3	
	2	
500	4	
	3	
	2	
260	3	
	2	
200	3	
	2	



LOCATION OF ICI TUBE 58

FIGURE A.1-5

A.2 Hydraulic Forcing Functions for UGS Assembly

A.2.1 Periodic Forcing Function

The most significant dynamic force on the upper guide structure assembly is due to flow induced forces on the tube bank. The periodic components of these forces could be due to pressure pulsations at harmonics of the pump rotor and blade passing frequencies and possible vortex shedding due to crossflow over the tubes. A series of tests on full size tubes, (Ref. 22) at reactor pressure and temperature conditions indicated no evidence of periodic vortex shedding at the Reynolds Number and turbulence levels expected in the tube bank. Thus the only significant periodic force is that due to pump pulsations. Reactor test data from plant are used to determine the magnitude of these pulsations at the pump rotor, twice the rotor, the blade passing and twice the blade passing frequencies. To consider coupling effects, pump pulsation loads on the Fuel Alignment Plate, Upper Guide Structure support plate and Upper Guide Structure Barrel are also computed.

The rms pump pressure pulsation force exerted on the UGS region components can be calculated with the expression:

$$\bar{F}(\omega_p) = \bar{P}_0 A_p \sin(\omega_p \frac{\Delta x}{C_0}) \quad (1)$$

where:

- $\bar{F}(\omega_p)$ = Force at pump rotational frequency ω_p
- \bar{P}_0 = Pump rms pressure fluctuation at pump rotational frequency ω_p
- Δx = Component diameter or thickness
- C_0 = Velocity of sound
- A_p = Projected or frontal area of component

The magnitude of the pump RMS pressure fluctuation in the upper plenum region is determined from reactor test data taken with one

operating pump. These data are given as PSDs, in units of psi^2/Hz and are for a particular band width. For a particular pump frequency, the RMS pressure is given by,

$$\bar{P}_{1p} = \text{Band Width} \cdot (\text{Sop})_{1p}^{1/2} \quad (2)$$

Where $(\text{Sop})_{1p}$ is the pressure power spectral density with 1 pump operating.

$$\bar{P}_{1p} = (\text{Sop})_{1p}^{1/2} \quad (3)$$

For multiple pump operation, with the band width taken to be 1Hz, the principle of superposition gives:

$$\bar{P}_0 = N \quad \bar{P}_{1p} = N \cdot (\text{Sop})_{1p}^{1/2} \quad (4)$$

where:

N = number of operating pumps

The pump pressure pulsation force exerted on the UGS region components can then be expressed as:

$$\bar{F}(\omega_p) = N \cdot (\text{Sop})_{1p}^{1/2} A_p \sin(\omega_p \frac{\Delta x}{C_o})$$

Forces are calculated at the pump rotor, twice the rotor, the blade passing and twice the blade passing frequencies.

Predictions of the periodic force on the CEA tubes, fuel alignment plate (FAP), upper guide structure support plate (UGSSP) and upper guide structure (UGS) cylinder are provided at the pump rotor, twice rotor, blade passing and twice blade passing frequencies for both hot and cold conditions for a variety of multiple pump operating configurations. The pump pressure pulsation forces on the CEA tube #6 and FAP are presented in Table A.2-1 in terms of the rms force exerted on the component at the pump rotational frequencies. The pump pressure pulsation forces on the UGSSP and UGS cylinder are presented in Table A.2-2. CEA tube 6 is located adjacent to the outlet nozzle as shown in Figure A.2-1.

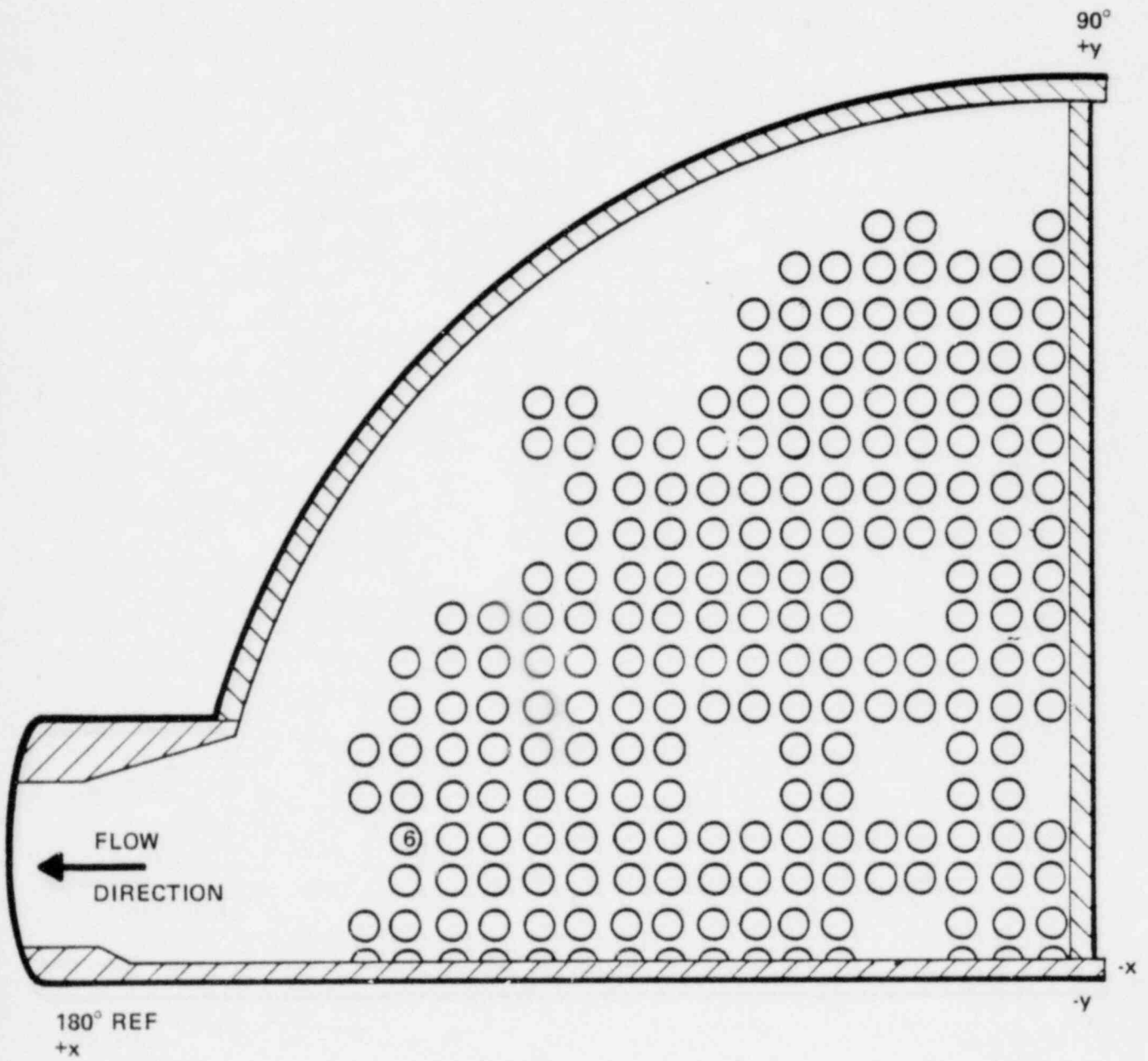
A.2.2 Random Forcing Function

Results from quarter-scale CEA tube bank tests (Ref. 31) indicate that at normal operating conditions, the CEA tubes are excited by upstream and wake produced turbulent buffeting. The response of selected CEA tubes to the random pressure forces was measured during the quarter-scale tests with strain gauges located 1/2 inch below the upper guide structure support plate. These test results are used to predict the CEA tube responses.

The pressure spectral density $S_p(\omega)$ was measured during the quarter-scale CEA tube bank tests with a pressure transducer mounted on the upper guide structure support plate downstream of the CEA tubes near the outlet nozzle, Figure A.2-2. The pressure PSD's from this pressure transducer were used to predict the pressure PSD's for the pressure transducer mounted in the upper guide structure region for the CVAP test program. The upper guide structure pressure transducer locations are identified in Section 6.2.2. The predicted pressure power spectral density function for the upper guide structure pressure transducers is provided in Figure A.2-3

TABLE A.2-2
 PUMP PULSATION LOADS ON THE UPPER GUIDE
 STRUCTURE COMPONENTS (LBS)

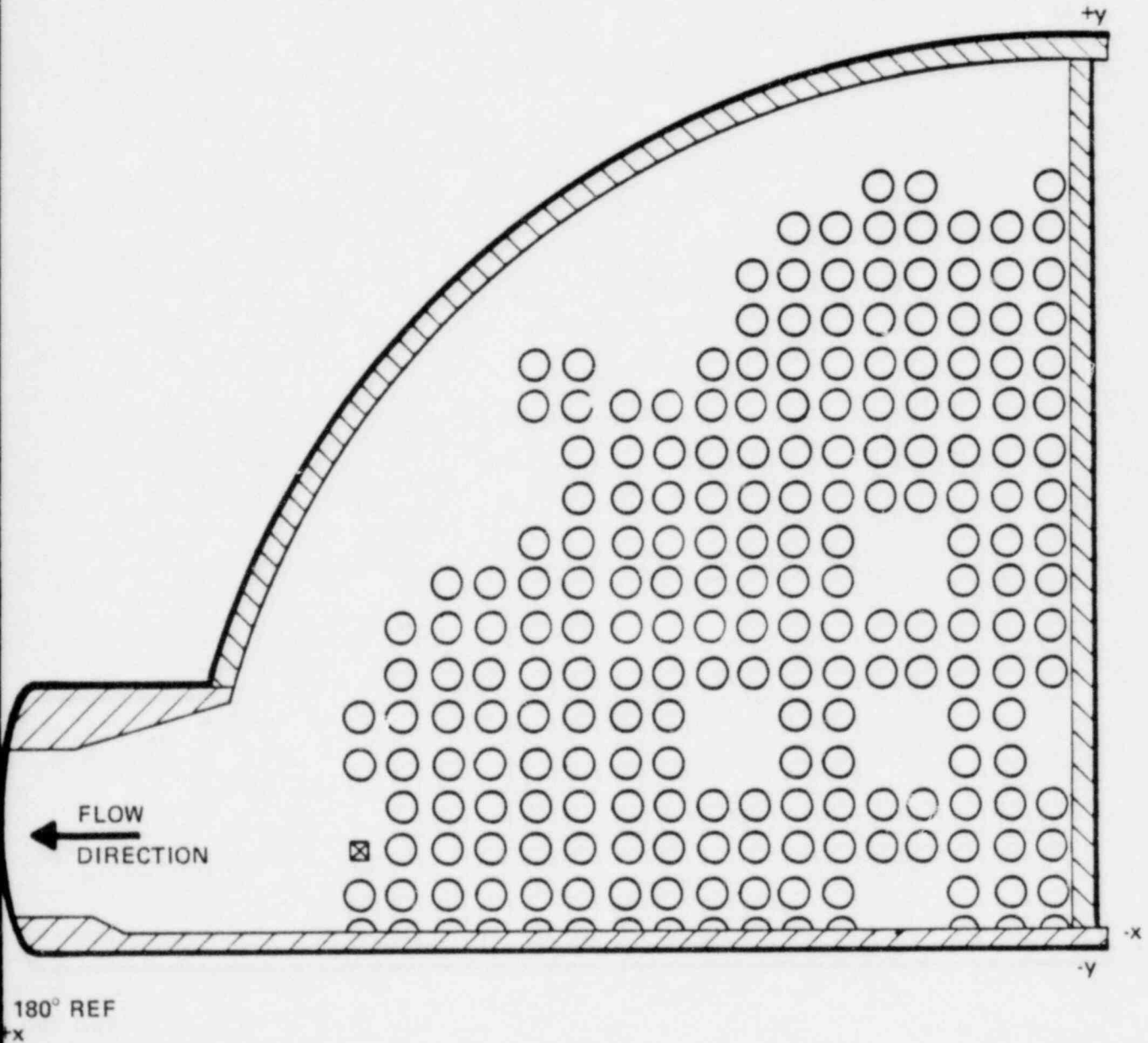
Temperature °F	No. Pumps	Upper Guide Structure Support Plate				Upper Guide Structure Cylinder			
		20Hz	40Hz	120Hz	240Hz	20Hz	40Hz	120Hz	240Hz
564	4								
	3								
	2								
500	4								
	3								
	2								
260	3								
	2								
200	3								
	2								



LOCATION OF CEA TUBE No. 6

FIGURE A.2-1

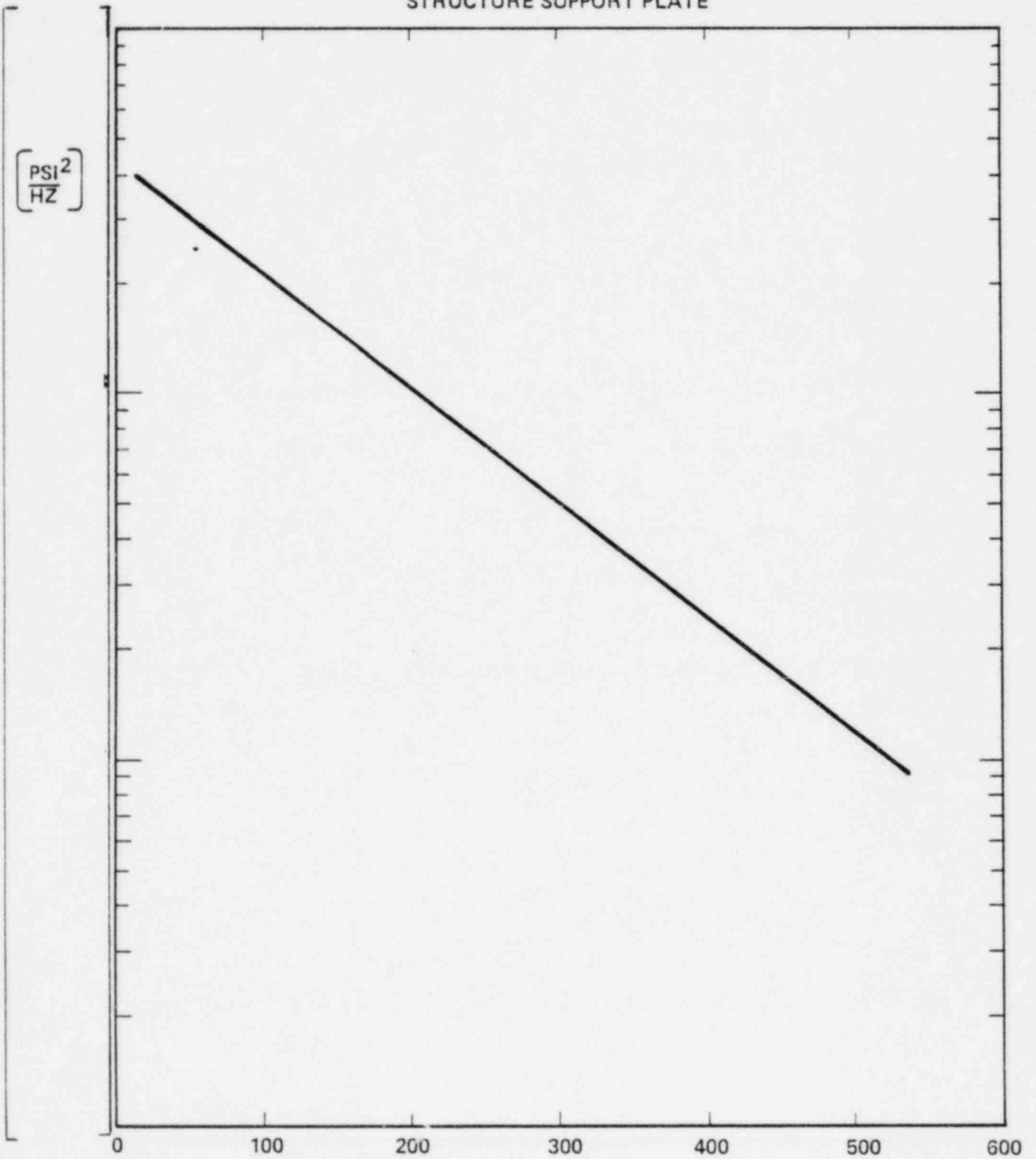
☒ PRESSURE TRANSDUCER MOUNTED ON UPPER GUIDE STRUCTURE SUPPORT PLATE



LOCATION OF PRESSURE TRANSDUCER DURING QUARTER-SCALE
FLOW INDUCED VIBRATION TEST

FIGURE A.2-2

PRESSURE PSD AT CVAP TEST CONDITIONS FOR PRESSURE
TRANSDUCERS MOUNTED ON CEA TUBES AND UPPER GUIDE
STRUCTURE SUPPORT PLATE



FREQUENCY, HZ
PRESSURE PSD AT CVAP CONDITIONS
FIGURE A.2-3

APPENDIX-B

DESCRIPTION OF COMPUTER CODES IN CVAP ANALYSISB.1 ASHSD

A. Description

The ASHD program uses a finite-element technique for the dynamic analysis of complex axisymmetric structures subjected to any arbitrary static or dynamic loading or base acceleration. The three-dimensional axisymmetric continuum is represented as an axisymmetric thin shell. The axisymmetric shell is discretized as a series of frustums of cones.

Hamilton's variational principle is used to derive the equations of motion for these discrete structures. This leads to a mass matrix, stiffness matrix, and load vectors which are all consistent with the assumed displacement field. To minimize computer storage and execution time, the non-diagonal "consistent" mass matrix is diagonalized by adding off-diagonal terms to the appropriate diagonal terms. These equations of motion are solved numerically in the time domain by a direct step-by-step integration procedure.

The assumptions governing the axisymmetric thin shell finite element representation of the structure are those consistent with linear orthotropic thin elastic shell theory. Further description is provided in Reference (A).

B. Application

ASHSD is used to obtain the dynamic response of the core support barrel under Normal Operating Conditions. An axisymmetric thin shell model of the structure is developed. The spatial Fourier series components of the time varying normal operating

hydraulic pressure loads are applied to the modeled structure. The program yields the dynamic shell and beam mode response of the structural system.

C. Verification

ASHSD has been verified by demonstration that its solutions are substantially identical to those obtained by hand calculations or from accepted experimental tests or analytical results. The details of these comparisons may be found in References (A) and (B).

REFERENCES

- A. Ghosh, S. and Wilson, E., "Dynamic Stress Analysis of Axisymmetric Structures under Arbitrary Loading," Dept. No. EERC 69-10, University of California, Berkeley, September 1969.
- B. Topical Report on "Dynamic Analysis of Reactor Vessel Internals Under Loss-of-Coolant Accident Conditions with Application of Analysis to C-E 800 Mwe Class Reactors," Combustion Engineering, Inc., Report CENPD-42, August 1972 (Proprietary).

B.2 MRI/STARDYNE

A. Description

The MRI/STARDYNE program uses the finite-element method for the static and dynamic analysis of two and three dimensional solid structures subjected to any arbitrary static or dynamic loading or base acceleration. In addition, initial displacements and velocities may be considered. The physical structure to be analyzed is modeled with finite elements that are interconnected by nodes. Each element is constrained to deform in accordance with an assumed displacement field that is required to satisfy continuity across element interfaces. The displacement shapes are evaluated at nodal points. The equations relating the nodal point displacements and their associated forces are called the element stiffness relations and are a function of the element geometry and its mechanical properties. The stiffness relations for an element are developed on the basis of the theorem of minimum potential energy. Masses and external forces are assigned to the nodes. The general solution procedure of the program is to formulate the total following equations:

$$[K] \cdot \{\delta\} = \{P\} \quad (1)$$

$$\omega^2 [M] \{q\} - [K] \{q\} = 0 \quad (2)$$

where:

$\{\delta\}$ = the nodal displacement vector

$\{P\}$ = the applied nodal forces

$[M]$ = the mass matrix

ω = the natural frequencies

$\{q\}$ = the normal modes

$[K]$ = stiffness matrix

Equation (1) applies during a static analysis which yields the nodal displacements and finite elements internal forces.

Equation (2) applies during an eigenvalue/eigenvector analysis, which yields the natural frequencies and normal modes of the structural system. Using the natural frequencies and normal modes together with related mass and stiffness characteristics of the structure, appropriate equations of motion may be evaluated to determine structural response to a prescribed dynamic load.

The finite elements used to date in C-E analyses are the elastic beam, plate and ground support spring members. The assumption governing their use are as follows: small deformation, linear elastic behavior, plane sections remain plane, no coupling of axial, torque and bending, geometric and elastic properties constant along length of element.

Further description is provided in reference (A).

B. Application

The MRI/STARDYNE code is used in the analysis of reactor internals. The program is used to obtain the mode shapes, frequencies and response of the internals to prescribed static and dynamic loading. The structural components are modeled with beam and plate elements. Ground support spring elements are used, at times, to represent the effects of surrounding structures. The geometric and elastic properties of these elements are calculated to be dynamically equivalent to those of the original structures. The response analysis is then conducted using both modal response spectra and modal time history techniques. Both methods are compatible with the program.

The program is also used to perform a static finite element analysis of the lower support structure to determine its structural stiffness.

C. Verification

MRI/STARDYNE is in the public domain and further verification is not required.

REFERENCE

- A. MRI/STARDYNE-Static and Dynamic Structural Analysis System: User Information Model, Control Data Corporation, June 1, 1970.

B.3 ICES/STRUDL-II

A. Description

The ICES/STRUDL-II computer program provides the ability to specify characteristics of framed structures and three-dimensional solid structures; perform analyses, static and dynamic, and reduce and combine results.

Analytic procedures in the pertinent portions of ICES/STRUDL-II apply to framed structures. Framed structures are two or three dimensional structures composed of slender, linear members and/or plate elements. Such a structure is modeled with joints (including support joints) and members connecting the joints. A variety of force conditions on members or joints can be specified. The member stiffness matrix is computed from beam and/or plate theory. The total stiffness matrix of the modeled structure is obtained by appropriately combining the individual member stiffnesses.

The stiffness analysis method of solution treats the joint displacements as unknowns. The solution procedure provides results for joints and members. Joint results include displacements and reactions and joint loads as calculated from member end forces. Member results are member end forces and distortions. The assumptions governing the element representation of the structure are as follows; linear, elastic, homogeneous, and isotropic behavior, small deformations, plane sections remain plane, and no coupling of axial, torque, and bending. Further description is provided in reference (A).

B. Application

The ICES/STRUDL-II code is used for the Normal Operations thermal stress analysis of the lower support structure grid beams, and

for the stiffness evaluation and stress analysis of the bottom plates and the instrument nozzle support plate.

C. Verification

ICES/STRUDL-II is in the public domain and further verification is not required.

REFERENCES

- A. ICES/STRUDL-II, The Structural Design Language: Engineering User's Manual, Volume I, Structures Division and Civil Engineering's Systems Laboratory, Department of Civil Engineering, MIT, Second Edition, June, 1970.

B.4 HYDRO

A. Description

The HYDRO Code is a computerized form of theory for finding the reduced frequencies of a cylindrical shell with arbitrary end conditions due to the existence of a surrounding liquid media.

B. Application

The HYDRO Code is utilized to determine the reduced frequencies of the reactor CSB due to the surrounding liquid.

C. Verification

HYDRO has been verified by demonstrating that its solutions are substantially identical to those obtained by hand calculations. Details of the HYDRO theory are contained in Reference (A).

REFERENCE

- A. Penzes L. E. and Bhat S. K., "Generalized Hydrodynamic Effects of a Double Annuli on a Vibrating Cylindrical Shell", 3rd Int. Conf. on Structural Mechanics in Reactor Technology, Vol, II, Part F.

B.5 DPVIB

A. Description

The DPVIB program utilizes a continuum approach to determine the response of an acoustic medium confined in a cylindrical annulus of finite length to a surface excitation.

B. Application

DPVIB is used to determine the acoustic pressure acting on the CSB due to pump pulsations.

C. Verification

DPVIB has been verified by demonstrating that its solutions are substantially identical to those obtained by hand calculations. Details of the DPVIB theory are contained in Reference (A).

REFERENCE

- A. Penzes, L. E., "Theory of Pump Induced Pulsating Coolant Pressure in PWRs", 2nd Int. Conf. on Structural Mechanics in Reactor Technology, Vol. II, Part E-F.

B.6 STEADY STATE

A. Description

The STEADY STATE code calculates the response of a cylindrical shell to a general spatial pressure distribution with harmonic time dependence. The cylindrical shell can have arbitrary boundary conditions, changes in shell thickness and variations in material properties. The STEADY STATE code also incorporates the hydrodynamic mass effects of a surrounding liquid.

B. Application

The STEADY STATE code is used to determine the response of the CSB to deterministic pump induced pressure pulsations. Dynamic stress, strain and displacement are obtained.

C. Verification

The STEADY STATE computer code has been verified by demonstrating that its solutions are substantially identical to those obtained by hand calculations.

APPENDIX-C

DEVELOPMENT OF RELATIONSHIPS FOR ACCEPTANCE CRITERIAC.1 Ratio of Measured to Predicted Stress

Shown schematically in Figure C.1-1 are the relative differences between the peak values of alternating stress intensity for design conditions and for both predicted and measured CVAP conditions. In this figure and the subsequent analysis:

S_e ; endurance limit

$S_{a, n}$; peak alternating stress intensity for condition n ,
where n ; d (design), cp (CVAP prediction), cm (CVAP measured)

Δ_m difference in measured and predicted peak alternating stress intensities

Δ_d difference in endurance limit and design peak stress intensities

The difference between the endurance limit stress and the peak stress intensity is,

$$\Delta_d = (S_e - S_{a,d}) \quad (1)$$

Upon rearranging,

$$\Delta_d = S_{a,d} [(S_e/S_{a,d}) - 1] \quad (2)$$

where the ratio of $S_e/S_{a,d}$ has been defined as the fatigue margin (Section 1.5.2).

For CVAP conditions considering only the case where the measured stress is greater than the predicted stress, the difference between the two is,

$$\Delta_m = (S_{a,cm} - S_{a,cp}) \quad (3)$$

or

$$\Delta_m = S_{a,cp} [(S_{a,cm}/S_{a,cp}) - 1] \quad (4)$$

The difference between the endurance limit and the design stress sets an upper bound on the allowable error, or difference, between the measured and predicted stress for the CVAP. Thus the difference

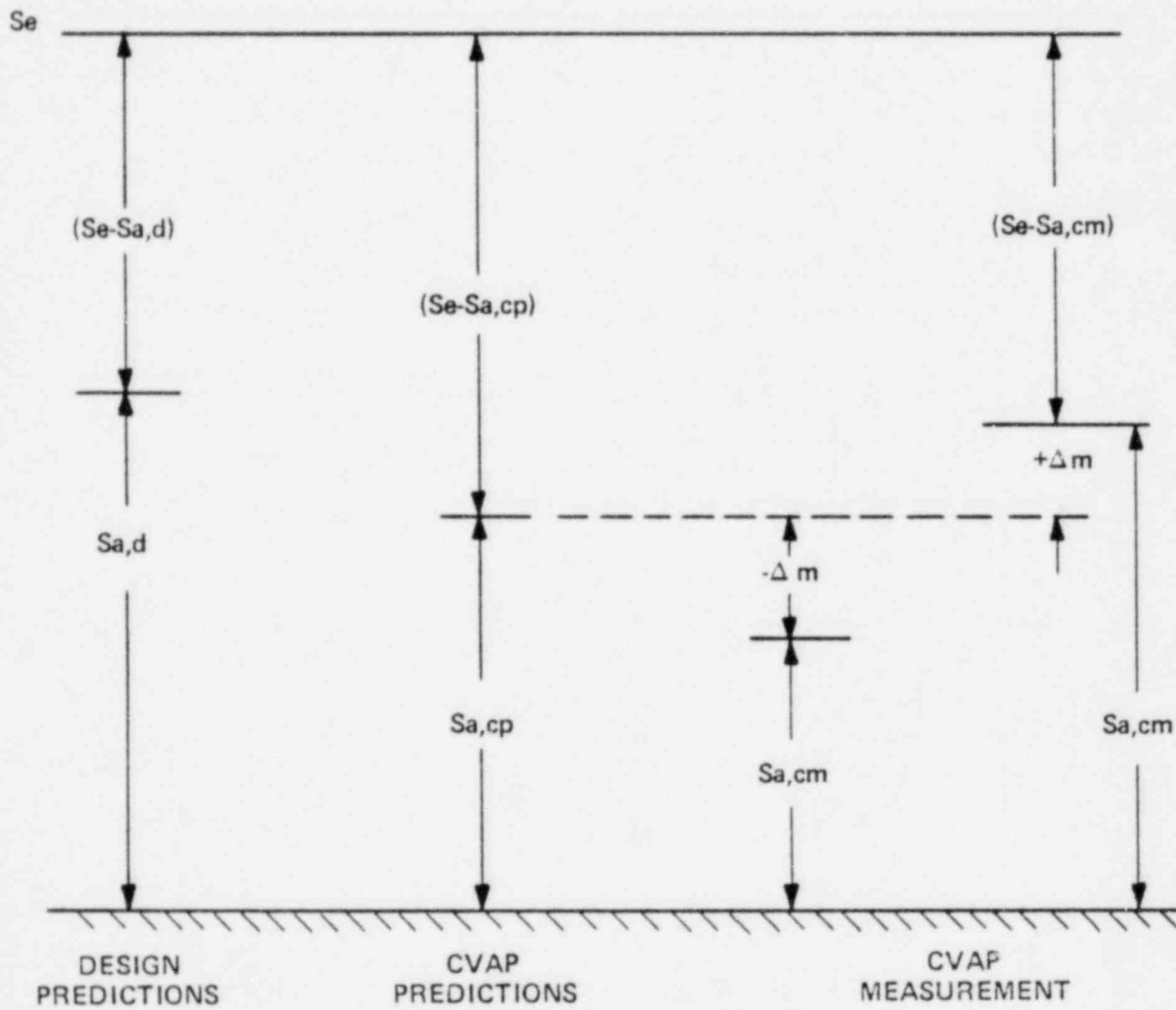
between the endurance and design values of stress must be greater than or, in the limit, equal to the difference between the measured and calculated values for the corresponding CVAP conditions. From equations (1) and (3),

$$\Delta d \geq \Delta m \quad (5)$$

A ratio of equations 4 and 2 gives,

$$\frac{\Delta m}{\Delta d} = \frac{S_{a,cp}}{S_{a,d}} \left[\frac{S_{a,cm}/S_{a,cp} - 1}{S_e/S_{a,d} - 1} \right] \leq 1 \quad (6)$$

With the value equal to one, equation 6 is solved for the ratio of the maximum acceptable value of measured to predicted stress for the CVAP.



DESIGN AND CAVP STRESS INTENSITIES

FIGURE C.1-1

C.2 Acceptance Criterion Based on RMS Value of the Measured Response

Consider a spectral density representation of combined random and periodic response, shown schematically in Figure C.2-1. The problem is to develop a criteria that, based on the RMS value of this spectrum, will insure the response is within the limit on endurance limit stress allowed by the ASME Code.

Assume this spectrum can be divided into the sum, in the mean square, of a random plus periodic spectra (Figure C.2-1A). The random portion is assumed to be wide band white noise from zero to some limiting frequency f_L (Figure C.2-1B). For the random portion, the RMS value σ_{RMS_R} , is limited to being less than one third the ASME limit.

$$\sigma_{RMS_R} \leq \sigma_{ASME}/3 \quad (1)$$

The periodic portion (Figure C.2-1C) is assumed to be narrow band so that its peak value is $\sqrt{2}$ times its RMS value;

$$\sigma_{RMS_{P,N}} = \sigma_{PN} / \sqrt{2} \quad (2)$$

For convenience, all N peaks are assumed to be of the same magnitude;

$$\sigma_{P1} = \sigma_{P2} = \sigma_{PN} \quad (3)$$

Then the total mean stress squared for the periodic part is

$$\sigma_{RMS_P}^2 = N \cdot \sigma_{PN}^2 / 2 \quad (4)$$

Response analysis, for the structure producing the spectrum shown in Figure C.2-1A, would normally use modal superposition to calculate the total response.

$$\sigma_{PT} = \sigma_{P1} + \sigma_{P2} + \dots + \sigma_{PN} = N\sigma_{PN} \quad (5)$$

This sum must be less than the ASME allowable limit;

$$\sigma_p = N\sigma_{pN} \leq \sigma_{ASME} \quad (6)$$

Upon substitution, into (4),

$$\sigma_{RMS_p}^2 \leq \frac{(\sigma_{ASME})^2}{2N} \quad (7)$$

The larger the value of N the smaller the σ_{RMS_p} value so as not to exceed the ASME code limit.

The total mean squared value for the spectrum is,

$$\sigma_{RMS_T}^2 = \sigma_{RMS_R}^2 + \sigma_{RMS_p}^2 \quad (8)$$

Substitution of (1) and (7) into (8) gives,

$$\sigma_{RMS_T}^2 \leq \left(\frac{\sigma_{ASME}}{3}\right)^2 \left(1 + \frac{3^2}{2N}\right) \quad (9)$$

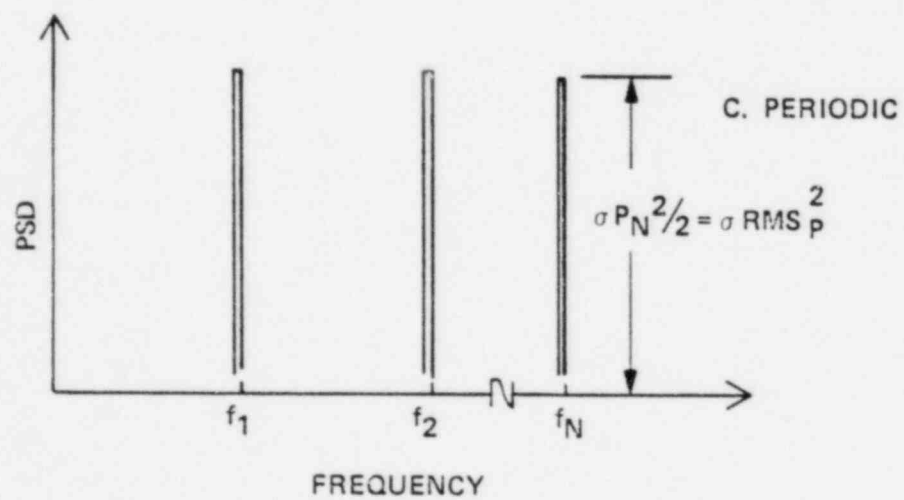
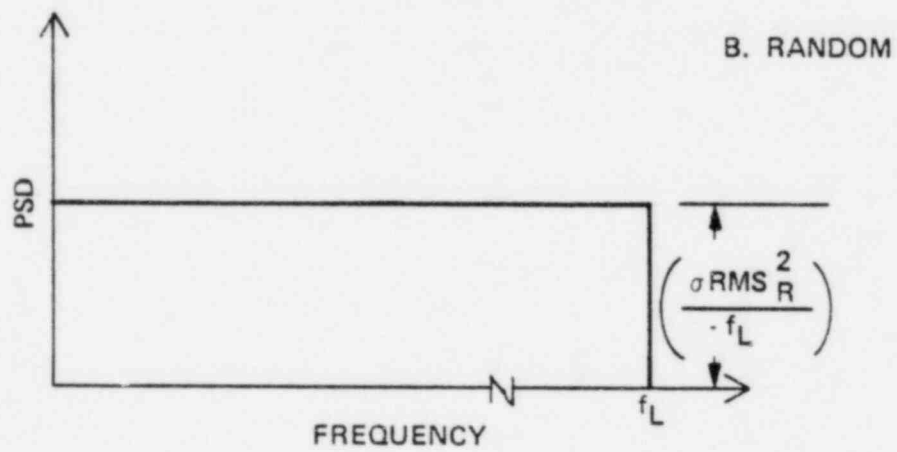
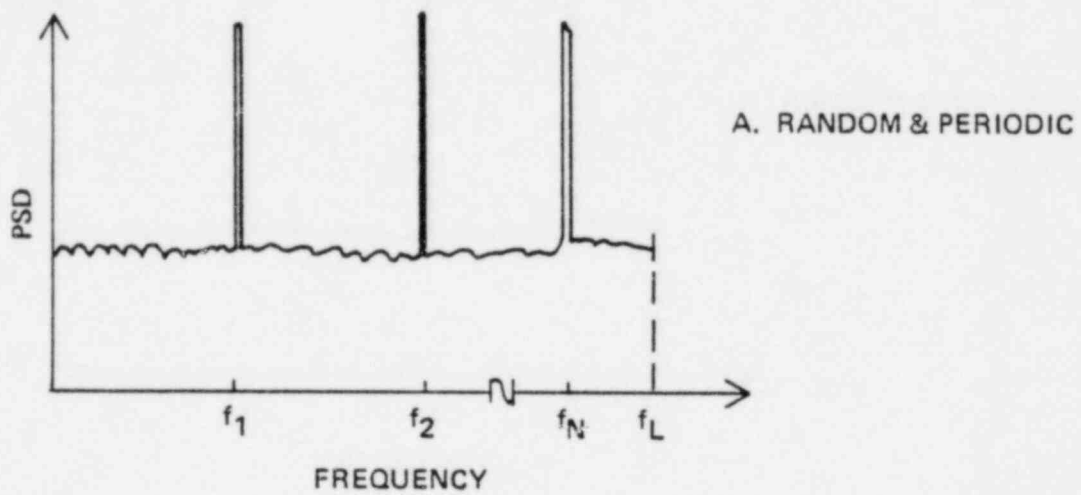
or,

$$\sigma_{RMS_T} \leq \left(\frac{\sigma_{ASME}}{3}\right) \sqrt{\left(1 + \frac{3^2}{2N}\right)} \quad (10)$$

Since $N \geq 1$, a criteria based on one-third the ASME code limit is conservative.

IDEALIZED RESPONSE PSDs FOR DEVELOPMENT
OF ACCEPTANCE CRITERIA

FIGURE C.2-1



COMBUSTION ENGINEERING, INC.